

# Sheffield Hallam University

*Adhesive bonding of stainless steel :Strength and durability.*

BOYES, Robert.

Available from the Sheffield Hallam University Research Archive (SHURA) at:

<http://shura.shu.ac.uk/19379/>

## A Sheffield Hallam University thesis

This thesis is protected by copyright which belongs to the author.

The content must not be changed in any way or sold commercially in any format or medium without the formal permission of the author.

When referring to this work, full bibliographic details including the author, title, awarding institution and date of the thesis must be given.

Please visit <http://shura.shu.ac.uk/19379/> and <http://shura.shu.ac.uk/information.html> for further details about copyright and re-use permissions.

LEARNING CENTRE  
CITY CAMPUS, POND STREET,  
SHEFFIELD, S1 1WB.

101 585 621 7



## REFERENCE

Fines are charged at 50p per hour

07 FEB 2003 4:05.

30 APR 2003 3:50

16 MAR 2004 5:20

25 MAR 2004 8:22 pm

29 MAR 2006

4.22

ProQuest Number: 10694260

All rights reserved

INFORMATION TO ALL USERS

The quality of this reproduction is dependent upon the quality of the copy submitted.

In the unlikely event that the author did not send a complete manuscript and there are missing pages, these will be noted. Also, if material had to be removed, a note will indicate the deletion.



ProQuest 10694260

Published by ProQuest LLC (2017). Copyright of the Dissertation is held by the Author.

All rights reserved.

This work is protected against unauthorized copying under Title 17, United States Code  
Microform Edition © ProQuest LLC.

ProQuest LLC.  
789 East Eisenhower Parkway  
P.O. Box 1346  
Ann Arbor, MI 48106 – 1346

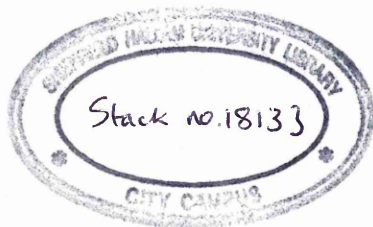
**ADHESIVE BONDING OF  
STAINLESS STEEL:  
STRENGTH AND DURABILITY**

Robert Boyes

A thesis submitted in partial fulfilment of the requirements  
of Sheffield Hallam University for the degree of Doctor of  
Philosophy

May 1998

Collaborating Organisation: Avesta Sheffield AB



At the top of Pentonville Road  
I saw the sun setting  
The town laid out before me  
Looked beautiful to me  
Away from all the sighing  
The suffering and the dying  
I dreamed of the future  
The young and the free

Shane MacGowan

## ABSTRACT

Adhesive bonding as an alternative method of joining materials together has many advantages over the more conventional joining methods such as fusion and spot welding, bolting and riveting. For example, adhesives can be used to bond dissimilar materials, adhesive joints have a high stiffness to weight ratio and the stress distribution within the joint is much improved. Stainless steels are commonly used in applications that would clearly benefit from adhesive bonding; architectural cladding, because of the large bond areas involved, and in the railway industry, due to improved acoustic insulation and greater fatigue resistance. The work presented in this thesis is concerned with adhesive bonding of stainless steels intended for structural applications.

As a starting point to the investigation, a review of the literature was conducted, covering the intrinsic mechanisms of adhesion, the significance of the chemical and physical nature of the adherend surface, the types of structural adhesives, the methods of testing adhesive joints and surface characterisation techniques. The first experimental stage, involved a screening programme to evaluate a number of candidate adhesive systems and adherend surface pre-treatments. Standard single overlap shear and floating roller peel tests conducted in ambient conditions were employed in the discrimination and the degree of compatibility between adhesive and adherend, as measured by the proportion of cohesive failure on the post-fracture face, was also considered. In the second stage of the experimental work, lap shear tests were used to evaluate the affects of surface contamination on joint strength. In addition, lap shear and peel tests were considered to assess the significance of the adhesive bondline and primer thickness. In order to assess the environmental durability of adhesive joints, lap shear and peel tests were conducted after ageing in ambient and high humidity environments. To compliment the data, Boeing wedge crack extension tests were also carried out on adhesive bonded joints incorporating adherends with different surface conditions, to investigate the contribution to joint strength in ambient and adverse environments afforded by surface pre-treatment. The next stage of the experimental work was designed to evaluate the significance of the adherend type and its thickness on initial lap shear strength. Several different commercial grades and gauges of stainless steel were used in the tests, which were conducted at room temperature. The final stage of the experimental work was concentrated on the room temperature creep and dynamic fatigue performance of adhesive joints. Throughout the course of study a number of different surface analytical techniques were employed to physically and chemically characterise the surfaces of pre-bonded adherends and to identify the locus of failure on post-fracture faces.

The single overlap shear and floating roller peel tests were able to differentiate between the candidate adhesives; epoxy systems, particularly the toughened variants, were considered the most suitable structural adhesives for bonding stainless steels in load bearing applications. However, these tests and subsequent tests using lap shear and peel, failed to discriminate conclusively between the different surface pre-treatments (except untreated or crudely prepared surfaces) and ageing environments. The Boeing wedge crack extension tests were found to be sensitive to the condition of the adherend surface and the environment in which the joint is located; roughening the surface of the adherend either chemically or physically was found to enhance joint durability in ambient, high humidity and sub-zero environments. The use of surface primers and coupling agents may protect the un-bonded surface and benefit joint durability, but excessively thick primer layers may reduce joint strength. The stiffness of the adherend material was found to significantly influence lap shear strength. Stiffer adherends, either thicker or inherently stronger, give higher joint strengths because they resist joint rotation and the peel stresses at the extremes of the overlap are minimised. Lap joints with low stiffness adherends will fail by peel-dominated, adherend-controlled failure and lap joints with high stiffness adherends will fail by shear-dominated, adhesive-controlled failure. Two elastic models were proposed for determining the elastic rotation and the line peel force as a function of the shear stress. The room temperature creep results showed an endurance limit of ~40% mean static failure load (design load = 250 N.mm<sup>-1</sup>). The dynamic fatigue results were favourable compared to those of spot welded and weldbonded joints and an endurance limit of ~ 40% mean static failure load (design load = 250 N.mm<sup>-1</sup>) was observed. Finally, leaving the hard fillets of cured adhesive squeeze-out, intact at the extremes of the overlap, will reinforce the joint and minimise the rotation-induced peel stresses that will lead to premature failure when the adherend plastically deforms under static or dynamic loading.

## ADVANCED STUDIES

As part of the course of study I attended the following conferences, short courses and taught lectures combined with a number of informal research seminars presented at Sheffield Hallam University by academic staff and research students from the Materials Research Institute.

### *Conferences:*

- **Duplex '94**

Glasgow, UK. November 1994.

- **Micromechanisms of Fracture and their Structural Significance**

The Institute of Materials Second Griffith Conference. Sheffield, UK. 13 - 15 September 1995.

- **Stainless Steels for the Architect and Engineer**

Avesta Sheffield AB, Sheffield, UK. 29 November, 1995.

- **Euradh '96**

European Adhesion Conference. Churchill College Cambridge, UK. 3 - 6 September 1996.

- **Adhesion and Adhesives**

35<sup>th</sup> Annual Conference. Oxford Brookes University, Oxford, UK. 9 April 1997.

- **Adhesives in Transport**

Institute of Materials: Adhesive Section. London, UK. 2 December 1997.

- **Structural Adhesives in Engineering V**

5<sup>th</sup> International Conference. Bristol, UK. 1 - 3 April 1998.

### ***Short Courses:***

- **Advanced Adhesive Bonding**

Dr. J. F. Watts

University of Surrey, Guilford, UK. November 1995.

- **Adhesion Science Technology**

Professor K. L. Mittal

YTKEMISKA INSTITUTET - Institute of Surface Chemistry. Stockholm, Sweden.

19-20 November 1996.

### ***Taught Lectures:***

- **Analytical Scanning Electron Microscopy**

Dr. J. Cawley

Materials Research Institute, Sheffield Hallam University, 1995.

- **Polymers and Liquid Crystals**

Dr. S. Spells

Materials Research Institute, Sheffield Hallam University, 1995.

- **Crystallography**

Dr. J. Cawley

Materials Research Institute, Sheffield Hallam University, 1995.

- **Electron microscopy and X-Ray Techniques**

Professor J. Titchmarch

Materials Research Institute, Sheffield Hallam University, 1995.

- **Infra Red Spectroscopy**

Professor J. Yarwood

Materials Research Institute, Sheffield Hallam University, 1996.

- **Finite Element Analysis**

Dr. Mohammed Islam

School of Engineering, Sheffield Hallam University, 1996.

- **Fracture and Fatigue**

Professor J. Atkinson

School of Engineering, Sheffield Hallam University, 1996.

- **Materials Under Load**

Professor J. Fletcher

School of Engineering, Sheffield Hallam University, 1996.

***Miscellaneous:***

- Avesta Sheffield Research Foundation - annual review of research. Stockholm, Sweden 1994.
- Avesta Sheffield Research Foundation - annual review of research. Stockholm, Sweden 1995.
- Avesta Sheffield Research Foundation - annual review of research. Stockholm, Sweden 1996.
- Research studies. Luleå University of Technology, Luleå, Sweden. November 1996.
- Avesta Sheffield Research Foundation - annual review of research. Stockholm, Sweden 1997.

## ACKNOWLEDGEMENTS

The author would like to sincerely thank the following people and collaborating establishments for their helpful discussions and advice during the period of study.

- Professor H. Nordberg of the Avesta Sheffield Research Foundation.
- Dr. J. Cawley and Professor J. Yarwood of the Materials Research Institute, Sheffield Hallam University.
- Dr. C. Sammon, Dr. M. Webb and Dr. M. Ives, Mr. K. Blake, Mr. R. Day, Mr. G. Robinson, Mr. T. Hudson, Mr. P. Slingsby, Mrs. C. Shaw and Mrs. L. Davies of the Materials Research Institute, Sheffield Hallam University.
- Mr. S. McCann of the School of Engineering, Sheffield Hallam University.
- Mr. R. Wilkinson, Mr. K. Wright, Mr. P. Haythorne, Mr. C. Hague, Mr. B. Palmer, Mr. A. Earnshaw, Mr. M. Jackson, Mr. J. Bradshaw, and Mr. R. Grant from the School of Engineering and the engineers in the machine shop, Sides, Brian, Roger, Joe and Dick.
- Dr. D. Crowther of the School of Science, Sheffield Hallam University.
- Avesta Sheffield AB.
- 3M UK Plc.
- Dr. H. Groth and Dr. C. Olsson of Avesta Sheffield AB, Avesta, Sweden.
- Mr. M. Pavior of Avesta Sheffield AB, Sheffield, UK.

- Dr. B. Sikkel and Mr. A. Rance at 3M UK Plc, Bracknell, UK.
  
- Mr. J. Linder of the Swedish Institute for Metals Research, Stockholm, Sweden.
  
- Dr. F. Gaillard of Laboratoire de Sciences et Ingénierie des Surfaces, Université Claude Bernard, Lyon, France.
  
- Mr. C. M. Davies and Mr. T. English of Swinden Technology Centre, British Steel Plc, Rotherham, UK.
  
- Dr. T. B. Jones of the Welsh Laboratories, British Steel Plc, Port Talbot, UK.
  
- Mr. Per-Olof Danielsson of ADtranz AB, Kalmar, Sweden.
  
- Mrs M. Ring Groth, Mr. A. Olsson, Mr. Roger Andersson of Luleå University of Technology, Luleå, Sweden for their friendship, hospitality, good company and laughs during the visits to Sweden.
  
- Finally, I would like to thank my mother and father and close family for their support and encouragement throughout the course of study, with a very special thank you to Val for her understanding, tolerance and love during the ups and downs.

## NOMENCLATURE

a	half grip-to-grip distance (mm)
b	lap joint width (mm)
C	compliance ( $\text{MPa}^{-1}$ )
c	half overlap length (mm)
h	adherend thickness (mm)
I	inertia for rectangular plane ( $\text{mm}^4$ )
l	overlap length (mm)
M	bending moment (kN.mm)
P	load (kN)
$P_a$	load amplitude (kN)
$P_f$	line peel force ( $\text{N.mm}^{-1}$ )
$P_m$	mean load (kN)
$P_{\max}$	maximum load (kN)
$P_{\min}$	maximum load (kN)
$P_r$	load range (kN)
R	load ratio
$R_a$	arithmetic average roughness ( $\mu\text{m}$ )
$r_f$	surface roughness parameter
$R_p$	proof stress (MPa)
S	equilibrium spreading parameter
t	adhesive thickness (mm)
$T_g$	glass transition temperature (Deg.)
$W_A$	thermodynamic work of adhesion ( $\text{mN.m}^{-1}$ ( $\text{mJ.m}^{-2}$ ))
$Y_s$	yield strength (MPa)
$\gamma_l$	surface tension (surface free energy) of a liquid in a vacuum ( $\text{mN.m}^{-1}$ ( $\text{mJ.m}^{-2}$ ))
$\gamma_{lv}$	surface tension (surface free energy) of a liquid ( $\text{mN.m}^{-1}$ ( $\text{mJ.m}^{-2}$ ))
$\gamma_s$	surface tension (surface free energy) of a solid in a vacuum ( $\text{mN.m}^{-1}$ ( $\text{mJ.m}^{-2}$ ))
$\gamma_{sl}$	interfacial tension ( $\text{mN.m}^{-1}$ ( $\text{mJ.m}^{-2}$ ))

$\gamma_{sv}$	surface tension (surface free energy) of a solid ( $\text{mN.m}^{-1}$ ( $\text{mJ.m}^{-2}$ ))
$\delta$	crack opening displacement (mm)
E	Young's modulus of elasticity (MPa)
$\epsilon$	engineering strain
$\theta_a$	advancing contact angle (Deg.)
$\theta_f$	contact angle on rough surface (Deg.)
$\theta_m$	rotation due to moment (Radians)
$\theta_p$	rotation due to peel stresses (Radians)
$\theta_r$	receding contact angle (Deg.)
$\theta_s$	contact angle on smooth surface (Deg.)
$\theta_{\text{TOTAL}}$	total rotation (Deg.)
$\pi_s$	equilibrium spreading pressure
$\sigma$	engineering stress (MPa)
$\sigma_p$	line peel stress (MPa)
$\sigma_s$	mean apparent shear strength (MPa)

# CONTENTS

<b>1.0.</b>	<b>INTRODUCTION</b>	<b>1</b>
1.1.	PROJECT OBJECTIVES	3
<b>2.0.</b>	<b>REVIEW OF LITERATURE</b>	<b>4</b>
2.1.	INTRINSIC ADHESION	5
2.1.1.	MECHANISMS OF ADHESION	5
2.1.1.1.	MECHANICAL INTERLOCKING	5
2.1.1.2.	DIFFUSION THEORY	6
2.1.1.3.	ELECTROSTATIC THEORY	6
2.1.1.4	ADSORPTION THEORY	7
2.1.1.4.1.	PRIMARY BONDS	8
2.1.1.4.2.	SECONDARY BONDS	9
2.1.1.4.2.1.	INDUCED DIPOLE BONDS	9
2.1.1.4.2.2.	PERMANENT DIPOLE BONDS	10
2.1.1.4.2.3.	HYDROGEN BONDS	11
2.1.1.4.2.4.	LONDON DISPERSION FORCES	11
2.1.1.4.3.	DONOR-ACCEPTOR BONDS	12
2.1.2	INTERFACIAL CONTACT	12
2.1.2.1.	SURFACE TENSION AND SURFACE FREE ENERGY	12
2.1.2.2.	PARTIAL WETTING OF A SOLID SURFACE	13
2.1.2.2.1.	EFFECT OF SURFACE ROUGHNESS ON CONTACT ANGLE	15
2.1.2.3.	THERMODYNAMICS OF ADHESION	16
2.1.2.4.	SURFACE FREE ENERGIES	17
2.2.	PRACTICAL ADHESION	18
2.2.1.	SURFACE CLEANLINESS	18
2.2.2.	MECHANICAL PRE-TREATMENTS	19
2.2.3.	CHEMICAL PRE-TREATMENTS	21
2.2.4.	SURFACE PRIMERS	24

2.2.5.	SURFACE PREPARATION FOR STAINLESS STEELS	25
2.2.5.1.	AN INTRODUCTION TO STAINLESS STEELS	25
2.2.5.2.	SURFACE PRE-TREATMENTS	27
2.3.	STRUCTURAL ADHESIVES AND ADHESIVE SELECTION	33
2.3.1.	STRUCTURAL ADHESIVES	33
2.3.1.1.	CHARACTERISTICS OF STRUCTURAL ADHESIVES	33
2.3.1.1.1.	CHEMICALLY REACTIVE ADHESIVES	33
2.3.1.1.2.	EVAPORATION OR DIFFUSION ADHESIVES	34
2.3.1.1.3.	HOT MELT ADHESIVES	35
2.3.1.1.4.	DELAYED TACK ADHESIVES	35
2.3.1.1.5.	FILM ADHESIVES	35
2.3.1.1.6.	PRESSURE SENSITIVE ADHESIVES	36
2.3.1.1.7.	CONDUCTIVE ADHESIVES	36
2.3.1.2.	CHEMICAL FAMILIES USED AS STRUCTURAL ADHESIVES	36
2.3.1.3.	STRUCTURAL ADHESIVES FOR STAINLESS STEELS	37
2.3.1.4.	ADHESIVE SELECTION	38
2.4.	MECHANICAL TESTING OF ADHESIVE JOINTS	39
2.4.1.	TEST GEOMETRY'S	39
2.4.2.	JOINT DURABILITY	40
2.4.3.	STATIC AND DYNAMIC FATIGUE TESTING	43
2.5.	SURFACE ANALYTICAL TECHNIQUES	45
2.5.1.	SURFACE CHARACTERISATION	45
2.5.1.1.	PHYSICAL CHARACTERISATION	45
2.5.1.2.	CHEMICAL CHARACTERISATION	45
2.5.2.	FAILURE ANALYSIS	46
<b>3.0.</b>	<b>ADHESIVE SCREENING</b>	<b>47</b>
<b>4.0.</b>	<b>THE EFFECT OF WEAK BOUNDARY LAYERS ON THE MECHANICAL PERFORMANCE OF ADHESIVE-BONDED STAINLESS STEEL JOINTS</b>	<b>86</b>

<b>5.0.</b>	<b>ENVIRONMENTAL DURABILITY OF ADHESIVE-BONDED STAINLESS STEEL JOINTS</b>	<b>99</b>
<b>6.0.</b>	<b>COMPARISON OF THE MEAN APPARENT SHEAR STRENGTH OF STAINLESS STEEL LAP JOINTS INCORPORATING DIFFERENT GRADES AND SURFACE FINISHES</b>	<b>112</b>
<b>7.0</b>	<b>STATIC AND DYNAMIC FATIGUE PERFORMANCE OF ADHESIVE-BONDED STAINLESS STEEL LAP JOINTS</b>	<b>136</b>
<b>8.0.</b>	<b>SURFACE CHARACTERISATION</b>	<b>150</b>
<b>9.0.</b>	<b>DISCUSSION</b>	<b>168</b>
<b>10.0.</b>	<b>CONCLUSIONS</b>	<b>179</b>
<b>11.0.</b>	<b>FUTURE WORK</b>	<b>182</b>
	<b>REFERENCES</b>	<b>184</b>

## PLATES

<b>Plate 3.1.</b> SEM micrograph showing evidence of stressing in DP 490 adhesive due to ballotini.	58
<b>Plate 3.2.</b> Optical micrograph of DP 460 fracture face.	73
<b>Plate 3.3.</b> Scanning electron micrograph of DP 460 fracture face. Showing cliff- like fracture edges.	73
<b>Plate 3.4.</b> Optical micrograph of 7823 S fracture face.	74
<b>Plate 3.5.</b> Optical micrograph of 3532 B/A fracture face.	74
<b>Plate 3.6.</b> Optical micrograph of DP 490 fracture face.	75
<b>Plate 3.7.</b> Optical micrograph of 9323 B/A fracture face.	75
<b>Plate 3.8.</b> Scanning electron micrograph of DP 490 fracture face. Showing cohesive failure within adhesive.	76
<b>Plate 3.9.</b> Scanning electron micrograph of DP 490 fracture face. Showing cohesive and adhesive failure.	76
<b>Plate 3.10.</b> Scanning electron micrograph of DP 490 fracture face. Showing cracking.	77
<b>Plate 3.11.</b> Scanning electron micrograph of DP 490 fracture face. Showing interfacial failure.	77
<b>Plate 3.12.</b> Scanning electron micrograph of 9323 B/A fracture face. Showing adhesive and cohesive failure.	78
<b>Plate 3.13.</b> Scanning electron micrograph of 9323 B/A fracture face. Showing adhesive and cohesive Failure.	78
<b>Plate 4.1.</b> Adhesive failure. Weak adhesion at the adhesive / adherend interface.	94
<b>Plate 4.2.</b> Cohesive <sub>Adhesive</sub> failure. Weak cohesion within the bulk adhesive.	94
<b>Plate 4.3.</b> Interfacial <sub>Adhesive</sub> failure. Weak cohesion within the surface adhesive.	95
<b>Plate 4.4.</b> Interfacial <sub>Oxide</sub> failure. Weak adhesion between metallic oxide and parent metal.	95

<b>Plate 8.1.</b> Scanning electron micrograph of AISI 304L stainless steel with a 2B surface finish. Surface condition <i>As Received</i> (Ra = 0.1 $\mu\text{m}$ ).	156
<b>Plate 8.2.</b> Scanning electron micrograph of AISI 304L stainless steel with <i>Scotchbrite</i> <i>Abraded</i> surface (Ra = 0.2 $\mu\text{m}$ ).	156
<b>Plate 8.3.</b> Scanning electron micrograph of AISI 304L stainless steel with <i>Alumina</i> <i>Blasted</i> surface (Ra = 1.1 $\mu\text{m}$ ).	157
<b>Plate 8.4.</b> Scanning electron micrograph of AISI 304L stainless steel with <i>Acid</i> <i>Etched</i> ( $\text{H}_2\text{SO}_4$ - smut removed) surface (Ra = 1.8 $\mu\text{m}$ ).	157
<b>Plate 8.5.</b> Scanning electron micrograph of AISI 304L stainless steel with <i>Smutted</i> ( $\text{H}_2\text{SO}_4$ - smut un-removed) surface.	158
<b>Plate 8.6.</b> Scanning electron micrograph of AISI 304L stainless steel with <i>Passivated</i> surface.	158

## 1:0 INTRODUCTION

Structural adhesives are extensively used in the aerospace industry to join metals such as aluminium, titanium and their respective alloys and, increasingly, fibre-laminated adherends such as carbon-fibre and glass fibre reinforced plastics (1). Compared with joining by screws and riveting, adhesive bonding offers reduced fabrication costs, increased fatigue resistance of components, improved aerodynamics and considerable weight reduction (2). It was reported in 1986, that ~15% of the structural weight of aluminium constructed aeroplanes could be saved using bonding techniques as opposed to riveting and fastening with screws (2).

The construction of the modern car involves many different adhesive materials (3). However, their use to date can be considered as 'non-structural' since they have been mainly used in non-load bearing applications, or to supplement other joining methods (3), for example, sealing the seams in the manufacture of motor vehicle bodies (4). This situation is changing as developments in materials and processes are resulting in adhesives being used in both greater quantities and more demanding applications (3). Examples include; the bonding of the ring gear in a Renault differential, and the structural gasketing used in the Rover K Series engine (3).

In contrast with the structural adhesives used in aircraft, the development of adhesives for bonding steel has been governed not only by considerations of highest possible shear and peel strengths, and later, good durability, but more by the consideration of simple and economic processing properties (5). The search for increased efficiency and economy in the joining of assembled structures has historically moved from rivets to melt-weldments to spot-weldments to weld-bonding. The latest stage, weld-bonding, involves the combination of spot-welding and adhesive bonding (6, 7).

In order to convince the engineering industry of the possibilities and benefits of adhesive joining it must be demonstrated that these joints can carry pre-calculated loads not only at the time of manufacturing but over the lifetime of the products. These time periods may vary from a few years to three to four decades. Static loads (tensile strength and room temperature creep strength) as well as dynamic (fatigue strength) loads are important. The environment in which the joint operates is equally important, and

structural joints would be expected to endure loads in diverse range of environments. Thus, testing the mechanical properties of adhesive-bonded joints should be done in different environments, over a temperature range from - 40°C to + 60°C.

Stainless steel alloys have often proved difficult to bond, because of the inherent passive, non-interacting surfaces which characterise these alloys. As a consequence of this, mechanical and/or chemical pre-treatments are often employed to modify the surface of stainless steel adherends, in order to improve joint performance (8, 9). The development of the toughened adhesives has, to some extent, helped alleviate the problem; toughened acrylic and single-part and two-part epoxies will bond these alloys well, giving high initial joint strengths (10). Abrasion followed by a solvent wipe may be sufficient for low load applications, although chemical treatments will almost invariably be necessary where good durability in demanding environments is a requirement (11).

The sponsor of the research program was Avesta Sheffield AB, a company formed in 1992 by a merger between Avesta AB and the Stainless Steel Division of British Steel plc. Avesta Sheffield is one of the world's leading manufacturers of stainless steel, accounting for 15 percent of the world's production; in 1994, the Group produced 923,000 tonnes of stainless steel, an increase of 17 percent over the previous year (12). The Group have a commitment to research and development and have not over-looked the potential of adhesive bonding technology, particularly in structural applications such as architectural usage and, more specifically, as a possible alternative to spot welding the carriage panels of the ADtranz X2000 and the new X2 high speed trains. It is the potential of using adhesives for structural joining in applications such as this that was the main impetus of the research programme.

ADtranz Traction is one of largest manufactures of trains and carriage stock in Europe and it has recently entered the markets of the USA and Australia. The new X2 is based on the X2000 and its asynchronous operation and robust traction motors will guarantee performance to the maximum speed of 210 km/h. The majority of the sections in the unit underframe and the greater part of the car body are manufactured from stainless steel; the car bodies are currently spot welded, although ADtranz are

considering the potential offered by both weld-bonding and adhesive bonding, for economic reasons and because of the improved acoustic insulation.

The adhesives used in the research program are supplied by the Adhesives, Coatings and Sealants Division of 3M United Kingdom plc. 3M is a US company with a world-wide turnover exceeding \$ 14 billion and it is expanding; new products introduced within the last four years accounted for 30 % of sales. 3M have a commitment to research and development, investing over \$ 1 billion in 1993.

### **1.1. PROJECT OBJECTIVES**

1. - to evaluate a number of different adhesive systems, in order to find a structural adhesive that is compatible with stainless steel.
2. - to investigate the performance of simple adhesive - bonded stainless steel fabrications under tensile shear and peel loading.
3. - to assess the environmental durability of the aforementioned joints.
4. - to appraise the dynamic durability of adhesive - bonded stainless steel joints.
5. - to consider the practicalities of using adhesives to bond stainless steels.

## 2.0 REVIEW OF LITERATURE

The literature review is divided in to five parts: *2.1. Intrinsic Adhesion*; *2.2. Practical Adhesion*; *2.3. Structural Adhesives and Adhesive Selection*; *2.4. Mechanical Testing of Adhesive Joints*; and *2.5. Surface Analytical Techniques*. The first part deals with the theoretical aspects of adhesive bonding; the mechanisms of adhesion and surface wetting. The second part is concerned more with the practical aspects of adhesive bonding; adherend surface preparation to enhance adsorption, and use of primers. Section 2.3. describes the different types of structural adhesives and considers those with the potential for bonding stainless steels. Section 2.4. summarises the different types of test methods and joint configurations, and finally, Section 2.5., summarises surface analytical techniques for surface characterisation and fracture analysis.

## 2.1. INTRINSIC ADHESION

### 2.1.1. MECHANISMS OF ADHESION

There are four main theories that have been proposed to explain the phenomenon of adhesion. Although the most widely accepted is the adsorption theory, each of the others is appropriate in certain circumstances, and may contribute to some extent to intrinsic adhesion. The adhesion mechanisms are explained in detail by a number of authors (11,13-19) and are briefly described in the following text.

The four main theories are:

- (i) Mechanical interlocking.
- (ii) Diffusion theory.
- (iii) Electrostatic theory.
- (iv) Adsorption theory.

#### 2.1.1.1. MECHANICAL INTERLOCKING

This theory proposes that the major source of intrinsic adhesion is a result of mechanical interlocking of the adhesive into the irregularities of the adherend surface. However, adhesion has been attained on perfectly smooth surfaces (20, 21) and optically smooth surfaces (22), which would suggest that mechanical interlocking is not one of the major mechanisms, at least not on a molecular level. There is no doubt that mechanical interlocking is the appropriate mechanism in certain circumstances, for example, it is responsible for securing the mercury amalgam in tooth cavities (11).

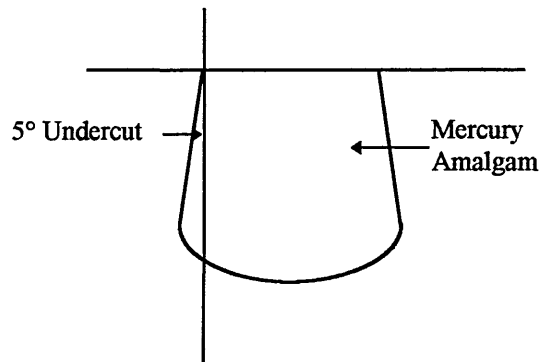


Figure 2.1. Mechanical interlocking: mercury amalgam in tooth cavity.

Another example is the bonding of leather, where the outer layer of leather is removed to free the ends of the corium fibers so that they can embed in the adhesive and the adhesive penetrate between them (15). Roughening the substrate surface prior to bonding, either by physical or chemical means, is often carried out to improve joint strength, although the enhanced performance is more likely to be due to the more rigorous cleaning afforded by these techniques or because of the increased surface area available for surface adsorption which results from surface roughening, rather than the increase in strength being as a consequence of mechanical interlocking. Therefore, it was considered more appropriate to discuss mechanical interlocking and the significance of surface roughening in Section 2.2. *Practical Adhesion*, rather than under the heading of intrinsic adhesion.

#### **2.1.1.2. DIFFUSION THEORY**

Voyutskii (23) first proposed that diffusion is the major driving force for polymer *autohesion* i.e. adhesion of polymers to themselves and to each other (14). Autohesion involves the mutual diffusion of polymer molecules across the interface, and it requires that molecules, or chain segments, of the polymers (adhesive and adherend) possess sufficient mobility and are mutually soluble (11). The concept is quite simple; one end of the polymer molecule chain from one surface diffuses into the structure of the second surface so that the molecule forms a bridge or bond across the interface (13). This theory however, is only relevant in the adhesion of a material to itself or a similar material, and therefore, is not an appropriate model for polymer-metal (metal oxide) adhesion, and thus, it is only discussed briefly in this section.

#### **2.1.1.3. THE ELECTROSTATIC THEORY**

If the adhesive and the adherend have different electronic band structures there will probably be some transfer of electrons on contact in order to balance Fermi levels, which will result in the formation of a double layer of electrical charge at the interface (11). This theory was primarily proposed by Deryaguin *et al* (24-26), and suggests that the electrostatic forces for such contact or junction potentials may contribute significantly to intrinsic adhesion (11). The adhesive and the adherend are likened to the two plates of a capacitor, and the work of separation is equated to that required to separate the two charged

capacitor plates (13). There is considerable controversy associated with this theory and it is not widely accepted as of general importance, but the mechanism is likely to contribute to certain rather special instances of adhesion.

#### **2.1.1.4. THE ADSORPTION THEORY**

The adsorption theory is the most widely accepted theory, and adequately explains metal (metal oxide) - polymer adhesion. This mechanism proposes that materials will adhere because of the inter-atomic and intermolecular forces which are established between the atoms and the molecules in the surface of the adhesive and adherend (11). The most common forces are Lifshitz - van der Waals forces. These forces give rise to *secondary* bonds and are subdivided into: permanent dipole - dipole interactions; dipole - induced dipole interactions; and London dispersion forces (11). Hydrogen bonds can also be formed across the adhesive / adherend interface, and these are similarly classed as secondary bonds. *Primary* bonds across the adhesive / adherend interface are possible (chemisorption), which incorporates ionic, covalent, and metallic interfacial bonds (11). Donor acceptor bonds may also occur and they have a bond strength intermediate between primary and secondary bonds. These bonds are subdivided into Bronsted acid - base interactions and Lewis acid - base interactions (11). The types of bond and their bond strengths are given in Table 2.1.

**Table 2.1.** Bond types and typical bond energies (27-29).

TYPE OF BOND	BOND ENERGY (kJ.mol <sup>-1</sup> )
<u>Primary Bonds</u>	
Ionic	600-1100
Covalent	60-700
Metallic	110-350
<u>Donor - Acceptor Bonds</u>	
Bronsted acid-base Interactions (i.e. up to a primary ionic bond)	↑ 1000
Lewis acid-base interactions	↑ 80
<u>Secondary Bonds</u>	
<i>Hydrogen Bonds</i>	
Hydrogen Bonds involving fluorine	↑ 40
Hydrogen Bonds excluding fluorine	10-25
<i>van der Waals bonds</i>	
Permanent dipole-dipole interactions	4-20
Dipole-induced dipole interactions	< 2
Dispersion (London) Forces	0.08-40

#### 2.1.1.4.1. PRIMARY BONDS

A pure ionic bond is one in which a positive ion and negative ion attract each other, each ion acting as a nucleus surrounded by a rigid spherical distribution of electrons (28). In covalent bonding stable electron configurations are assumed by the sharing of electrons between adjacent atoms. Two atoms that are covalently bonded will each contribute at least one electron to the bond, and the shared electrons may be considered to belong to both atoms (30). However, very few compounds exhibit pure ionic or covalent bonding, but rather, the inter-atomic and intermolecular bonds are usually partially ionic and partially covalent (30). When two atoms have different degrees of electronegativity, the bond between them will have at least partial ionic character. If the atomic orbitals of the two atoms are such that the (directed) orbitals may overlap, and if electrons are available to occupy the resulting orbitals the bond will have at least partial covalent character (28). Interfacial primary bonds, highly ionic in character, have been reported (31-33) between polymeric adhesives and metal oxides (11). Klein *et al* (34) found infrared evidence of primary covalent bonds between a polyurethane adhesive and epoxy-based primers, and such interactions gave the highest joint strength (11). The final type of primary bond is the metallic

bond. An ideal metal crystal consists of a regular array of 'ion cores' in a sea of valence electrons. The ion cores consist of atomic nuclei and the remaining non-valence electrons (30). The valence electrons are not attracted to any one particular atom and are, more or less, free to drift throughout the entire metallic mass. In addition to the interactions of the valence or 'conduction' electrons, there is a mutual attraction of the ion cores for each other; repulsion exists because the ion cores all have a net positive charge, and attraction exists due to the dispersion force of the non-valence electrons in the ion cores (28).

#### **2.1.1.4.2. SECONDARY BONDS**

The most common are Lifshitz van der Waals forces which exist between virtually all atoms and molecules. Lifshitz van der Waals bonds are much weaker than the primary bonds and their presence may be obscured if any of the primary bonding types are present (30). These secondary forces arise from atomic or molecular dipoles, which exist whenever there is some separation of positive and negative portions of an atom or molecule; the bonding results from the coulombic attraction between the positive and negative ends of the dipole (30).

##### **2.1.1.4.2.1. INDUCED DIPOLE BONDS**

A dipole may be induced in an atom or a molecule that is normally electronically symmetrical as shown in Figure 2.2. However, because atoms are continuously vibrating, instantaneous and short lived distortions of the electrical symmetry of the atoms or molecules occur, and thus, small electric dipoles are induced (30). One dipole can in turn produce a displacement of the electron distribution of an adjacent atom or molecule, thus a second dipole is induced that is weakly attracted to the first; this is one type of van der Waals bonding (30).

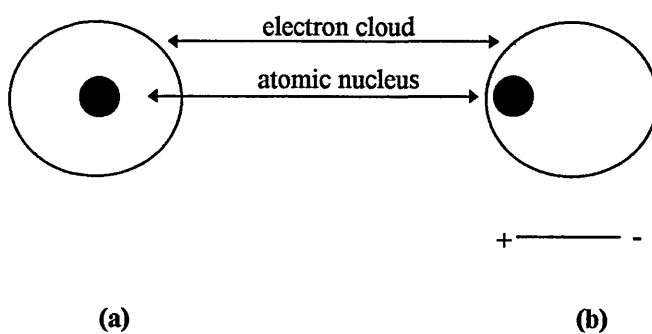


**Figure 2.2.** Schematic representations of (a) an electrically symmetrical atom and (b) an induced atomic dipole (30).

#### 2.1.1.4.2.2. PERMANENT DIPOLE BONDS

Permanent dipole moments exist in some molecules by virtue of an asymmetrical arrangement of positively and negatively charged regions; such molecules are called polar molecules. Consider a HCl molecule (Figure 2.3.); a permanent dipole arises from the net positive and negative charges that are associated with the hydrogen and chlorine ends of the HCl molecule (30).

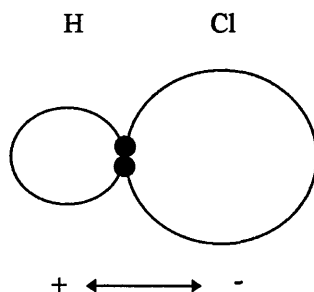


**Figure 2.3.** Schematic representation of a polar hydrogen chloride molecule (30).

Polar molecules can also induce dipoles in adjacent non-polar molecules, and a bond will form as a result of the attractive forces between the two molecules. Lifshitz van der Waal forces will also exist between adjacent polar molecules and the associated binding energies will be significantly greater than bonds involving induced dipoles (30).

### 2.1.1.4.2.3. HYDROGEN BONDS

The strongest secondary bonding mechanism is a special case of polar molecular bonding, the hydrogen bond. This occurs between molecules in which hydrogen is covalently bonded to an electronegative atom - usually fluorine, oxygen or nitrogen. In such cases the single hydrogen electron is shared with the other atom, thus, the hydrogen end of the bond is essentially a positively charged proton. This highly positively charged end of the molecule is capable of a strong attractive force with the negative end of an adjacent molecule. In essence, this single proton forms a bridge between two negatively charged atoms (30). The formation of hydrogen bonds across the interface appears to enhance the intrinsic adhesion and has often been observed by many authors, for example, Kusaka and Suetaka (35) employed 'Attenuated Total Reflectance Infrared Spectroscopy' to study the interfacial bonding between a cyanoacrylate adhesive and an anodized aluminum substrate. They observed a lowering of the C = O stretching frequency and a shift in the anti-symmetric stretching vibration of the C - O - C group to a higher frequency in the infrared spectrum of the cyanoacrylate when it was adsorbed onto the surface of the aluminium. These changes were interpreted as being due to the formation of interfacial hydrogen bonds between the carbonyl groups on the cyanoacrylate adhesive and hydroxyl groups on the surface of the aluminium oxide (11).

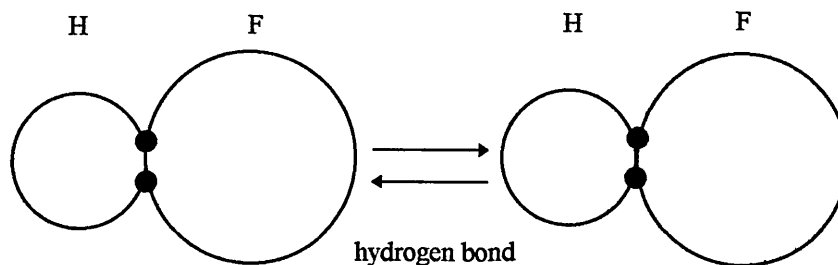


**Figure 2.4.** Schematic representation of hydrogen bonding in hydrogen fluoride (30).

### 2.1.1.4.2.4. LONDON DISPERSION FORCES

London dispersion forces explain the attraction between non-polar molecules (28). A succinct qualitative explanation of the forces was given by Hirschfelder *et al* (36). At any instant the electrons in molecule 'a' have a definite configuration, so that molecule 'a' has an instantaneous dipole moment

(even if it possess no permanent electric dipole moment). This instantaneous dipole in molecule 'a' induces a dipole in molecule 'b'. The interaction between these two dipoles results in a force of attraction between the two molecules. The dispersion force is then the instantaneous force of attraction averaged over all instantaneous configurations of the electrons in -molecule 'a'.

#### **2.1.1.4.3. DONOR - ACCEPTOR BONDS**

Besides the Lifshitz - van der Waals interactions, there are short-range forces due to donor - acceptor interactions (14). Fowkes *et al* (29, 37-41) have argued that the formation of acid-based interactions between adhesive and substrate may represent a major type of intrinsic adhesion force that operates across the interface (11). This classification includes hydrogen bonds, which are considered as a sub-set of acid-base interactions. Liquid and polymer surfaces can have one of three types of hydrogen bonding capability (42): (a) proton acceptors (electron donors or bases); (b) proton donors (electron acceptors or acids); and (c) both proton acceptors and proton donors. If the intermolecular distance is short range ( $<3 \text{ \AA}$ ) a stronger molecular interaction can take place between a donor (acid) and an acceptor (base).

#### **2.1.2. INTERFACIAL CONTACT**

Interfacial contact and surface wetting has been comprehensively described by many authors (11,14,15,43), and the basic principle are explained in the subsequent text. Adsorption is believed to be one of the most important mechanisms in achieving polymer-metal adhesion. Thus, surface free energies and surface wettability are important factors to consider; since the extent of atomic or molecular interaction will increase as the degree of intimacy between adhesive and adherend increases. Before explaining wettability it is necessary to define surface tension and surface free energy.

##### **2.1.2.1. SURFACE TENSION AND SURFACE FREE ENERGY**

Within the bulk of a liquid the attractive forces exerted on molecules by adjacent molecules are balanced in all directions. However, at the liquid surface there is an imbalance of attractive forces which results in the surface molecules experiencing a net inward attraction towards the bulk liquid.

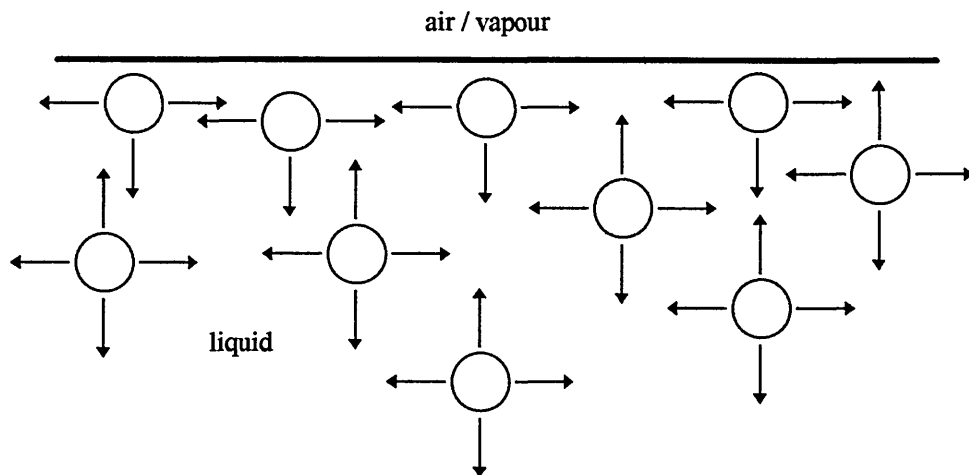


**Figure 2.5.** The imbalance of attractive forces at a liquid surface gives rise to surface tension and surface energy (13).

This attraction tends to reduce the number of molecules in the surface region, which consequently increases the intermolecular distance. To bring new molecules into the surface region, work must be done, and therefore, surface molecules will have higher energy than those of the bulk liquid. This extra energy of the surface molecules is called 'surface free energy' or 'surface energy', and is expressed as energy per unit area ( $\text{mJ. m}^{-2}$ ); this is the energy needed to create a unit area of new surface. The higher energy surface molecules make the liquid surface behave as if it were in tension, as if constrained by an elastic membrane, and this tension is expressed as force per unit length ( $\text{mN. m}^{-1}$ ). Surface energy and surface tension are numerically and dimensionally equivalent, and the terms are often used interchangeably.

#### **2.1.2.2. PARTIAL WETTING OF A SOLID SURFACE**

In 1805, Young (44) showed that the surface tensions acting at the surface of the three phase contact point of the liquid drop resting at equilibrium on a solid surface may be resolved in a direction parallel to the surface.

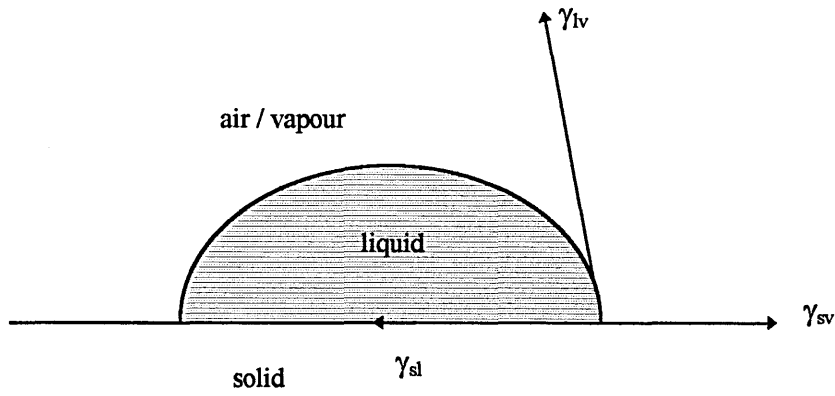


**Figure 2.6.** A liquid drop resting at equilibrium on a solid surface (11).

$$\gamma_{sv} = \gamma_{sl} + \gamma_{lv} \cos\theta \quad \text{The Young Equation} \quad (2.1.)$$

where  $\gamma_{sv}$  = surface tension or surface free energy of the solid,

$\gamma_{lv}$  = surface tension of the liquid,

$\gamma_{sl}$  = interfacial tension.

The term  $\gamma_{sv}$  is the surface tension or the surface free energy of the solid surface resulting from adsorption of vapour from the liquid, and will be lower than the surface energy of the solid surface in a vacuum,  $\gamma_s$  by an amount known as the equilibrium spreading pressure,  $\pi_s$ .

$$\gamma_{sv} = \gamma_{lv} - \pi_s \quad (2.2.)$$

substituting into equation (2.1.),

$$\gamma_s = \gamma_{sl} + \gamma_{lv} \cos\theta + \pi_s \quad (2.3.)$$

When  $\theta > 0^\circ$ , the liquid is non-spreading. But the liquid will spread spontaneously over the surface when,  $\theta = 0^\circ$ . Thus, for complete wetting to occur,

$$\gamma_{sv} \geq \gamma_{sl} + \gamma_{lv} \quad (2.4.)$$

$$\gamma_{sv} \geq \gamma_{sl} + \gamma_{lv} + \pi_s \quad (2.5.)$$

These criteria may be expressed by defining a parameter termed the equilibrium spreading,  $S$ , where:

$$S = \gamma_{sv} - \gamma_{sl} - \gamma_{lv} \quad (2.6.)$$

or alternatively,

$$S = \gamma_s - \gamma_{sl} - \gamma_{lv} - \pi_s \quad (2.7.)$$

When  $S \geq 0$ , the liquid will completely wet a solid surface. However, it is also possible for a liquid spread across a solid surface even when  $\theta > 0^\circ$ , but this will of course require an external pressure to forcibly spread the liquid (11).

#### 2.1.2.2.1. EFFECT OF SURFACE ROUGHNESS ON CONTACT ANGLE

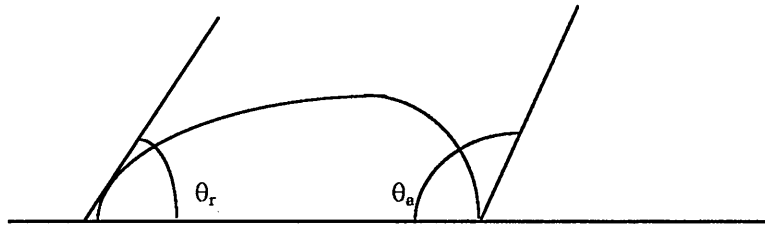


**Figure 2.7.** A liquid drop showing advancing and receding contact angles, where  $\theta_a$  is the advancing contact angle and  $\theta_r$  is the receding contact angle.

Contact angle hysteresis occurs because solid surfaces are seldom smooth or chemically homogenous, and thus different values of the equilibrium contact angle,  $\theta$ , may be obtained depending upon whether the liquid drop is *advanced* or *withdrawn* across the solid surface. It has been shown (45) that surface roughness can change the apparent advancing contact angle and may be expressed by,

$$\cos\theta_f = r_f \cos\theta_s \quad (2.8.)$$

Where,  $\theta_s$  is the contact angle of a liquid drop on a smooth surface,

$\theta_f$  is the contact angle of a liquid drop on a rough surface,

$r_f$  is a surface roughness parameter; = actual area / projected area.

If on a smooth surface  $\theta_s$  is less than  $90^\circ$ , then roughening the surface will further decrease the contact angle to  $\theta_f$  and thereby increase the wettability. However, if on a smooth surface  $\theta_s$  is greater than  $90^\circ$ , roughening the surface will only increase the contact angle to  $\theta_f$  and thereby decrease the wettability.

For a more detailed account on the dynamics and kinetics of wetting, the reader is referred to the work of de Gennes (43).

### 2.1.2.3. THERMODYNAMICS OF ADHESION

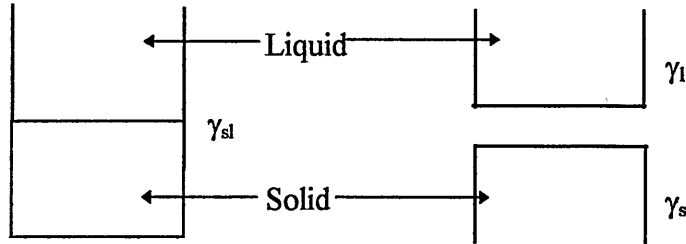


**Figure 2.8.** The physical representation of Dupré's analysis (13).

In 1869, Dupré (46) considered the work needed to separate a liquid from a solid surface. He defined the thermodynamic work of adhesion,  $W_A$ , as the sum of the surface free energies of the solid and liquid phases *minus* the interfacial energy, i.e. the energy of new surface created *minus* the energy of interface destroyed.

$$W_A = \gamma_s + \gamma_{lv} - \gamma_{sl} \quad \text{The Dupré equation} \quad (2.9.)$$

Note: In the Dupré equation (2.9),  $\gamma_s$  represents the surface free energy of the solid surface in a vacuum. But in the Young equation (2.1.),  $\gamma_{sv}$  is used, which represents the surface free energy of the solid surface in equilibrium with vapour. Thus, to make the two equations compatible, the Dupré equation may be rewritten, substituting  $\gamma_s$  for  $\gamma_{sv}$  using equation (2.2.)

Thus,

$$W_A = \gamma_{sv} + \pi_s + \gamma_{lv} - \gamma_{sl} \quad (2.10.)$$

Now substituting  $\gamma_{sv}$  from the Young equation,

$$W_A = \gamma_{lv}(1 + \cos\theta) + \pi_s \quad (2.11.)$$

The above equation accurately describes the situation of a drop of *liquid* adhesive on a solid surface, but because surface energies do not change much on solidification, it also may be used to represent a drop of *solid* adhesive on a solid surface.

#### **2.1.2.4. SURFACE FREE ENERGIES**

Organic materials, such as polymers, are classified as low energy surfaces, with surface free energies usually less than 100 mJ.m<sup>-2</sup>. Metals, metal oxides and ceramics, with surface free energies typically greater than 500 mJ.m<sup>-2</sup>, are classified as high energy surfaces (11). Zisman *et al* (47-51) developed an empirical approach to characterising low energy surfaces. He established that, for low energy surfaces and a series of liquids, a rectangular relationship frequently existed between the cosine of the contact angle,  $\cos \theta$ , and the surface tension of the wetting liquid,  $\gamma_{lv}$ . Zisman defined a critical surface tension of wetting,  $\gamma_c$ , by the value to which  $\gamma_{lv}$  extrapolated as  $\cos \theta$  tends to unity, i.e. as  $\theta$  tends to 0°. Thus,  $\gamma_c$  is the surface tension of a liquid which will just spread on the surface giving a zero contact angle (11). The work of Zisman and others is well documented and is detailed in most text books on the subject of theoretical adhesion. Contact angles on low energy surfaces are easily measured, however, it is much more difficult to achieve on high energy surfaces because they will always be covered with low surface energy contamination, although, many techniques have been used to determine the values of surface free energies of high energy surfaces (52-55).

## **2:2 PRACTICAL ADHESION**

The strength of an adhesive joint depends not only on the cohesive strength of the adhesive (or adherends), but also on the bond strength at the adherend / adhesive interface (56). Adhesion at the interface occurs within a layer of molecular dimensions and the presence of surface contaminants, which are themselves weakly adherent and which prevent contact between the adhesive and the adherend, can reduce the bond strength considerably. Certain adhesives are available which can tolerate contaminants such as light-machine or protective oils, but, even so, the type of contaminant needs to be carefully matched to the adhesive type and its thickness controlled, to enable the adhesive to dissolve and displace the contaminant adequately (11). Rosty *et al* (57) has claimed some success bonding oil-coated 1020 steel using an epoxy adhesive.

Although in many applications no, or very little, surface pretreatment is employed to the substrate materials prior to adhesive bonding, to attain the maximum in joint performance some form of surface pre-treatment is almost always necessary and this is particular relevant to structural applications where durability is a very important consideration. Therefore, for optimum adhesion, the adherend materials must be cleaned or converted to a suitable condition prior to adhesive bonding and this is the purpose of all surface pre-treatments (56).

### **2:2:1 SURFACE CLEANLINESS**

Metallic surfaces will almost certainly be contaminated with some form of grease or oil and a degreasing pre-treatment is therefore essential. Common pre-treatments for metallic surfaces range from, wiping the bond surface with a solvent-wetted cloth, to much more effective methods such as, solvent vapour degreasing or immersing the substrates in liquid solvent degreasing baths, often incorporating an ultrasonic agitator. Whatever method is adopted, the degreasing must be thorough and contaminants must not be re-deposited on the surface as the solvent evaporates.

Common organic solvents used include 1,1,1-trichloroethane or perchloroethylene. These solvents are very effective although they must be checked periodically for the formation of corrosive acid.

Trichloroethylene and other organic solvents are becoming less favourable in industry due to their hazardous nature and indeed, in some countries their use is restricted or even prohibited.

Following solvent degreasing, residual inorganic contaminants are removed using alkaline cleaners or detergent solutions, which are commercially available or may be prepared from existing formulations. Uninhibited (etching type) strong alkaline cleaners are used for ferrous materials, titanium and certain copper alloys, whilst aluminium requires inhibited solutions if etching is to be avoided. Alkaline cleaning leaves the substrates non-receptive to many adhesives and is therefore often followed by a mechanical or chemical treatment (11).

### **2:2:2 MECHANICAL PRE-TREATMENTS**

Mechanical treatments involve the abrasive action of wire brushes, abrasive pads, sand and emery papers, or shot/grit blasting techniques to remove weak surface layers which complicate the bonding operation. In addition to cleaning the substrates and removing weak oxide layers, abrasion techniques create a macro-rough surface, that increases the surface area available for bonding. Mechanical roughening also increases the surface activity of the surface, which enhances the bonding mechanism. The techniques of grit (sand) or shot blasting are preferred in industry (11), because they give the most reproducible results compared with other abrasion methods. Generally however, abrasion methods are less uniform and more difficult to control than chemical treatments, and they may produce a roughened surface which is susceptible to penetration by liquids and corrosive media (58).

The variables associated with grit blasting are grit size, pressure of blast, exposure time, angle of incidence, and distance between the blast nozzle and the adherend (59). A variety of abrasive media is available for grit/shot blasting processes; alumina, quartz and carborundum grits being the most suitable for steels and light alloys (58). The most favourable results are generally obtained with sharp-edged grits, as round blasting media such as iron shot and glass beads tend to create an unsuitable peened surface. The abrasive is typically angular chilled iron of size G04 to BS 254 or angular alumina of 180/220 mesh (11). However, Atkins *et al* (60) has shown that variations in pressure in grit blasting, the angle of incidence of the jet, or the abrasive type have little influence on the resultant joint strength.

Grit blasting may be a dry or wet process; dry abrasion produces dust which must be removed before bonding, and wet abrasion, although it is capable of rinsing away dust residues, must use water of sufficient purity to combat corrosion and prevent deposition of salt residues on drying. In each case it is important to degrease the surface before and after abrasion and to ensure that the abrasion medium is free of substances which are likely to contaminate the surface.

As referred to earlier, abrasion techniques produce a roughened surface which results in an increased surface area available for bonding. It might be expected therefore, that an improvement in joint strength will not only be due to the increased area available for bonding, but also due to the increased mechanical locking affect of the roughened surface. Jennings (61) conducted detailed comparisons between bonding to polished surfaces of aluminium and stainless steel substrates, and rough, machined or abraded surfaces. An epoxy-polyamide adhesive was employed to bond the adherends and the results from room temperature tests are shown in Table 2.2.

**Table 2.2.** Joint strength as a function of surface roughness. Jennings (61).

SURFACE CONDITION	BUTT JOINT STRENGTH (MPa)	COEFFICIENT OF VARIATION (%)
<i>Aluminium Alloy (6061)</i>		
Polished 1 $\mu\text{m}$ diamond paste	28.8	24.4
Abraded through 600 SiC paper	30.9	24.9
Abraded through 280 SiC paper	39.0	17.5
Abraded through 180 SiC paper	36.7	20.4
Sandblasted with 40 to 50 mesh SiC <sub>2</sub> grit	48.5	14.4
<i>Stainless Steel (AISI 304)</i>		
Polished 1 $\mu\text{m}$ diamond paste	27.8	20.8
Regular machined grooves	35.2	20.0
Sandblasted with 40 to 50 mesh SiC <sub>2</sub> grit	53.4	10.8

It may be seen that the rougher the surface the stronger the joint, with sandblasting giving the strongest joints. As the test temperature was increased, making the adhesive more ductile, the differences in joint strengths resulting from the smooth and rough surfaces disappeared. Jennings considered that the better wetting and increased surface area afforded by the roughened substrates probably made some contribution to the higher joint strengths, although this could not explain the observed effect of

temperature; he suggested that the effect of surface topography on the local stress distribution was possibly the main factor. As Kinloch (11) explained: if the macroscopic surface was random as for sandblasting, it could be effective in preventing cracks aligning and propagating along any line of interfacial weakness in the joints. Such alignment and propagation are more likely for a smooth, polished substrate surface. Also, the effect of surface roughness on the ease of crack propagation would be expected to be less important as the adhesive becomes less brittle and more ductile.

Thus, it appears that roughening the surface of the substrates may lead to increased joints strengths, but that such improvements do not generally arise from simple mechanical locking (11). They may arise from the very effective cleaning action associated with the abrasion process, the increased surface area available for bonding, the increased surface energy, the often improved kinetics of wetting, and from the more subtle affects due to changes in the local stress distribution; for example, an increase in roughness may increase localised energy dissipation in the adhesive near the interface and prevent any cracks at, or close to, the interface from aligning and then readily propagating.

### **2:2:3 CHEMICAL PRE-TREATMENT**

Chemical and electrochemical treatments are employed to chemically modify the surfaces of adherends in order to improve initial joint strengths and enhance durability. In addition to the cleaning action, chemical treatments can be used to increase the micro roughness of substrates, and may be employed to produce a strong, chemically resistant surface layer that, for example, may improve bond strength retention in service (56). The treatments involve immersing the substrates in reagents (which range from dilute or concentrated acid or alkaline solutions) at room or elevated temperatures. The acids and bases attack metal oxides preferentially to the base metal and remove these potential mechanically weak layers. With some metals, for example aluminium, further immersing under controlled conditions and with milder solutions such as acid dichromates, may produce stable and mechanically strong oxide layers of controlled structure and thickness. Anodising is a common electrochemical pretreatment employed on aluminium and its alloys to develop preferred oxide layers on surfaces prior to adhesive bonding, and is used extensively in the aerospace industries. In anodising, the adherend acts as the anode and an inert electrode acts as the cathode; a typical electrolyte would be phosphoric acid.

Anodising is performed only after the adherend has been etched, to enable a porous oxide layer to develop on top of that oxide layer formed after etching (59). This porous layer enables the adhesive (or primer) to readily penetrate the pores to form a strong bond. In the subsequent text, reference is made to the "anodising" of stainless steels, however, the term anodising is a misnomer when applied to these materials since the mechanism involved is one of passivation. The procedure, however, is essentially the same.

With nearly all high energy surfaces, in order to achieve the maximum durability to aqueous environments, a chemical pretreatment and/or a primer should be considered (11). Particular attention should be paid in the selection of chemical surface pre-treatment, with the practical and economic implications also being assessed. Chemical pre-treatment may require careful monitoring of the various baths and also, may present a waste disposal problem. It is also very important that the selected treatment does not adversely affect the adherend material being treated; certain titanium alloys and martensitic steels may become embrittled if hydrogen is generated during the process.

The ultimate performance of adhesive bonded stainless steel joints is observed when the substrates are chemically pre-treated (62-65). A typical pretreatment consists of degreasing and water rinsing, followed by etching in sulphuric acid (60°C), water rinsing, de-smutting in chromic acid (60°C), water rinsing and drying (11). Some workers (8, 11) consider complete de-smutting (removal of iron oxide, formed during the etching process) to be essential if high joint strengths are to be realised, since the un-removed smut acts as a weak boundary layer. In the case of stainless steels little is known about the mechanisms, whereby a treatment such as the typical one given above leads to improved joint performance; especially as to why the environmental resistance at the interfacial regions is much improved in comparison with that observed when an abrasion treatment is employed. However, the effectiveness of the pretreatment appears to be very sensitive to the manufacturing path used for the steel (63-65), as may be seen from the data shown in Figure 2.9.

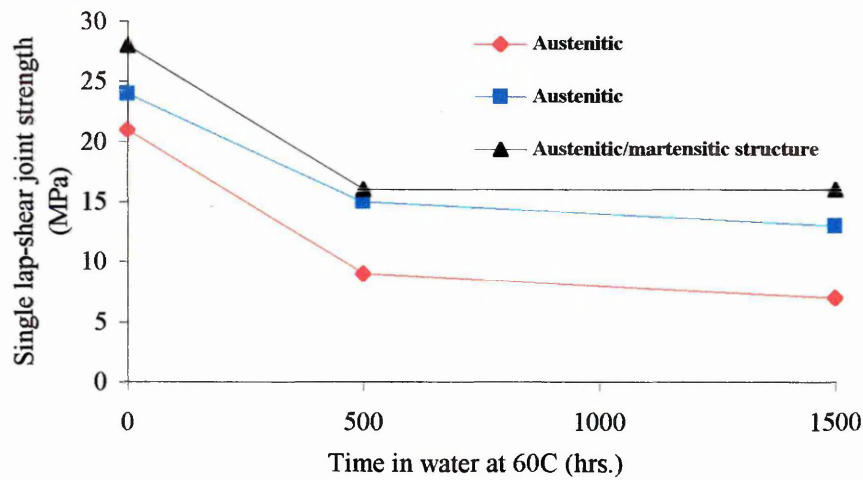


**Figure 2.9.** Single-lap shear strength of joints prepared from stainless steels as a function of immersion time in water: Gettings *et al* (63). The stainless steels had nominally the same bulk chemical composition but had followed somewhat different manufacturing paths, as shown below. The steels were etched in sulphuric acid and de-smutted in chromic acid prior to bonding.

	<i>Melting</i>	<i>Rolling</i>	<i>Flattening</i>	<i>Heat Treatment</i>	
				<i>1st</i>	<i>2nd (In Air)</i>
(a) In air	Yes		Roller level	Air anneal and pickle	240-260 °C
(b) In vacuum	No		None	Bright anneal (NH <sub>3</sub> )	340-360 °C
(c) In air	Yes		Stretch flatten	Bright anneal (NH <sub>3</sub> )	340-360 °C

It was observed that, the relative amounts of austenite and martensite present, which are influenced by the manufacturing path, appear to control the rate of etching within the acid bath, and hence the topography of the etched substrate. Martensitic structures, lead to a faster etching rate and a rougher surface on the etched substrate, and also one which was a somewhat different chemical composition.

It is not only the material structure that may effect the etching rate, contaminants present in the treatment tanks may also have an effect: For several years Bell Helicopter Company (USA) have successfully used strong sulphuric acid solutions in the preparation of 300 series stainless steels for adhesive bonding (66). Although the solutions have proved very effective, problems of stainless steel weight loss, due to the heavy etching, have been experienced. Therefore, a new process, based on a mixture of sulphuric acid and sodium bisulphate, was developed, to produce a lightly etched surface that was still receptive to adhesives.

Initial assessment work on the new process revealed no problems, however, after several weeks use, two effects were observed: (i) the etching action on some components was difficult to initiate; (ii) other components failed to etch uniformly. An investigation was carried out and small quantities of lead in the bisulphate etch solution (dissolved from the tank lead lining and the lead heating coils) were found to be responsible for changes in the characteristics of the etched stainless steel surfaces. The investigation concluded that as little as 5 ppm of lead will change the etching activity of the solution.

#### **2:2:4 SURFACE PRIMERS**

The use of primers as a pretreatment for high energy surfaces prior to adhesive bonding is becoming of increasing importance in industrial applications, where they are most commonly applied as the final stage in a multistage pretreatment operation (11). The main reasons why primers are employed are:

- (i) To improve the performance of the bonded component
  - (a) Some adhesives, for example high-temp polyimides, have too high a viscosity to adequately wet the substrate. Therefore, a primer is formulated (essentially a solvent diluted version of the adhesive) and applied to the substrate prior to the application of the adhesive to ensure complete wetting of the surface. The primer may also incorporate ingredients to improve properties such as thermal stability and environmental resistance.
  - (b) The joint strengths of 'difficult to bond' substrates can be improved by employing a primer, where the role of the primer is to establish strong interfacial forces to both the adhesive and the substrate.
  - (c) In addition to improving the initial joint strength, primers may be used to improve joint durability; the primer may establish strong and moisture resistant interfacial bonds, protecting the substrate from hydration and corrosion which may form a weak boundary layer.

(d) Joints incorporating brittle adhesive types often have poor peel strengths. However, the peel strength of the joint may be improved by priming the substrate with a lower-modulus, tough primer.

(ii) To increase production flexibility in the bonding operation.

Following surface pretreatment, high energy substrates will readily adsorb atmospheric contamination as a consequence of the increased surface activity resulting from the surface pretreatment. After a certain surface exposure time, which may be only a few hours for chemically treated substrates, the contamination may be to such an extent that joint performance will be adversely affected, particularly with respect to durability (67-70). To overcome this problem the substrates may be treated with a primer, within a few hours of the surface pretreatment. Such primers are air-and/or oven-dried and are usually non-tacky and thus, may be then handled, and if necessary stored for several months prior to the application of the adhesive. These primers are typically based on epoxy polyurethane or phenolic materials and are often formulated so that they assist in providing good environmental resistance to the bonded component.

## **2.2.5. SURFACE PREPARATION FOR STAINLESS STEELS**

### **2.2.5.1. AN INTRODUCTION TO STAINLESS STEELS**

Iron and the usual iron alloy, steel, are from a corrosion view point relatively poor materials since they rust in air, corrode in acids and scale in furnace atmospheres. In spite of this there is a group of iron-base alloys, the iron-chromium-nickel alloys known as *stainless steels*, which do not rust in sea water, are resistant to hot, concentrated acids and which do not scale up to 1100°C. It is this largely unique usefulness, in combination with good mechanical properties and manufacturing characteristics, which gives the stainless steels their *raison d'être* and makes them an indispensable tool for the designer (71).

The four main types of stainless steel are so-called because of their room temperature microstructure; austenitic, martensitic, ferritic and duplex: the latter comprising a combined structure of austenite and ferrite. The type of microstructure produced is determined by the chemistry of the steel, and is responsible for the physical and chemical properties peculiar to these alloys, although, the physical properties of the steel can be influenced by the extent of mechanical working during production, for example by cold rolling. A convenient but very approximate method of relating composition and microstructure in stainless steels is by means of the Schaeffler diagram, given in Figure 2.10. (72). In this diagram, the elements that behave like chromium in promoting the formation of ferrite are expressed in terms of a *chromium equivalent*:

$$\text{Cr equivalent} = (\text{Cr}) + (2\text{Si}) + (1.5\text{Mo}) + (5\text{V}) + (5.5\text{Al}) + (1.75\text{Nb}) + (1.5\text{Ti}) + (0.75\text{W})$$

In a similar manner, the austenite-forming elements are expressed in terms of a *nickel equivalent*:

$$\text{Ni equivalent} = (\text{Ni}) + (\text{Co}) + (0.5\text{Mn}) + (0.3\text{Cu}) + (25\text{N}) + (30\text{C})$$

all concentrations being expressed as weight percentages.

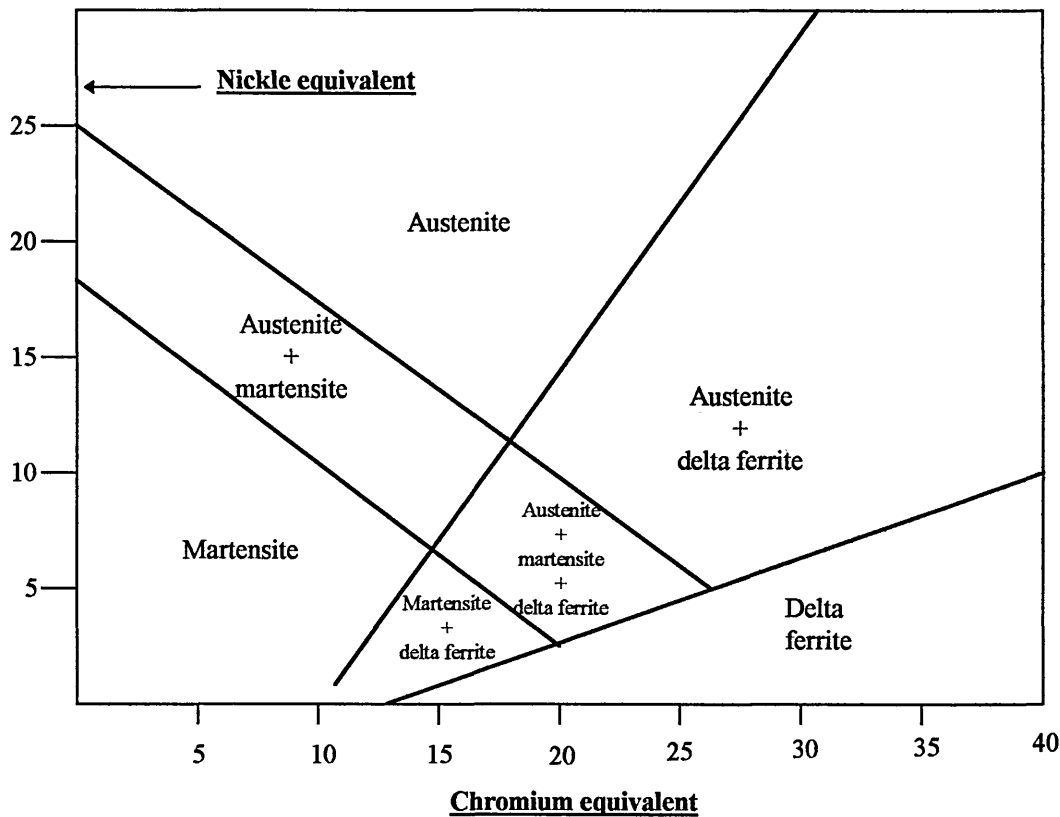


Figure 2.10. Schaeffler diagram.

Stainless steels are sub-divided into different grades, comprising carefully alloyed steels, chemically engineered to afford a diverse range of properties, for example, oxidation resistance at high temperatures, formability, and structural strength and toughness, etc. The chemical and physical nature of the inherent surface oxide, which helps to protect these alloys from corrosion, is also determined by the alloy chemistry and influenced by the subsequent production route, for example, acid pickling is used to create a dull, matt *2B* surface finish and a reflective, *bright annealed* surface finish is achieved by annealing in cracked ammonia. Thus, the composition and structure of the intrinsic surface oxide will vary depending upon the particular grade of stainless steel and its production route.

#### 2.2.5.2. SURFACE PRE-TREATMENTS

In 1965 Botrell (73) evaluated several pre-bonding treatments for stainless steel (FV 520 - martensitic stainless steel). The treatments employed were: vapour degreasing; mechanical abrasion; hydrofluoric-nitric acid etching, hydrochloric acid-formalin-hydrogen peroxide etching; and hydrochloric acid etching. He found that joints incorporating adherends subjected to mechanical abrasion and those

treated by etching gave higher lap-shear strengths than joints including vapour degreased adherends. He attributed the increase in apparent lap shear strength to the increased surface roughness afforded by mechanical and chemical roughening.

Allen *et al* (62) investigated seven chemical treatments for stainless steel (FV 520 - martensitic stainless steel): sulphuric acid etching; sulphuric and oxalic acid etching; sulphuric acid and sodium sulphate etching; hydrochloric acid etching; hydrochloric acid and sodium chloride etching; hydrochloric acid and ferric chloride etching; and hydrofluoric etching. In each case the smut was removed by dipping in concentrated nitric acid. The adhesives used were an epoxy-phenolic, an epoxy, and a polyimide. The adhesive bond properties were tested in torsional shear using napkin ring test pieces, polished using successive grades of emery paper to 600 grit, then polished with diamond paste. Allen found that etching in any reducing acid would improve joint performance, especially sulphuric and hydrofluoric acids.

In 1983 Haak and Smith (74) evaluated the mechanical performance of adhesive-bonded stainless steel joints. No less than 19 surface pre-bonding treatments were considered. The adherend material employed was a duplex alloy (austenitic and martensitic) AM355. Wedge tests were performed according to ASTM-D3762 at 50°C and 100 % relative humidity; stress durability tests (ASTM D2919) at 60C and 100 % relative humidity and lap shear tests (ASTM 1002-72) were also carried out. The adhesive used was Hysol EA 9628H and the adherend surfaces were primed before applying the adhesive using Hysol EA 9210. The oxides formed on the steel as a result of the surface treatments were characterised using Auger Electron Spectroscopy (AES), X-ray photoelectron spectroscopy (XPS), ellipsometry, surface potential difference (SPD), photoelectron emission, and water contact angle methods. Considering hydrothermal-stress endurance, cost and simplicity, the optimum surface treatments for AM355 stainless steel were found to be sulphuric acid / sodium dichromate and nitric acid anodising (passivating). It was found that the bond endurance increases for those treatments that allow the formation of a stable (passive) chromium oxide layer. Mechanical interlocking was also thought to improve bond endurance, which resulted from the formation of a capillary network or micro-roughness layer if the treatment could selectively dissolve iron and re-precipitate a dendritic (micro-rough film).

Pocius *et al* (65) observed a wide variation in the floating roller peel strengths of AISI 301 austenitic stainless joints, adhesively bonded with AF-163-2K/EC-3924 adhesive/pimer system;  $0.88 \text{ N.mm}^{-1}$  to  $8.5 \text{ N.mm}^{-1}$ , at  $152 \text{ mm.min}^{-1}$ . The stainless steel adherends were subjected to a surface treatment prior to priming and bonding; the samples were etched in sulphuric acid and sodium bisulphate solution, followed by de-smutting in a sulphuric acid and sodium dichromate. The workers used XPS and AES to examine the chemical nature of the etched surfaces and scanning electron microscopy (SEM) to evaluate the physical topography. Surface profilometry was also employed to measure the surface roughness of the etched steel surface, micro-hardness readings and electrochemical polarisation measurements were also taken. They concluded that the variation in peel strength was due to the variation in surface micro-roughness (increasing with increasing roughness) and the thickness of the adherend (increasing with increasing thickness). The variations in surface micro-roughness (SEM magnification X 8,000) were attributed to variations in electrochemical reactivity of the surfaces, which in turn, were thought to be due to variations in the steel composition, i.e. variations in the relative amounts of austenite and martensite, the austenite being the predominant phase and the martensite generated as a result of work hardening during the cold rolling operations.

Gaillard *et al* (75) attempted to develop strong and durable stainless steel /epoxy adhesive joints, by subjecting the surfaces to various surface pre-bonding treatments. Surface characterisation was achieved by Low Energy Electron Induced X-ray Spectrometry (LEEIXS), AES, XPS and SEM techniques, and the bond strengths were evaluated, after ageing under hydrothermal conditions (72 hours at  $70^\circ\text{C}$  and 95% relative humidity), by means of a mechanical three-point flexure test. The adherend material employed was AISI 304 L austenitic stainless steel, acetone degreased in an ultrasonic bath and etched in a 5% hydrofluoric -15% nitric acid aqueous solution at  $20^\circ\text{C}$  for 5 minutes, in order to remove contaminants and residual oxides. The adhesive used was a two-component epoxy resin (Araldite AY103 with Hardener HY991 from Ciba-Geigy), which was applied at  $20^\circ\text{C}$ , 35% relative humidity and cured for 2 hours at  $80^\circ\text{C}$ . The pre-treatments considered were: (i) thermal oxidation in air at  $600^\circ\text{C}$ ; (ii) phosphating in an  $\text{HCl-H}_3\text{PO}_4\text{-HF}$  solution at  $80^\circ\text{C}$ ; (iii) etching in 5 to 40% sulphuric acid solutions at 30 to  $90^\circ\text{C}$  (62, 76-78), followed by de-smutting in a sodium dichromate/sulphuric acid

solution (62, 76); (iv) immersing in concentrated ( $400 \text{ g}^{-1} \text{ K}_2\text{Cr}_2\text{O}_7$ ,  $470 \text{ g}^{-1} \text{ H}_2\text{SO}_4$ ) sulpho-chromic solutions at  $85 \text{ }^\circ\text{C}$ , followed by "anodising" in the same solution at  $70 \text{ }^\circ\text{C}$  for 15 minutes (current density  $1 \text{ mA cm}^{-2}$ ); and (v) "anodising" in a 50 % nitric acid solution at room temperature.

As a result of the investigation Gaillard offered the following conclusions:-

- (i) Surface and near-surface sensitive techniques, together with a mechanical three-point flexure test, allow determination of the optimum treatment conditions in order to produce strong, durable stainless steel/epoxy joints.
- (ii) Thermal oxidation, phosphating and smut layer formation, all lead to the formulation of thick surface films, which undergo failure within a weak boundary layer, as determined by SEM and AES.

Although smut (iron oxide) removal is desirable and easily achieved by wire brushing and immersion in an sodium dichromate/sulphuric acid solution, any un-removed smut can be tolerated when epoxies are employed, with no adverse effects on subsequent joint performance (79).

- (iii) Anodising in a nitric acid solution, immersing in a hot, concentrated sulpho-chromic bath, and especially anodising in this last medium, all lead to the formation of thick (up to 90 nm), highly chromium (as Cr (III) ) -enriched surface oxides, which exhibit good cohesion properties. The high surface chromium enrichment seems to be a predominant factor with respect to the bonded joint resistance, notwithstanding the oxide layer thickness (LEEIXS) or the surface morphology (SEM). A strong correlation exists between joint strength and the Cr/Fe intensity ratio (LEEIXS, AES and XPS).

Gaillard's final comments included:- A possible mechanism for the improved durability is an improvement in corrosion resistance due to surface chromium enrichment (74). The nature of the surface pretreatment may also influence the properties of the adhesive itself (80), especially the cross linking near the interface; this last parameter being a great influence in water-induced bonded joint degradation (5). At last, it seems possible that the electronic properties of the substrate surface may play a great role in the mode of adhesive polymerisation (81).

Bouquet and others (9) evaluated the lap shear and peel performance of AISI 304 stainless steel joints, bonded with an epoxy system and incorporating adherends subjected to 15 surface pre-bonding treatments. The assembled joints were subsequently aged for 750 hours at 70°C and 98 % relative humidity before being mechanically tested. They found that joints incorporating nitric acid anodised and sulfuric/chromic acid anodised adherends gave the optimum performance in a moist, warm environment.

Gaskin *et al* (8) investigated the influence of four different surface pre-treatment on the low temperature peel strengths and durability of adhesive joints incorporating three types of stainless steel; a low chromium austenitic AISI 301, a high chromium austenitic with niobium AISI 347 and a martensitic precipitation hardened stainless steel AISI 15-5PH. Wedge crack extension tests were employed to assess joint durability; 24 hours at 60 °C and 100 % relative humidity. For each assembly the adhesive system used was a supported film adhesive AF163-2K and spray applied primer EC3917, manufactured by 3M. Specimens were bonded under 275 kPa pressure at 120°C for 1.5 hours. The surface pre-treatment investigated were: (i) Wet hone abrasion (WHA); (ii) Sulphuric acid pickle (SAP), followed by a sodium dichromate de-smutting solution; (iii) Wet hone/sulphuric acid-naconol etch (SANE), followed by nitric-hydrofluoric acid de-smutting solution; and (iv) Ferric chloride-hydrochloric acid etch (FCHAE), followed by a sodium dichromate de-smutting solution.

Gaskin found the SAP pretreatment to be the most successful compared to the FCHAE treatment for both the AISI 301 and 15-5 PH stainless steels, and the AISI 347 adhesive joints subjected to the SANE pretreatment, to be superior to the AISI 347 adhesive joints subjected to the other three treatments.

However, no treatment proved particularly effective, since all failures were either adhesive or interfacial, i.e. occurring at the adhesive/adherend interface or occurring through the complex interfacial, primer/oxide, region. Like Kinloch (11), Gaskin considers the complete de-smutting to be essential for optimum joint performance and observed the nitric-hydrofluoric acid solution to be the most effective in removing the oxide residue (smut) produced by the etching pre-treatment. In later work (82), Gaskin incorporated an additional pretreatment; sulphuric acid pickle, followed by a nitric-hydrofluoric acid de-smutting stage (SAP II). This pretreatment proved to be most effective, in terms of peel and wedge crack extension tests, for the AISI 301 stainless steel.

De Lacy and Tavakoli (83) evaluated the shear performance of AISI 303 stainless steel bonded with two adhesives; an epoxy and an UV curing anaerobic system. Three surface pre-bonding treatments were considered; grit blasting with alumina, oxalic and chromic acid etching, and priming using a silane primer. Joints incorporating untreated adherends were also tested to act as controls. Initial joint strengths and those after ageing were determined. The ageing conditions were 85C and 85% R.H. for up to 1000 hours with intermediate tests at 100 and 500 hours. They conclude that the durability of adhesive bonds to stainless steel components under exposure to severe damp heat conditions can be dramatically improved by the use of suitable pre-treatment of the metal surfaces prior to bonding.

## **2:3 STRUCTURAL ADHESIVES AND ADHESIVE SELECTION**

There is no single system that adequately classifies the many types of adhesives that are commercially available. However, some distinction may be made when classification is based upon criteria such as: physical form; chemical composition; method of application; processing factors such as curing mechanism; suitability for particular service requirements or environments; or end use such as metal-to-metal adhesives (56). This sub-chapter considers the factors which effect the selection of structural adhesives.

### **2:3:1 STRUCTURAL ADHESIVES**

Although there is no accepted definition for structural adhesives and they may, to some extent, be classified by anyone of the above criteria (2.3.), they are usually defined in terms of their suitability for particular service requirements. Several definitions for a structural adhesive have been offered: a material used to transfer loads between adherends in service environments to which the assembly is typically exposed (84); one which is employed where joints or load-bearing assemblies are subjected to large stresses (56); an adhesive based upon a monomer composition which polymerises to give a high modulus, high strength adhesive, between relatively rigid adherends, so that a load bearing joint is constructed (11); a material of proven reliability in engineering structural applications in which the bond can be stressed to a high proportion of its maximum failing load for long periods without failure (85).

Most materials used in structural adhesives are thermosets, although some thermoplastics, for example cyanoacrylates and anaerobics, are used. Thermoplastics harden rapidly, but have limited heat and creep resistance. The advantage of thermosets as structural adhesives is their heat and creep resistance (84).

#### **2.3.1.1. CHARACTERISTICS OF STRUCTURAL ADHESIVES**

##### **2.3.1.1.1. CHEMICALLY REACTIVE ADHESIVES**

These adhesives are divided into two groups, one-component systems and two-component systems (84). One-component systems are sub-divided into systems that cure in the presence of moisture and systems that are heat-activated. Two-component systems are sub-divided into mix-in and no-mix systems.

One-component systems that are activated by moisture, either from the surrounding air or from the adherend material itself, include; cyanoacrylates "super glues", polyurethanes and silicones. One-component, heat-activated systems, which eliminate the need for metering and mixing equipment, include; epoxies and epoxy-nylons, polyurethanes, polyimides, polybenzimidazoles and phenolics.

Anaerobic adhesives are also chemically reactive, one-component systems. However, they are considered to be a special case, since they harden in the absence of air, or more precisely oxygen, rather than in the presence of moisture or heat. Generally, anaerobics are based on methacrylates, acrylics and acrylic-ester co-polymers.

Two-component systems cure by chemical reaction as a result of intimate interaction between the adhesive and an hardening agent. Mix-in systems, as they are termed, require accurate proportioning and mixing prior to application; chemical families in this group include epoxies, modified acrylics, polyurethanes, silicones and phenolics. Some mix-in, two-component systems cure at room temperature, but heat is often applied to accelerate curing and improve bond quality. In no-mix systems, the adhesive is applied to one adherend and the accelerator to the other; since no mixing is required, careful metering is unnecessary. These systems will cure at room and elevated temperature; modified acrylics are included in this group.

#### **2.3.1.1.2. EVAPORATION OR DIFFUSION ADHESIVES**

These adhesives are divided into two groups; materials that are based on organic solvents and materials that are based on water (84). In solvent-based systems the solvent escapes by evaporation, and/or, absorption into the adherend material(s); for absorption to occur, it is usually required that at least one of the adherends be porous. However, non-porous materials, such as metals, can be bonded using these adhesives, although heat and pressure are usually required to activate the adhesive. Chemical families included in this group are natural, reclaimed and synthetic rubbers, phenolics, polyurethanes, vinyls, acrylics and other natural occurring materials. Water-base adhesives comprise materials that are entirely soluble (solutions) or dispersive (latex) in water. These adhesives do not have the toxicity and

flammability problems that are associated with solvent-base adhesives, although they are slow setting and have poor water resistance.

#### **2.3.1.1.3. HOT-MELT ADHESIVES**

Hot-melt adhesives are 100% solid thermoplastics, remaining solid up to ~ 80 °C. These adhesives melt rapidly and are applied to the adherend materials in the liquid state, where cooling results in rapid setting (84). Hot-melt adhesives are loosely classified as structural, since most will not withstand elevated-temperature loads without suffering from creep. Chemical families included in this group include ethylene-vinyl acetate copolymers, polyolefins, polyamides, polyesters and thermoplastic elastomers. High-performance hot melts, including polyamides and polyesters, will withstand limited loads.

#### **2.3.1.1.4. DELAYED-TACK ADHESIVES**

These adhesives remain tacky following heat activation and cooling; tack can remain from minutes to days, and over a wide temperature range (84). Chemical families used in delayed-tack adhesives include styrene-butadiene copolymers, polyvinyl acetates, polystyrene and polyamides.

#### **2.3.1.1.5. FILM ADHESIVES**

Film adhesives are available as one-sided or double-sided films and tapes. They usually consist of a high molecular weight backbone polymer, which affords toughness, elongation, and peel strength; a low molecular weight cross-linking resin, such as an epoxy or a phenolic; and a curing agent for the cross-linking resin (84). The adhesives are either unsupported or are supported by a carrier, such as glass cloth, nylon or paper. Some film adhesives will cure at room temperature, but most require elevated temperature and nominal pressure. Chemical families used in making film adhesives include nylon-epoxies, elastomer-epoxies, nitrile-phenolics, vinyl-phenolics, epoxy-phenolics and high-temperature-resistant aromatics, including polyimides and polybenzimidazoles.

### **2.3.1.1.6. PRESSURE-SENSITIVE ADHESIVES**

These adhesives do not harden, but remain permanently tacky. They are capable of holding adherends together when they are brought into contact under brief pressure at room temperature (84). Like film adhesives, pressure-sensitive adhesives are either unsupported or are supported by various carriers, including paper, cellophane, plastic films, cloth and metal foil. Most pressure-sensitive adhesives are based on rubbers compounded with various additives, including tackifiers. Rubber-base materials, however, have poor ageing characteristics and thus, they are often replaced by polyacrylates or polyvinylalkylethers.

NB Tack is defined as the property of an adhesive that enables it to form a bond of measurable strength immediately after adhesive and adherend are brought into contact under low pressure (86). A tackifier is an additive to the formulation that promotes tack.

### **2.3.1.1.7. CONDUCTIVE ADHESIVES**

These adhesives are used for structural applications where electrical and/or thermal conductivity is required (84). They contain flaked or powdered filler materials, such as gold, silver, copper or aluminium, to provide electrical conductivity and contribute to thermal conductivity. In addition, non-electrically conductive oxide fillers, such as aluminium oxide (alumina) and beryllium oxide (beryllia), are used to afford thermal conductivity to the adhesive. The chemical families that are used most often to provide electrical and/or thermal conductivity include epoxies, polyurethanes, silicones and polyimides.

### **2.3.1.2. CHEMICAL FAMILIES USED AS STRUCTURAL ADHESIVES**

The chemically reactive adhesives most commonly used as structural adhesives are epoxies, polyurethanes, modified acrylics, cyanoacrylates and anaerobics (84). Epoxies provide strong joints and their excellent creep properties make them ideal for structural applications, but un-modified epoxies have only moderate peel and low impact strength. Whenever the absolute maximum performance is demanded, the toughened epoxies that incorporate a resilient rubbery phase must be considered to offer

the ultimate in adhesive performance (10). The advantages and limitations of the five most popular structural adhesives are summarised in Table 2.3.

### 2.3.1.3. STRUCTURAL ADHESIVES FOR STAINLESS STEELS

The majority of workers who have investigated the adhesive bonding of stainless steels have used epoxies (8, 9, 61, 87, 75). Brockmann (88), however, employed a diverse range of adhesives in his work on joint durability. The shear strengths of Cr/Ni 18/8 adhesive joints are shown in Figure 2.11.

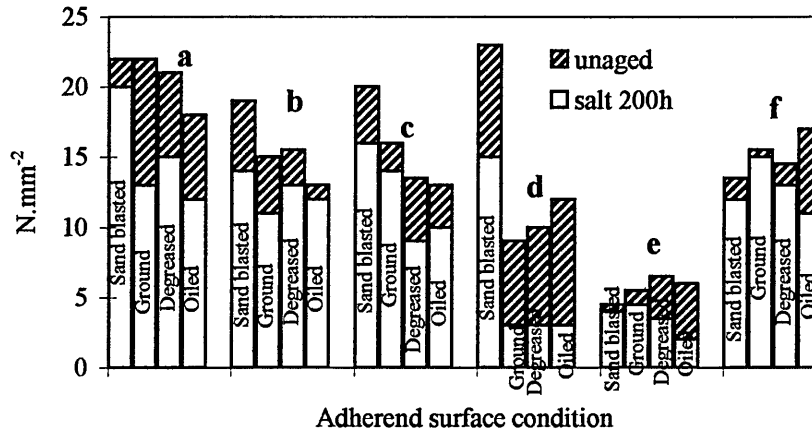


Figure 2.11. Shear strengths of Cr/Ni 18/8 stainless steel joints: Brockmann (88).

(a) Two-part, cold-cured epoxy; (b) Two-part acrylic; (c) Anaerobic acrylic; (d) Cyanoacrylate; (e) PVC plastisol; (f) One-part, hot-cured epoxy.

The cyanoacrylate on the sand blasted surface showed the highest initial joint strength ( $\sim 22 \text{ N.mm}^{-2}$ ), however, after ageing the bond strength was reduced to  $\sim 15 \text{ N.mm}^{-2}$ . Similar reductions were observed for the ground, degreased and oiled surfaces, where the shear strengths after ageing were all less than  $5 \text{ N.mm}^{-2}$ . The plastisol adhesive gave the poorest initial bond strength for all surface conditions, although the sand blasted and ground surfaces exhibited good durability. Both the two-part acrylic and anaerobic acrylic adhesives exhibited reasonable initial bond strengths and good durability, particularly the two-part acrylic used in conjunction with the oiled surface. The one-part, hot-cured epoxy showed reasonable initial bond strengths and good durability. The two-part, cold-cured epoxy, although having high initial bond strength, showed poor durability, with the exception of the sand blasted surface.

**Table 2.3.** Advantages and limitations of the five most widely used chemically reactive structural adhesives. Gauthier (84).

<b>EPOXY</b>	<b>POLYURETHANE</b>	<b>MODIFIED ACRYLIC</b>	<b>CYANOACRYLATE</b>	<b>ANAEROBIC</b>
<p><b>Advantages</b></p> <p>High strength.                      Good solvent resistance.                      Good gap filling capabilities.                      Good elevated-temperature resistance.                      Wide range of formulations.                      Relatively low cost.</p>	<p>Varying cure times.                      Tough.                      Excellent flexibility even at low temperatures.                      One or two component, room- or elevated-temperature cure.                      Moderate cost.</p>	<p>Good flexibility.                      Good peel and shear strengths.                      No mixing required.                      Will bond dirty (oily) surfaces.                      Room-temperature cure.                      Moderate cost.</p>	<p>Rapid room-temperature cure.                      One component.                      High tensile strengths.                      Long pot life.                      Good adhesion to metal.                      Dispenses easily from package.</p>	<p>Rapid room-temperature cure.                      Good solvent resistance.                      Good elevated-temperature resistance.                      No mixing.                      Indefinite pot life.                      Non-toxic.                      High strength on some substrates.                      Moderate cost.</p>
<p><b>Limitations</b></p> <p>Exothermic reaction.                      Exact proportions needed for optimum properties.                      Two-component formulations require exact measuring and mixing.                      One-component formulations often require refrigerated storage and an elevated temperature cure.                      Short pot life.</p>	<p>Both un-cured and cured are moisture sensitive.                      Poor elevated-temperature resistance.                      May revert with heat and moisture.                      Short pot life.                      Special mixing and dispensing equipment required.</p>	<p>Low hot-temperature strength.                      Slower cure than with anaerobics or cyanoacrylates.                      Toxic.                      Flammable.                      Odour.                      Limited open time.                      Dispensing equipment required.</p>	<p>High cost.                      Poor durability on some surfaces.                      Limited solvent resistance.                      Limited elevated-temperature resistance.                      Bonds skin.</p>	<p>Not recommended for permeable surfaces.,                      Will not cure in air as a wet fillet.                      Limited gap cure.</p>

From the above; cyanoacrylate and plastisol adhesives are not considered suitable for the adhesive bonding of stainless steels; the former having poor durability and the latter, although durable, having inadequate strength. However, both acrylic and epoxy systems are deemed worthy of consideration for stainless steel applications, particularly the durable one-part, hot-cured epoxy.

#### **2.3.1.4. ADHESIVE SELECTION**

Adhesive selection is influenced by many factors, which include; the materials to be bonded (compatibility of adherends and adhesives); the surface pre-treatment requirements; the desired joint design; the assembly, processing and storage requirements; the desired properties and service requirements (of both the adhesive itself and the joint); and the cost (56). Lees (10) and Shields (56) have both presented procedures designed to simplify adhesive selection, in terms of the most appropriate family or families of adhesives for a particular application. However, the specific characteristics and requirements of individual adhesive types must be weighed against factors such as cost, space requirement and any conflict of subsequent production processes. Discussion of these factors with adhesive manufacturers will help to secure the most suitable adhesive for a given application at the lowest overall cost for material and processing.

## 2.4. MECHANICAL TESTING OF ADHESIVE JOINTS

Before considering a test programme for assessing the mechanical properties of adhesive bonded joints, one should have knowledge of the type of loading and environment to which the assembled structures are likely to be exposed. For example, the assemblies may need to withstand impact and/or fatigue loading at high, low or fluctuating temperatures and/or in aggressive environments in which attack from moisture or chemicals is probable. In addition, it is also important to know the time scale over which the assembly is expected to satisfactorily perform under the particular service conditions.

Having defined the service conditions in terms of loading, environment and life expectancy, one should decide upon, or develop, a suitable test procedure that will provide reliable data that can be confidently applied in the design of the final assembly. However, there are complications associated with testing and design of adhesive assemblies: (i) any test on a bonded joint is not a test on a single material, but a test on a multi-component *system* (89). In the case of stainless steel adhesive joints this system is comprised of the adherends, adhesive, primer, surface oxides and the inter-phase regions which exist between the distinct phases. Thus, the overall joint performance is a measure of the performance of the system, where success or failure is determined by its weakest link; (ii) design is further complicated, because all adhesive joint test geometry's are non-ideal, since they all give rise to complicated, non-uniform, three-dimensional stress distributions and most also exhibit singular stress fields at certain locations within the bond (89). Thus, considering the above points, it is essential to appreciate that the mechanical test results obtained will represent the adhesive system performance when used in the specific structure of the given test geometry (89).

### 2.4.1. TEST GEOMETRY'S

Test geometry's such as the thin adherend, single lap-shear and the Boeing wedge crack extension tests are simple and inexpensive to manufacture and assemble. They are employed for *qualitative comparison and preliminary screening purposes*, for example, to allow discrimination between adhesives and/or surface pre-bonding treatments (90). When more accurate quantitative results for design use are required, thick adherend specimens are necessary. These are more expensive to

manufacture than the above, and the loads required to test them may be higher and require more sophisticated methods of application and monitoring. Testing of structural configurations is employed as the final stage in a testing and design program for verification purposes. Although expensive and limited in terms of the extent of statistical data produced, this testing procedure is invaluable in assessing "fitness for purpose" of adhesive structural assemblies.

#### **2.4.2 JOINT DURABILITY**

Adhesive joints are notoriously prone to degradation with time, due to ageing of the adhesive and also, due to persistent attack from moisture which penetrates the interfacial regions, thus, it is necessary to assess the durability of adhesive joints. This is achieved by maintaining bonded joints for a certain period of time in a particular environment prior to testing, be it ambient, at high or low temperatures, either in air or submerged in water or some aggressive medium. However, more realistic results are obtained if the joints are stressed and aged in an appropriate medium simultaneously. The Boeing wedge crack extension test is ideally suited to this approach, since it is self stressing and, thus, can be sited in any environment immediately after the joint is loaded. Lap-shear specimens can be loaded in sustained load rigs, where a pre-loaded spring applies a constant load to several joints placed in series; these rigs can then be exposed to almost any environmental conditions. These rigs, however, are awkward to assemble and are cumbersome to work with, since whenever a joint fails it must be replaced with a dummy specimen in order to continue loading the remaining, non-failed joints. Thick adherend shear tensile, peel, creep and fatigue tests are particularly difficult to conduct in controlled environments, since special environmental chambers need to be constructed around the specimens. Although this can be achieved to a degree by wrapping the joints in, for example, wetted cotton wool, the problem of temperature control still remains. The most widely used durability tests are summarised in Table 2.4.

**Table 2.4.** Summary of the most widely used durability tests: DTI Report (91).

TEST CHARACTERISTICS	GEOMETRY			
	1. WEDGE TEST ASTM D 3762-79	2. DOUBLE CANTILEVER (static and cycled) ASTM D 1062-78, 3807-79, 3433-75	3. WET PEEL ASTM D 1876-72 or D 903-49	4. UNSTRESSED LAP SHEAR ASTM D 1002
POPULARITY	Widely adopted	Not widely used in industry	Not widely used	Very popular
UTILITY AND EASE OF USE	Some difficulties in interpretation; easy to use	Care required in testing and data analysis	Generally easy to carry out tests	Samples are easy to test
ACCURACY AND REPRODUCIBILITY	Generally accurate; highly reproducible	Usually very good	Unknown	Generally good if well prepared
RELEVANCE TO INDUSTRIAL SECTOR	Very relevant, especially for QA	Only used where fracture mechanics is accepted	Used sometimes in preference to wedge tests	Geometry resembles some applications
LIMITATIONS ON MATERIALS	Not good for very tough adhesives or flexible adherends	Generally for linear elastic materials	Flexible adherends	None
ENVIRONMENTAL AND SERVICE CONSIDERATIONS	Usually 55 °C and 100% R.H.	Mostly exposed or aged specimens	Water immersed samples	Various, tropical, seacoast, jungle, etc.
IN-SERVICE CORRELATION	Good	Unknown	Good	Fair
QUALITATIVE OR QUANTITATIVE DATA	Qualitative	Quantitative	Qualitative	Qualitative
PARAMETERS RECORDED	Crack growth	Fracture toughness, crack growth	Peel force	Lap shear strength; failure mode
INTERPRETATION AND USE OF INFORMATION	Quality/Process control	Can be complex to interpret; used for design	Relatively straightforward	Can be used for comparison of adhesives, pre-treatment, etc.
ACCEPTANCE OR PASS/FAIL CRITERIA	Crack growth > 19 mm in 1 hour	Fracture toughness > in-service stress intensity	Peel strengths > specified values	Lap shear strength > minimum specified, cohesive failure mode
COST	Low	High	Low	Moderate to low
LIMITATIONS OF PROCEDURE	Plastic deformation of adherends	Only linear elastic fracture conditions considered	Unknown	None
TYPE OF TEST	Standard/routine	Analytical	Developmental	Standard/routine

**Table 2.4. (continued) Summary of the most widely used durability tests: DTI Report (91).**

TEST CHARACTERISTICS	GEOMETRY				
	5. STRESSED LAP SHEAR (plain/perforated/reduced area) ASTM D 1002	6. CLIMBING DRUM ASTM D 3167-76 FLOATING ROLLER ASTM D 1781-76	7. HONEYCOMB SANDWICH PANEL FLEXURE ASTM D 1184-86	8. BUTT TENSILE or TORSION ASTM D 897, 2094, 299	9. OTHER, E.G. THICK ADHEREND SHEAR ASTM D 3983
POPULARITY	Widely used by industry	Mainly aerospace material suppliers	Aerospace material suppliers and designers	Research/engineering design data	Not widely used
UTILITY AND EASE OF USE	Commercial stressing rigs available	Commercial fixtures available; easy to carry out tests	Used to evaluate materials and design of panel	Difficulty of alignment, data analysis, etc.	Difficult to carry out good quality measurements
ACCURACY AND REPRODUCIBILITY	Accurate and reproducible data	Dependent on peeling rates chosen	Dependent on test geometry and bonding conditions	Dependent on sample preparation	Very accurate but depends on sample preparation
RELEVANCE TO INDUSTRIAL SECTOR	Very relevant to industry	Laminated or honeycomb sandwich structures	Laminated or honeycomb sandwich structures	Not a realistic geometry	Not a realistic geometry
LIMITATIONS ON MATERIALS	None, mostly aluminium alloys studied	Honeycomb sandwich laminates	Honeycomb or laminated sandwich panels	Rigid adherends	Rigid adherends; adhesives with $G < 0.7$ GPa
ENVIRONMENTAL AND SERVICE CONSIDERATIONS	Outdoor exposure, simulated freeze-thaw, salt spray, etc.	Various, DTD 5577 specifies temperature limitations	Various	Various	Various
IN-SERVICE CORRELATION	Excellent	Good where data is available	Unknown	Unknown	Unknown
QUALITATIVE OR QUANTITATIVE DATA	Qualitative	Quantitative	Quantitative	Quantitative	Quantitative
PARAMETERS RECORDED	Time to failure, strength, failure mode	Peel strength, failure mode	Flexural stiffness, failure mode	Shear modulus, strength, failure mode	Shear modulus, strength, failure mode
INTERPRETATION AND USE OF INFORMATION	Comparison of adhesives, pre-treatment, etc.	Quality control or materials specification	Design or materials specification	Design data or quality control	Design
ACCEPTANCE OR PASS/FAIL CRITERIA	Time to failure > specified value	Cohesive failure, peel strength > specified value	Stiffness > specified value, cohesive failure	Properties within manufacturers' specification	Unknown
COST	Exposure trials and correlation of results - moderate	Samples/testing straightforward - moderate	Samples expensive, tests can be difficult to get good data	Difficult to get good alignment	High
LIMITATIONS OF PROCEDURE	Geometry's limited to fit stressing rigs	Laminated materials	Laminated or sandwich structures	Extensometry is required to get shear modulus	Accurate extensometry required
TYPE OF TEST	Developmental	Standard/routine	Standard/routine	Analytical	Analytical

### 2.4.3. STATIC AND DYNAMIC FATIGUE TESTING

Adhesive bonded joints may exhibit fatigue failure in service because of sustained or exposure to cyclic loads and hostile environments. In studying the fatigue behaviour of adhesive bonded joints, the following factors, which have the potential to affect joint durability, should be considered: the stress and strain levels and their modes of application with regard to time and joint geometry; exposure to thermal environments, including high- and low-temperature environments; exposure to water; exposure to chemicals; and exposure to radiation. In studying the durability of adhesively bonded joints under exposure to the above degradation parameters, one needs to consider three entities: the bulk of adhesive, which often exhibits viscoelastic constitutive behaviour; the inter-phase, which exists between the adhesive and the adherend (the region immediately adjacent to the interface within adhesive and adherend) and has properties different from that of the bulk adhesive because of the action of the mechanical and chemical adhesion process, adherend surface treatment, and surface topography; the adherend, which may act viscoelastically and can react to chemical and thermal environments. The nature of load transfer between the substrates by means of the adhesive and the inter-phase is quite complex, especially when any or all of the three constituents, adhesive, inter-phase, and adherend, exhibit viscoelastic behaviour.

Joseph *et al* (92) evaluated crack growth rates within epoxy/aluminium and epoxy/steel joints (using double cantilever beam specimens) as a function of: (a) surface pretreatment; (b) water soak; (c) fatigue cyclic rate; (d) adhesive thickness and; (e) type of epoxy adhesive. He found that for both adherends, aluminium and steel, the fatigue behaviour improved significantly with the incorporation of the mercaptoester coupling agent. After an eight day, 57°C water soak, the metal surfaces which were pre-treated with the coupling agent or by a phosphoric acid anodisation treatment still resulted in cohesive failure, and the crack growth rates were higher in the control samples and showed more scatter. A room temperature cured epoxy (Epon 828, Shell Chemicals) with coupling agent-treated aluminium showed a less dramatic improvement, probably because of a difference in the application procedure of the coupling agent, which resulted in different coupling agent thickness', 50 Å for the room temperature cured adhesive compared with 150 Å for a heat-cured, one-component epoxy adhesive (FM-73, American Cyanamid Co.). For the steel joints and room temperature adhesive the improvement in the fatigue

behaviour of coupling agent-treated samples was maintained after an eight day hot water soak. After water soaking the fatigue performance for the steel joints was even better than before exposure. This was attributed to the plasticising effect of the water on the room temperature curing epoxy system. A similar effect was observed with the anodised aluminium joints incorporating the room temperature cured epoxy. No significant change was found in the fatigue crack growth rate over a frequency range of 1-5 Hz., but a significant change was found as a function of the bondline thickness; the greater the thickness, the higher the fatigue crack growth rate. The thickness bondline studied was 0.38 mm. The room temperature curing epoxy evaluated exhibited a much lower fatigue residence than the heat-cured commercial structural adhesive FM-73.

Su, *et al* (93, 94) carried out investigations into the effect of ageing and environment on the fatigue life of grit blasted, mild steel adhesive joints. Su observed that some adhesives (high strength, high fracture toughness, high Young's modulus epoxies, cured with a polyamine hardener) showed excellent durability properties and that the fatigue life of some specimens actually improved with age. Other adhesives (low strength, low Young's modulus epoxies, cured with polysulphide hardener) were adversely affected by environment, particularly high humidity (90% relative humidity at room temperature) or exposure to a natural environment (roof top conditions, Dundee).

Harris and Fay (95) investigated the fatigue behaviour of two adhesives (Elastosol M51, Evode and XW 1012, Ciba-Geigy) intended for use in automotive body shell construction, using un-treated, oily mild steel single lap-shear test pieces. They found that, over a wide temperature range that included the glass transition temperature ( $T_g$ ) of both adhesives, fatigue life was dominated by a crack initiation phase, which was associated with the build up of creep deformation in the adhesive layer. It was also observed that thicker glue lines have a detrimental effect on static strength, over the range of -30 to 90°C, for both adhesives.

## **2.5. SURFACE ANALYTICAL TECHNIQUES**

### **2.5.1. SURFACE CHARACTERISATION**

It is necessary to characterise the surface of the adherends to be bonded, both physically and chemically, to allow the mechanical test results and the natures of the failure to be related to the surface condition.

This section highlights surface analytical techniques used to physically and chemically characterise pre-bonded and post-fracture surfaces.

#### **2.5.1.1. PHYSICAL CHARACTERISATION**

The degree of surface roughening resulting from mechanical pre-bonding treatments (macro-roughening) can easily be characterised using Talysurf or laser profilometry, which will quantify the surface roughness in terms of, for example, Ra values (see 4:2:1 of *Results*). In order to characterise macro-rough surfaces and micro-rough surfaces resulting from chemical pre-bonding treatments, in terms of surface morphology and topography, it is necessary to employ Scanning Electron Microscopy (SEM), because of the high resolution and depth of field characteristics. Because of the scale of the micro-rough oxides generated by chemical passivating pre-bonding treatments, it is often necessary to use different techniques such as Transmission Electron Microscopy (TEM) or Scanning Transmission electron Microscopy (STEM). However, to observe the morphology and physical structure of these oxides by TEM or STEM, involves the development of surface replicas which is time consuming (96).

#### **2.5.1.2. CHEMICAL CHARACTERISATION**

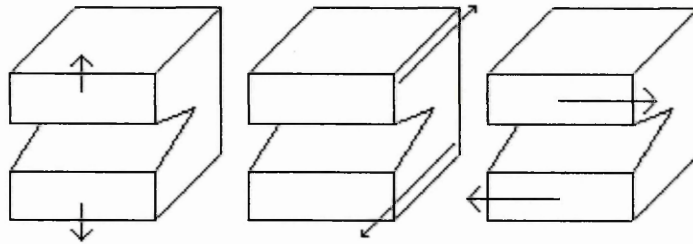
Although Low Energy Electron Induced X-ray Spectrometry (LEEIXS) and Infra Red Spectroscopy (IRS) have been used to chemically characterise adherend surfaces prior to bonding (75, 88) the most commonly employed techniques are X-ray Photoelectron Spectroscopy (XPS); Auger Electron Spectroscopy (AES); Secondary Ion Mass Spectrometry (SIMS); and Secondary Neutral Mass Spectrometry (SNMS). The most widely used surface analytical techniques are summarised in Table 2.5.

Table 2.5. Advantages and limitations of XPS, AES, SIMS and SNMS: Czanderma (97).

TECHNIQUE	ADVANTAGES	DISADVANTAGES
<p>XPS .....</p>	<p>Sensitive to 2-10 monolayers; metals &lt; oxides &lt;&lt; polymers            Can detect <math>\sim 10^{-3}</math> at. %            Quantitative to <math>\sim 10</math>-20 % without standards            Especially useful for chemical shifts from same element in different compounds            Least destructive of all techniques (x-ray excitation)            Sensitivity range within factor of 10 for most atomic numbers            Minimal sample charging</p>	<p>Relatively poor lateral resolution and poor imaging capability            Requires deconvolution techniques (e.g. surface monolayer)            Has adequate data acquisition rates for compositional depth profiles; inferior to other methods</p>
<p>AES .....</p>	<p>Sensitive to 2-10 monolayers            Can detect <math>\sim 10^{-3}</math> at. %            Outstanding for compositional depth profiles            Quantitative to <math>\pm 10</math> % with standards            Superb lateral resolution (20-50 nm, or 0.6-2.0 min beam)            Fastest of four methods            Superb imaging and lateral mapping capabilities            Useful for chemical shifts for some elements</p>	<p>May alter surface composition from ESD            May have severe charging problems            Will form carbon from polymers (electron beam cracking)            Has a slow rate of element mapping</p>
<p>SIMS .....</p>	<p>Sensitive down to 1-2 monolayers            Can detect 10 ppm or less            Superb for compositional depth profiles            Can detect isotopes            Can detect hydrogen and deuterium present            Can acquire data rapidly            Has lateral imaging capability</p>	<p>Requires sample destruction            Is quantitative with difficulty, at best            Has varying elemental sensitivity            Has complex spectra            May have chemical state changes from ion bombardment</p>
<p>SNMS .....</p>	<p>Has first six advantages of SIMS            Quantitative with modest use of standards (a major improvement over SIMS)</p>	<p>Requires sample destruction            May have chemical state changes from ion bombardment</p>

## 2.5.2. FAILURE ANALYSIS

Considerable information about fracture modes and natures of failure can be obtained by examining the physical appearance of the fracture surface once a specimen or component has completely failed (96). This can be achieved by visual inspection, SEM, STEM or TEM techniques. Chemical characterisation is possible using XPS, AES, SAM (Scanning Auger Microscopy) and IR (Infra Red) microscopy (98), although analysis is complicated by surface contamination of the fracture surfaces in the period between fracture and fracture analysis, and, for example, being unable to distinguish between interfacial failure and failure entirely within the oxide layer, due to the fact that freshly exposed metal will re-oxidise immediately on fracture (99). The three fracture modes, and the three types of failure associated with adhesive joints are given in Figures 2.12. and 2.13., respectively.



**Figure 2.12.** Fracture modes: Left to right: Mode I (tensile opening or cleavage mode); Mode II (in-plane shear mode); Mode III (tearing or antiplane shear mode).



**Figure 2.13.** Types of failure: Top to bottom: Cohesive failure; adhesive failure; interfacial failure.

### 3.0. ADHESIVE SCREENING

#### The Initial Shear-Tensile and Peel Strength of Adhesive-Bonded AISI 304L Stainless Steel

#### Joints and their Subsequent Fracture Surfaces

##### *Abstract*

*Standard-single-overlap-shear tensile tests, and floating roller peel tests were conducted on AISI 304L stainless steel / adhesive joints, to discriminate between six candidate adhesives considered to be suitable for bonding metals. To study the effects of adherend surface preparation on joint performance, a number of pre-bonding treatments were considered: Alkaline Degreasing; Mechanical Roughening; Alumina Blasting; Acid Rinsing; and Acid Etching. The highest mean apparent single-overlap-shear strengths were realised by the joints bonded with epoxy adhesive systems, and the highest mean peel strengths were given by the joints bonded with a polyurethane system. There was little evidence to suggest that surface modification contributed to the mechanical performance of the bonded-steel joints, although heavy contamination on the surface of the pre-bonded adherend was shown to adversely affect joint strength.*

### 3.1. INTRODUCTION

As a result of the literature review, and considering 'adhesive-selection' software and following discussions with 3M UK plc., six candidate adhesives representing three chemical families, epoxies, acrylics, and urethanes, were considered to have the potential to bond stainless steels intended for structural applications, and a screening schedule incorporating these adhesives was devised. The primary objective of the screening program was to discriminate between the candidate adhesives in terms of the shear and peel strength performance of AISI 304L stainless steel / adhesive bonded joints. The subsequent fracture faces were also evaluated as part of the regime to assess adherend / adhesive compatibility as measured by the extent of cohesive failure achieved; the preferred candidate would have both optimum shear and peel strength, and the locus of failure would be entirely cohesive within the adhesive, which would imply that the adhesive strength between adhesive and adherend was greater than the cohesive strength of the adhesive. The apparent standard lap-shear strength and floating roller peel strength of AISI 304L stainless steel / adhesive joints were determined in accordance with BS 5350: Parts C5 and C7, respectively, in conjunction with the American equivalents, ASTM D1002-94 and ASTM D3167-93. The subsequent fracture surfaces were examined, both visually and using SEM, to ascertain the loci of failure. The cost of the adhesives and practical aspects such as ease of application were also considered as additional criteria, to find the most suitable adhesive out of those considered, for bonding stainless steels. In order to investigate the role of the adherend surface condition in enhancing joint performance, different surface pre-bonding treatments were incorporated in the schedule. The introduction of more than one adherend surface condition necessitated some degree of surface characterisation, and this was achieved using surface profilometry and SEM; the details and results of which are given in Chapter 8.0. *Surface Characterisation*.

The following account details adherend surfaces preparation, the bonding procedures, mechanical testing and fracture analysis of the failed surfaces. Any deviation from the original program, and there were several, have been, hopefully, clearly indicated and referred to.

## 3.2. EXPERIMENTAL WORK

### 3.2.1. MEASUREMENT OF THE APPARENT SHEAR STRENGTHS AND PEEL STRENGTHS OF AISI 304L ADHESIVE-BONDED JOINTS

#### 3.2.1.1. TEST MATERIAL PREPARATION AND JOINT CONFIGURATION

##### 3.2.1.1.1. STANDARD LAP SHEAR

AISI 304L stainless steel strip with a matt surface finish, designation 2B; cold-rolled to 1.5 mm, and stretch-flattened to meet the flatness tolerances in BS 5350: Pt. C5, was supplied by Avesta Sheffield AB, Shepcote Lane works. Oversized blanks were pressed from the test material and the edges along the length of the specimens milled square. The milled blanks were guillotined to approximate length and the end faces milled square to the final length. The dimensions of the single lap shear test piece are given in Figure 3.1.

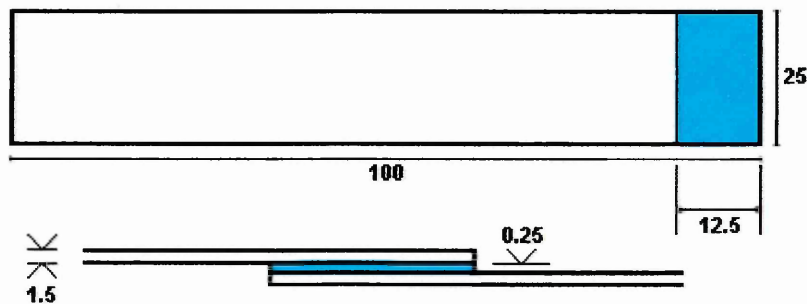


**Figure 3.1.** Standard, single overlap, shear-tensile test-piece and section through joint. All dimensions in mm.

##### 3.2.1.1.2. FLOATING ROLLER PEEL

A peel test piece consisted of a thin strip of adherend material (300 x 25 x 0.5 mm), bonded to a thicker strip of adherend material (300 x 25 x 1.5 mm). The two strips, the *flexible* adherend and the *rigid*

adherend, were bonded together along two thirds of the joint length; the remaining third was not bonded, to enable the flexible adherend to be peeled away from the rigid adherend during the test. The test material for the flexible adherend ((0.5 mm gauge with a 2B surface finish) was provided by Avesta-Sheffield AB, Avesta, Sweden. The dimensions of the test piece are given in Figure 3.2.

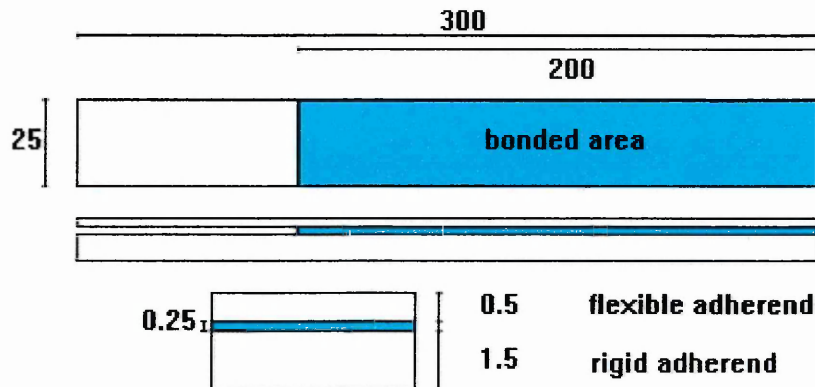


**Figure 3.2.** Floating peel roller test piece. All dimensions mm.

The first batch of test specimens were machined from pre-bonded coupons (300 x 100 mm). Two test pieces were prepared from each coupon; the test-pieces were guillotined to approximate size, away from the sides of the coupon to avoid edge effects, and then machined to the final dimensions. In addition, the coupons were held together during curing in specially constructed jigs. However, in subsequent batches, the test pieces were machined to the final dimensions prior to bonding, and the joints were held together during curing using special spring clips. The different methods are described in 3.2.1.3. *Joint Assembly* and highlighted in 3.3. *Results*.

### 3.2.1.2. SURFACE PRE-BONDING TREATMENTS

#### 3.2.1.2.1. STANDARD LAP SHEAR

The machined test pieces were de-burred, washed in hot soapy water to remove heavy contamination, such as machine oil, and then allowed to dry over night. A line was scribed on each test piece; 12.5 mm from, and parallel to, the milled end-faces. This was to mark the area to be bonded. The 216 test pieces (sufficient to make 108 lap joints) were then divided into three batches for one of the following surface pre-treatments:

**Table 3.1.** Initial pre-bonding treatments.

SURFACE TREATMENT	STAGES	
<i>ALKALINE DEGREASING</i>	STAGE I STAGE II	ALKALINE DEGREASING PRIMING
<i>MECHANICAL ROUGHENING</i>	STAGE I STAGE II STAGE III STAGE IV	ALKALINE DEGREASING MECHANICAL ROUGHENING ALKALINE DEGREASING PRIMING
<i>ACID RINSING</i>	STAGE I STAGE II STAGE IV	ALKALINE DEGREASING ACID RINSING PRIMING

**N.B.** The individual stages are described in the subsequent text.

### **3.2.1.2.1.1. THE ALKALINE DEGREASING PROCEDURE**

Samples were degreased using the surface engineering cleaning line at Sheffield Hallam University.

The procedure is given in Table 3.2.

**Table 3.2.** Alkaline degreasing procedure.

STAGE	MEDIUM	TEMPERATURE (°C)	TIME (MINUTES)	ULTRASONIC AGITATION
Preliminary degrease	Everclean™ : 2 % HT 107 A, 2 % HT 107 B, tap water	70	3	Yes
Rinse	Tap water	23	0.5	No
Secondary degrease	Bannerclean™ 16 : 0.16 %, tap water	70	3	Yes
Rinse	Tap water	23	0.5	No
Tertiary degrease	Bannerclean™ 13: 0.16%, tap water	70	3	Yes
Rinse	Tap water	23	0.5	No
Clean rinse	De-ionised water	23	3	Yes
Soak	De-ionised water	23	1	No
Dry	Hot air blast	70	10	N/A

### 3.2.1.2.1.2. MECHANICAL ROUGHENING

In order to evaluate and compare two different surface-roughening procedures simultaneously, the batch of test-pieces allocated for *Mechanical Roughening* was further divided: one half of the test pieces were blasted with alumina particles, and the other half abraded manually with Scotchbrite™, supplied by 3M UK plc. Adherends subjected to alumina blasting were bonded to adherends which had been abraded with Scotchbrite to make thirty-six *Mechanically Roughened* hybrid joints, i.e. one half of the lap joint being *Alumina Blasted* and the other *Scotchbrite Abraded*.

### 3.2.1.2.1.2.1. ALUMINA BLASTING

Thirty-six *Alkaline Degreased* test pieces were prepared; each test piece was masked below the scribed line, so only the bond area was exposed, and then blasted with in a jet of high purity alumina for several seconds.

**Table 3.3** Grit blasting parameters.

<b>Blast medium:</b>	High purity aluminium oxide (99.99%) BS 871
<b>Blast pressure:</b>	5 Kg cm <sup>-2</sup>
<b>Blast distance:</b>	300 mm
<b>Blast angle:</b>	0 °
<b>Blast duration:</b>	30 seconds

### 3.2.1.2.1.2.2. SCOTCHBRITE ABRADING

The bond areas of thirty-six *Alkaline Degreased* test pieces were roughened with Scotchbrite, in a direction parallel to the milled end-face (perpendicular to the tensile-axis), for a few minutes to uniformly abrade the bond area.

### 3.2.1.2.1.3. ACID RINSING

Seventy-two *Alkaline Degreased* test-pieces (sufficient for thirty six joints) were rinsed in hydrochloric acid solution at room temperature for several minutes. The test pieces were then rinsed in agitated de-ionised water to remove the acid residue, and finally dried by a hot air blast.

**Table 3.4.** Acid rinsing procedure.

<b>Bath composition:</b>	50 % by vol. HCl solution (S.G. 1.6) bal. de-ionised water
<b>Bath conditions:</b>	23 °C for 30 min. (ultrasonically agitated)

#### **3.2.1.2.1.4. PRIMING**

Since it is realistic to assume that primers would always be used in practical situations, all the substrates were primed following the pre-bonding treatments, unless otherwise specified. The primer chosen is commercially available, "off the shelf", from 3M UK plc and has been used successfully in adhesive bonded metallic applications. The silane based primer (3901) was supplied suspended in methanol, and it was simply applied with a clean lint-free cloth. The methanol evaporated from the steel surface within a few seconds, leaving behind a residue of primer, visible to the naked eye. The treated substrates were then wrapped in clean, dry cloth and stored overnight in a desiccator to allow the primer to dry completely. After 24 hours, the test pieces were wiped repeatedly with an acetone wetted cloth to remove the excess primer, they were then dried and stored in a desiccator, ready to be bonded. The primed surfaces were bonded within 4 days of priming.

#### **3.2.1.2.2. FLOATING ROLLER PEEL**

Three pre-bonding treatments were employed in the peel tests: *Alkaline Degreasing*, as for the lap shear evaluation; *Alumina Blasting*, to replace the hybrid mechanical treatment used in the lap shear tests; and *Acid Etching*, to produce a macro-rough surface by chemical means, instead of by mechanical roughening. *Mechanical roughening* was replaced by *Alumina Blasting* because in hind sight it was considered bad practice to attempt to evaluate two surface conditions simultaneously, and *Acid Rinsing* was subsequently replaced by *Acid Etching* in order to produce a chemically roughened surface of comparable roughness to those surfaces physically roughened by blasting with alumina.

**Table 3.5.** Pre-bonding treatments.

<i>ALKALINE DEGREASING</i>	STAGE I STAGE II	ALKALINE DEGREASING PRIMING
<i>ALUMINA BLASTING</i>	STAGE I STAGE II STAGE III STAGE IV	ALKALINE DEGREASING ALUMINA BLASTING ALKALINE DEGREASING PRIMING
<i>ACID ETCHING</i>	STAGE I STAGE II STAGE III STAGE IV	ALKALINE DEGREASING ACID ETCHING DE-SMUTTING PRIMING

**N.B.** The individual stages are described in the subsequent text.

### 3.2.1.2.2.1. ACID ETCHING

#### (i) The Etching Procedure

**Table 3.6.** Acid etching procedure.

<b>Bath composition:</b>	30 % by vol. H <sub>2</sub> SO <sub>4</sub> (S.G. 1.85) bal. de-ionised water
<b>Bath conditions:</b>	80 °C for 5 min. (UT agitated)

Etching austenitic stainless steel in sulphuric acid under such conditions results in the formation of a black, velvety, iron oxide on the steel surface, referred to as smut. The smut is so weakly adhered to the surface that it is easily removed by wire brushing and is even easier to remove by chemical means. Thus, a de-smutting stage was introduced to remove the smut.

**(ii) The De-smutting Procedure**

**Table 3.7.** The de-smutting procedure.

<b>Bath composition:</b>	12 % by vol. H <sub>2</sub> SO <sub>4</sub> (S.G. 1.85) 2 % by volume K <sub>2</sub> Cr <sub>2</sub> O <sub>7</sub> bal. de-ionised water
<b>Bath conditions:</b>	80°C for 5 min. (UT agitated)

**3.2.1.3. JOINT ASSEMBLY**

**3.2.1.3.1. STANDARD LAP SHEAR**

The joints were assembled in purpose-built jigs to ensure accurate joint alignment along the length and width of the joints, and to maintain an overlap of 12.5 mm, marked by the scribed line referred to in 3.2.1.2. *Surface Preparation Treatments.* Mild steel weights were used to apply a nominal pressure to the curing joints; each weight (~1 Kg ) applied a uniform pressure of 1.6 g mm<sup>-2</sup> to two adjacent joints. Silicon-waxed, release paper was placed between the jigs and the curing joints, and between the curing joints and the mild steel weights; this facilitated easy removal of the cured joints.

**3.2.1.3.1.1. BONDLINE CONTROL**

The thickness of the adhesive, the bondline, was maintained at 0.25 mm. This was achieved by sprinkling tiny glass balls (ballotini), to act as spacers, into the adhesive immediately after its application to the joints. The diameter of the ballotini varied, although the maximum diameter was 0.25 mm, and this was exactly the thickness of the desired bondline. To isolate the larger 0.25 mm diameter balls, approximately 15% by weight of the total, the ballotini were sieved through a 210 μ ( No. 72) sieve.

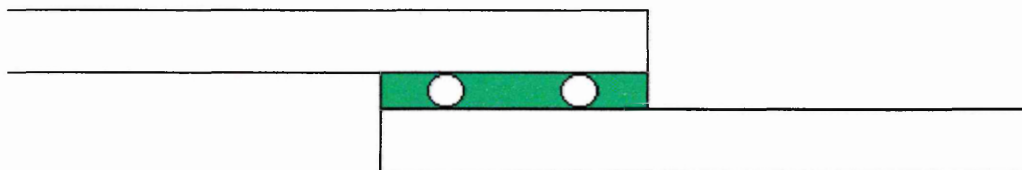


**Figure 3.3.** 0.25 mm diameter ballotini spacers.

The 0.25 mm ballotini were applied using a small spatula containing a conical indentation stamped in one end. The spatula was first wiped dry with tissue paper, then dipped into the ballotini, removed, and then shaken to remove any excess, before adding the ballotini to the newly applied adhesive. In order to evaluate the repeatability of this method, 20 samples were taken using the spatula, and alternately examined under an optical microscope: the average number of balls / sample was found to be 10.45; the median 10.5; the mode 10; and the range, 6 to 14. This was considered reasonable since even if 20 balls were delivered to the adhesive, the volume of the joint occupied by the ballotini, would still be only 0.2% of the total volume of the joint, and thus, not adversely effect the bond performance.

This method of controlling the bondline was used for the first sequence of tests, however for subsequent tests, a different method was employed; two, three millimeter lengths of steel wire, 0.25 mm diameter (No. 06 guitar string), were placed in each joint. The wires were positioned parallel to the joint length (tensile axis), at mid-overlap length, and at one quarter and three quarters of the overlap width, respectively.

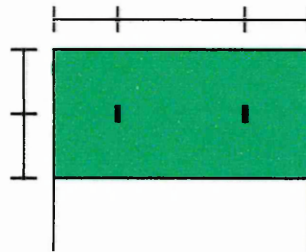
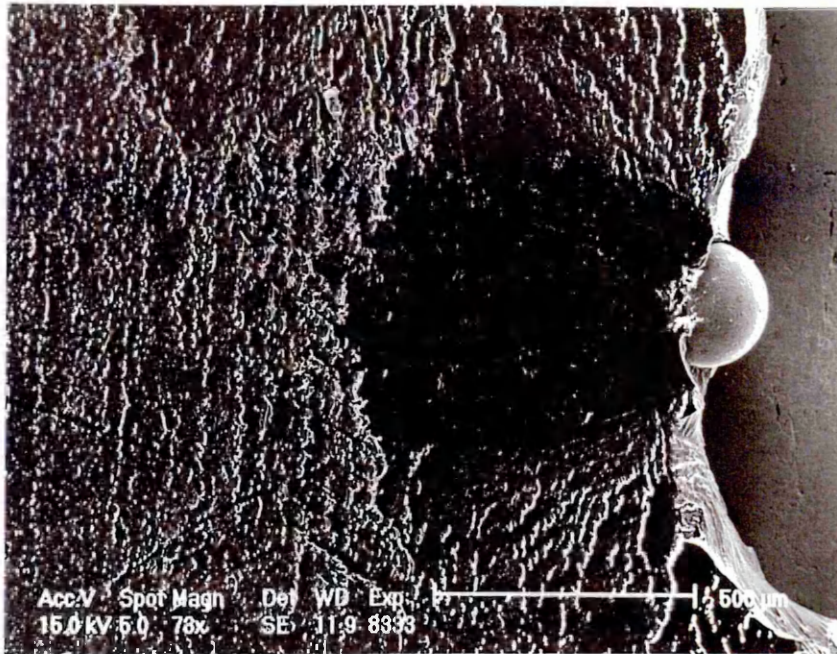


**Figure 3.4.** Position of wire spacers.

The problem with the glass ballotini was sticking ; be it due to surface tension, static charge, or because of the presence of moisture, the ballotini were difficult to separate from one another, and this resulted in clumps of unevenly distributed ballotini, which could have led to inconsistent bondlines. There also appeared to be a degree of incompatibility between the ballotini and the adhesive; SEM revealed evidence of stressing in the adhesive in areas adjacent to ballotini, possible due to the adhesive contracting around the ballotini as it cured; this effect is shown in Plate 3.1. There were no such problems experienced with the steel wire. Bryant *et al* (100,101), have used steel wire without it adversely affecting bond strength.



SEM micrograph showing evidence of stressing in DP 490 adhesive due to ballotini.

### 3.2.1.3.2. FLOATING ROLLER PEEL

#### 3.2.1.3.2.1. METHOD I

The first batch of test-specimens were machined from pre-bonded coupons (300 x 100 mm), see Figure 3.5. Two test-pieces were produced per test-coupon. Piano wire, 0.25 mm diameter was situated in the coupons at positions A, B, and C, in order to control the bondline. The un-bonded section of the test coupon was protected by masking the area using three layers of 0.8 mm thick P.T.F.E. strip (D).

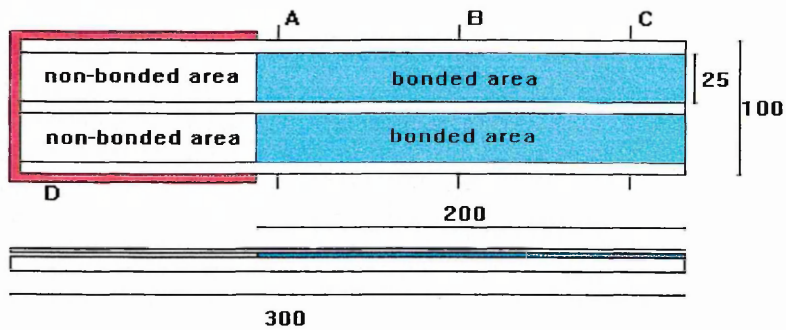
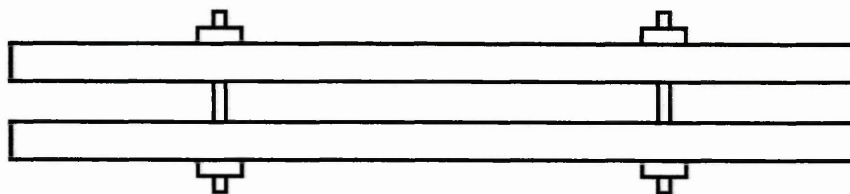


Figure 3.5. Method I test coupon. Dimensions mm.

Jigs were constructed to hold the test-coupons together during curing, see Figure 3.6. Silicon release paper was placed between the coupons and the jigs to facilitate easy removal after curing. The loaded jigs were hand-tightened to apply sufficient pressure to hold the test-coupons together.



**Figure 3.6.** Jigs used in assembly Method I.

### 3.2.1.3.2.2. METHOD II

The remaining test-specimens were machined to the final dimension prior to bonding. The reason for the change in procedure was financial, although Method II did prove to be the simplest and quickest procedure. In Method II, small, steel spring-clips were employed to hold the curing joints together, see Figure 3.7. The clips were delivered by a device called the Superclip 40, which was the tool provided to position the spring-clips; it opened the jaws of the clip to enable it to be positioned. As with Method I, Method II used 0.25 mm piano wire and silicon release paper to control the bondline and facilitate easy removal of the cured joints, respectively. The joints bonded using Methods I and II are highlighted in 3.3. *Results* section.

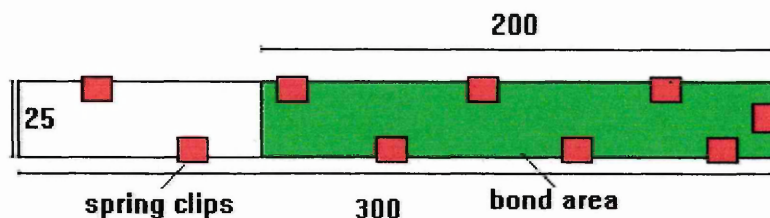


**Figure 3.7.** Bonded peel test-piece (Method II) held together by spring-clips during curing.

### 3.2.1.4. ADHESIVES APPLICATION AND CURING PROCEDURES

The candidate adhesives and their curing requirements are listed in Table 3.8.

**Table 3.8.** The candidate adhesives and their curing requirements.

ADHESIVE	CURING REQUIREMENT
<b>DP 460:</b> Two-component, cold-cure epoxy	7 days at 23 °C
<b>DP 490:</b> Two-component, cold-cure epoxy	7 days at 23 °C
<b>9323 B/A:</b> Two-component, cold-cure epoxy	5 days at 23 °C
<b>7823 S:</b> One-component, heat-cure epoxy	40 minutes at 180 °C
<b>3532 B/A:</b> Two-component, cold-cure polyurethane	2 days at 23 °C
<b>DP 801:</b> Two-component, cold-cure modified acrylic	30 minutes at 23 °C

#### 3.2.1.4.1. ADHESIVE APPLICATION AND WORKING LIFE

Both the DP 460 and DP 490 epoxies, were supplied in Duo-Pak's, double-tube cartridges, incorporating the adhesive and the hardener. The adhesives were applied using a special gun applicator which forces the two components, in the correct proportions, through a pre-mixing nozzle attached to the cartridge (3M EPX applicator). For both the 9323 B/A epoxy and 3532 B/A polyurethane two-component, cold-cure adhesives, the two components were supplied separately and thus, manual mixing, by weight, in the correct proportions was necessary: 100 A : 101 B and 27 A : 100 B for the two adhesives, respectively. In each case, the adhesive was applied to each joint in excess of the theoretical volume required, 80.65 mm<sup>3</sup> (25.4 mm x 12.7 mm x 0.25 mm). Thus, as the joints were closed the excess adhesive was squeezed out, and this ensured that the required volume was delivered to each joint. It is important to remember at this point, that this 'squeeze-out', as it is known, was allowed to cure and not removed at any stage, and thus, the joints were mechanically tested with the hardened squeeze-out intact.

The epoxy adhesives DP 490, 9323 B/A, and 7823 S were sufficiently fluid to allow easy spreading, but were viscous enough to be retained within the required volume, and to resist sagging during the curing cycle. The DP 460 adhesive was much less viscous, and consequently more difficult to apply successfully; a number of the bondline dimensions were observed to be less than the desired 0.25 mm, as a result of adhesive escaping from the joint. The polyurethane adhesive 3532 B/A was difficult to apply, because of the low work life of this adhesives: the adhesive began to harden approximately 5 minutes after mixing, which meant that small amounts of the adhesive had to be mixed at regular intervals.

The modified acrylic EP 801 was so difficult to work with that this adhesive system was omitted from the screening program at an early stage; the adhesive was beginning to harden too quickly to allow satisfactory application of the adhesive.

#### **3.2.1.4.2. CURING**

After bonding, the cold-curing adhesives were allowed to stand overnight, before being stacked and stored for the appropriate time, until they were fully cured. The ambient temperature and relative humidity were recorded continuously throughout the application procedure and the curing cycle of the adhesives. The ambient temperature and relative humidity ranged from 19 °C to 25 °C and 40 to 60 %, respectively. For adhesives cured at the lower end of the temperature range, 19 °C, the curing period was extended to 10 days, to ensure complete curing. The heat-cured epoxy, 7323 S, was cured in a pre-heated oven. The mild steel weights for applying the nominal pressure, referred to in 3.2.1.3. *Joint Assembly*, were also pre-heated to minimize the re-heating time in the oven, once the joints had been loaded. The cured adhesive joints were all tested within 4 days of finishing the curing cycle, i.e. tested 10 to 14 days after assembly.

N.B. When closing the joints just prior to curing excess adhesive was squeezed out, and this so-called 'squeeze-out' was left in position, allowed to cure, and the joints were subsequently tested with these squeeze-out fillets intact. However, it was suspected that the un-removed fillets may have contributed to the joint strength, and thus, in subsequent bonding the hardened fillets were removed prior to

mechanical testing. The joints tested with the fillets intact and those tested with the fillets removed are clearly indicated in the results.

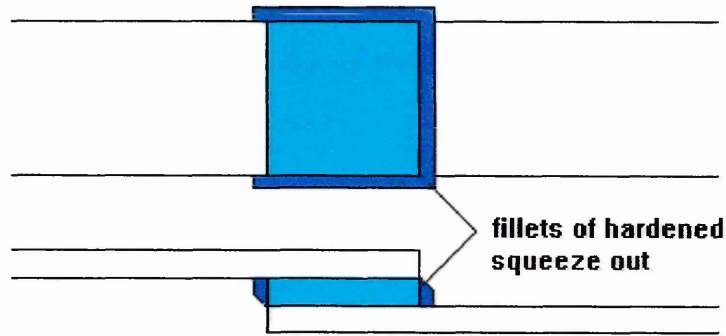


**Figure 3.8.** Squeeze cut occurring during joint assembly.

### 3.2.1.4.3 COST OF ADHESIVES

**Table 3.9.** Cost of the six candidate adhesives. Price list supplied by 3M UK plc, August 1997.

ADHESIVE SYSTEM	SMALLER SIZE		LARGER SIZE	
	UNIT COST	~ COST PER LITRE	UNIT COST	~ COST PER LITRE
DP 460 Epoxy	£11.62 / 37 ml	£314	£54.70 / 400 ml	£138
DP 490 Epoxy	£11.62 / 37 ml	£314	£52.71 / 400 ml	£132
9323 Epoxy	£56.50 / 1	£57	£1092.62 / 20 l	£55
7823 Epoxy (heat cured)	£31.47 / 150 ml	£210	£1286.49 / 20 l	£64
3532 Polyurethane	£15.81 / 113 ml	£139	-	-
DP 801 Acrylic	£9.92 / 50 ml	£198	-	-

The most expensive adhesives are the DP 460 and DP 490 systems, particularly in the smaller sizes at almost £12 for 37 ml. The heat-cured epoxy (7823) costs about the same as the acrylic system (DP 801) at around £200 per litre; although the latter is only available in the smaller size, as is the polyurethane, which is moderately priced at just below £140 per litre. The most economical, however, is the 9323

epoxy system, which is by far the cheapest and there is little difference in the 'costs per litre' between the two quantities, at round £60 per litre.

### **3.2.1.5. MECHANICAL TESTING**

Single lap-shear tests were conducted in accordance with BS 5350: Part C5 (ASTM D1002-94). The specification states that a strain rate shall be adopted such that the joint is broken in a period of  $65 \pm 20$  seconds. However, this is impossible if comparisons between adhesives are to be made, since this would entail varying the cross-head speed for different adhesives to satisfy the above criteria. Thus, after initial trials a test rate of  $1.5 \text{ mm min}^{-1}$  was considered most appropriate. Temperature and relative humidity were recorded at the times of the tests. The results of the single lap-shear tests are given in *3.3. Results*.

Floating roller peel tests were conducted in accordance with BS 5350: Part C7 (ASTM D3167-93). The test were carried out at the 3M Technical Centre in Bracknell, using a Instron hydraulic test machine. The rate of the tests used was  $150 \text{ mm min}^{-1}$ . The results of the floating roller peel tests are given in *3.3. Results*.

#### **3.2.1.5.1. TREATMENT OF RAW DATA**

Mean apparent overlap shear strengths were obtained from a sample size of 6. A normal distribution was assumed and the standard deviation calculated. Accuracy was to  $\pm 1$  standard deviation, and the degree of scatter was monitored by calculating the coefficient of variation; the standard deviation as a percentage of the mean.

Mean peel strengths were estimated by bisecting the peel curve (as shown in Figure 3.9.) and also by taking the average of 20 readings of peel load at positions equally spaced along the peel length.

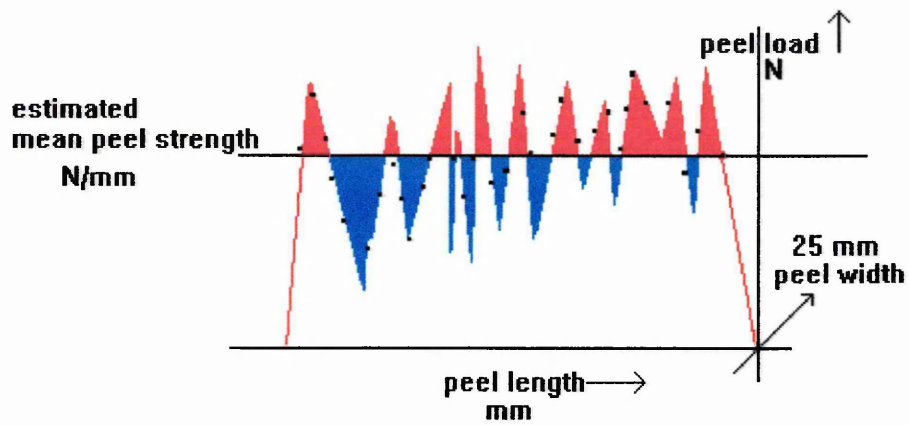


Figure 3.9. Typical Peel Curve.

### 3.2.2. FRACTURE ANALYSIS

The surfaces of the failed joints were evaluated physically to ascertain the type of failure, be it cohesive, adhesive or interfacial, and in addition, to identify the failure mechanism, be it Mode I, II, III or mixed mode. The physical evaluation was carried out by visual inspection and using scanning electron microscopy. The results of the fracture analysis are given in 3.3. *Results*.

### **3.3. RESULTS**

#### **3.3.1. APPARENT SHEAR STRENGTHS OF ADHESIVE BONDED AISI 304L STAINLESS STEEL JOINTS**

The results of the lap shear tests are given in Tables 3.10. and 3.11., and represented graphically in Figures 3.10 and 3.11. Table 3.10. (Figure 3.10.) detail the mean apparent shear strength of the original adhesive / adherend joint combinations, tested with the fillets un-removed, and Table 3.11. (Figure 3.11.) detail the mean apparent shear strength of the adhesive / adherend joint combinations, tested with the fillets removed. Figure 3.12. compares the mean apparent shear strength of joints, tested with the fillets un-removed, and tested with the fillets removed.

**Table 3.10.** Initial overlap shear strengths of AISI 304 L / adhesive joints with the fillets un-removed prior to testing.

ADHESIVE SYSTEM	ADHEREND SURFACE CONDITION	MEAN FAILURE LOAD (kN)	S.D. (kN)	MEAN APPARENT SHEAR STRENGTH (N.mm <sup>-2</sup> )	S.D. (N.mm <sup>-2</sup> )	COEFFT. OF VARIATION $\frac{S.D.}{\bar{x}} \times 100$ (%)
DP 460	<i>Alkaline Degreased</i>	9.5	0.7	30.3	2.3	7.6
	<i>Mechanical Roughened</i>	9.4	0.7	30.2	2.3	7.5
	<i>Acid Rinsed</i>	9.8	0.8	31.5	2.6	8.1
DP 490	<i>Alkaline Degreased</i>	8.0	0.3	25.6	1.0	3.8
	<i>Mechanical Roughened</i>	8.2	0.3	26.2	0.9	3.4
	<i>Acid Rinsed</i>	8.7	1.1	27.7	3.4	12.2
9323 B/A	<i>Alkaline Degreased</i>	7.8	1.6	24.9	5.0	20.1
	<i>Mechanical Roughened</i>	8.8	0.4	28.0	1.3	4.8
	<i>Acid Rinsed</i>	8.9	0.8	28.5	2.5	8.8
7823 S	<i>Alkaline Degreased</i>	7.4	0.8	23.8	2.6	10.8
	<i>Mechanical Roughened</i>	7.0	0.6	22.3	1.8	8.1
	<i>Acid Rinsed</i>	8.0	0.4	25.6	1.3	4.9
3532 B/A	<i>Alkaline Degreased</i>	3.8	1.0	12.2	3.2	25.8
	<i>Mechanical Roughened</i>	4.1	0.3	13.1	0.9	7.1
	<i>Acid Rinsed</i>	4.4	0.4	14.1	1.2	8.2

**Table 3.11.** Initial overlap shear strengths of AISI 304 L / DP 490 epoxy joints with fillets removed prior to testing.

DP 490	<i>Alkaline Degreased</i>	6.1	0.8	19.4	2.4	12.4
	<i>Alumina Blasted</i>	7.7	0.7	24.6	2.2	9.0
	<i>Acid Etched</i>	7.7	0.4	24.7	1.3	5.4

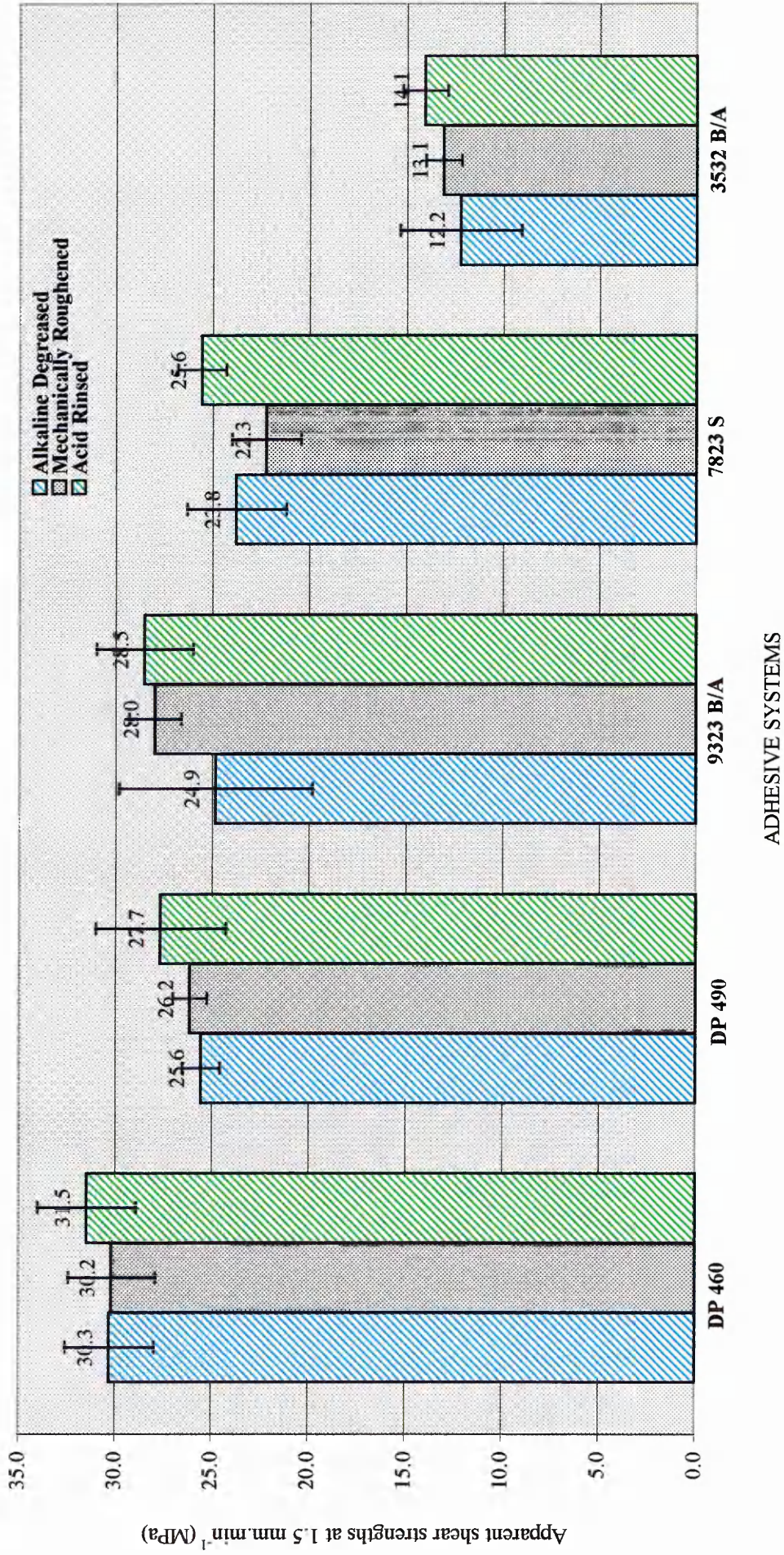
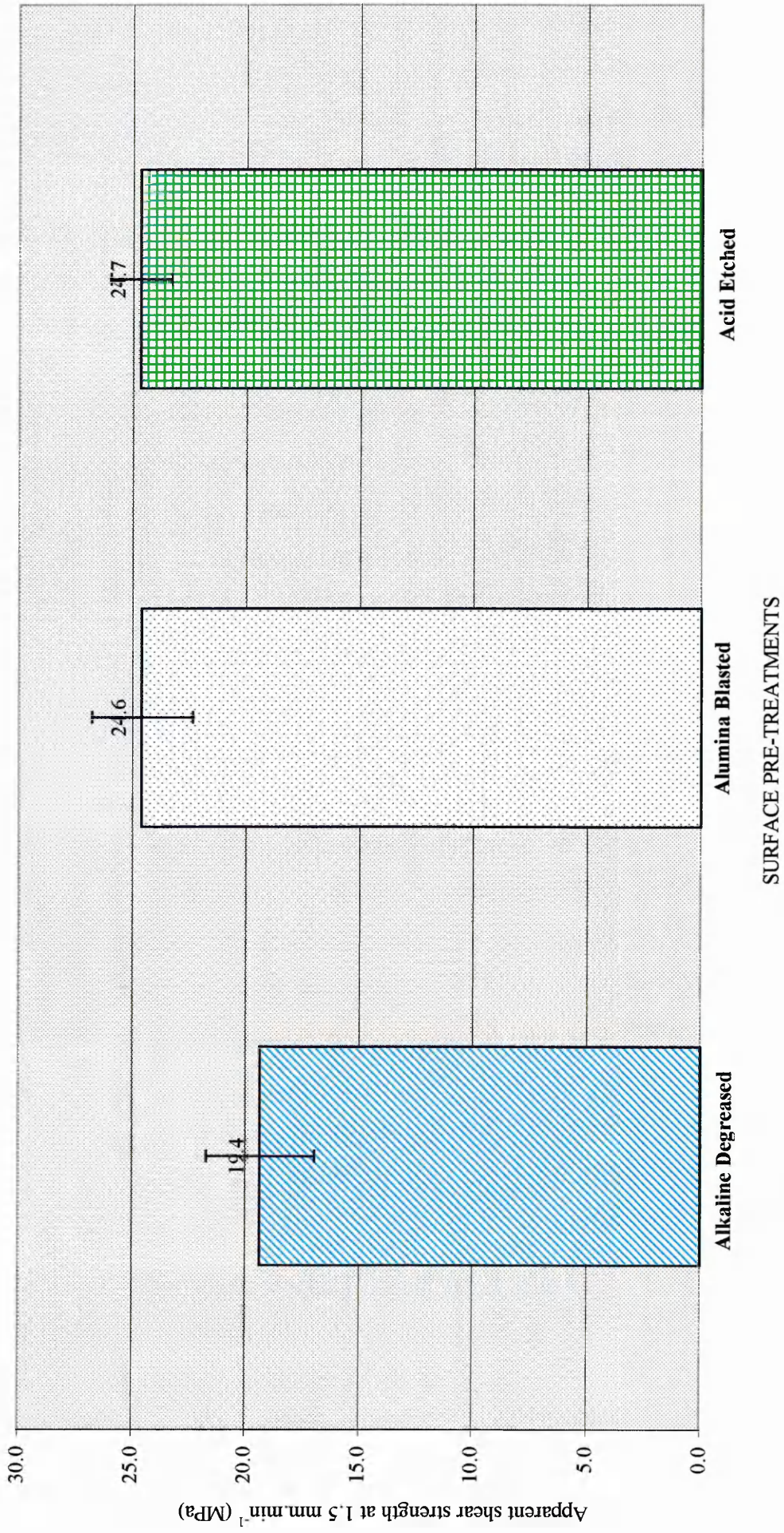


Figure 3.10. Initial lap shear strengths of AISI 304L stainless steel adhesive joints (fillets un-removed).



**Figure 3.11.** Initial lap shear strengths of AISI 304L stainless steel / DP 490 epoxy joints (fillets removed).

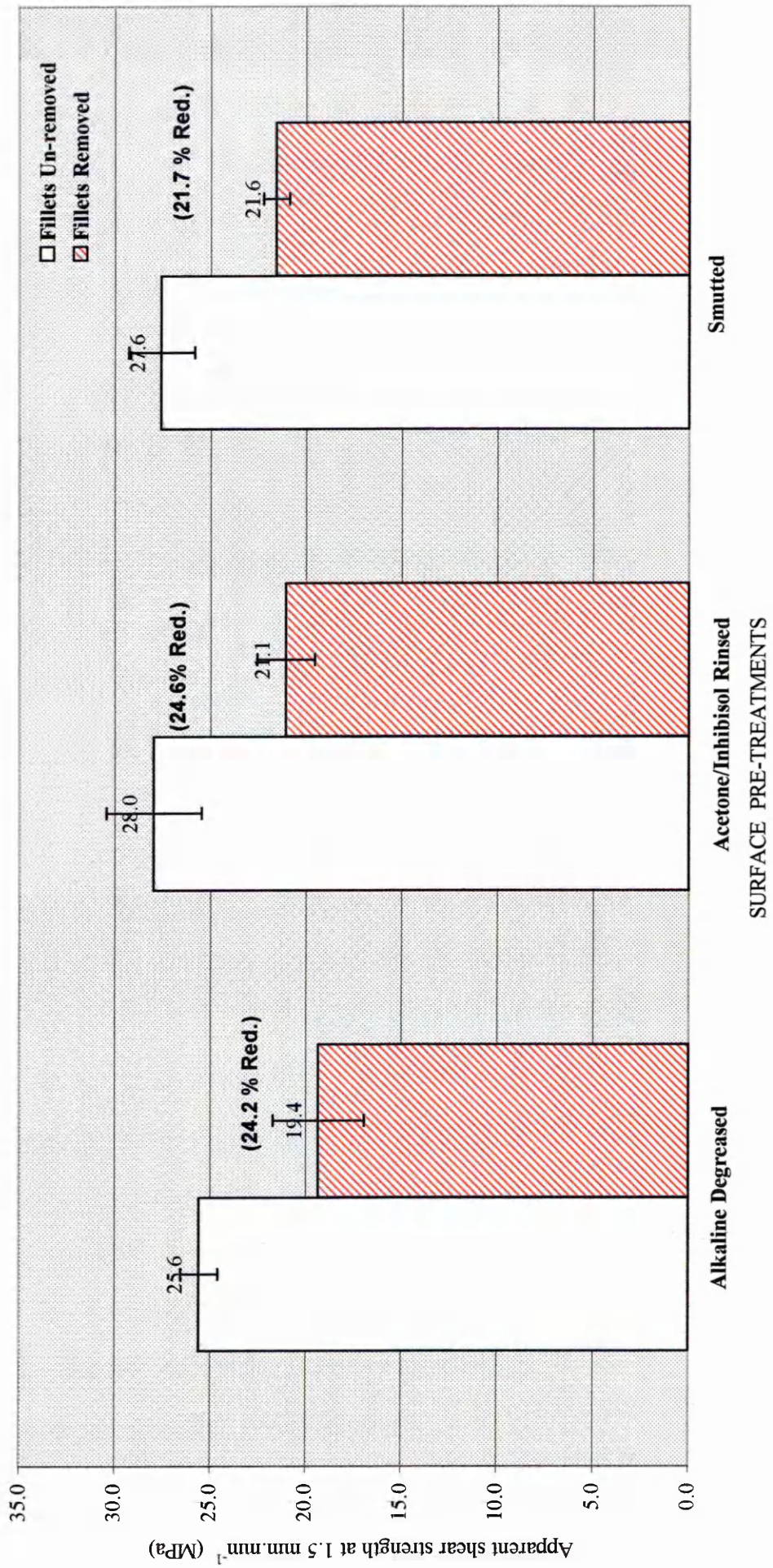


Figure 3.12. Effect of removing adhesive fillets on lap-shear strength.

**Considering Table 3.10. and Figure 3.10.**

The best performance in terms of mean apparent shear strength came from those joints bonded with the two-part, cold-cure epoxy system DP 460; the mean strength of the joints incorporating the *Alkaline Degreased* adherends and the *Mechanically Roughened* adherends was essentially the same at 30.3 ( $\pm 1$  standard deviation,  $\pm 2.3$ ) MPa and 30.2 ( $\pm 2.3$ ) MPa, respectively. The joint incorporating the *Acid Rinsed* adherends performed only slightly better at 31.5 ( $\pm 2.6$ ) MPa.

The joints bonded with the two-part, cold-cure epoxy system DP 490 performed well in the tests. The mean apparent shear strength of the joints incorporating the *Alkaline Degreased*, and the *Mechanically Roughened* adherends were similar at 25.6 ( $\pm 1.0$ ) MPa and 26.2 ( $\pm 0.9$ ) MPa, respectively. The joints incorporating the *Acid Rinsed* adherends performed slightly better at 27.7 ( $\pm 3.4$ ) MPa, although this result was marred by the extent of the scatter displayed by these joints (c.o.v. 12.2 %).

The joints bonded with the two-part, cold-cure epoxy system 9323 B/A also performed well in the tests. The mean strengths of the joints incorporating the *Mechanically Roughened* adherends and the *Acid Rinsed* adherends were similar at 28.0 ( $\pm 1.3$ ) MPa and 28.5 ( $\pm 2.5$ ) MPa, respectively. The joints incorporating the *Alkaline Degreased* adherends gave a much poorer performance at 24.9 ( $\pm 5.00$ ) MPa, and further more this result was marred by the degree of scatter displayed by these joints (c.o.v. 20.1 %).

The heat cured system 7323 performed least well out of the epoxies considered. The joints incorporating the *Acid Rinsed* adherends gave the highest mean strength at 25.6 ( $\pm 1.3$ ) MPa. The joints including the *Alkaline Degreased* surfaces gave a slightly lower mean strength at 23.8 ( $\pm 2.6$ ) MPa. However, the poorest performance was displayed by the joints with the *Mechanically Roughened* adherends at 22.3 ( $\pm 1.8$ ) MPa.

The poorest performance came from those joints bonded with the two-part, cold-cure polyurethane system 3532 B/A; 12.2 ( $\pm 3.2$ ) MPa, 13.1 ( $\pm 0.9$ ) MPa, and 14.1 ( $\pm 1.2$ ) MPa for those joints

incorporating the *Alkaline Degreased*, *Mechanically Roughened*, and *Acid Rinsed* adherends, respectively. Although a slight improvement was observed, the improvement was small, and the result was marred by the degree of scatter displayed by the joints incorporating the *Alkaline Degreased* adherends (c.o.v. 25.8 %).

Overall, the joints incorporating the adherends subjected to *Acid Rinsing* gave the highest mean shear strength, and generally, the lowest mean shear strength came from those joints including the *Alkaline Degreased* adherends; with two exceptions. The mean shear strength of the joints bonded with DP 460 were essentially the same for joints including the *Alkaline Degreased* and the *Mechanically Roughened* adherends, 30.3 ( $\pm 2.3$ ) MPa and 30.2 ( $\pm 2.3$ ), respectively. For the joints bonded using the heat cured system, 7323, the joints with the *Mechanical Roughened* adherends gave the lowest mean shear strength at 22.3 ( $\pm 1.8$ ) MPa.

**Considering Table 3.11. and Figure 3.11.**

For those joints tested with the fillets removed prior to testing, the joints incorporating the *Alumina Blasted* and the *Acid Etched* adherends performed best at 24.6 ( $\pm 2.2$ ) MPa and 24.7 ( $\pm 1.3$ ) MPa, respectively. However, the joints incorporating the *Alkaline Degreased* adherends gave a relatively poor mean strength at 19.4 ( $\pm 2.4$ ) MPa and displayed the highest degree of scatter at 12.4 %. The joints containing the *Acid Rinsed* adherends gave the least degree of scatter at 5.4 %.

The effect of removing the fillets prior to testing can be seen from Tables 3.10. and 3.11. and Figure 3.12. The mean shear strength of the joints bonded with DP 490 and incorporating the *Alkaline Degreased* adherends decreased by  $\sim 24$  %, from 25.6 ( $\pm 1.0$ ) MPa to 19.4 ( $\pm 2.4$ ) MPa, when the fillets were removed. This reduction in strength was accompanied by an increase in the degree of scatter; c.o.v 3.8 % for the joints tested with fillets un-removed, compared with 12.4 % for the joints tested with the fillets removed. This is shown clearly in Figure 3.12., together with two other examples which show similar reductions in mean shear strength as a result of removing the fillets prior to testing. Joints incorporating *Acetone / Inhibisol Rinsed* adherends showed a reduction of  $\sim 25$  % in shear strength, 28.0 ( $\pm 2.5$ ) MPa to 21.1 ( $\pm 1.5$ ) MPa. The joints incorporating *Smuted* adherends showed a reduction

of ~ 22 % in shear strength; 27.6 ( $\pm$  1.7) MPa to 21.6 ( $\pm$  0.7) MPa. *Acetone / Inhibisol Rinsing* and *Smutting* are detailed in Section 4.2.1.2. *Surface Pre-bonding Treatments*.

N.B. Although there were differences in the adherend surface conditions referred to as *Mechanically Roughened* and *Alumina Blasted*, both were induced by physical roughening of the substrate surface, and thus, some degree of comparison was thought justified. The mean strength of the joints incorporating *Alumina Blasted* adherends, when tested with the fillets removed, was only 6 % less than that of the joints incorporating *Mechanically Roughened* adherends, tested with the fillets un-removed, 24.6 ( $\pm$  2.2) MPa and 26.2 ( $\pm$  0.9) MPa, respectively. However, the degree of scatter was better for the joints tested with the fillets un-removed; c.o.v. 3.4 % compared with c.o.v. 9.0 %, respectively.

In addition, the mean shear strength of the joints tested with the fillets removed, incorporating *Alumina Blasted* and *Acid Etched* adherends, were both comparable with the mean shear strength of the joints incorporating the *Alkaline Degreased* adherends, but tested with the fillets un-removed; 24.6 ( $\pm$  2.2) MPa and 24.7 ( $\pm$  1.3) MPa, respectively, compared with 25.6 ( $\pm$  1.0) MPa. This was a considerable achievement considering these joints were tested with the fillets removed, and therefore in a weakened state.

### **3.3.2 FLOATING ROLLER PEEL STRENGTHS OF ADHESIVE-BONDED AISI 304L STAINLESS STEEL JOINTS**

The results of the floating roller peel tests are given in Tables 3.12. and 3.13. and represented graphically in Figures 3.13. and 3.14.

The first batch of peel test specimens to be assembled comprised three adhesives and three adherend surface conditions; two epoxy systems DP 460 and DP 490 and the urethane system 3532 were used to bond joints incorporating *Alkaline Degreased*, *Alumina Blasted* and *Acid Etched* adherends. These joints were machined to final dimensions from pre-bonded coupons and were held together using special jigs during curing, as described in 3.2.1.3.2.1. *Floating Roller Peel: Method I*. Identified in Tables

**Table 3.12.** Floating roller peel strengths of stainless steel / adhesive joints.

ADHESIVE SYSTEM	ADHEREND SURFACE CONDITION	ASSEMBLY PROCEDURE	PEEL LENGTH (mm)	PEEL LOAD (N)			MEAN PEEL STRENGTH (N.mm <sup>-1</sup> )	S.D. (N.mm <sup>-1</sup> )	COEFF. OF VARIATION (%)
				MIN.	MAX.	MEAN			
DP 460	<i>Alkaline Degreased</i>	Method I	380	28	185	62.3	2.5	0.9	36.6
	<i>Alumina Blasted</i>	Method I	380	85	165	112.5	4.5	0.5	12.0
	<i>Acid Etched</i>	Method I	360	153	248	184.0	7.4	0.9	12.5
DP 490	<i>Alkaline Degreased</i>	Method I	380	66	205	102.0	4.1	1.1	25.7
	<i>Alumina Blasted</i>	Method I	400	35	182	136.8	5.5	1.2	22.1
	<i>Acid Etched</i>	Method I	380	70	193	136.0	5.4	1.0	18.5
9323 B/A	<i>Alkaline Degreased</i>	Method II	160	77	120	94.0	3.8	0.3	9.2
7823 S	<i>Alkaline Degreased</i>	Method II	160	67	100	81.5	3.3	0.3	8.5
3532 B/A	<i>Alkaline Degreased</i>	Method I	380	178	359	300.8	12.0	1.3	11.2
	<i>Alumina Blasted</i>	Method I	280	260	424	351.8	14.1	1.4	10.00
	<i>Acid Etched</i>	Method I	380	170	327	264.5	10.6	1.3	12.1

**Table 3.13.** Floating roller peel strengths of stainless steel / DP 490 epoxy joints, comparing curing fixtures, clips and jigs.

DP 490	<i>Alkaline Degreased</i>	Method I	380	66	205	102.0	4.1	1.1	25.7
		(from Table 3.12.)							
		Method II	160	62.5	91.5	76.4	3.1	0.3	8.3
		Method III	160	65.5	84	73.8	3.0	0.2	6.2

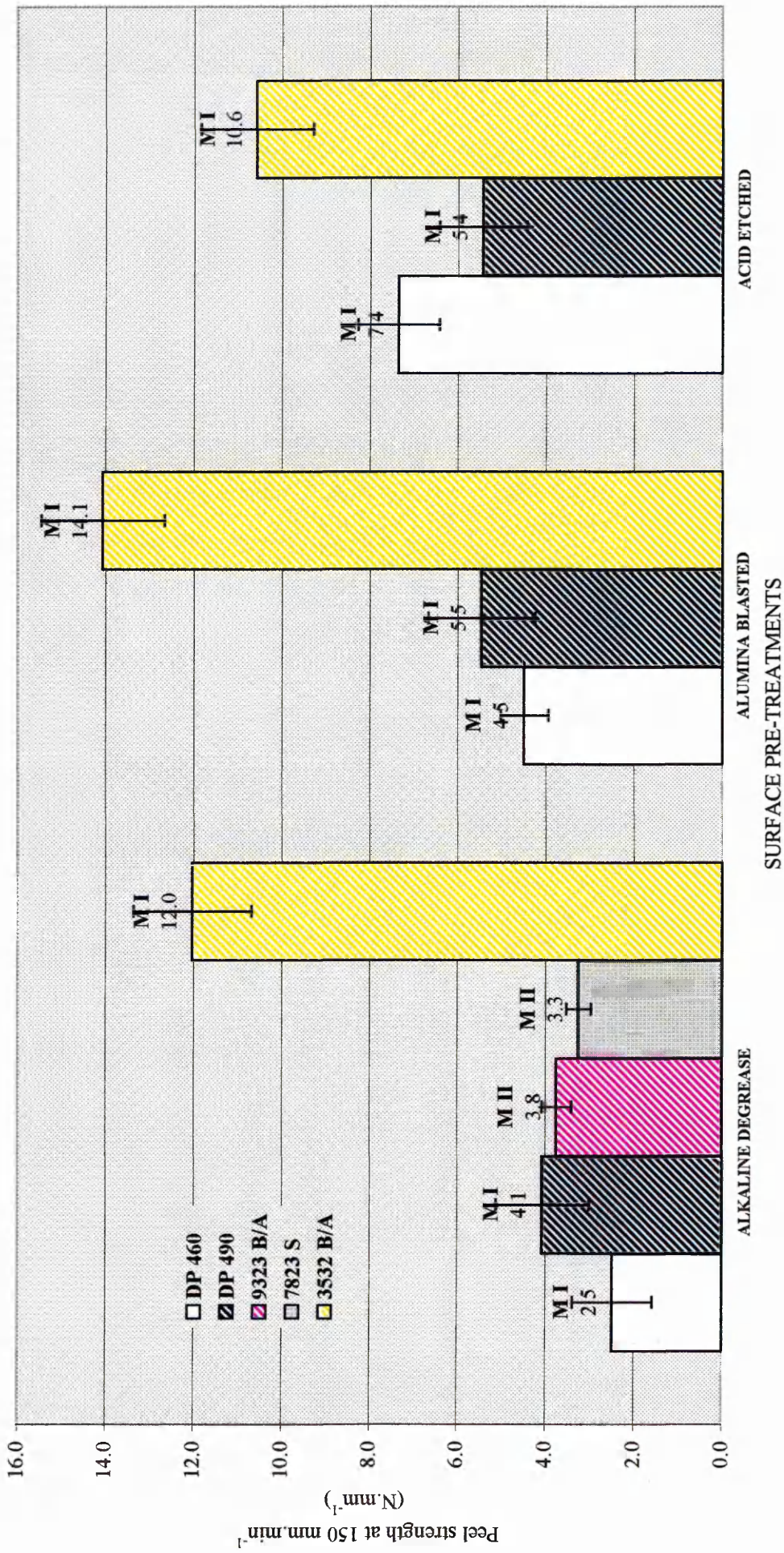


Figure 3.13. Floating roller peel strengths of AISI 304 L stainless steel / adhesive joints.

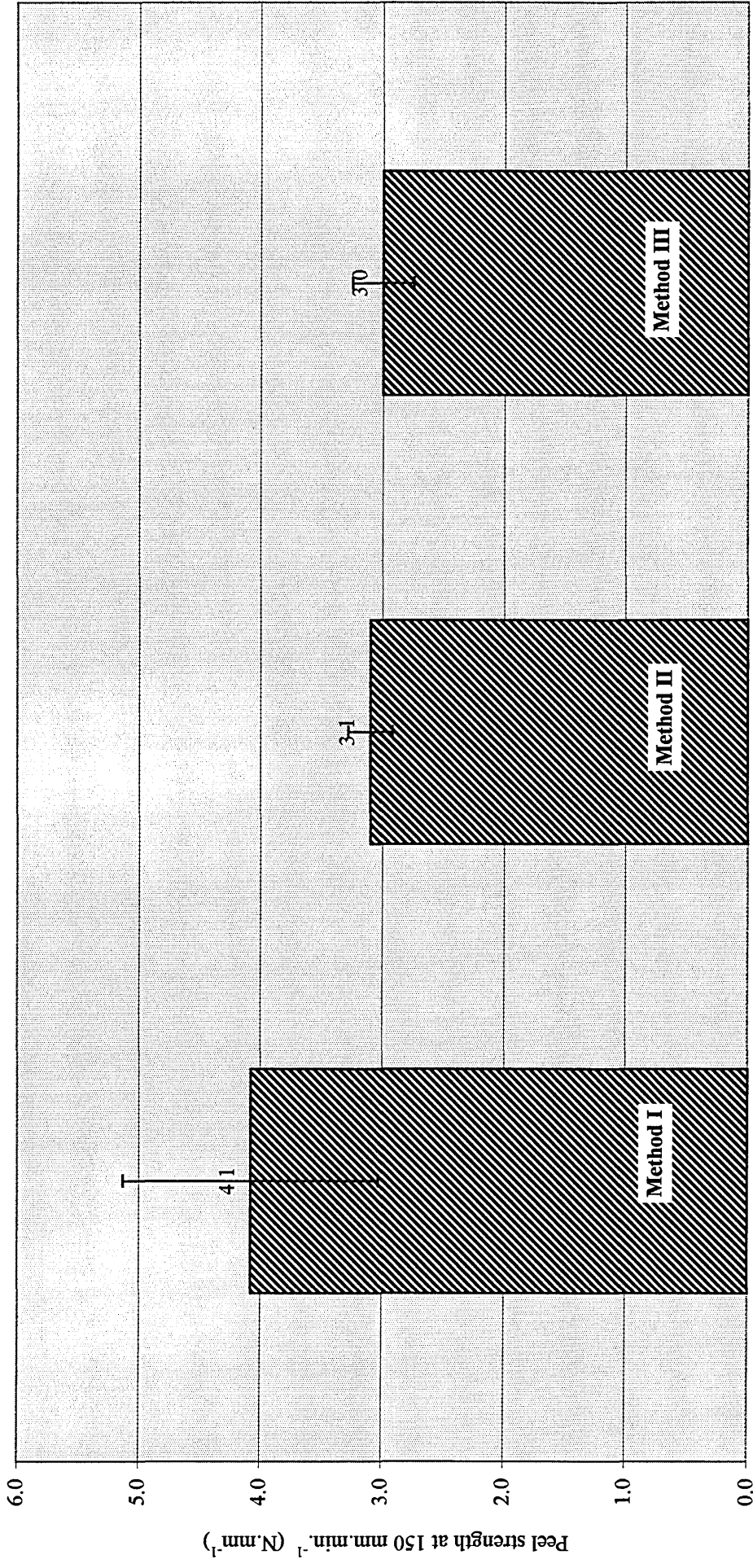


Figure 3.14. Floating roller peel strengths of AISI 304L stainless steel / DP 490 epoxy bonded joints

3.12. and 3.13, and Figures 3.13. and 3.14. by M I (Method I). However, due to a logistical problem, it became impossible to produce the peel test specimens by this method and an alternative method was developed. Subsequent joints were machined to the final joint dimensions prior to bonding, and special spring clips were used instead of the jigs to facilitate curing, as described in 3.2.1.3.2.2. *Method II*. Identified in Tables 3.12 and 3.13, and Figures 3.13. and 3.14. by M II (Method II).

**Considering Table 3.12. and Figure 3.13.**

**For joints assembled by Method I**

The polyurethane system, 3532, clearly gives the best performance at  $10.6 (\pm 1.3) \text{ N mm}^{-1}$ ,  $12.0 (\pm 1.3) \text{ N mm}^{-1}$  and  $14.1 (\pm 1.4) \text{ N mm}^{-1}$ , for the *Acid Etched*, *Alkaline Degreased* and *Alumina Blasted* adherends, respectively. The poorest performance came from the joints bonded with DP 460 and incorporating the *Alkaline Degreased* adherends at  $2.5 (\pm 0.9) \text{ N mm}^{-1}$ , although higher mean peel strengths were realised for those joints including *Alumina Blasted* and *Acid Etched* adherends at  $4.5 (\pm 0.5) \text{ N mm}^{-1}$  and  $7.4 (\pm 0.9) \text{ N mm}^{-1}$ , respectively. The joints bonded with DP 490 and incorporating the *Alumina Blasted* adherends gave essentially the same mean peel strength as those including the *Acid Etched* adherends at  $5.5 (\pm 1.2) \text{ N mm}^{-1}$ , and  $5.4 (\pm 1.0) \text{ N mm}^{-1}$ , respectively. However, the joints incorporating the *Alkaline Degreased* adherends gave a lower mean peel strength at  $4.1 (\pm 1.1) \text{ N mm}^{-1}$ .

**For joints assembled by Method II**

The joints incorporating the *Alkaline Degreased* adherends and bonded with the epoxy 9323, performed slightly better than those bonded with the heat cured system 7823 at  $3.8 (\pm 0.3) \text{ N mm}^{-1}$  and  $3.3 (\pm 0.3) \text{ N mm}^{-1}$ . However, these results could not be compared directly with the above results because of the two different methods involved during joint construction and assembly. Thus, to allow comparison, the mean peel strength of DP 490-bonded joints (*Alkaline Degreased*) assembled using Method II was determined and is given in Table 3.13. and Figure 3.14.

**Considering Table 3.13. and Figure 3.14.**

The joints assembled using Method II gave a mean peel strength almost 25% less than those joints assembled using Method I;  $3.1 (\pm 0.3) \text{ N.mm}^{-1}$  and  $4.1 (\pm 1.1) \text{ N.mm}^{-1}$ , respectively. However, there

were two essential differences between Methods I and II: Firstly, in Method I the joints were machined from pre-bonded coupons, whereas, in Method II the joints were machined to size prior to bonding; and secondly, in Method I the joints were 'jig-held' during curing, whereas, in Method II the joints were held together with spring clips. Therefore, it is difficult to say whether the reduction in mean peel strength observed between joints assembled using Method I and Method II is due to the machining/bonding sequence, or whether, it is due to the type of fixture employed to keep the joints together during curing. Thus, in order to evaluate the significance of the type of holding fixture employed to facilitate curing, the mean peel strength was determined for joints incorporating adherends pre-machined prior to bonding *but* held together during curing using the jigs originally designed for holding coupons rather than individual joints. This was designated Method III and is given in Table 3.13. and Figure 3.14.

**Method I** - joints machined directly to size from pre-bonded coupons and held in jigs during curing.

**Method II** - joints bonded after machining and held together with spring clips during curing.

**Method III** - joints bonded after machining (as with Method II) and held in jigs during curing (as with Method I).

The mean peel strength of the joints, incorporating adherends pre-machined prior to bonding, were almost the same at  $3.0 (\pm 0.2) \text{ N.mm}^{-1}$  and  $3.1 (\pm 0.3) \text{ N.mm}^{-1}$ , for the joints held using spring clips and those jig-held, respectively (Methods II and III). Thus, it would suggest that the reduction in strength observed between the joints assembled using Methods I and II, had little to do with the type of fixture employed to facilitate curing, but must be due to the machining/bonding sequence.

### 3.3.3. FRACTURE ANALYSIS

The fracture faces of the failed joints were examined visually and using SEM; the fractures were mounted and gold coated before SEM examination. Table 3.14. contains the estimated proportions of adhesive, cohesive, and interfacial failure; it is appreciated that these results are subjective. N.B. The

terms *adhesive*, *cohesive*, and *interfacial* failure are often confused, thus, the following interpretations of the definitions are included to clarify the situation.

**Table 3.14.** Loci of Failures.

ADHESIVE SYSTEM	LOCUS OF FAILURE IN SHEAR TEST SAMPLES			LOCUS OF FAILURE IN PEEL SAMPLES
	ADHESIVE %	INTERFACIAL %	COHESIVE %	
DP 460	75	20	5	ADHESIVE
DP 490	20	30	50	ADHESIVE
9323 B/A	60	25	15	ADHESIVE
7823 S	0	99	1	ADHESIVE
3532 B/A	50	40	10	ADHESIVE

*Adhesive failure:* - complete separation of adhesive and adherend.

*Cohesive failure:* - failure entirely within adhesive or failure entirely within adherend.

Denoted by  $cohesive_{Adhesive}$  or  $cohesive_{Adherend}$ .

*Interfacial failure:* - failure within the surface layer of adhesive, or, at adhesive / primer

interface. Denoted by  $interfacial_{Adhesive}$  or  $interfacial_{Adhesive/primer}$ .

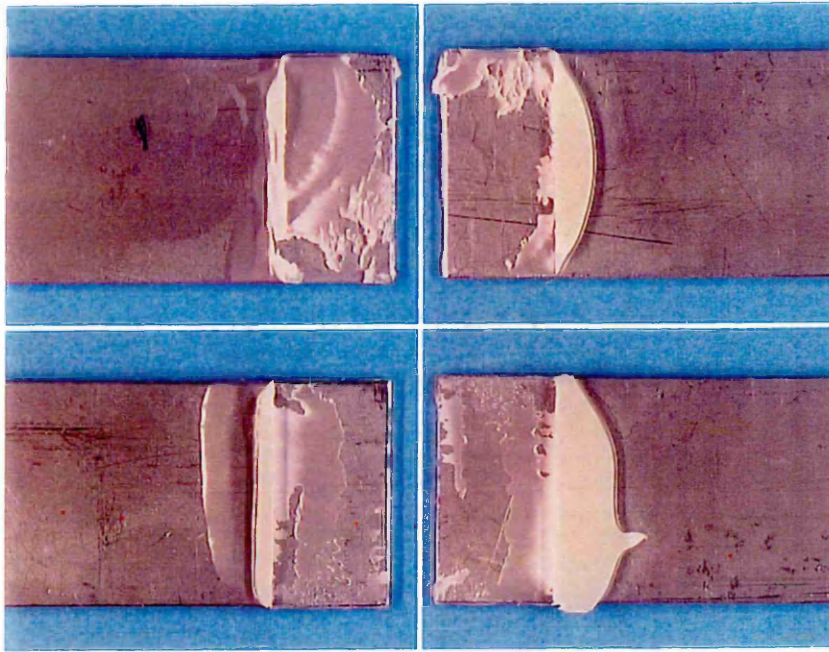
- failure within primer, or, at primer / oxide interface. Denoted

$interfacial_{Primer}$  or  $interfacial_{Primer/oxide}$ .

- failure within the oxide layer or, at oxide / bulk metal interface. Denoted by

$interfacial_{Oxide}$  or  $interfacial_{Oxide/adherend}$ .

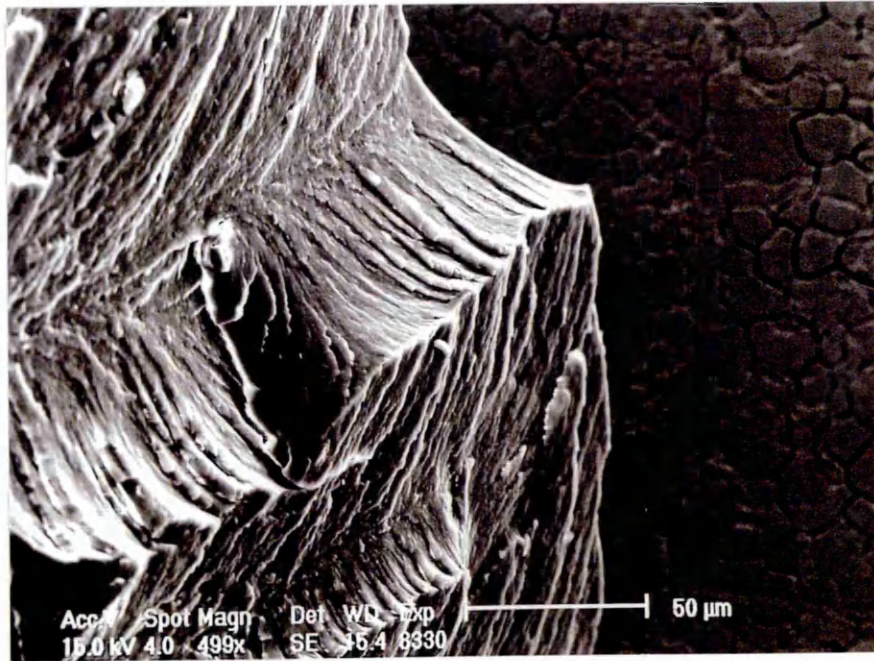
Plate 3.2.



AISI 304: ALK. DEG: DP 460: PREDOM. I/FACIAL FAILURE -1:1

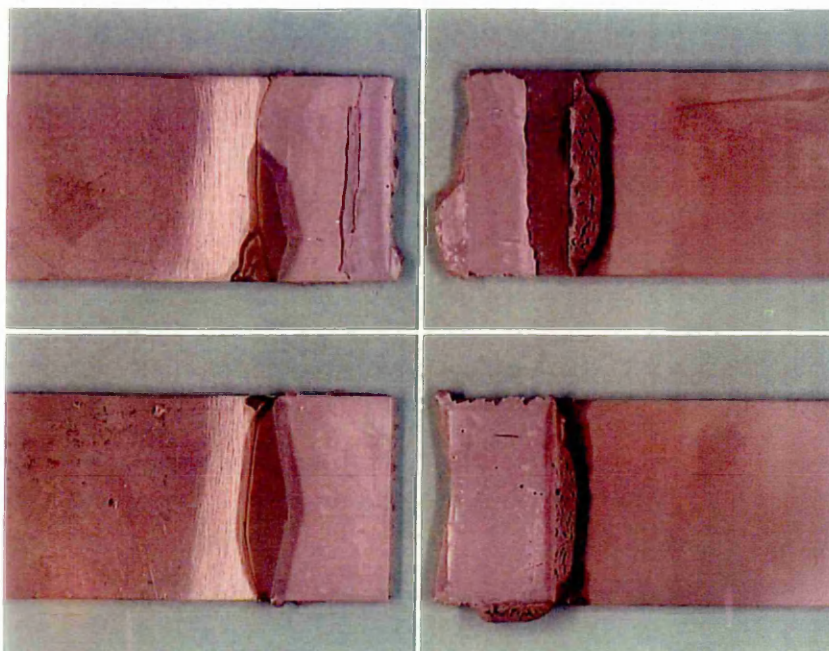
Optical micrograph of DP 460 fracture face.

Plate 3.3.



Scanning electron micrograph of DP 460 fracture face. Showing cliff-like fracture edges.

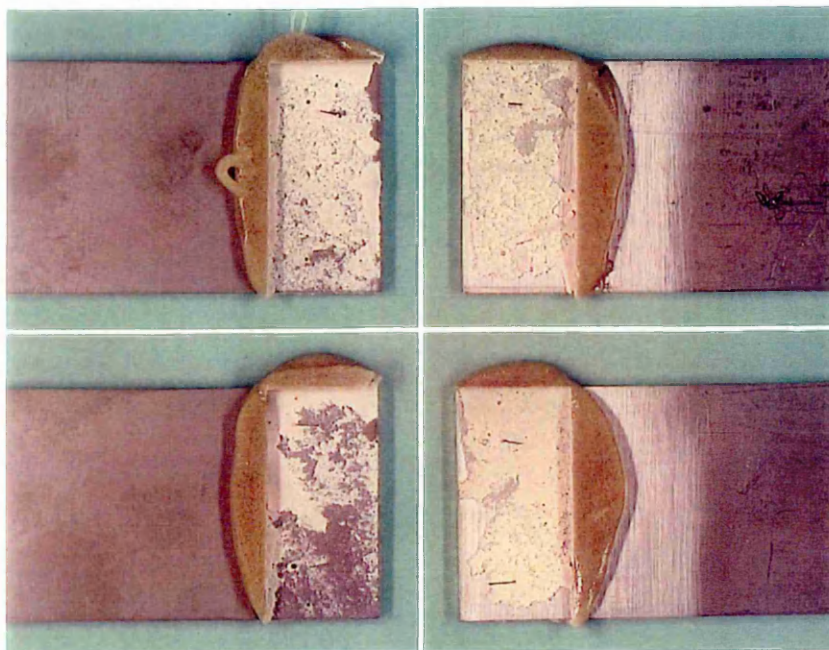
**Plate 3.4.**



AISI 304: GB/SB: HEAT CURED. COH. FAILURE.

Optical micrograph of 7823 S fracture face.

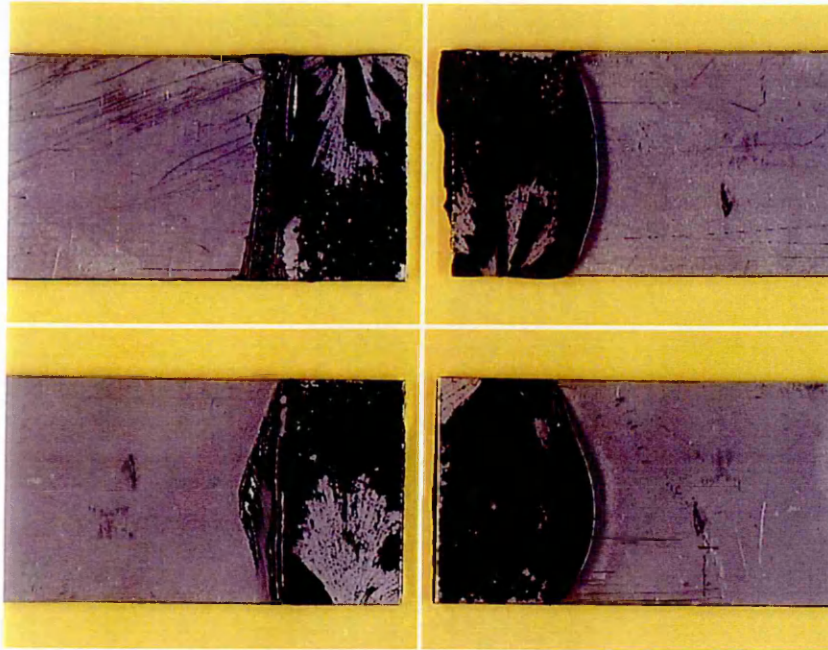
**Plate 3.5.**



AISI 304: GB/SB: POLY.

Optical micrograph of 3532 B/A fracture face.

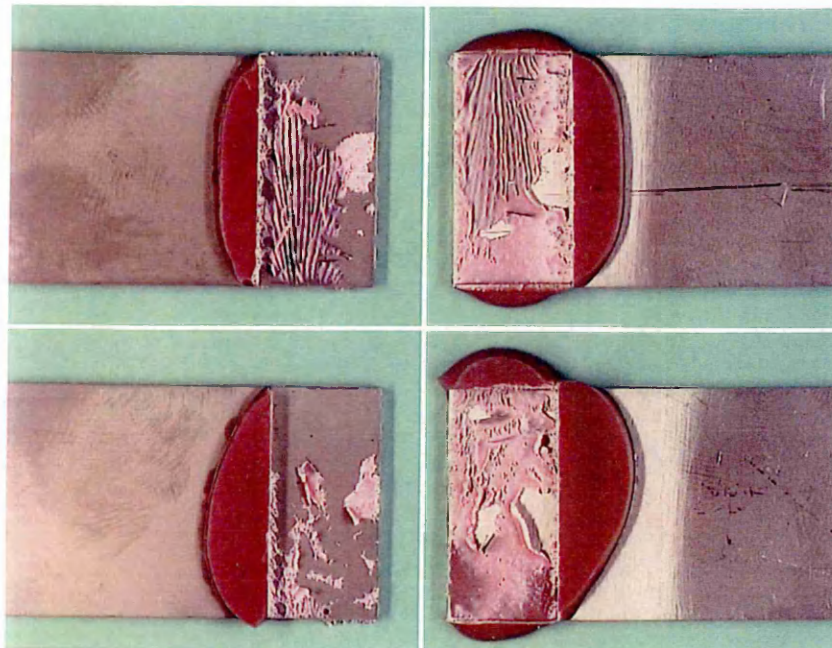
**Plate 3.6.**



AISI 304: ALK. DEG: DP 490: PREDOM. I/C FAILURE -1: 1

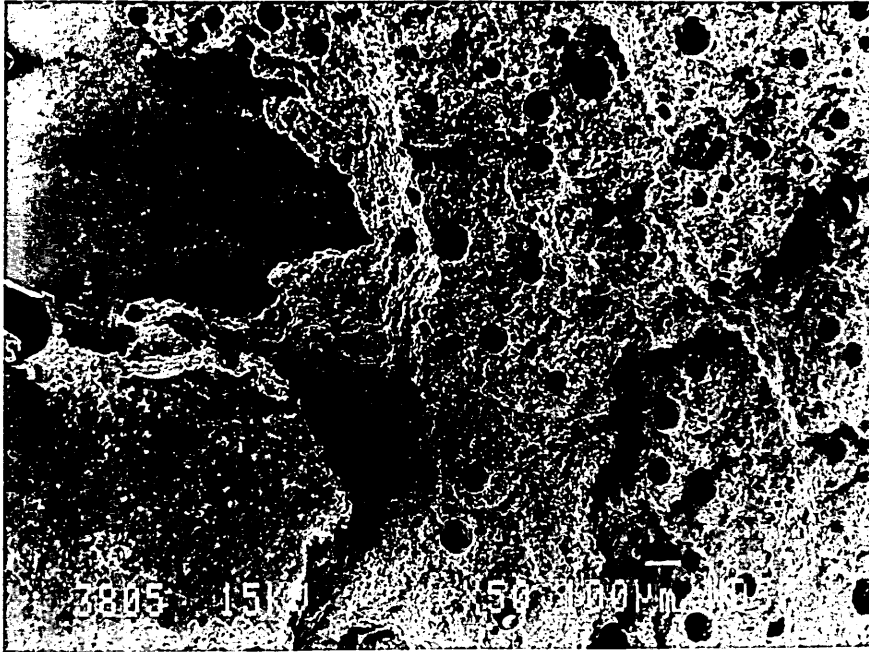
Optical micrograph of DP 490 fracture face.

**Plate 3.7.**

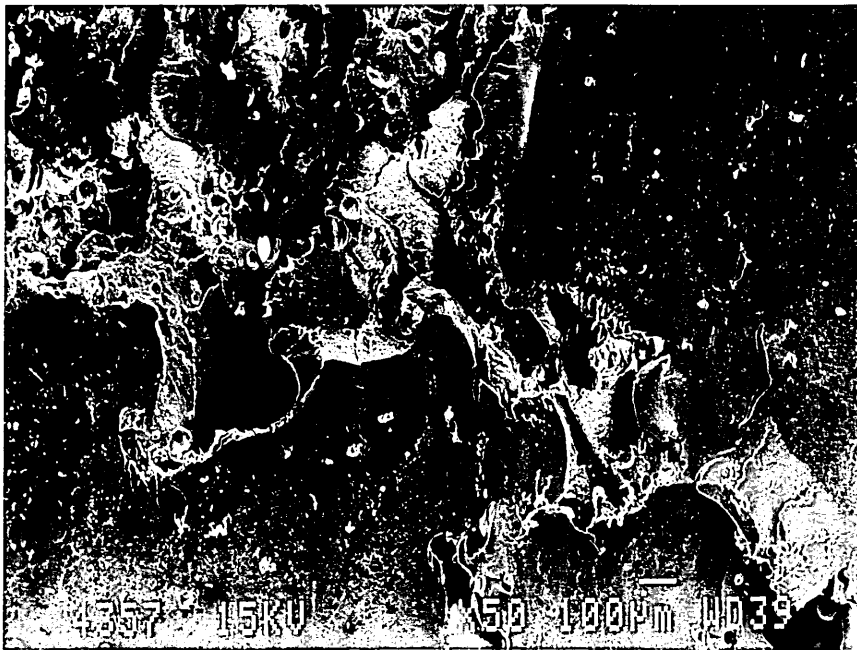


AISI 304: GB/SB: 2 COMP.

Optical micrograph of 9323 B/A fracture face.



Scanning electron micrograph of DP 490 fracture face. Showing cohesive failure within adhesive.

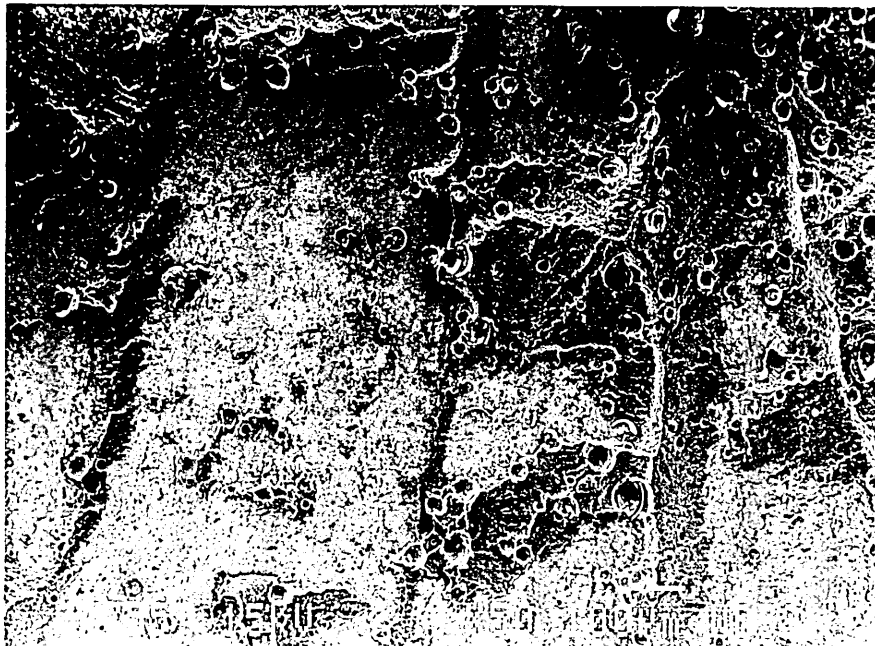


Scanning electron micrograph of DP 490 fracture face. Showing cohesive and adhesive failure.



Scanning electron micrograph of DP 490 fracture face. Showing cracking.

Plate 3.11.



Scanning electron micrograph of DP 490 fracture face. Showing interfacial failure.

Plate 3.12.



Scanning electron micrograph of 9323 B/A fracture face. Showing adhesive and cohesive failure.

Plate 3.13.



Scanning electron micrograph of 9323 B/A fracture face. Showing adhesive and cohesive failure.

**Plate 3.2.**

The fracture faces of the failed lap shear joints bonded with the epoxy system DP 460 showed predominantly regions of adhesive failure. Remnants of the adhesive were observed, as large broken islands, on both halves of each joint, distributed evenly between the two halves, and to a height equal to that of the bondline (0.25 mm). These islands corresponded to similar shaped areas of exposed steel substrate on the opposite fracture face, and any two corresponding halves fitted together like jigsaw pieces. Both the surface of the adhesive and that of the adherend had a gloss lustre, as if the two materials had never been intimate. For the most part, the adhesive surface was smooth and featureless, although the edges of the islands had a distinct pattern, and were in fact cliff-like, see Plate 3.3.

**Plate 3.4.**

The fractures of the joints bonded using the hot-cured epoxy system 7823S, also had a distinct appearance. The adhesive, relatively smooth and featureless, was present on both corresponding faces of each joint, and it appeared to be an entirely cohesive failure within the adhesive. However on closer inspection it was apparent that failure had occurred within the near-surface layers of the adhesive, leaving a thin layer of adhesive on one half of the joint and approximately 0.25 mm of adhesive (almost the entire bondline thickness) on the other. The surface of the adhesive on both faces of each corresponding joint no longer had a gloss sheen, but was of a dull, matt appearance. This was characteristic of interfacial<sub>Adhesive</sub> failure, which was the predominant locus of failure observed on the post-fracture faces. This was attributed to peel stresses induced at the extremes of the overlap due to the elastic and plastic rotation of the joint. As the joint rotates, cracks due to peel propagate from both ends of the overlap towards the centre, where fast fracture occurs through the adhesive by shear as the joint rotation reaches a maximum and this results in cohesive<sub>Adhesive</sub> failure. The latter explains the 1% cohesive failure reported from the post-fracture faces of joints bonded with the 7823S system (see Table 3.14.).

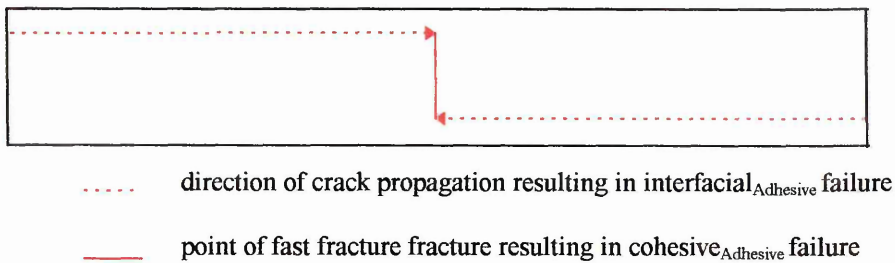


**Figure 3.15.** Locus of failure in 7823S bonded joints.

**Plate 3.5.**

The fracture of the lap shear joints bonded with the polyurethane system 3532 B/A consisted of around 50% adhesive failure, with approximately equal amounts of adhesive on the corresponding halves of each joint. The remainder consisted predominantly of interfacial failure, with discrete regions of cohesive failure, 40% and 10%, respectively.

**Plate 3.6.**

The fracture faces of the joints bonded with the epoxy system DP 490, showed a reduced proportion of adhesive failure, the remainder being predominately cohesive failure with associated interfacial failure, 20% 50% and 30%, respectively. Less cohesive failure was observed on those joints incorporating the alkaline degreased adherends, than on those incorporating the mechanical roughened and the acid rinsed adherends, 35%, 60% and 50%, respectively. Plates 3.8. and 3.9. show areas of cohesive and adhesive failure.

**Plate 3.7.**

The fracture faces of the joints bonded with the epoxy system 9323 were very similar to those of the DP 490 System, but with a higher proportion of adhesive failure (60% c.f. 20%), and a lower proportion of cohesive failure (15% c.f. 50%). The extent of interfacial failure was similar at 30% and 35%, respectively.

Both the DP 490 and 9323 B/A systems displayed a similar pattern of cracking running perpendicular to the tensile axis at one edge and veering to approximately 45° to the tensile axis towards the centre of the fracture faces. In the DP 490 system the pattern was finer than that displayed by the 9323 system. The cracks in the DP 490 were angled at 45° to the tensile axis. The cracking pattern was not observed in any of the other adhesives. Plates 3.10. and 3.11., show the cracking in the DP 490, and Plates 3.12. and 3.13., show a similar pattern in the 9323 system.

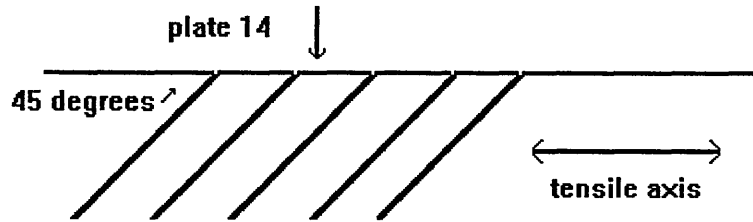


**Figure 3.16.** Locus of cracking observed in DP 490 and 9323 epoxy systems.

### 3.4. DISCUSSION

It is clear from the results that it is possible to discriminate between different adhesive systems using a regime which includes single-overlap-shear testing. But, whether or not it is possible to differentiate between different adherend pre-treatments using this technique is less clear. A slight trend was observed, however, in favour of the lap shear joints incorporating the *Acid Rinsed* adherends, which might suggest that this cleaning procedure is more effective than *Alkaline Degreasing* or *Mechanical Roughening*. In addition, the lap shear strengths resulting from the joints incorporating the *Mechanically Roughened* adherends were the most consistent, and this might indicate that *Mechanical Roughening* removes contamination in a manner more uniform than that achieved by either *Alkaline Degreasing* or *Acid Rinsing*. Similarly, floating roller peel testing was able to discriminate effectively between different adhesive systems. But once again, it is less clear as to whether or not floating roller peel testing is capable of discriminating between different adherend surface conditions. Again a slight trend was observed, this time in favour of the joints including *Alumina Blasted* and *Acid Etched* adherends, and this may be attributed to the increased degree of mechanical interlocking, resulting from the physical and chemical roughening action of these techniques, or, it may simply be because these methods are more effective at cleaning than *Alkaline Degreasing*.

In the lap shear tests, the epoxy systems, as expected, performed much better than the polyurethane system, because of the high inherent shear strength associated with this family of adhesives. However, joints incorporating the polyurethane adhesive gave a much superior mean peel strength than any of the epoxy systems, which is probably due to the high flexibility commensurate with this family of adhesives. The joints incorporating the two-component epoxy DP 460 gave the highest mean apparent shear strength, although all the epoxy systems performed well in the lap shear tests. The poor performance of the polyurethane under shear loading, however, would limit the use of this adhesive type to non-structural applications. Although the peel performance of joints bonded with the epoxy systems were inferior to those bonded with the polyurethane, the strengths obtained were reasonable, and could be tolerated, providing the peel stresses within the joint were minimised by careful joint design.

It is worth noting that peel strength appears to be sensitive to changes in the assembly procedure. The higher mean peel strength obtained from joints machined from pre-bonded coupons (Method I), compared with those of joints bonded from pre-machined adherends (Methods II and III), may be attributed to edge effects, such as the extent of which any mechanical clinching incurred during guillotining and machining contributed to peel performance. It may even be due to a plasticising effect of the machine oil or coolant on the DP 490 adhesive.

On the assumption that cohesive failure within the adhesive implies that the strength of adhesion at the adhesive / adherend interface is greater than the cohesive strength of the adhesive, the two-part epoxy DP 490 was considered to be the most 'stainless-compatible' system, since the subsequent fracture faces of the joints bonded with this system gave the highest percentage of cohesive failure within the adhesive.

The subsequent fracture faces of the lap shear joints revealed areas of adhesive failure at the adhesive / adherend interface, and areas of interfacial and cohesive failure within the adhesive, the approximate proportions of which are given in Table 3.14. The areas of adhesive failure observed on the fracture faces were generally restricted to the two extremes of the overlap, where the peel stresses would have been the greatest during the test, as a result of an induced bending moment. The areas of interfacial and cohesive failure, however, were located towards the centre of the fracture face where the peel stresses would have been minimal during the test. Thus, adhesive failure is likely to have initiated at both ends of the joint due to intense peel stresses induced by the bending moment, the adhesive finally failing, cohesively, as the two planar cracks approached one another.

With respect to the application of the adhesives and their curing requirements. The one-component heat-cured epoxy 7323 displayed a reasonable mean shear strength, just two hours after the joints were assembled, after allowing for the joints to cool down before testing. This, together with its indefinite working life at room temperature, would make this the ideal choice of adhesive for many applications. The main disadvantage with this type of system, however, is that a heat source is required, and this may be impractical or too expensive to accommodate. The two-component adhesives that required mixing by hand, the epoxy 9323 and the polyurethane system 3532 had the advantage of curing at room

temperature, but reaching handling strength after 24 hours. The main problems with these systems were in the time taken, and the accuracy required, to mix the two components. In addition to this, the urethane 3532 had a short working life, so short the adhesive had to be mixed in very small quantities at a time. The adhesives considered the easiest to work with must be the two-component epoxies DP 460 and DP 490; both reaching handling strength within 24 hours and with no weighing, proportioning and mixing required, as these adhesives are both supplied in a pre-proportioned, double cartridge, and applied with a gun and self-mixing nozzle. From the aforementioned adhesive the preferred choice would be the DP 490 system, because of its optimum viscosity, its sag resistance and its gap filling properties; sufficiently liquid to wet the surface, but sufficiently solid to be controlled.

From considered opinion, Table 3.15. gives a rating, from 1 to 5, from worse to best, for each of the candidate adhesives, as judged by the following criteria: Mechanical properties (apparent lap shear and floating roller peel strength); adhesive / adherend compatibility (degree of cohesive failure); application and curing; and cost.

**Table 3.15. Adhesive ratings.**

<b>ADHESIVE SYSTEM</b>	<b>SHEAR RATING</b>	<b>PEEL RATING</b>	<b>ADHESION RATING</b>	<b>APPLICATION RATING</b>	<b>COST RATING</b>	<b>TOTAL RATING</b>
<b>EPOXY DP 460</b>	5	4	1	4	2	16
<b>EPOXY DP 490</b>	4	3	5	5	1	18
<b>EPOXY 9323</b>	3	2	4	2	5	16
<b>EPOXY 7323</b>	2	1	3	3	4	13
<b>POLY. 3532</b>	1	5	2	1	3	12

Finally, removing the fillets of hardened adhesive 'squeeze-out' from around the perimeter of the lap shear joints prior to mechanical testing, results in a dramatic reduction in apparent shear strength, up to 25 %. This is probably because the fillets minimise the peel stress at the extremes of the overlap, and thereby, offset failure until a higher load.

### 3.5. CONCLUSIONS

1. Apparent overlap shear strength tests and floating roller peel tests are useful methods for discriminating between different types of adhesive. However, these techniques are less sensitive to changes in the condition of the surface of the adherend.
2. Measured peel strength of is sensitive to manufacturing route.
3. If the bond performance is improved by roughening the surface, by physical or chemical means, it is more likely to be a result of the improved degree of cleanliness attained and/or the increase in surface area available for bonding, rather than from the contribution afforded by mechanical interlocking.
4. If stainless steels are to be joined using adhesives, with the intention of employing the resulting fabrications in structural applications, toughened epoxy systems must be considered. The epoxy system DP 490 would be the preferred choice out of those systems considered in this programme.
5. The surface condition of the adherend is important with respect to the degree of surface cleanliness attained. However, the contribution to bond strength afforded by physical and chemical induced modifications are considered negligible, and may be out-weighed by the economic considerations.
6. Adhesive 'squeeze-out' fillets should be left un-removed in adhesive-metallic bonds to optimise performance. However, if aesthetic considerations are paramount, the fillets may be removed, but this will result in a subsequent reduction in the shear strength observed.

#### **4.0. The Effect of Weak Boundary Layers on the Mechanical performance of Adhesive-Bonded Stainless Steel Joints**

##### *Abstract*

*Shear tensile tests were conducted on AISI 304L stainless steel lap joints, bonded with a toughened epoxy system, DP 490, and incorporating adherends which had been pre-treated by a number of different methods; As-Received surfaces were also included for comparison. The highest apparent shear strengths were obtained from those joints comprising adherends cleaned by mechanical and chemical roughening, and ones containing Acetone/Inhibisol Rinsed, Alkaline Degreased and Acid Rinsed surfaces. Joints incorporating adherends subjected to little or no surface preparation (As-Received and Dry Wiped surfaces) gave inferior mean apparent shear strengths; approximately 25 % lower. Single overlap shear and floating roller peel tests were also conducted on joints with different bondline thickness', and on others incorporating adherends primed to different degrees. The mean apparent shear strength was found to decrease with increasing bondline thickness, although the mean peel strength stayed about the same. The presence, or absence, of a surface primer appeared to make little difference to both the mean apparent shear strength and the mean floating roller peel strength.*

## 4.1. INTRODUCTION

Metallic surfaces are high energy surfaces and thus naturally susceptible to contamination. Air-borne contaminants, organic and inorganic, will be readily adsorbed by metallic surfaces, or more correctly, metallic oxide surfaces. Contamination will also come from more obvious sources; from handling, or as a result of the production process, for example, oil and coolant from machining, or grease from lubrication and storage. These surface contaminants can act as barriers to intrinsic adhesion, preventing, or impairing, intimate union between adhesive and adherend surface, by forming what are effectively weak boundary layers.

However, it is not only surface contamination that can act as weak boundary layers. Primers, employed to promote adhesion and/or to help protect 'cleaned surfaces' from re-contamination, may impart brittleness to the joint if the primer layer is excessive; in this case, the primer is the weak boundary layer. Inherent surface oxides, or those created or modified by chemical reaction (etching and anodising), can also constitute weak boundary layers. Indeed, the adhesive itself may act as the weak link, if the bondline thickness is too great.

In order to investigate surface contamination as a potential weak boundary layer, joints incorporating untreated *As-Received* material were prepared and the mean apparent shear strength determined. For comparison, similar tests were carried out on joints containing adherends that had received some degree of surface preparation, ranging from basic *Dry Wiping* to more comprehensive surface cleaning such as *Acetone / Inhibisol Rinsing* or *Acid Rinsing II*. Stainless steel surfaces were also etched in sulphuric acid, before being bonded, to generate the black iron oxide known as smut, which has been observed to act as a weak boundary layer (62).

In order to evaluate the primer as a potential weak boundary layer, both the mean single-overlap-shear strength and mean floating roller peel strength were determined for joints incorporating under-primed and over-primed adherends. Similarly, to assess the bondline as a potential weak boundary layer, both the mean single-overlap-shear strength and mean floating roller peel strength were determined for joints incorporating reduced and increased bondlines, 0.1 mm and 0.5 mm, respectively.

## **4.2. EXPERIMENTAL WORK**

### **4.2.1. MEASUREMENT OF THE MEAN APPARENT SHEAR STRENGTH AND FLOATING ROLLER PEEL STRENGTH**

#### **4.2.1.1. TEST MATERIAL PREPARATION AND JOINT CONFIGURATION**

AISI 304L stainless steel strip, with a matt surface finish (designation 2B), cold-rolled to 1.5 mm, was used as the adherend material for the single overlap shear joints, and as the rigid adherend for the peel joints; the flexible adherend used in the peel tests was made from AISI 304L, with a 2B surface finish, cold rolled to 0.5 mm. The adherends used in the lap joints and those used in the peel joints were manufacture to the same dimensions, and by the same methods, as those given and detailed in *3.2.1.1. Test Material Preparation and Joint Configuration*.

#### **4.2.1.2. SURFACE PRE-BONDING TREATMENTS**

Prior to bonding, the adherends were subjected to a number of surface treatments, and these are given in Table 4.1., together with descriptions of the various stages involved.

#### **4.2.1.3. JOINT ASSEMBLY**

Single-overlap shear joints were constructed following the procedure detailed in *3.2.1.3. Joint Assembly*, and floating roller peel joints were assembled by 'Method II', which is also described in *3.2.1.3. Joint Assembly*. In order to control the bondline thickness of both lap shear and peel joints, 0.1 mm, 0.25 mm and 0.5 mm diameter wire (guitar strings) were carefully positioned into the lap and peel joints just prior to joint closure. All the joints were bonded using the toughened epoxy system DP 490, selected because of its performance in the screening program. The bonded joints were stored in a desiccator and allowed to stand for the appropriate curing period.

Table 4.1. Surface pre-treatments.

SURFACE CONDITION	STAGES INVOLVED	DESCRIPTION OF STAGE
<i>AS RECEIVED</i>	NO SURFACE PREPARATION	N/A
<i>DRY WIPED NO PRIMER</i>	STAGE I DRY WIPING	I. Surfaces were wiped repeatedly with a clean, dry, lint-free cloth, to remove heavy contamination.
<i>DRY WIPED STAND. PRIME</i>	STAGE I DRY WIPING STAGE II PRIMING	I. As above. II. As given in 3.2.1.2.1.4. Priming..
<i>DRY WIPED OVER PRIMED</i>	STAGE I DRY WIPING STAGE II OVER-PRIMING	I. As above. II. Surfaces primed as per 3.2.1.2.1.4. Priming. The surfaces were then allowed to dry overnight before the procedure was repeated. This resulted in a heavy layer of primer, visible to the naked eye.
<i>ACETONE / INHIBISOL RINSED</i>	STAGE I ACETONE RINSE STAGE II INHIBISOL RINSE STAGE III PRIMING	I. Surfaces were cleaned in ultrasonically agitated acetone for 15 minutes at room temperature. II. Surfaces were cleaned in ultrasonically agitated Inhibisol (a trichloroethylene-based solvent) for 15 minutes at room temperature. III. As given in 3.2.1.2.1.4. Priming.
<i>ACID RINSED II</i>	STAGE I ALKALINE DEGREASE STAGE II ACID RINSE II STAGE III PRIMING	I. As given in 3.2.1.2.1.1. The Alkaline Degreasing Procedure. II. Surfaces were cleaned in an ultrasonically agitated sulphuric acid solution (30 % by vol. H <sub>2</sub> SO <sub>4</sub> ) for 15 minutes at room temperature. III. As given in 3.2.1.2.1.4. Priming.
<i>SMUTTED</i>	STAGE I ALKALINE DEGREASE STAGE II ACID ETCHING (SMUT GENERATION) STAGE III PRIMING	I. As given in 3.2.1.2.1.1. The Alkaline Degreasing Procedure. II. As given in 3.2.1.2.2.1. (I) The Etching Procedure. However, the de-smutting stage was omitted so that the black iron oxide (smut) remained undisturbed. The surfaces were allowed to dry thoroughly before priming and subsequent bonding. III. As given in 3.2.1.2.1.4. Priming.

#### **4.2.1.4. MECHANICAL TESTING**

Single lap-shear tests were conducted in accordance with BS 5350: Part C5 (ASTM D1002-94) at a rate of 1.5 mm min.<sup>-1</sup>. Floating roller peel tests were conducted in accordance with BS 5350: Part C7 (ASTM D3167-93) at a rate of 150 mm min.<sup>-1</sup>. The mean apparent shear strength was calculated using a sample size of six. The mean floating roller peel strength was calculated using a sample size of two, since the peel is a continuous test (see 3.2.1.5.1. *Treatment of Raw Data*). N.B. All joints were tested with the fillets of hardened 'squeeze-out' un-removed, with the exception of the lap shear joints incorporating 0.1, 0.25 and 0.5 mm bondline thickness'.

#### **4.2.2. FRACTURE ANALYSIS**

The surfaces of the failed joints were evaluated physically to ascertain the type of failure, be it cohesive, adhesive or interfacial, and in addition, to identify the failure mechanism, be it Mode I, II, III or mixed mode. The physical evaluation was carried out by visual inspection and using SEM.

### 4.3. RESULTS

The results of the standard single-overlap shear tests are given in Tables 4.2. and 4.3., and Figures 4.1. and 4.2. The floating roller peel test results are given in Table 4.4. and Figure 4.2. Table 4.5. details the loci of failure observed under shear and peel loading.

**Table 4.2.** Mean apparent shear strength of AISI 304 L / adhesive joints, bonded with DP 490 toughened epoxy and incorporating adherends with different surface conditions. Fillets un-removed.

ADHEREND SURFACE CONDITION	MEAN FAILURE LOAD (kN)	S.D. (±1 S.D.) (kN)	MEAN APPARENT SHEAR STRENGTH (N.mm <sup>-2</sup> )	S.D. (±1 S.D.) (N.mm <sup>-2</sup> )	COEFFICIENT OF VARIATION $\frac{S.D.}{\bar{x}} \times 100$ (%)
<i>AS-RECEIVED</i>	6.8	1.4	21.8	4.5	20.6
<i>DRY WIPED NO PRIMER</i>	6.9	0.7	22.0	2.4	10.7
<i>DRY WIPED STAND. PRIME</i>	6.9	1.3	22.0	4.2	19.1
<i>DRY WIPED OVER PRIMED</i>	6.8	1.1	21.8	3.4	15.7
<i>ACETONE/INHIBISOL RINSED</i>	8.7	0.8	28.0	2.5	9.0
<i>ALKALINE DEGREASED</i> (From Table 3.10.)	8.0	0.3	25.6	1.0	3.8
<i>ACID RINSED</i> (From Table 3.10.)	8.7	1.1	27.7	3.4	12.2
<i>ACID RINSED II</i>	8.4	0.3	26.9	1.0	3.9
<i>MECHANICALLY ROUGHENED</i> (From Table 3.10.)	8.2	0.3	26.2	0.9	3.4
<i>SMUTTED</i>	8.6	0.5	27.6	1.7	6.3

NB Standard prime (see 3.2.1.2.1.4. Priming)

**Table 4.3.** Mean apparent shear strength of AISI 304 L / adhesive joints, bonded with DP 490 toughened epoxy, showing the effect of increasing the bondline. Fillets removed.

<i>ALKALINE DEGREASED 0.1 mm BONDLINE</i>	8.3	0.4	26.4	1.2	4.7
<i>ALKALINE DEGREASED STAND. BONDLINE</i> (From Table 3.11.)	6.1	0.8	19.4	2.4	12.4
<i>ALKALINE DEGREASED 0.5 mm BONDLINE</i>	4.3	0.9	13.7	2.9	20.9

NB Standard bondline = 0.25 mm

Table 4.4. Effect of primer thickness and bondline thickness on floating roller peel strength.

ADHEREND SURFACE CONDITION AND BONDLINE	PEEL LENGTH (mm)	PEEL LOAD (N)			MEAN PEEL STRENGTH (N.mm <sup>-1</sup> )	S.D. (± 1 S.D.) (N.mm <sup>-1</sup> )	COEFF. OF VARIATION $\frac{S.D.}{\bar{x}} \times 100$ (%)
		MIN.	MAX.	MEAN			
<i>ALKALINE DEGREASED</i> NO PRIMER STAND. BONDLINE	160	40	92	67	2.7	0.4	14.5
<i>ALKALINE DEGREASED</i> OVER PRIMED STAND. BONDLINE	160	46	110	68.5	2.7	0.3	11.6
<i>ALKALINE DEGREASED</i> 0.1 mm BONDLINE STAND. PRIME	160	60	92	75	3.0	0.3	10.3
<i>ALKALINE DEGREASED</i> 0.5 mm BONDLINE STAND. PRIME	160	47	105	69	2.8	0.4	12.7
<i>ALKALINE DEGREASED</i> STAND. BONDLINE STAND. PRIME (From Table 3.13.)	160	62.5	91.5	76.5	3.1	0.3	8.3

NB All peel joints bonded by Method II (see 3.2.1.3. Joint Assembly)

Standard bondline = 0.25 mm

Standard prime (see 3.2.1.2.1.4. Priming)

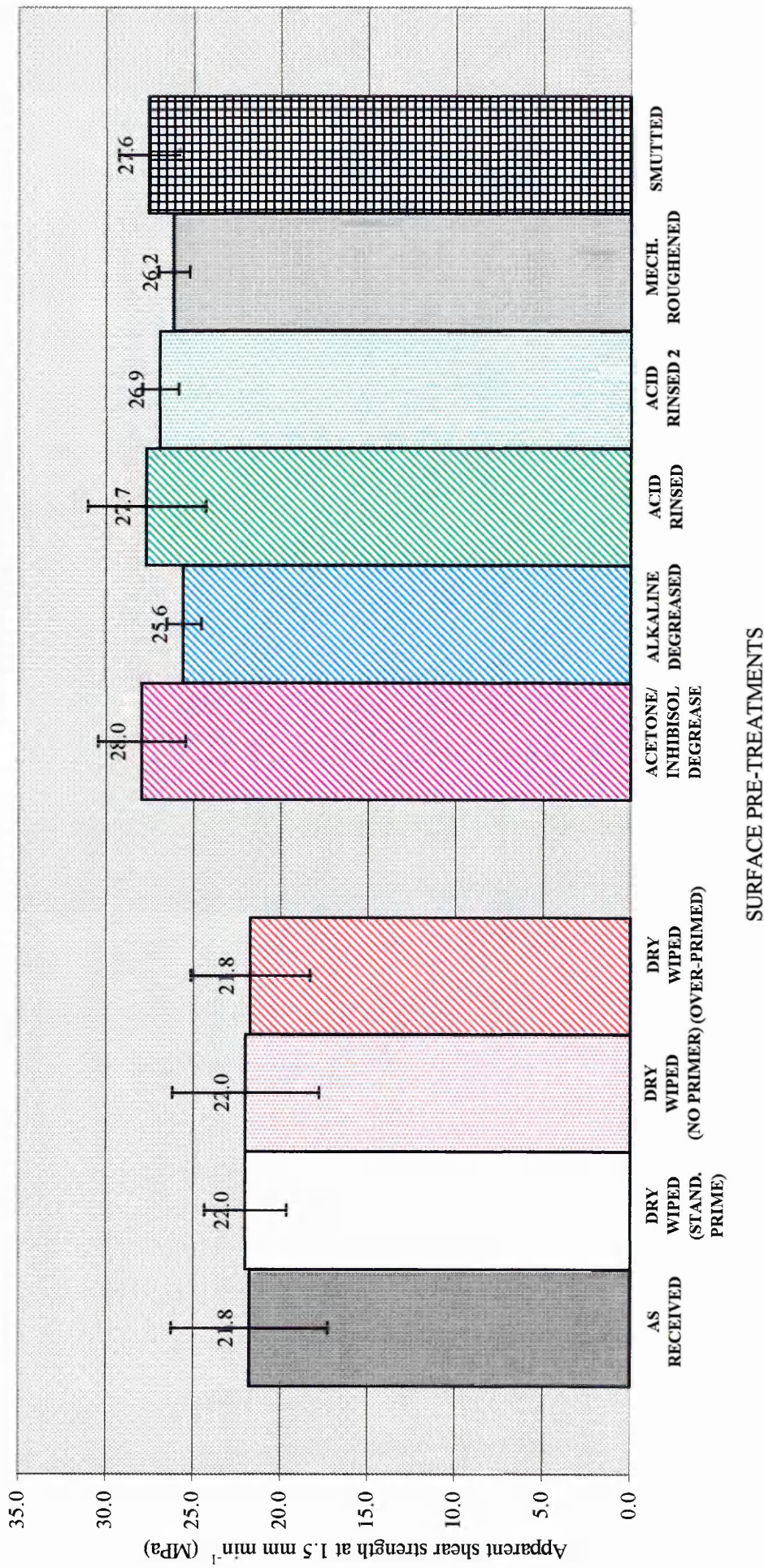


Figure 4.1. Effect of weak boundary layers on apparent overlap shear strength. Fillets un-removed.

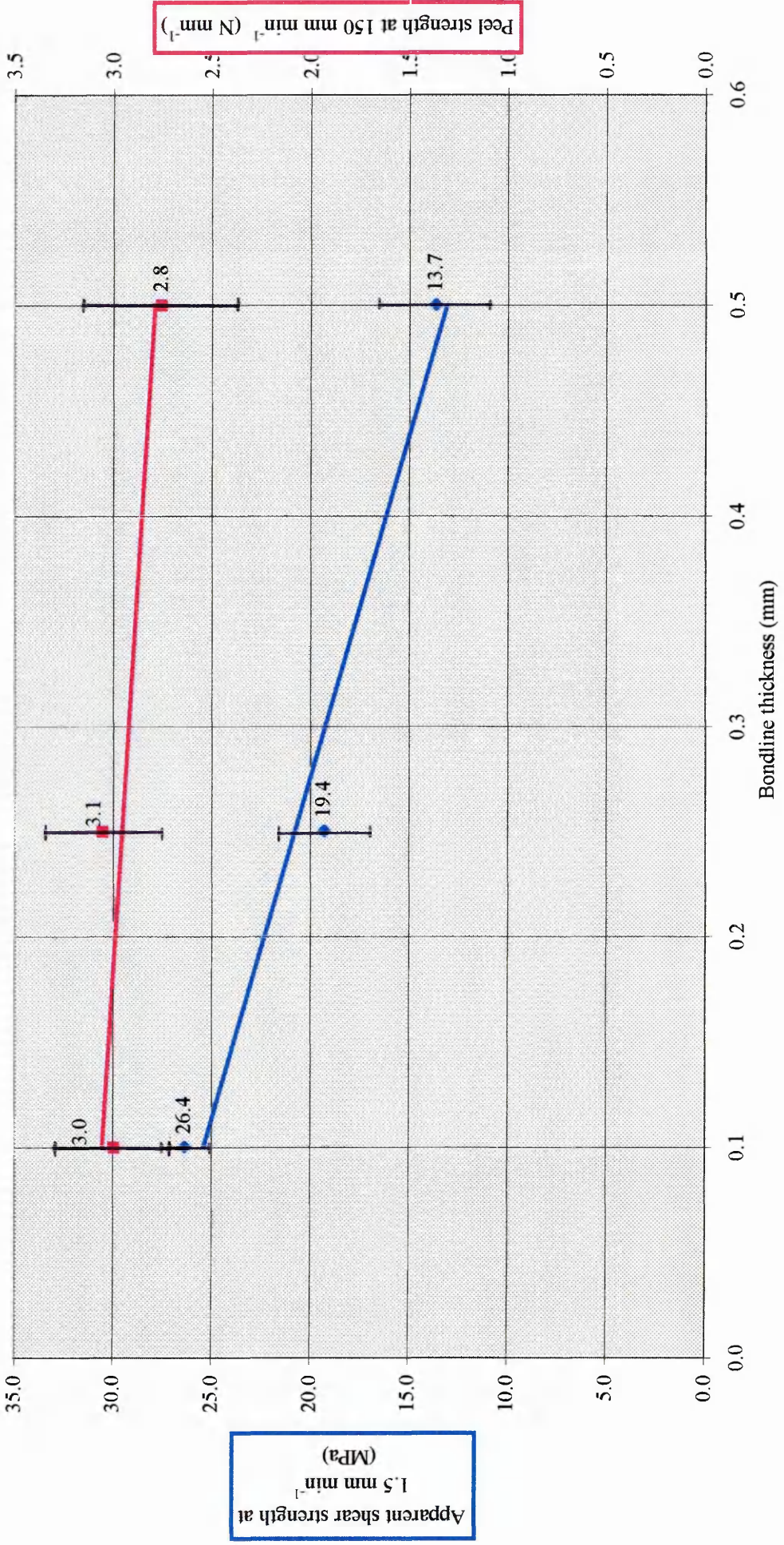


Figure 4.2. Effect of bondline thickness on apparent overlap shear and peel strength. Fillets removed w.r.t. overlap shear joints.

**Table 4.5. Loci of Failures.**

TYPE OF TEST	ADHEREND SURFACE CONDITION	LOCI OF FAILURE		
		ADHESIVE %	INTERFACIAL %	COHESIVE %
LAP SHEAR	<i>AS-RECEIVED</i>	85	10 (adhesive)	5
	<i>DRY WIPED NO PRIMER</i>	75	20 (adhesive)	5
	<i>DRY WIPED STAND. PRIME</i>	75	10 (adhesive)	15
	<i>DRY WIPED OVER PRIMED</i>	75	20 (adhesive)	5
	<i>ACETONE/INHIBISOL RINSED</i>	45	35 (adhesive)	20
	<i>ACID RINSED II</i>	10	50 (adhesive)	40
	<i>SMUTTED</i>	0	95 (oxide)	5
	<i>ALKALINE DEGREASED 0.1 mm BONDLINE</i>	60	35 (adhesive)	5
	<i>ALKALINE DEGREASED 0.5 mm BONDLINE</i>	80	15 (adhesive)	5
PEEL	<i>ALKALINE DEGREASED NO PRIMER</i>	100	0	0
	<i>ALKALINE DEGREASED OVER PRIMED</i>	90	10 (primer)	0
	<i>ALKALINE DEGREASED 0.1 mm BONDLINE</i>	100	0	0
	<i>ALKALINE DEGREASED 0.5 mm BONDLINE</i>	100	0	0

Considering Table 4.2. and Graph 4.1.

Joints incorporating *Acetone/Inhibisol Rinsed*, *Acid Rinsed II* and, surprisingly enough, *Smuted* surfaces, gave high mean apparent shear strengths, comparable with those of joints comprising *Alkaline Degreased*, *Mechanically Roughened*, and *Acid Rinsed* adherends (see Section 3.0. *Adhesive Screening*). Joints with *Acetone/Inhibisol Rinsed* adherends gave a mean apparent shear strength slightly higher than that of joints incorporating adherends pre-treated by the more involved *Alkaline Degreasing* method, 28.0 (± 2.5) MPa and 25.6 (± 1.0) MPa, respectively. The mean apparent shear strength of joints including adherends rinsed in hydrochloric acid (*Acid Rinsed*) was only slightly higher than that of joints incorporating surfaces rinsed in sulphuric acid (*Acid Rinsed II*), 27.7 (± 3.4) MPa and 26.9 (± 1.0) MPa, respectively. Joints incorporating adherends, plastically deformed by

*Mechanically Roughening*, also performed well, as indeed, did joints comprising surfaces chemically roughened by *Smutting* at 26.2 ( $\pm$  0.9) MPa and 27.6 ( $\pm$  1.7) MPa, respectively. The lowest mean apparent shear strengths, and the largest scatter, came from joints incorporating adherends subjected to little or no surface preparation: 21.8 ( $\pm$  4.5) MPa for joints incorporating *As-Received* surfaces; and 22.0 ( $\pm$  4.2) MPa for the joints incorporating *Dry Wiped* (standard prime) surfaces. Removing the primer stage, or deliberately adding excess primer, appeared to do nothing to adversely affect, or improve, mean apparent shear strength; 22.0 ( $\pm$  2.4) MPa and 21.8 ( $\pm$  3.4) MPa, for the joints incorporating *Dry Wiped (no primer)* and *Dry Wiped (over-primed)* surfaces, respectively.

**Considering Table 4.3. and Figure 4.2.**

Higher mean apparent shear strengths were obtained from joints with smaller bondline thickness'; 26.4 ( $\pm$  1.2) MPa, 25.6 ( $\pm$  1.0) MPa and 13.7 ( $\pm$  2.9) MPa, for 0.1 mm, 0.25 mm and 0.5 mm thick bondlines, respectively.

**Considering Table 4.4. and Figure 4.2.**

The mean peel strength of joints with 0.1 mm, 0.25 mm and 0.5 mm were similar at 3.00 ( $\pm$  0.3) N.mm<sup>-1</sup>, 3.1 ( $\pm$  0.3) N.mm<sup>-1</sup> and 2.8 ( $\pm$  0.4) N.mm<sup>-1</sup>, respectively. There was also little difference between the mean peel strengths of joints incorporating non-primed, standard primed and over-primed adherends, 2.7 ( $\pm$  0.4) N.mm<sup>-1</sup>, 3.1 ( $\pm$  0.3) N.mm<sup>-1</sup> and 2.7 ( $\pm$  0.3) N.mm<sup>-1</sup>, respectively. These results are not represented graphically.

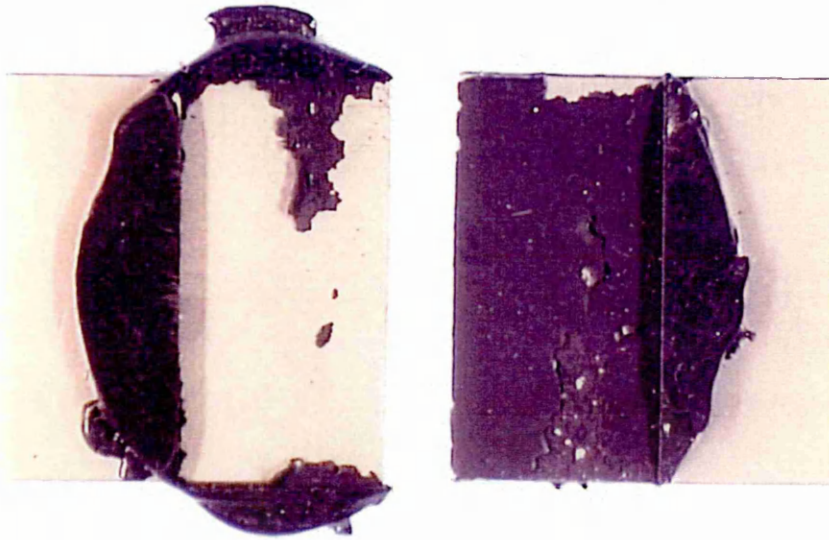
**Considering Table 4.5.**

The lap shear fracture faces of the joints incorporating adherends which were subjected to little or no surface preparation (*Dry Wiped* and *As-Received*), revealed the largest proportion of adhesive failure. Whereas, the fractures of joints comprising adherends pre-treated by more sophisticated techniques (*Acetone/Inhibisol Rinsing*, *Alkaline Degreasing*, *Acid Rinsing*, *Acid Rinsing II*, and *Mechanical Roughening*), revealed higher proportions of interfacial and cohesive failure.

N.B. The loci of failure in fractured lap joints incorporating *Alkaline Degreased* (standard 0.25 mm bondline), *Mechanically Roughened*, and *Acid Rinsed* adherends, are not included in Table 4.5., because the loci of failure were originally determined from all lap joints considered in the adhesive screening regime that were bonded with the toughened epoxy DP 490, regardless of the surface condition of the adherend (see 3.3.3. *Fracture Analysis*). However, generally there was a high percentage of cohesive failure observed (~50%), and the remainder, comprised about equal proportions of adhesive and interfacial failure, ~20% and ~30%, respectively. For the same reason, the loci of failure in fractured peel joints of standard bondline and standard prime are not included in Table 4.5. In these cases, 100% adhesive failure was typical (see 3.3.3. *Fracture Analysis*).

Most of the interfacial failures observed were, clearly within the adhesive, but so close to the surface that it could not be deemed truly cohesive. However, the fracture faces of the *Smutted* surfaces showed predominantly interfacial failure at the interface of the metallic oxide (smut) and the parent metal. There was also some evidence of interfacial failure within the primer layer, i.e. the characteristic hue of the primer, a shocking pink, was clearly visible on both sides of the peel joint. Plates 4.1. to 4.4. show examples of adhesive failure, cohesive<sub>adhesive</sub>, interfacial<sub>adhesive</sub>, and interfacial<sub>oxide/adherend</sub> failure.

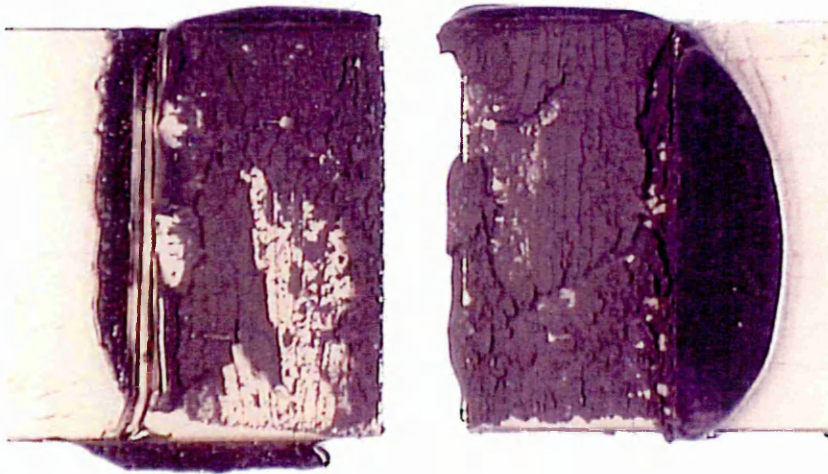
**Plate 4.1.**



ADHESIVE FAILURE

Adhesive failure. Weak adhesion at the adhesive / adherend interface.

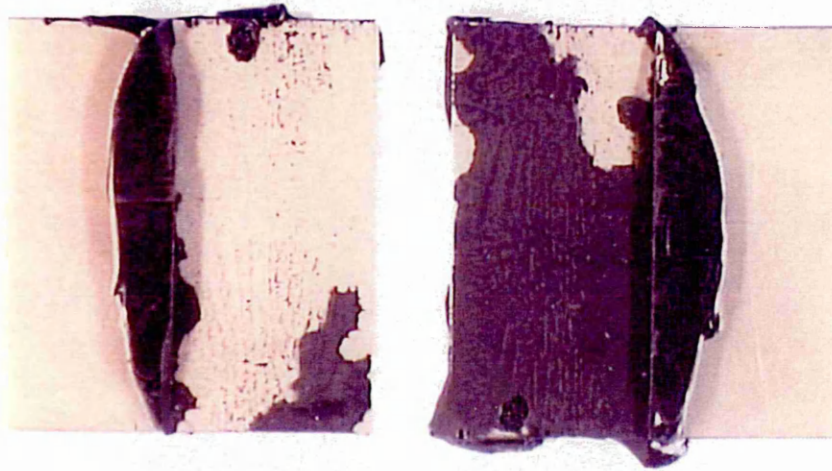
**Plate 4.2.**



INTERFACIAL/COHESIVE FAILURE

Cohesive<sub>Adhesive</sub> failure. Weak cohesion within the bulk adhesive.

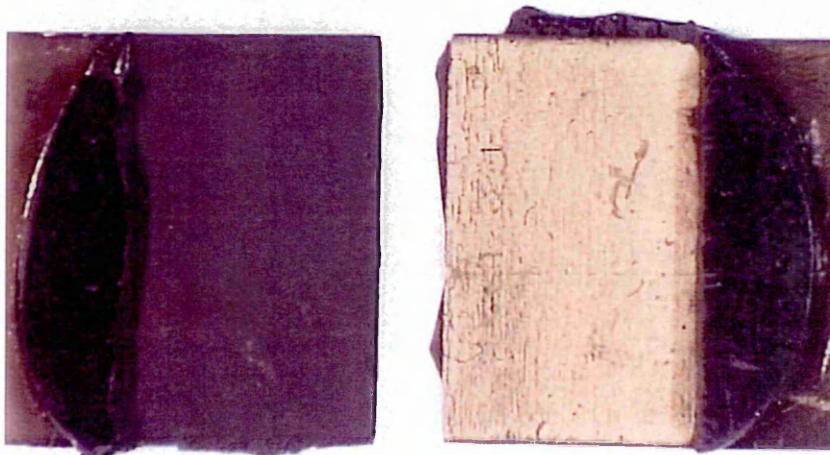
**Plate 4.3.**



ADHESIVE FAILURE

Interfacial<sub>Adhesive</sub> failure. Weak cohesion within the surface adhesive.

**Plate 4.4.**



INTERFACIAL FAILURE

Interfacial<sub>Oxide</sub> failure. Weak adhesion between metallic oxide and parent metal.

#### 4.4. DISCUSSION

Considering the mean apparent lap shear strengths. It would appear that cleaning the surface of the adherend before bonding optimises the strength of the joint. The joints incorporating surfaces subjected to little or no surface pre-treatment, *Dry Wiped* and *As-Received* surfaces, showed a significant reduction in mean apparent shear strength (~ 25%). This suggests that heavy contamination, such as that likely to be present on as-received surfaces, can act as weak boundary layers preventing or marring adhesion, and wiping the surface with a clean, dry cloth will do little more than smear the contaminants from one place to another. The fracture faces of the failed joints supported this evidence; a greater proportion of adhesive failure was observed on the fractures of adherends subjected to the least stringent treatments, and a greater proportion of interfacial and cohesive failure was observed on the surfaces treated more thoroughly (the fractures in general, showed large proportions of adhesive failure at the extremes of the overlap where the peel stresses would have been at a maximum, with areas of interfacial and cohesive failure towards the middle of the fractures, more typical of failure by shear). In addition, the strength of the joints comprising adherends cleaned by more stringent methods gave higher, and generally more consistent, apparent shear strengths. It would seem that *Acetone/Inhibisol Rinsing*, *Alkaline Degreasing*, *Acid Rinsing* (in hydrochloric or sulphuric acid), and *Mechanical Roughening*, are all effective methods of preparing the pre-bonded surface of stainless steel. However, it is conceded that the strength of joints incorporating mechanical roughened adherends, may owe more to mechanical interlocking than to the cleanliness of the adherend surface.

The high mean apparent shear strength of joints incorporating *Smuted* surfaces was obfuscating, since it is reported to be such a weak boundary layer (62). Although failure did occur at the oxide interface, indicating that the smut is indeed very weakly adhered to the etched steel surface, the mean apparent shear strength attained was still one of the highest at nearly 28 MPa. It was probable that final failure occurred as a result of the intense peel forces acting on the extremes of the overlap as the joint rotated during the test, with rapid fracture occurring at the weakest point, the smut, even though a considerable strength was achieved before failure.

Priming the surface of the *Dry Wiped* adherends prior to bonding did nothing to improve lap shear strength. On the other hand, deliberately over-priming the surface did nothing to weaken lap shear strength. The peel test results for joints incorporating *Alkaline Degreased* adherends with non-primed, standard prime and over-primed adherends were equally inconclusive. Perhaps the advantages of priming becomes more obvious with time, and therefore, durability testing might be a better approach to assessing the role of the primer. However, one thing is certain, when a surface primer is employed additional interfaces are created within the joint and this may complicate adhesion. From practical experience, it is considered very difficult indeed to control the amount and distribution of the primer, and very easy to deposit an layer of non-uniform thickness.

Increasing the bondline thickness of the lap shear joints resulted in a reduction in apparent shear strength, which would be expected since the bending moment, induced during the test, would increase with increasing bondline thickness. The peel tests, however, failed to discriminate between joints with reduced and increased bondlines.

Finally, if *Alumina Blasting* is used to physically roughen and/or clean stainless steel there is always the possibility that particles of alumina may be implanted in the steel surface, and thus, galvanic corrosion may result. In addition, *Acid Etching* stainless steels in sulphuric acid could prove very costly, because of the chromium and nickel lost during the violent exothermic reaction.

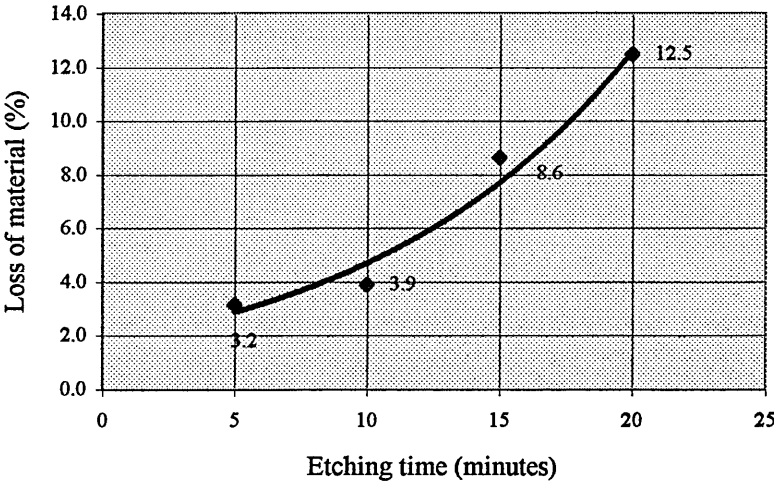


Figure 4.3. Affect of acid etching on stainless steel (weight % loss) (102).

## 4.5. CONCLUSIONS

1. Cleaning the adherend surface prior to bonding improves the mean apparent shear strength, and the cleaning procedure need not be as sophisticated as was first imagined, in fact, simple solvent degreasing e.g. Acetone / Inhibisol Rinsing will probably suffice.
2. Surface priming does little to enhance joint performance, or for that matter, detract from it. Certainly, it is not easy to apply, and controlling its thickness and distribution is difficult.
3. Increasing the bondline thickness of lap joints will result in a lower mean apparent shear strength. Optimum strength is realized at thinner bondlines.
4. Etching stainless steel in sulphuric acid can result in the formation of an iron oxide (smut) on the surface of the etched steel. Although high lap shear strengths may be realised, the oxide is weakly adhered to the metal surface, as the loci of failure were observed to be at the metal / metal oxide interface. The bond between the adhesive and the metallic oxide proved to be more resilient than the bond between the metal and its oxide.
5. *Alumina Blasting* will roughen and effectively clean stainless steel surfaces, but may not be suitable for treating stainless and carbon steels, because the subsequent joint will be susceptible to galvanic corrosion.
6. Etching is an expensive pre-treatment for stainless steel. The inherent oxide present on the stainless surface is destroyed, or at least, compromised, and up to 12 % weight loss can occur within 20 minutes.

## 5.0. Environmental Durability of Adhesive Bonded Stainless Steel Joints

### *Abstract*

*Standard single overlap shear tests and floating roller peel tests were conducted on AISI 304L stainless steel joints bonded with DP 490 toughened epoxy adhesive. The pre-bonded adherends were subjected to minimal surface preparation, i.e. Alkaline Degreasing and priming. Some of the cured lap shear and peel joints were stored in a high relative humidity atmosphere (25 °C, 95% R.H.) for up to 100 days and the remaining joints were aged in ambient conditions. Boeing wedge crack extension tests were also carried out on joints bonded with the toughened epoxy and a polyurethane system 3532. The bonded joints were loaded and kept; at ambient temperature and relative humidity, under high humidity conditions, at -16 °C, or submerged in water. A number of surface pre-treatment were considered: Alkaline Degreasing (with and without priming); Alumina Blasting; Acid Etching; and an acid anodising (Passivating) treatment. The lap shear and peel strengths recorded after ageing were comparable with those obtained initially, and the presence of moisture seemed to do little to adversely affect joint strength. In the wedge tests, however, the surface condition of the adherend material seemed to play an important role in joint durability, and the presence of moisture appeared to have an adverse affect on performance. The epoxy adhesive gave better results than the polyurethane system in the Boeing wedge tests.*

## 5.1. INTRODUCTION

One of the major drawbacks to using adhesives for joining metal members intended for structural applications concerns the perceived poor environmental durability of the bonded structures. Metal-to-metal adhesive-bonded joints often give high initial shear strengths, but in time the strength of adhesion at the metal / adhesive interface may have deteriorated to zero; in a period of time which is much reduced by the presence of moisture. In order to evaluate the environmental durability of adhesive-bonded metal-to-metal joints, the overlap-shear tests and/or peel tests are often employed; joints are prepared and exposed to some deleterious environment for a certain length of time, and then subsequently removed and mechanically tested. However, it is much preferred if the joint is stressed *and* exposed to adverse environments, simultaneously. It is possible to test lap shear test-pieces using purpose-built jigs, in which several pre-bonded joints are mechanically fastened together in series. A tensile load is applied to the series by means of a relaxing, pre-compressed spring. The loaded jigs may then be placed into whatever environment is desired. The main problem with these devices is that if one of the joints fail, it must be replaced with a dummy-bar. This can be time consuming and results in an un-intended relaxation in the tensile load being applied to the other joints in series.

The Boeing wedge crack extension test, is an alternative method of exposing joints to detrimental environments and stress, simultaneously. Wedges are inserted into pre-bonded joints, and the joints are located in some harsh environment, for example, a humidity chamber. Providing no plastic deformation of the adherend occurs, a tensile load is generated and maintained at the tip of the crack that is initiated by the insertion of the wedge. The loaded joints are then exposed for a certain period and the resultant crack growth is monitored.



**Figure 5.1.** Loaded wedge test specimen.

As the crack propagates the effective cleavage load (P) on it decreases because,

$$P = \frac{\delta}{C} \quad (5.1.)$$

where,  $\delta$  is the crack opening displacement (COD) and C is the compliance. The decrease in effective load provides a self arrest capability for the wedge test, which enables the establishment of the threshold level (90) in terms of the Mode I load (P).

Single overlap shear tests and floating roller peel tests (exposed prior to testing) and wedge crack extension tests were used in this investigation as a means of assessing the environmental resistance of DP 490 toughened-epoxy and 3532 B/A polyurethane adhesive-bonded AISI 304L stainless steel joints. DP 490 was selected as a result of its overall performance in the screening programme, and the urethane (used only in the wedge crack extension tests) was chosen because of the excellent peel strength displayed by this adhesive during the screening schedule. This investigation also presented the opportunity to compare two different approaches to investigating durability, one a pre-exposed durability test, the other a sustained load test.

## **5.2. EXPERIMENTAL WORK**

### **5.2.1. MEASUREMENT OF SINGLE LAP-SHEAR STRENGTH AND FLOATING ROLLER PEEL STRENGTH**

Single overlap shear joints and floating roller peel joints were assembled, following the same procedures detailed in *3.0 Adhesive Screening*. AISI 304L stainless steel with a 2B surface finish was employed as the adherend material, and the joints were bonded with the toughened epoxy DP 490. The adherends were alkaline degreased, again by that procedure detailed in *3.0. Adhesive Screening*. The bondline was kept constant at 0.25 mm. Seventy two single overlap shear joints were produced. Half of the joints were stored at 23 °C and 40 to 50 % relative humidity, and the other half were stored at 23 °C and 95 % relative humidity. Six joints, the sample size, were taken from each batch after 1 day, 5 days, 10 days, 55 days, 84 days and 100 days from the day when the joints were assembled. The joints were subsequently tested and the resultant fracture faces analysed. N.B. the fillets of hardened squeeze out were removed prior to testing. Twenty eight peel test joints were also produced; fourteen of which were stored under ambient conditions, and the other fourteen were stored in a high humidity environment. Because the peel test is a continuous test a sample size of two was considered sufficient and two joints were removed from each batch after 1 day, 3 days, 4 days, 5 days, 10 days, 55 days and 100 days. The joints were subsequently tested and the resultant fracture faces analysed. The results of the lap shear and peel tests are given in *5.3. Results*.

### **5.2.2. WEDGE CRACK EXTENSION TESTS**

#### **5.2.2.1. BATCH I**

##### **5.2.2.1.1. TEST MATERIAL AND JOINT CONFIGURATION**

Two hundred blanks (sufficient for 100 joints) were laser cut from 1.5 mm gauge AISI 304L stainless steel with a 2B surface finish. Laser cutting was employed because of its simplicity, accuracy and cost; test pieces could be cut directly to size, 'fash-free', and relatively clean, i.e. there were no contamination from oil and grease that is usually associated with machining. A schematic of a wedge test specimen is given in Figure 5.2.

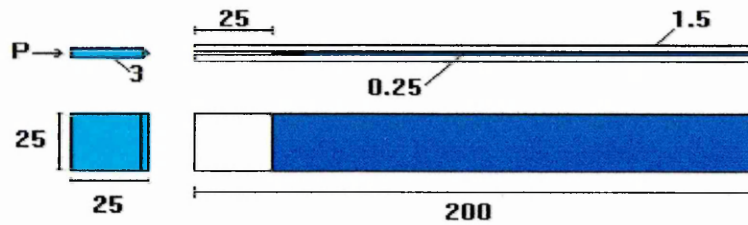


**Figure 5.2.** Wedge crack extension specimen.

### 5.2.2.1.2. SURFACE PRE-BONDING TREATMENTS CONSIDERED

The adherends were divided into 5 sets, each containing 40 blanks (sufficient for 20 joints). Each set was subjected to a different pre-bonding treatment. Most of the treatments have been given previously, however, the passivating treatment is new. The different treatments are listed in Table 5.1. and the details of *Passivating* are given in Table 5.2.

**Table 5.1.** Surface preparation of the adherends for the wedge test joints. Batch I.

SURFACE CONDITION	STAGES INVOLVED	
<b>ALKALINE DEGREASED STANDARD (SILANE) PRIME</b>	STAGE I	<b>ALKALINE DEGREASING</b>
	STAGE II	<b>PRIMING</b>
<b>ALKALINE DEGREASED NO PRIMER</b>	STAGE I	<b>ALKALINE DEGREASING ONLY -NO PRIMER</b>
<b>ALUMINA BLASTED NO PRIMER</b>	STAGE I	<b>ALKALINE DEGREASING</b>
	STAGE II	<b>ALUMINA BLASTING</b>
	STAGE III	<b>ALKALINE DEGREASING -NO PRIMER</b>
<b>ACID ETCHED NO PRIMER</b>	STAGE I	<b>ALKALINE DEGREASING</b>
	STAGE II	<b>ACID ETCHING</b>
	STAGE III	<b>DE-SMUTTING -NO PRIMER</b>
<b>PASSIVATED (NO PRIMER)</b>	STAGE I	<b>ALKALINE DEGREASING</b>
	STAGE II	<b>PASSIVATING - NO PRIMER</b>

**Table 5.2.** Details of passivating stage.

<b>Bath composition:</b>	12% vol. H <sub>2</sub> SO <sub>4</sub> 5% K <sub>2</sub> Cr <sub>2</sub> O <sub>7</sub> bal. de-ionised water
<b>Bath conditions:</b>	Temperature 75°C Current density 1 mA m <sup>-2</sup> Time 15 min Agitated

### 5.2.2.1.3. JOINT ASSEMBLY

The pre-treated adherends were bonded together to make 100 joints; 50 joints were bonded using the toughened epoxy system DP 490 and the remaining 50 were bonded using the polyurethane adhesive 3532 B/A. The spring clips described in 3.0. *Adhesive Screening*, were used to hold the joints together during curing. A schematic showing the assembly method is given in Figure 5.3. The bonded joints were allowed to cure in ambient conditions for 10 days. The spring clips were then released and the excess adhesive removed from the edges. Correction fluid was applied to the edges of the joints, to make monitoring the crack growth easier. Finally the wedges were inserted and the initial crack growth recorded. The loaded joints were then placed in the appropriate environments and the crack extensions monitored with time. The results are given in 5.3. *Results*.

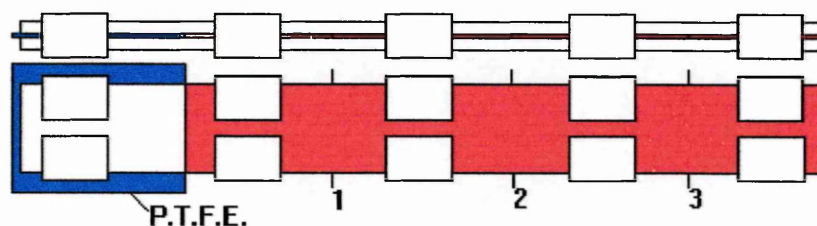


**Figure 5.3.** Assembly method for wedge crack extension test. Piano wire (0.25 mm diameter) was placed at positions 1, 2 and 3.

### 5.2.2.2. BATCH II

When the bonded and cured joints from *Batch I* were loaded, i.e. the wedges were inserted, some of the stainless adherends deformed plastically, and thus, a second batch of test pieces were prepared, this time incorporating 2 mm gauge adherends instead of 1.5 mm; in other respects the steel employed was the same grade as that used in *Batch I*, AISI 304L with a 2B surface finish.. The surface pre-treatments

used have been detailed in previous sections, although an additional primer was introduced, Accomet C, the application of which is given below. The pre-bonding treatments considered were: *Alkaline Degreasing* (no primer); *Alkaline Degreasing* (standard silane primed); *Alkaline Degreasing* (Accomet primed); and *Alumina Blasting* (no primer).

#### **5.2.2.2.1. ACCOMET PRIMING**

The adherends were *Alkaline Degreased* and the clean substrates allowed to dry. The surfaces were then coated with a solution (20 % by volume) of Accomet C™ (Brent Europe Ltd.), which is essentially a chromic acid solution that has been used successfully to bond stainless steels (103). The primed adherends were dried using a hot drier and then stored in a desiccator for 24 hours before they were bonded.

The joints were bonded, cured and prepared by the same procedures used for *Batch I*. The joints were loaded and the initial crack extension recorded, and then they were placed in a domestic freezer (-16°C) for 24 hours, after which the joints were removed and submerged in de-ionised water at room temperature and left to stand for another 24 hours. The results are given in *5.3. Results*.

### 5.3. RESULTS

The lap shear and peel result are given in Tables 5.3. and 5.4., and in Figures 5.4. and 5.5. The Boeing wedge test results (*Batch I*) are given in Figures 5.6. to 5.9., and the results from (*Batch II*) are given in Figures 5.10. and 5.11. N.B. With respect to Table 5.4., data for samples aged for 55 days is limited because the peel curves were destroyed before they could be properly analysed.

**Table 5.3.** Mean apparent shear strengths of DP 490-bonded AISI 304L adhesive joints. Fillets removed prior to testing.

ENVIRONMENT	AGEING TIME	MEAN FAILURE LOAD (kN)	S.D. (± 1 S.D.) (kN)	MEAN APPARENT SHEAR STRENGTH (N.mm <sup>-2</sup> )	S.D. (± 1 S.D.) (N.mm <sup>-2</sup> )	COEFFICIENT OF VARIATION $\frac{S.D.}{\bar{x}} \times 100$ (%)
	(Days)					
Ambient 23°C and 40-50% R.H.	1	4.4	0.1	14.0	0.2	1.2
	5-6	6.1	0.5	19.7	1.5	7.6
	10	6.1	0.8	19.4	2.4	12.4
	55	7.2	0.3	23.0	1.1	4.7
	84	7.4	0.5	23.7	1.5	6.2
	100	6.5	0.4	20.7	1.4	6.6
23°C and 95% R.H.	5-6	5.9	0.8	18.8	2.6	13.6
	10	6.2	0.3	19.9	1.0	5.2
	55	6.2	0.2	19.9	0.5	2.4
	84	4.9	0.8	15.8	2.5	16.0
	100	5.6	0.2	18.0	0.7	3.8

**Table 5.4.** Floating roller peel strengths of DP 490-bonded AISI 304L adhesive joints.

ENVIRONMENT	AGEING TIME (DAYS)	PEEL LENGTH (MM)	PEEL LOAD (N)			MEAN PEEL STRENGTH (N.MM <sup>-1</sup> )	S.D. (± S.D.) (N.MM <sup>-1</sup> )	C.O.V. (%)
			MIN.	MAX.	MEAN			
Ambient 23°C and 40-50% R.H.	1	160	110	176	143.8	5.8	0.5	8.9
	3	160	70	102	84.3	3.4	0.3	9.4
	4	140	69.5	94.5	78.5	3.1	0.2	4.7
	5-6	160	66	140	96.3	3.9	0.7	19.3
	10	150	62.5	91.5	76.5	3.1	0.3	8.3
	55					3.1		
	100	200	65	102	83.3	3.3	0.3	8.1
23°C and 95% R.H.	5-6	160	40	86	68.8	2.8	0.4	13.6
	10	160	42	93	68.6	2.8	0.4	15.4
	55					2.2		
	100	200	55	92	72.5	2.9	0.4	12.6

NB C.O.V. = coefficient of variation

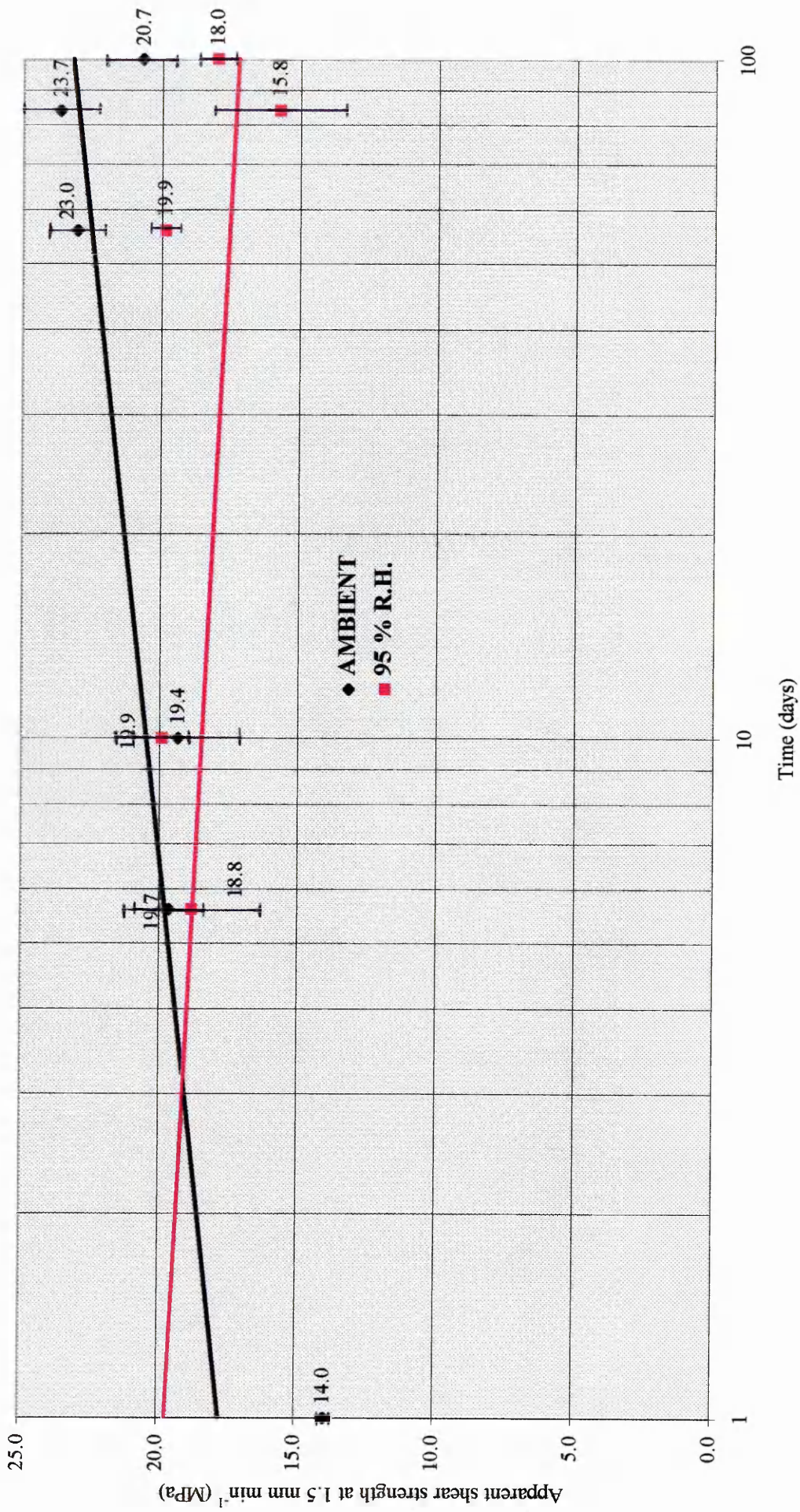


Figure 5.4. Effect of ageing on mean apparent shear strength. Fillets removed prior to testing.

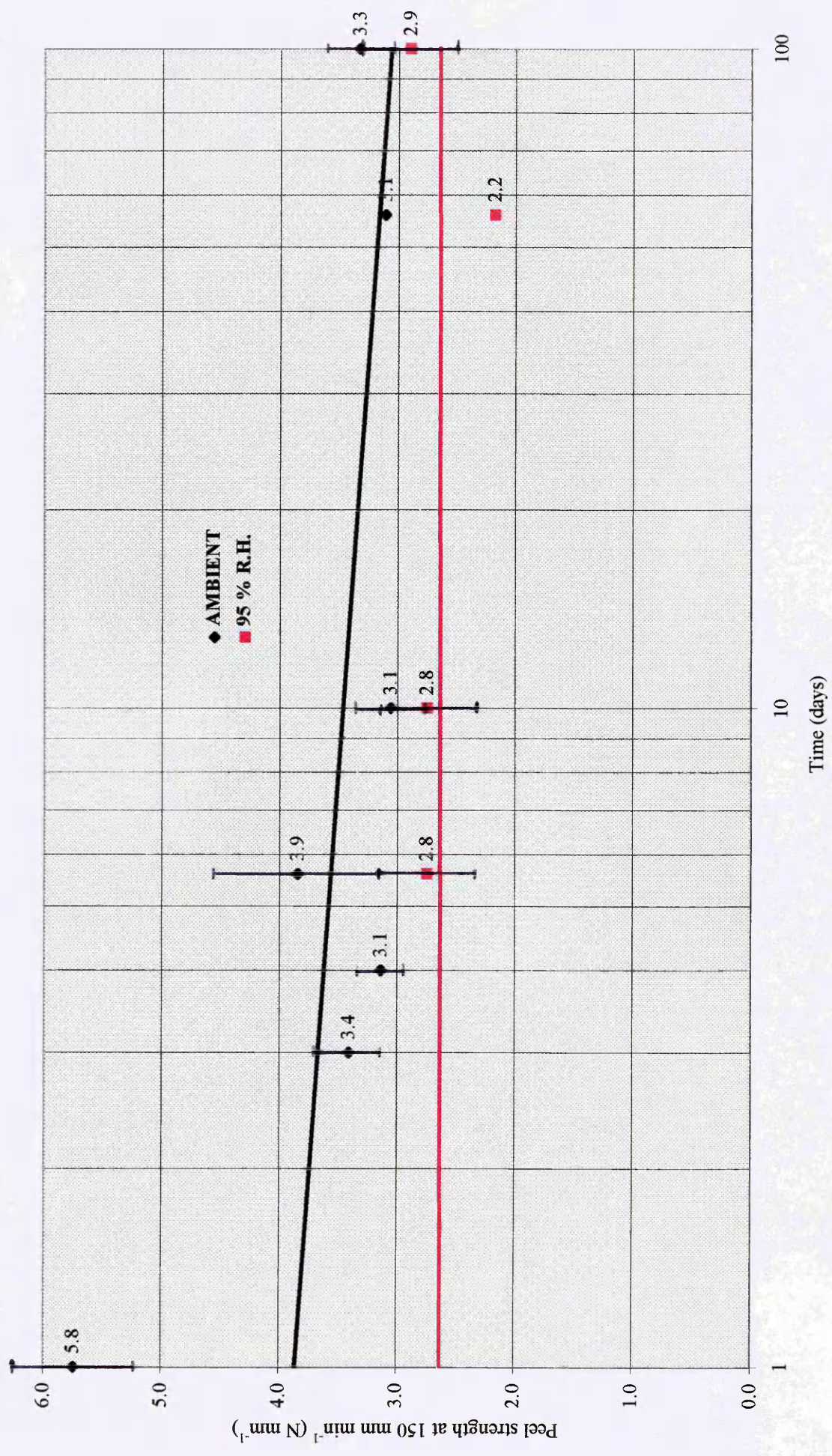


Figure 5.5. Effect of ageing on mean floating roller peel strength.

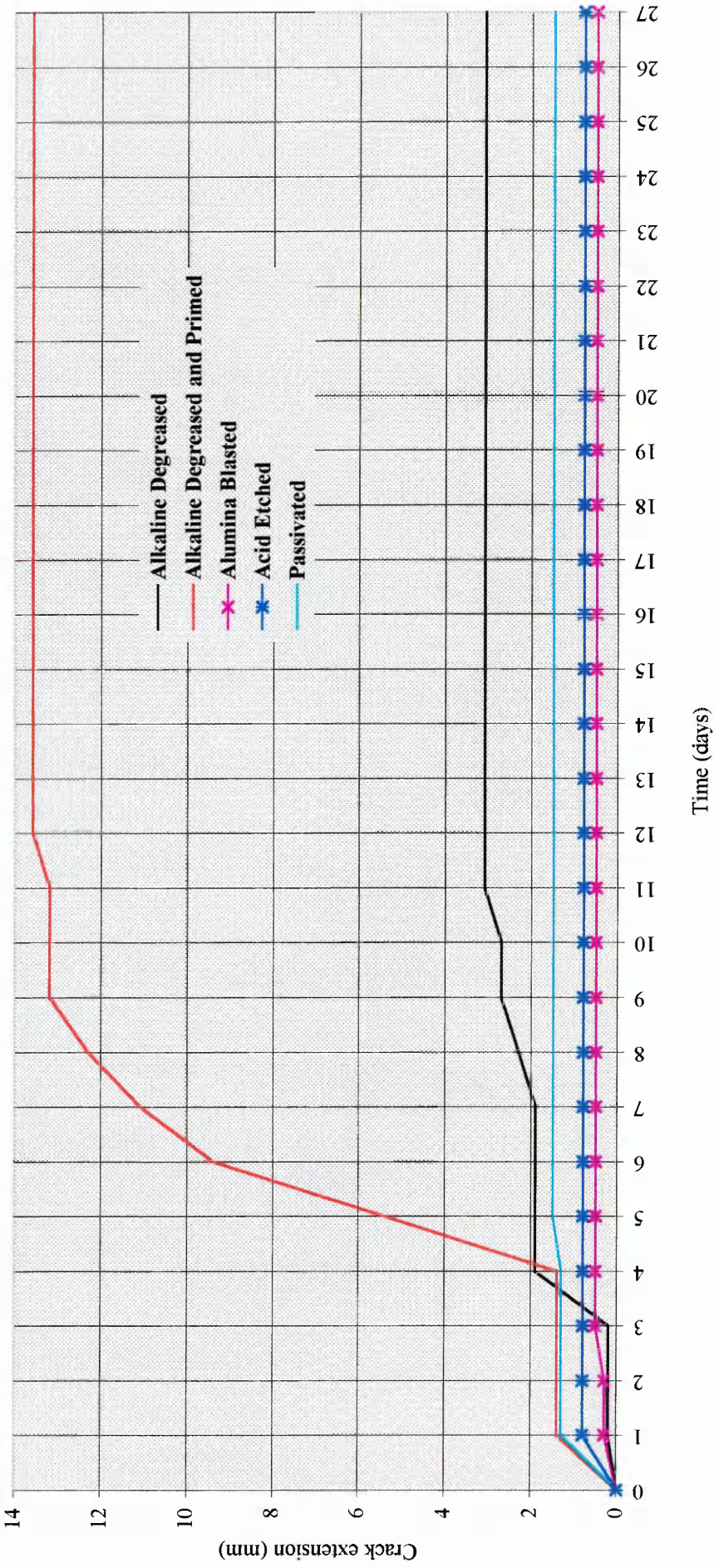
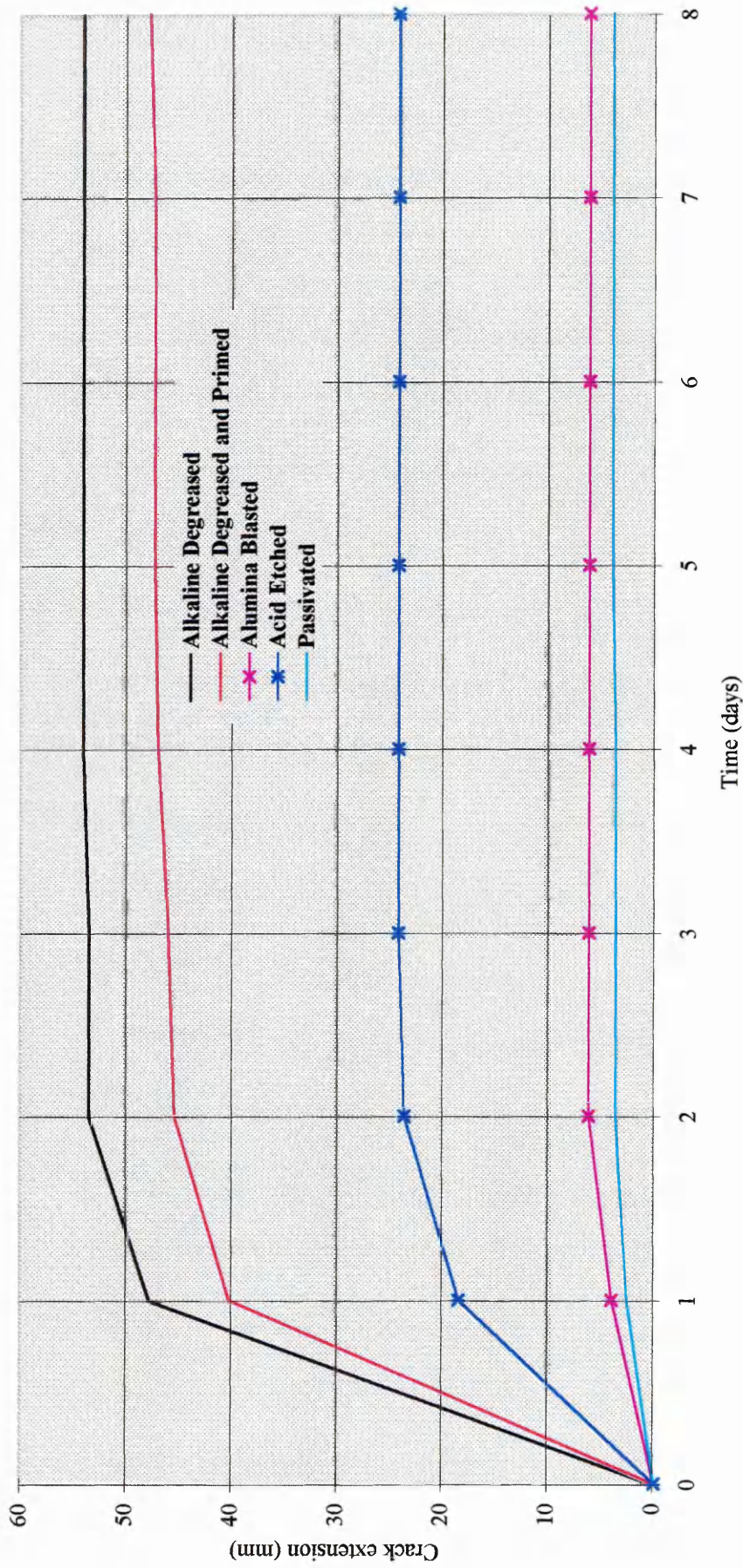


Figure 5.6. Wedge crack extension curve for AISI 304L stainless steel joints bonded with DP 490 toughened epoxy system (Ambient).  
Batch I.



**Figure 5.7.** Wedge crack extension curve for AISI 304L stainless steel joints bonded with DP 490 toughened epoxy system (95% R.H.).  
Batch I.

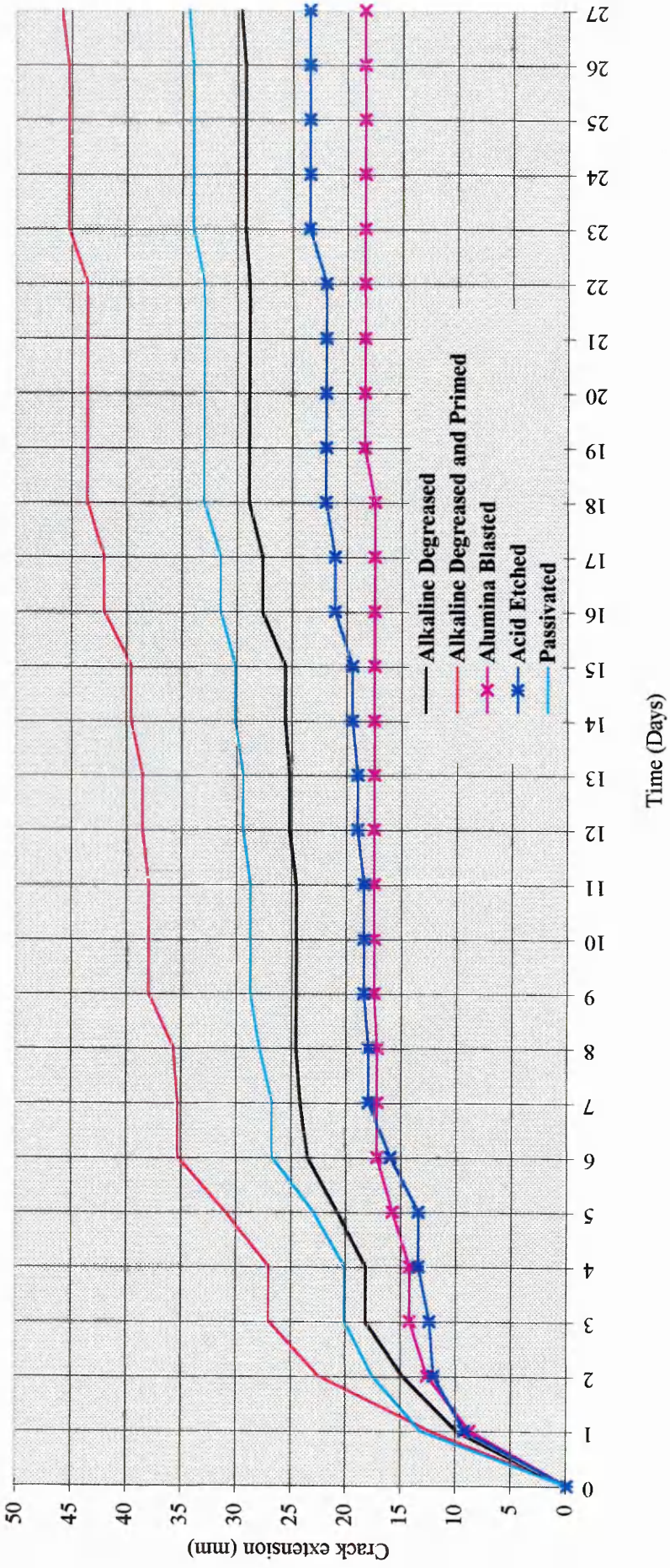


Figure 5.8. Wedge crack extension curve for AISI 304L stainless steel joints bonded with 3532 polyurethane system (Ambient). Batch I.

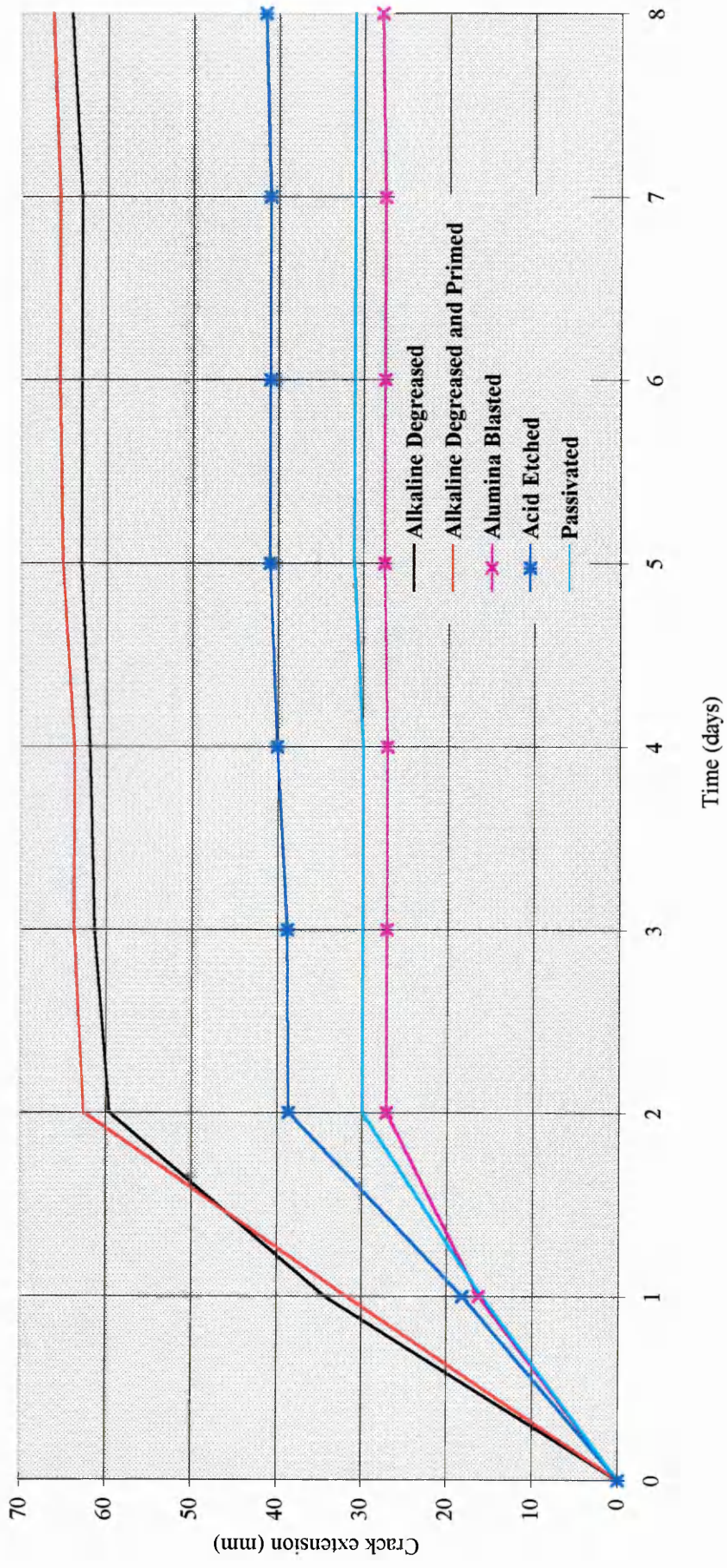


Figure 5.9. Wedge crack extension curve for AISI 304L stainless steel joints bonded with a polyurethane system (95% R.H.). Batch I.

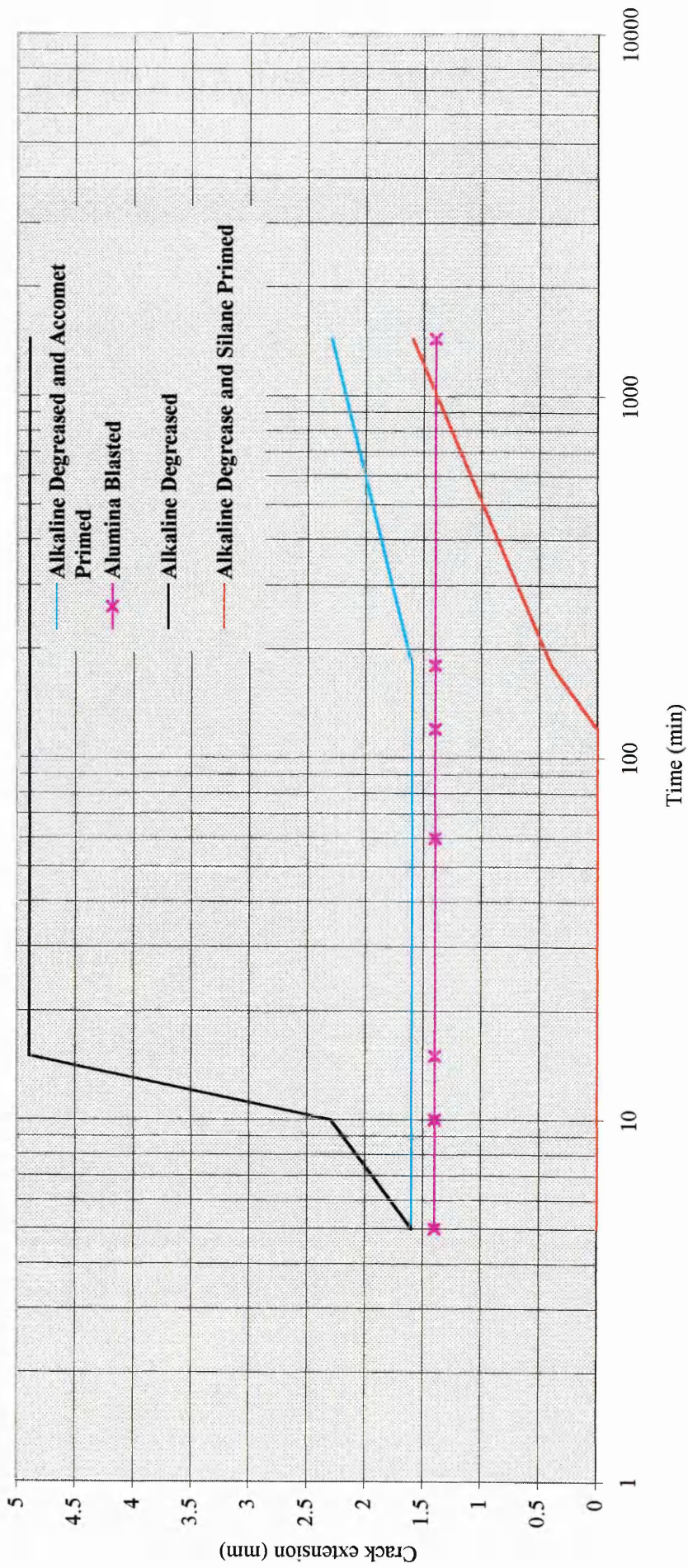


Figure 5.10. Wedge crack extension data for 2mm gauge AISI 304L stainless steel joints bonded with DP 490 toughened epoxy system (-16C). Batch II.

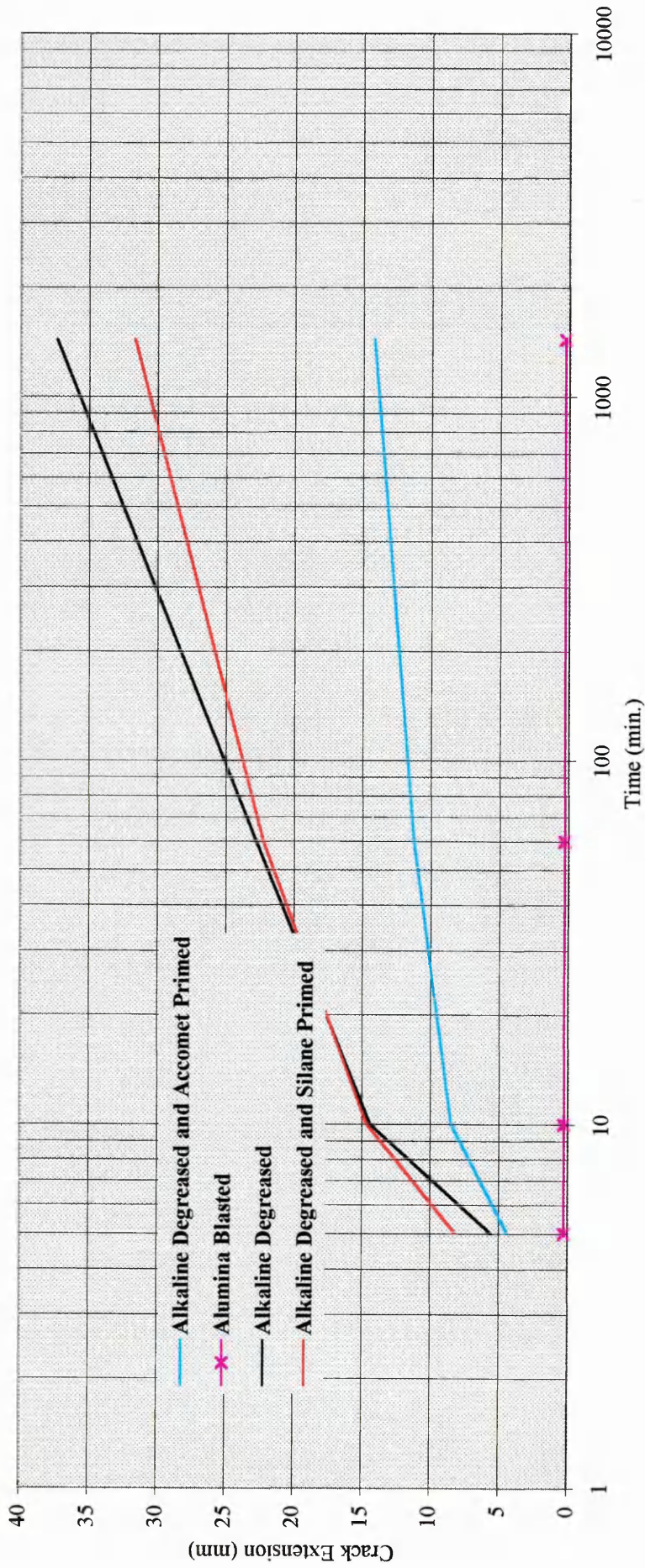


Figure 5.11. Wedge crack extension data for 2mm gauge AISI 304L stainless steel joints bonded with DP 490 toughened epoxy system (Water Soak). Batch II.

### **Considering the lap shear performance.**

The strength of the joints aged at ambient temperature generally showed an improvement with age, from 14 to 20.7 N.mm<sup>2</sup>, optimising at somewhere around 80 days (23.7 N.mm<sup>2</sup>). Although generally lower than the above, the strength of the joints aged in the humid environment remained reasonably constant throughout (~18 to 20 N.mm<sup>2</sup>), the exception being at 84 days, when 15.8 N.mm<sup>2</sup> was recorded.

### **Considering the peel performance.**

For the joints aged at ambient temperature, similar strengths were recorded between 3 and 100 days (3 to 4 N.mm<sup>-1</sup>). However, the strength recorded after only 1 day curing/ageing was surprising high at 5.8 N.mm<sup>-1</sup>. The joints aged in the humid environment gave slightly lower strengths than the above, although they remained generally constant with time (~2.8-2.9 N.mm<sup>-1</sup>), the exception being at 2.2 N.mm<sup>-1</sup> recorded after 55 days.

### **Considering the Boeing wedge tests**

#### **Batch I: Bonded with DP 490**

**Ambient environment** The joints incorporating *Alumina Blasted*, *Acid Etched*, and *Passivated* adherends proved to be very durable, the crack growth not exceeding 2 mm, with the crack arresting after only 1 day. The joints with the *Alkaline Degreased* (un-primed) surfaces also proved to be reasonably durable, although crack growth reached 11 mm before arresting. The joints incorporating the *Alkaline Degreased* (primed) adherends gave poor durability, with rapid crack growth occurring after 4 days, from 2 mm to 15 mm.

**High humidity environment** The joints incorporating *Alumina Blasted* and the *Passivated* adherends proved to be very durable, with crack growth not exceeding 2 mm. For joints with the *Acid Etched* adherends, the crack extension reached 20 mm before arresting, after about 2 days. The joints incorporating the *Alkaline Degreased* adherends (primed and un-primed) proved to be the least durable, with rapid crack growth to about 40 to 50 mm in 1 to 2 days.

### **Batch I: Bonded with 3532**

**Ambient environment** All the joints showed rapid crack growth within the first day, up to around 10 mm. After this time, gradual but continuous crack growth was observed. The joints with the *Alumina Blasted* adherends reached about 17 mm in 6 days before arresting. The cracks in the joints incorporating the *Acid Etched* adherends kept on growing, reaching 22 mm in 27 days. Similarly, the cracks in the joints incorporating the *Passivated*, the *Alkaline Degreased* (primed), and the *Alkaline Degreased* (un-primed) surfaces continued growing, reaching 28 mm, 33 mm, and 45 mm, respectively, in 27 days.

**High Humidity environment** The joints incorporating the *Alumina Blasted*, *Acid Etched* and *Passivated* surfaces displayed rapid crack growth within the first 2 days, up to about 25 to 40 mm. The joints with the *Alkaline Degreased* adherends (primed and un-primed), gave an even poorer performance, the crack extension reaching about 60 mm, within 2 days.

### **Batch II: Bonded with DP 490**

**Sub-zero (-16°C) environment** The joints with the *Alkaline Degreased* (un-primed) adherends performed poorly, showing significant crack growth (~ 5 mm) after only about 15 minute, after which time no further crack growth was observed. The joints incorporating the standard silane primed adherends and those with Accomet primed surfaces showed no crack propagation until almost 2 hours had elapsed, when gradual crack growths were observed. The joints with the *Alumina Blasted* surfaces performed extremely well, with hardly any crack growth observed at all after 24 hours.

**Submerged in water at 23 °C** Once again the joints incorporating the *Alumina Blasted* adherends gave an outstanding performing, with no crack growth whatsoever. The joints with the *Alkaline Degreased* adherends (standard silane primed and un-primed) performed about the same, showing considerable crack growth, starting after about 5 minutes and gradually increasing to ~ 30 mm after 24 hours. The joints with the Accomet primed surfaces gave a moderate performance, showing gradual but steady crack growth with time. Generally, the crack extensions for the joints exposed to water were considerably greater than those of joints exposed to - 16°C.

## 5.4. DISCUSSION

The mean apparent shear strengths of the stainless/epoxy-bonded joints stored in a dry environment appeared to improved with age, only giving inferior strengths when the joints were tested before the recommended curing period had elapsed. During curing the base resin and the hardener are cross linking, and most of the cross linking occurs quickly, within the first few days. However, the remaining cross linking will occur gradually, thus, testing prematurely means testing joints that are insufficiently cured and low joint strengths will be realised. The reason for the mean apparent shear strength increasing with age, probably means that good adhesion between the adhesive and adherend was achieved when the joints were first bonded, and this remained an intimate union because the ambient air was kept dry throughout the ageing period. The lap joints aged in a humid environment remained about the same strength throughout the ageing period and appeared not to be adversely affected by the presence of moisture, although the strength of joints aged under humid conditions were generally lower than those of joints aged in the dry environment. Thus, it is reasonable to assume that some weakening of the bond occurred as result of water impregnation.

The floating roller peel strengths remained reasonable constant throughout the ageing period, in both dry and humid environments. This indicates again that the adhesive must have been intimate with the adherend during bonding and a strong bond was thus achieved and maintained. However, the peel strengths were slightly lower for the joints aged in the presence of water, compared to the strengths of those aged in dry conditions. The disadvantage of lap shear and peel testing is that the joints are loaded after they have been aged, rather than being loaded and aged simultaneously, thus, the results may be misleading.

The wedge crack extension tests were much more conclusive. Joints incorporating mechanically or chemically roughened surfaces appeared to be much more durable than those joints with physically unmodified adherends, blasting with alumina seeming to be the optimum adherend pre-bonding treatment, out of the ones considered. The least durable, by far, were the joints incorporating adherends that had received minimal surface preparation, i.e. *Alkaline Degreased*, (primed and non-primed). Priming the surface did little to improve durability, in fact it may have proved detrimental, because there was some

visual evidence on the fracture faces of failure within the primer layer (characteristic shocking pink observed on corresponding halves of fracture). The high durability of joints with physically modified adherends was attributed to surface roughening, in that the movement of the crack between adhesive and adherend under Mode I loading was somehow impaired by the peaks and troughs of the roughened surfaces, as shown in Figure 5.12.

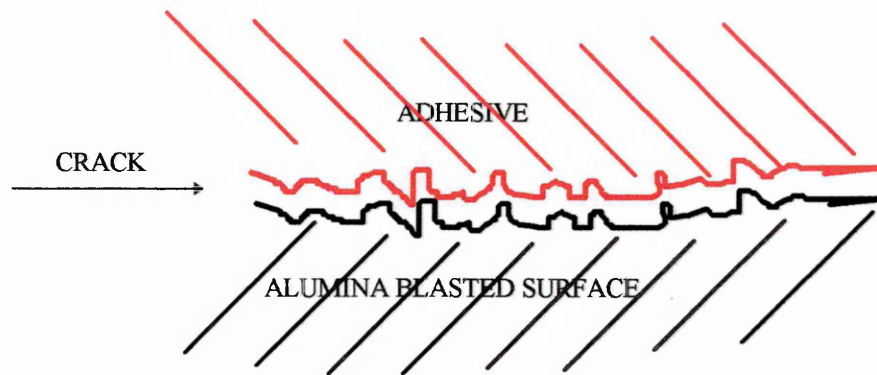


**Figure 5.12.** Schematic of crack propagation in wedge test; adhesive failure.

Alternatively, the improvement in durability may be attributed to the increased surface area available for bonding or because of the higher energy of the surfaces, both afforded by roughening the surface. It may even be due to an increased degree of mechanical interlocking, or simply, to the more rigorous cleaning action of the mechanical and chemical roughening treatments.

The wedge joints bonded using the toughened epoxy (DP 490) proved to be more durable than those bonded with the polyurethane system 3532, which was surprising considering the excellent performance of the urethane in the peel tests detailed in 3.0. *Adhesive Bonding*. The performance of the toughened epoxy, therefore, was attributed to the filler within the adhesive preventing or at least hindering crack growth. Joints bonded with the toughened epoxy gave excellent durability at sub-zero temperatures which was encouraging, although the durability displayed in the presence of moisture was generally poor, and independent of the adherend surface condition. The durability of joints bonded with the polyurethane system also deteriorated in the presence of moisture.

## 5.5. CONCLUSIONS

1. Mean apparent shear strength was not adversely affected by ageing in a dry environment.
2. Mean apparent shear strength was only moderately affected by ageing in a humid environment.
3. Under cured lap joints (prematurely tested) gave low mean apparent shear strengths.
4. Floating roller peel strength was not adversely affected by ageing in a dry, or a humid, environment.
5. Floating roller peel strength reaches an optimum after curing for 24 hours.
6. Roughening the surface of the adherend prior to bonding, either by mechanical or chemical means, will impair crack propagation and thus improve joint durability.
7. Toughened epoxy system gave a better performance than polyurethane system.
8. Durability of adhesive joints under peel or Mode I loading was adversely affected by the presence of moisture.
9. AISI 304L stainless steel joints bonded with the toughened epoxy system DP 490 were durable at temperatures down to -16 °C for 24 hours.

## **6.0. Comparison of the Mean Apparent Shear Strength of Stainless Steel Lap Joints Incorporating Different Steel Grades and Surface Finishes**

### *Abstract*

*Single-overlap-shear tests were carried out on adhesive-bonded stainless steel joints in order to evaluate the significance of the adherend condition. Four distinct grades of stainless steel, in two gauges and with three types of surface finish, were incorporated in the schedule. The condition of the surface appeared to have little effect on subsequent joint strength, although an increase of ~25 % was observed between joints with 1.25 mm and 2 mm thick adherends. The greatest difference in strength, however, was observed between those joints incorporating the different grades; joints with the stiffest adherends gave the highest joint strengths.*

## 6.1. INTRODUCTION

At this point in the dissertation reference is made to the first of the project objectives (1.0 *Introduction*):

*- to evaluate a number of different adhesive systems, in order to find a structural adhesive that is compatible with stainless steel.*

The mean apparent shear and floating roller peel strengths have been used as criteria, together with the locus of failure, ease of application and cost, to screen a number of adhesive systems considered to have the potential to bond stainless steels (3.0. *Adhesive Screening*). Thus, the first objective has in part been addressed. However in the screening programme and subsequent work, only one adherend material was considered; AISI 304L - a low carbon, austenitic grade. But stainless steels are a range of alloys of unique composition with a diverse range of physical and mechanical properties (2.2.5.1. *An Introduction to Stainless Steels*). Thus, the first objective has in part been neglected. To remedy the situation a testing schedule was devised which incorporated four different types of adherend material representing the main families of stainless steels: austenitic; ferritic; martensitic; and duplex.

Because the chemistry of the bulk stainless steel to a large extent determines the physical and chemical nature of the inherent surface oxide, which in turn may, or may not, influence adhesion, the four different families were selected to provide a diverse range of bonding surfaces, each chemically and physically unique. Different surface finishes were also considered in the investigation since the chemical and physical properties of the intrinsic oxide can also be influenced by the production route, which will also determine the macro-roughness of the surface, which may be significant to adhesion. During the lap shear tests carried out in previous work, the joints were observed to rotate under tensile loads to an extent sufficient to plastically deform the adherends, just prior to fracture. Thus, the stiffness of the adherends was thought to contribute to lap shear strength, and therefore, two adherend thickness' were also considered in the investigation. The thickness and surface finish of the four grades of stainless steel evaluated was subject to availability rather than through design.

The single overlap shear test was the mechanical test method selected to evaluate joint integrity, because of its 'simplicity' and cost, and because the single overlap configuration is typical in adhesive bonded fabrications. The surface pre-bonding treatment was kept to a minimum to avoid modifying the as-received surfaces and no surface primers were used for the same reason. The joints were simply cleaned and dried before they were bonded. The joint preparation, bonding and mechanical testing detailed in this chapter was carried out jointly with Margereta Groth-Ring at Luleå University.

## 6.2. EXPERIMENTAL WORK

### 6.2.1. MATERIAL AND TEST PIECE DIMENSIONS

The test pieces were cut from sheet material using two different techniques, laser and a high pressure water jet. Both these methods proved to be accurate ( $\pm 0.05$  mm) and cost effective; laser at £ 0.65 / sample compared with milling at £ 6.25 / sample. The test pieces cut using laser and water were also relatively clean compared to the milled test pieces, which were contaminated with machine oil, coolant and fash. This necessitated additional stages, to allow the heavy contamination and fash to be removed, before final cleaning and subsequent bonding, whereas, the laser and water cut test pieces were ready to clean and bond immediately. The test piece dimensions are given in Figure 6.1.

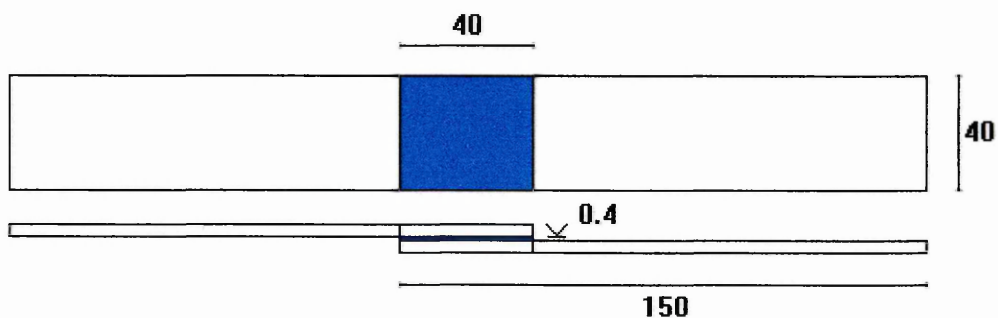


**Figure 6.1.** Single lap joint showing test piece dimensions (mm).

The material grades included in the regime were representative of the four main types of stainless steel. In addition, three surfaces finishes were represented, and two gauges considered. The stainless steels used are detailed are in Table 6.1. and the chemical composition and mechanical properties of the different grades are given in Tables 6.2. and 6.3., respectfully.

**Table 6.1.** Stainless steel grades and surface finishes.

DESIGNATION	GRADE	GAUGE	SURFACE FINISH
EN 1.4512	Ferritic	2 mm	2B
EN 1.4462	Duplex	2 mm	2D
AISI 304L	Austenitic	2 mm	2B
AISI 304L	Austenitic	1.25 mm	2B
AISI 304L	Austenitic	1.25 mm	BA
AISI 420	Martensitic	1.25 mm	2B

Where 2B is the designation for a matt surface finish; BA represents a bright annealed surface finish; and 2D designates a semi-bright surface finish. Ninety six test pieces were produced, sufficient for forty eight lap joints: sample size 8 joints per condition.

**Table 6.2.** Chemical compositions of the stainless steels.

	% C	% Ni	% Cr	% Mn	% Mo	% Si	% N	% P	% S
EN 1.4512 Ferritic	0.02	-	12.0	-	-	-	-	-	-
EN 1.4462 Duplex	0.02	5.5	22.0	-	3.0	-	0.17	0.025	-
AISI 304L Austenitic	0.04	9	18.5	-	-	-	-	0.025	0.001
AISI 420 Martensitic	0.21	0.4	13.2	0.45	-	0.4	-	0.025	0.015

**Table 6.3.** Mechanical properties of the stainless steels.

<b>MATERIAL</b>	<b>0.2% PROOF STRESS (MPa)</b>	<b>ULTIMATE TENSILE STRENGTH (MPa)</b>	<b>YOUNG'S MODULUS OF ELASTICITY (GPa)</b>
EN 1.4512 Ferritic	340	540	220
EN 1.4462 Duplex	540	780	200
AISI 304L Austenitic	310	620	195
AISI 420 Martensitic	1320	1670	220

Data and test material supplied by Avesta Sheffield AB and Uddeholm Strip (martensitic). The values given are for the cold rolled condition, with the exception those of the martensitic grade which are for the cold rolled, hardened and tempered condition.

Note: Because stress/strain curves for stainless steels exhibit no definite yield point, the proof stress is normally measured as an alternative to mark the onset of plastic deformation. The proof stress is determined by drawing a line parallel to the linear portion of the stress/strain curve at 0.2 strain. See Figure 6.2.

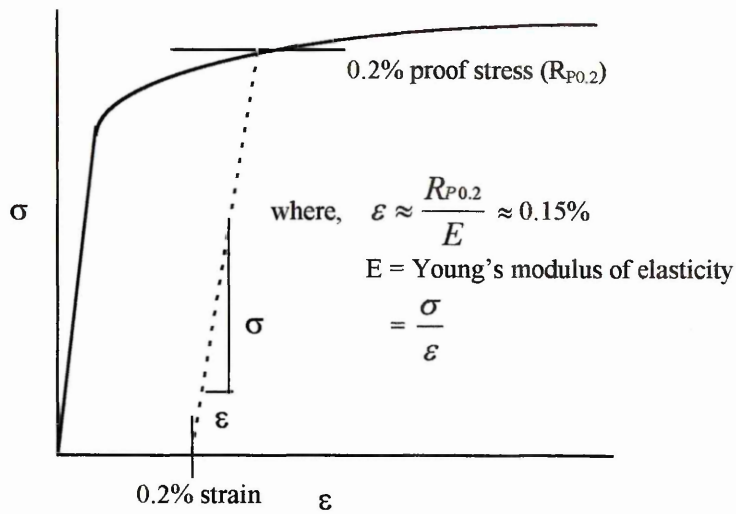


**Figure 6.2.** Typical stress/strain curve for stainless steels.

### 6.2.2. SURFACE PRE-BONDING TREATMENTS

Immediately prior to bonding, the adherends were subjected to minimal surface preparation by *Solvent Wiping*. They were first wiped with lint-free cloth wetted with isopropanol alcohol (IPA). The surfaces were then wiped with an acetone-wetted cloth. The cleaned substrates were wrapped in clean cloth and stored in a dry cabinet until they were needed for bonding.

### 6.2.3. JOINT ASSEMBLY

The joints were assembled manually using the modified epoxy DP 490. An assembled joint is shown in Figure 6.3. Piano wire, 0.4 mm diameter, was used to control the bondline (A) and the joints were held together during curing using bulldog clips (B). The assembled joints were allowed to cure for 10 days at 23 °C and 40 % relative humidity.

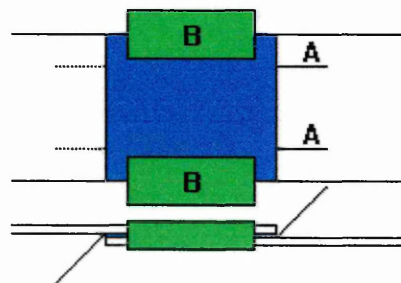


**Figure 6.3.** Lap shear joint assembly procedure.

#### **6.2.4. MECHANICAL TESTING**

The cured joints were tested at  $1.3 \text{ mm. min.}^{-1}$  in accordance with ASTM D1002 using a 50 kN servo-hydraulic MTS test machine. The subsequent fracture faces were examined visually and using SEM to ascertain the loci of failure. N.B. Hardened adhesive fillets around the perimeter of the joint resulting from 'squeeze-out' during joint closure were removed prior to testing.

## 6.3. RESULTS

### 6.3.1. MECHANICAL TEST RESULTS

The mechanical test results are given in Table 6.4. and in Figure 6.4.

**Table 6.4.** Initial overlap shear strengths of adhesive-bonded stainless steel joints. Fillets removed prior to testing.

TYPE OF STEEL AND DESIGNATION	SURFACE FINISH	GAUGE (mm)	MEAN APPARENT SHEAR STRENGTH (MPa)	S.D. (MPa)	COEFFICIENT OF VARIATION (%)
EN 1.4512 Ferritic	2B	2	16.0	1.0	6.1
EN 1.4462 Duplex	2D	2	22.9	0.9	4.1
AISI 304L Austenitic	2B	2	16.1	0.7	4.3
AISI 304L Austenitic	2B	1.25	13.1	0.3	2.0
AISI 304L Austenitic	BA	1.25	12.5	0.2	1.7
AISI 420 Martensitic	BA	1.25	23.9	0.7	2.8

#### Considering joints with 1.25 mm gauge adherends

No significant difference was observed between the joints including the 2B surfaces and those with the bright annealed surfaces, 13.1 ( $\pm 0.3$ ) MPa and 12.5 ( $\pm 0.2$ ) MPa, respectively. The mean apparent shear strength of the bonded austenitic joints with the 2B finish were 13.1 ( $\pm 0.3$ ) MPa and 16.1 ( $\pm 0.7$ ) MPa, for the joints with the 1.25 mm and 2 mm adherends, respectively. An increase of 23 %.

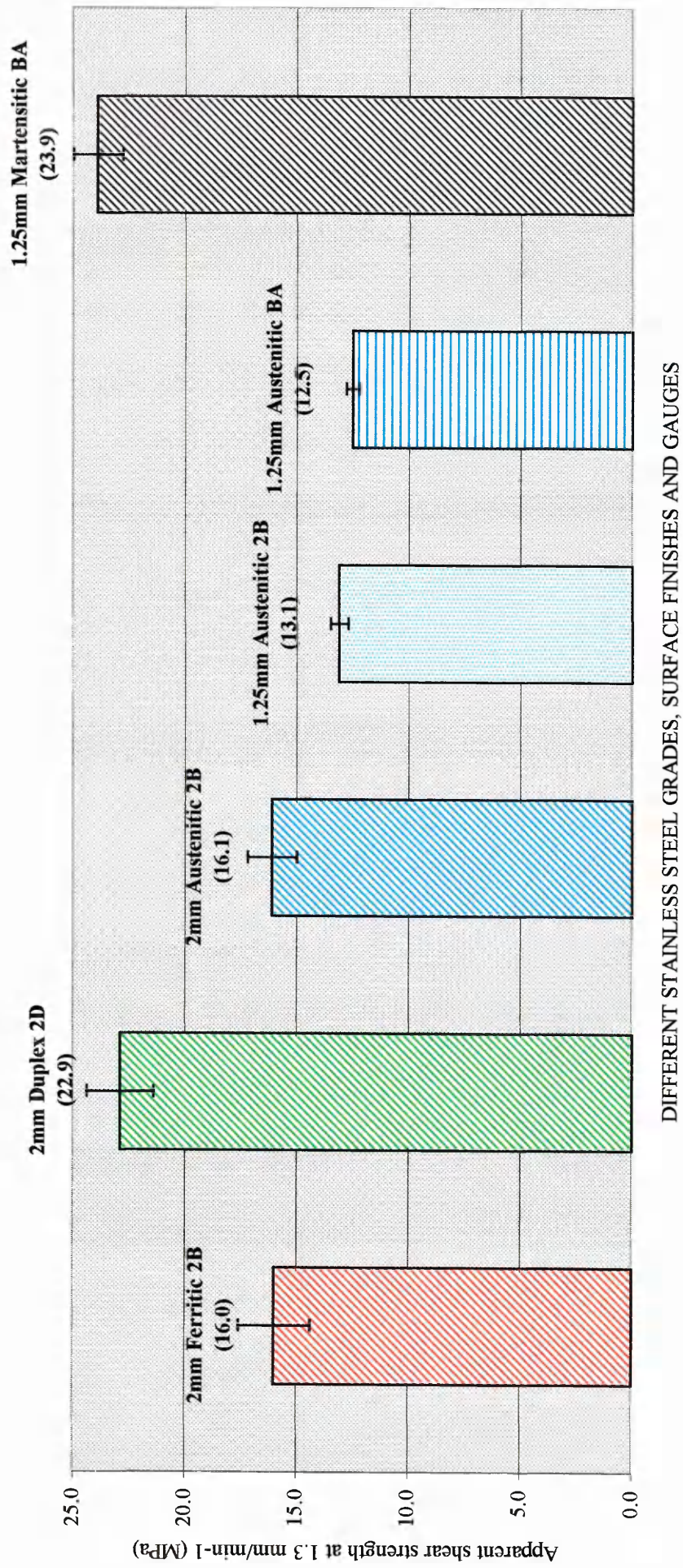


Figure 6.4. Mean apparent shear strength of DP 490-bonded AISI 304L stainless steel lap joints. Fillets removed prior to testing.

### Considering joints with 2 mm gauge adherends

The mean apparent shear strength for the joints incorporating the ferritic adherends was almost identical to that of the joints with the austenitic adherends; 16.0 ( $\pm 1.0$ ) MPa and 16.1 ( $\pm 0.7$ ) MPa, respectively. The joints with the duplex adherends, however, performed much better at 22.9 ( $\pm 0.9$ ) MPa. For the joints incorporating the 1.25 mm adherends. Similar values were observed between the austenitic grades (see above). The highest mean apparent shear strength was displayed by the joints with the martensitic adherends at 23.9 ( $\pm 0.7$ ) MPa. An excellent performance, more than equaling that of the joints incorporating the 2 mm duplex adherends (see above).

### 6.3.2. LOCI OF FAILURE

Figure 6.5. shows a typical fracture face. Evidence of adhesive failure was observed at the extremes of the fracture faces, and the interfacial and cohesive failure was restricted to the central regions.

Interfacial<sub>Adhesive</sub> represents failure within the surface of the adhesive.

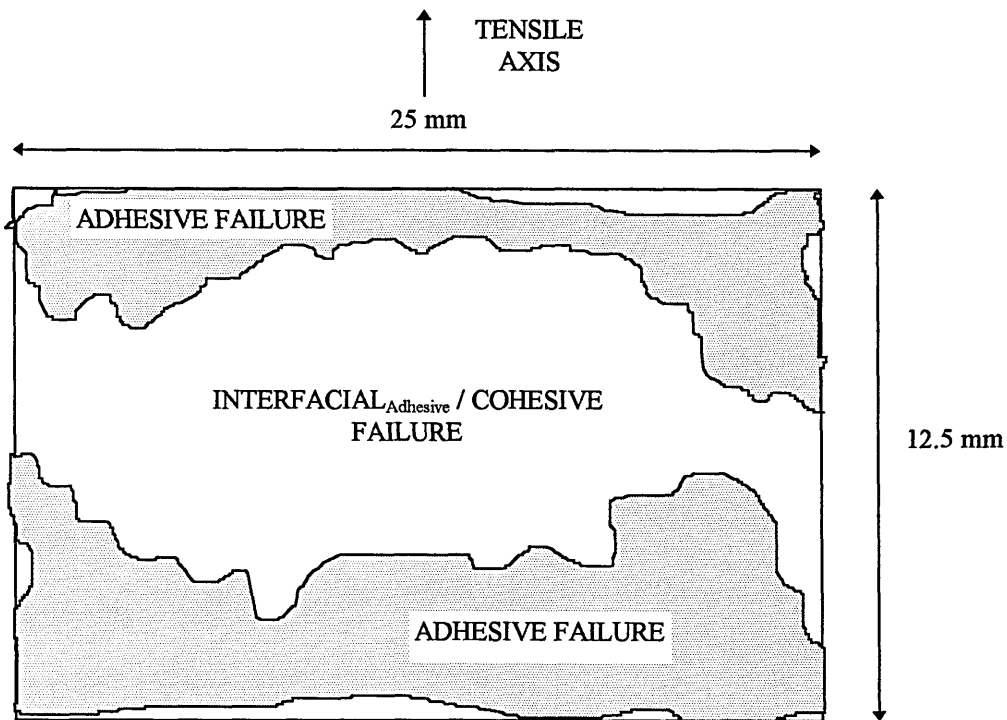


Figure 6.5. Schematic of typical fracture face showing predominant loci of failure.

## 6.4. DISCUSSION

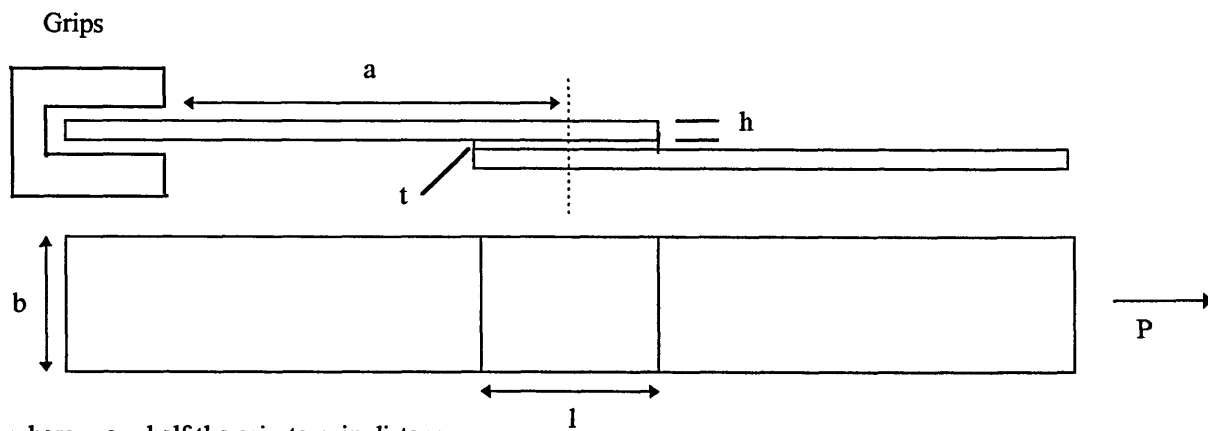
Generally, high joint strengths were realised even though the surface preparation of the pre-bonded adherends had been minimal, i.e. *Solvent Wiping*. The fracture faces also showed a high enough proportion of cohesive and interfacial<sub>Adh</sub> failure (within the adhesive) to suggest that a good bond had been achieved between the toughened epoxy and the steels. Thus, solvent wiping using IPA and acetone must be considered as adequate surface preparation for stainless steel adherends; at least with respect to initial joint strength.

The different surface finishes considered in the evaluation (2B, 2D and BA) would be expected to vary physically in terms of surface roughness (at least on a micro-scale), and in terms of the physical and chemical nature of the intrinsic oxide. But however great these variations might have been they did not observable contribute to, or detract from, the initial measured joint strength. Thus, the stainless steel surfaces were not characterised, either physically or chemically.

Before considering the thickness and yield strength of the adherend, it is worth noting that the mean apparent shear strengths recorded were much more consistent than those dealt with in previous chapters, even though the fillets of hardened adhesive ('squeeze-out') were removed prior to mechanical testing, a procedure that has been shown to adversely affect not only the joint strength but the consistency of the results (see Chapter 3.0. *Adhesive Screening*). The improved consistency was, therefore, attributed to the smoother operating mechanism of the hydraulic tensile test machine compared to that of the tensile test machine used previously that was mechanically driven.

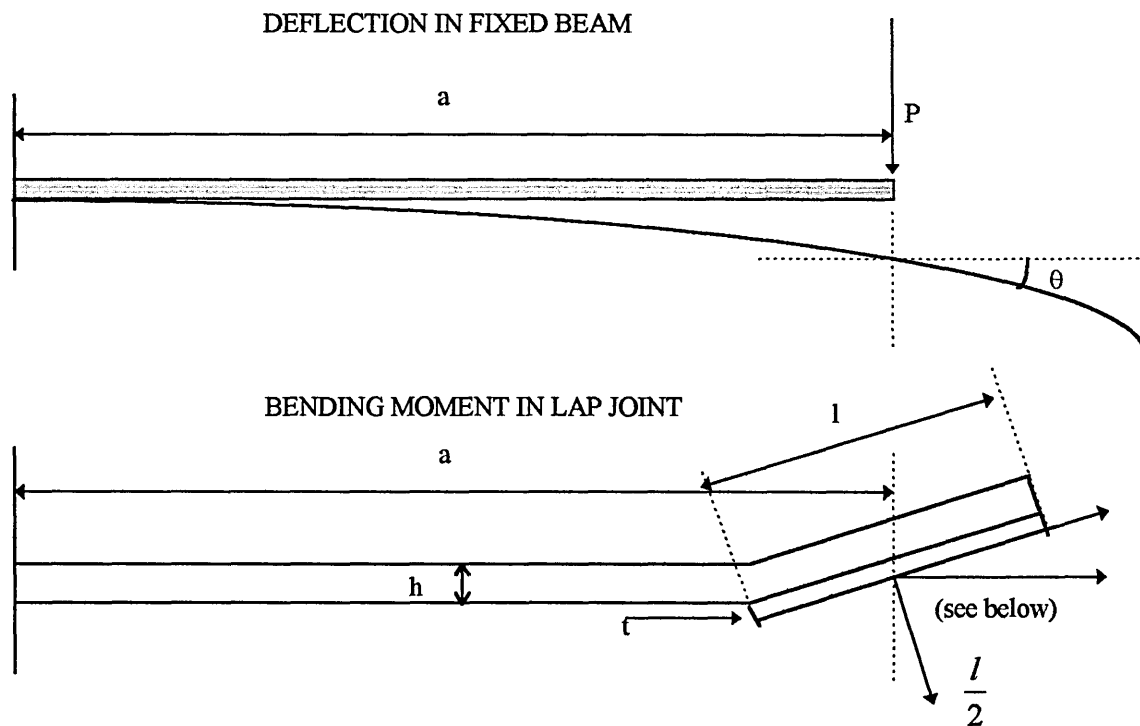
Now considering the significance of the adherend thickness and its intrinsic yield strength, which are both factors that appeared to significantly influence the apparent shear strength of the lap joint.

Consider a single overlap joint in tension:



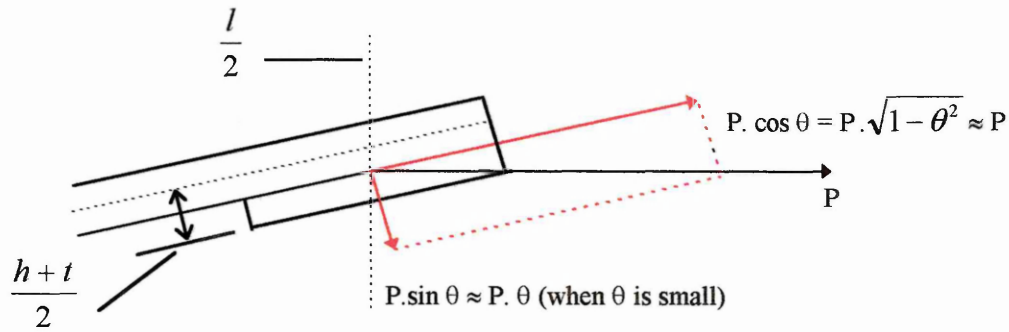
where  $a$  = half the grip-to-grip distance  
 $b$  = joint width  
 $h$  = adherend thickness  
 $l$  = length of overlap  
 $t$  = adhesive thickness  
 $p$  = applied load

Because the directions of the two forces ( $P \leftarrow \rightarrow P$ ) are not co-linear a bending moment is induced as the load is increased and the joint rotates to bring the line of action closer to the centre of the adherends in order to reduce the value of the bending moment. At this point the joint becomes analogous with the deflection of a fixed beam under load.



where  $\theta$  = angle of deflection / angle of rotation

Resolving the components of the load at the centre of the overlap,



The bending moment may be defined as,

$$M = P \cdot \frac{(h+t)}{2} \quad (6.1.)$$

Assuming that no rotation can take place at the grips, the rotation due to moment is given by,

$$\theta_m = \frac{M \cdot a}{E \cdot I} \quad (6.2.)$$

where  $\theta_m$  = rotation due to moment,

$E$  = Young's modulus of elasticity of adherend,

$I$  = inertia for a rectangular plane.

where inertia for a rectangular plane is,

$$I = \frac{b \cdot h^3}{12} \quad (6.3.)$$

Substituting (6.1.) and (6.3.) into (6.2.),

$$\theta_m = 6 \cdot \frac{P \cdot (h+t) \cdot a}{E \cdot b h^3} \quad (6.4.)$$

Rotation due to peel stresses,

$$\theta_p = \frac{P \cdot a^2}{2 \cdot E \cdot I} \cdot \theta_{TOTAL} \quad (6.5.)$$

where  $\theta_p$  = rotation due to peel stresses.

Substituting (6.3.) into (6.5),

$$\theta_p = 6 \cdot \frac{P \cdot a^2}{E \cdot b \cdot h^3} \cdot \theta_{TOTAL} \quad (6.6.)$$

where  $\theta_{TOTAL}$  = total rotation.

Thus, 
$$\theta_{TOTAL} = \theta_m - \theta_p \quad (6.7.)$$

Therefore, 
$$\theta_{TOTAL} = 6 \cdot \frac{P \cdot (h+t) \cdot a}{E \cdot b \cdot h^3} - 6 \cdot \frac{P \cdot a^2}{E \cdot b \cdot h^3} \cdot \theta_{TOTAL}$$

Thus, 
$$\theta_{TOTAL} = \frac{h+t}{a \cdot \left[ 1 + \frac{E \cdot b \cdot h^3}{6 \cdot P \cdot a^2} \right]} \quad (6.9)$$

now, 
$$P = \sigma_s \cdot b \cdot l \quad (6.10.)$$

where  $\sigma_s$  = mean apparent shear stress.

Therefore, 
$$\theta_{TOTAL} = \frac{h+t}{a \cdot \left[ 1 + \frac{E \cdot h^3}{6 \cdot \sigma_s \cdot l \cdot a^2} \right]} \quad (6.11.)$$

where  $h = 1.25$  or  $2.00$  mm,

$a = 80$  mm,

$l = 40$  mm,

$E \approx 190,000 - 200,000$  MPa for all grades (assumed to be 200,000 MPa).

Thus, joint rotation can be calculated as a function of the mean apparent shear stress using equation 6.11., and this is represented in Figure 6.6. Note equation (6.11.) gives the rotation in radians which are converted into degrees by multiplying  $\theta_{TOTAL}$  by  $\frac{180}{\pi}$ .

**Figure 6.6.** The elastic model predicts that joints with 2 mm gauge adherends will rotate more than the joints with 1.25 mm adherends, which one would expect due to the increased asymmetry of the load axis. It can be seen that most of the joint rotation occurs at relatively low shear stress, and as the shear stress increases further the joint almost stops rotating. This would suggest that the elasticity of the adherend determines the joint rotation, but when the rotation stops the shear properties of the adhesive determine the point at which the joint will fail. However, this does not explain why the joints with 2 mm duplex adherends failed at a higher shear stress than the joints with 2 mm ferritic and austenitic adherends, nor does it explain why the joints with 1.25 mm martensitic adherends failed at a higher shear stress than the joints with 1.25 austenitic adherends. In addition, this model assumes that all the joint rotation is elastic, which was certainly not the case.

Now continuing from (6.11), 
$$\sigma_p = \sigma_s \cdot \theta_{TOTAL} \tag{6.12.}$$

where  $\sigma_p$  = line peel stress at  $\pm \frac{l}{2}$ .

Now, 
$$\sigma_p = P_f \cdot \frac{2}{l} \tag{6.13.}$$

where  $P_p$  = line peel force at  $\pm \frac{l}{2}$ .

Therefore, 
$$P_f = \sigma_p \cdot \frac{l}{2} \tag{6.14.}$$

Thus, the line peel stress and the line peel force can be plotted as a function of the mean apparent shear stress, and these plots are given in Figures 6.7. and 6.8., respectively. The plots  $h = 1.25$  and  $h = 2$  are linear, because it was assumed that the only rotation to occur during testing was elastic.

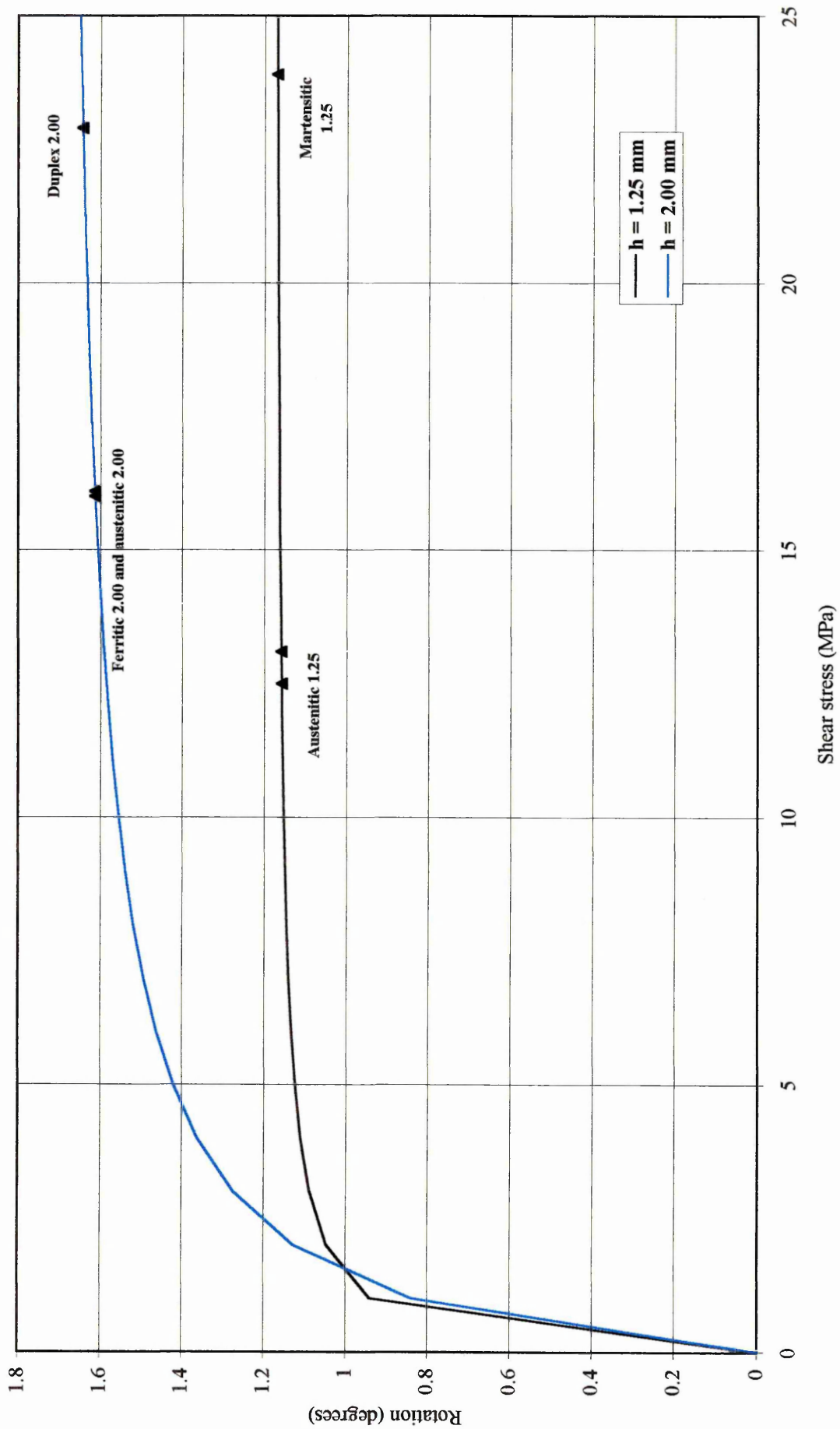


Figure 6.6. Joint rotation as a function of the mean apparent shear stress.

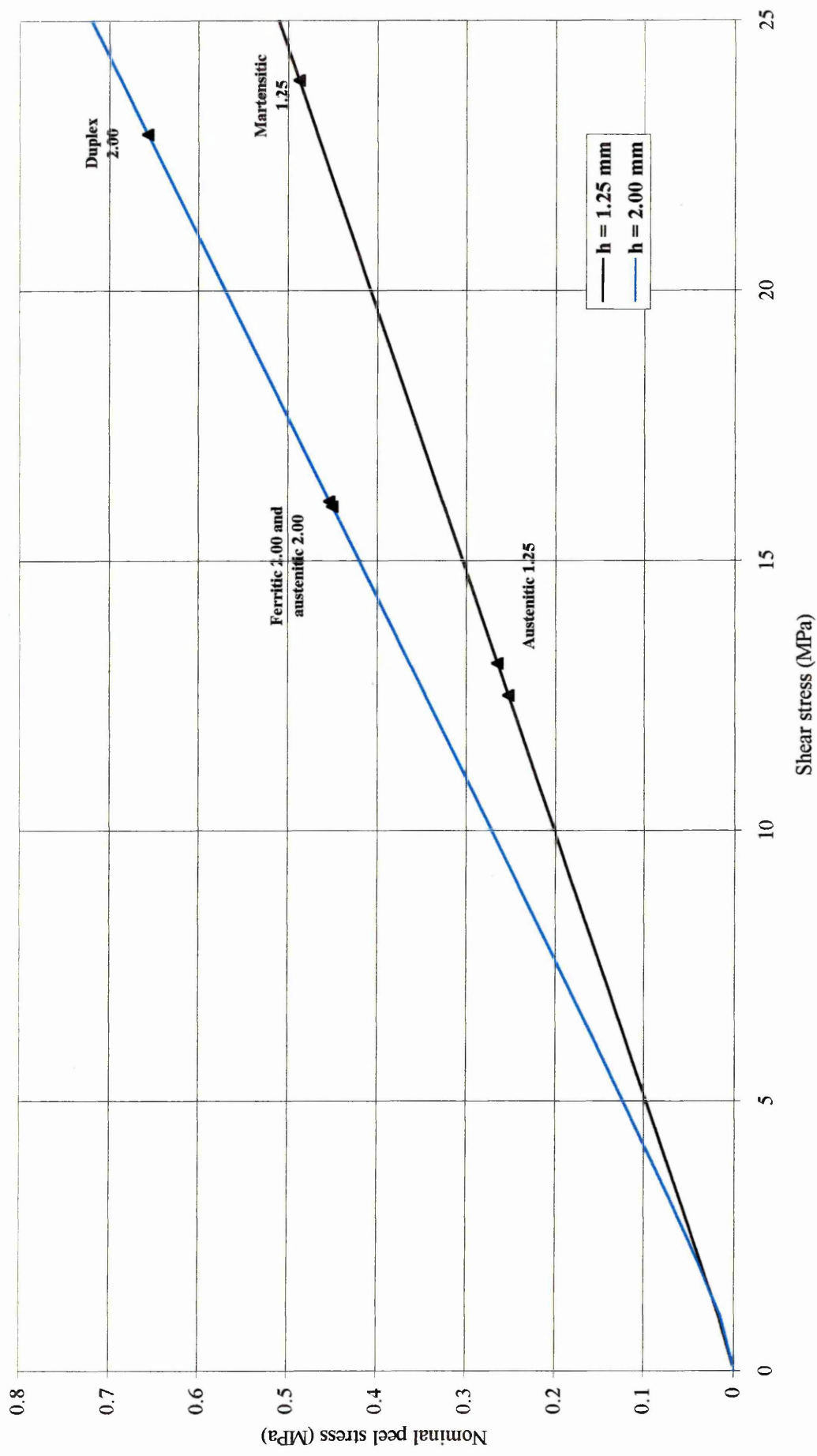


Figure 6.7. Nominal peel stress as a function of the mean apparent shear stress.

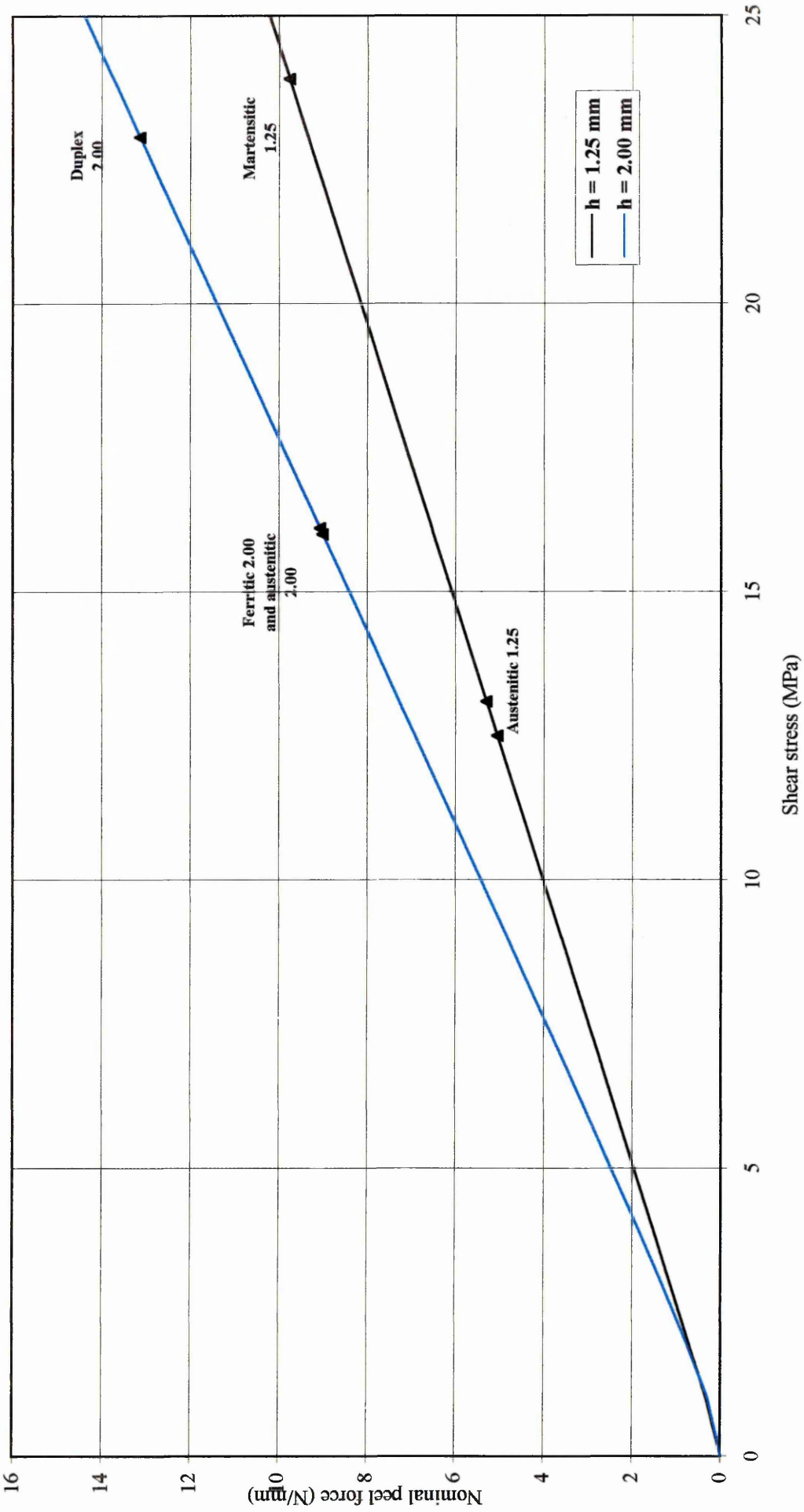


Figure 6.8. Nominal peel force as a function of the mean apparent shear stress.

Figures 6.7. and 6.8. The elastic model predicts that as the shear stress increases the peel stress/force will also increase as a result of elastic rotation, and that the peel stress/force (and hence the extent of elastic rotation) will continue increasing with increasing shear stress until fracture, and thus, joint failure must be determined either by the elastic properties of the adherend, or by the shear properties of the adhesive, or by both. But this contradicts with Figure 6.6., which shows that elastic joint rotation will be almost complete at much lower shear stresses than those represented in Figures 6.7. and 6.8. The simplification in the analysis of elastic rotation may introduce some errors in the elastic rotation.

However, it must be noted that the line peel stress and the line peel force in Figures 6.7. and 6.8., respectively, represent a nominal value at  $\frac{l}{2}$ . However, the peel stress distribution is at a maximum at the extremes of the overlap, therefore the line peel force at the extremes of the overlap must be considered.

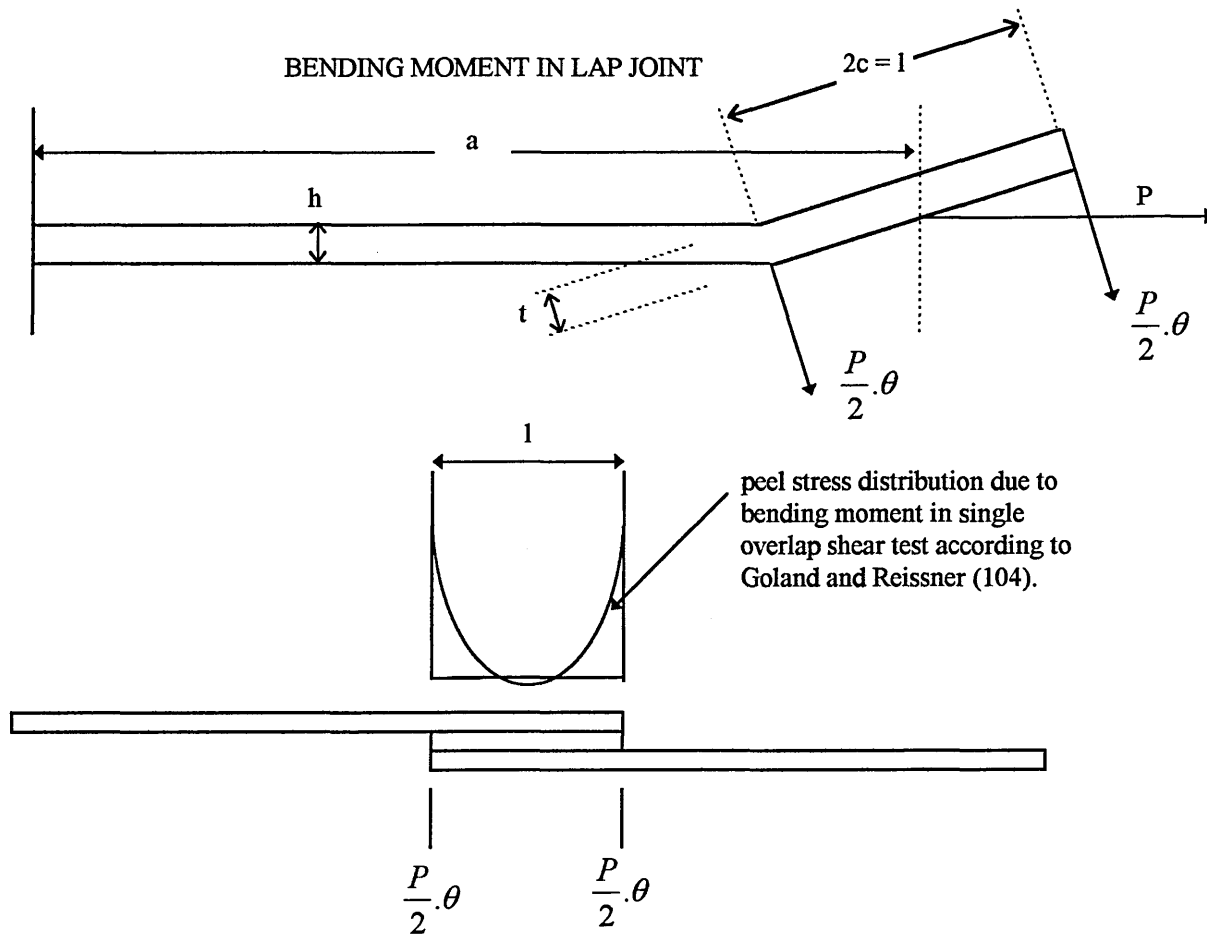


Figure 6.9. Transverse peel stresses in a single-lap joint (105).

Now,  $P = \sigma_s \cdot b \cdot 2c$  (6.15.)

where  $2c = 1$ .

Therefore,  $\sigma_s = \frac{P}{2 \cdot b \cdot c}$  (6.16.)

Thus,

$$\theta = \frac{12 \cdot P \cdot (h+t)(a-c)}{4 \cdot E \cdot b \cdot h^3} + \frac{12 \cdot P \cdot (h+t)(a+c)}{4 \cdot E \cdot b \cdot h^3} - \frac{12 \cdot P \cdot \theta(a-c)^2}{4 \cdot E \cdot b \cdot h^3} - \frac{12 \cdot P \cdot \theta(a+c)^2}{4 \cdot E \cdot b \cdot h^3}$$
 (6.17.)

Therefore,

$$\theta \left[ 1 + \frac{12 \cdot P}{4 \cdot E \cdot b \cdot h^3} 2(a^2 + c^2) \right] = \frac{12 \cdot P}{4 \cdot E \cdot b \cdot h^3} (h+t)(2a)$$
 (6.18.)

Thus,

$$\begin{aligned} &= \frac{\frac{12 \cdot P}{2 \cdot E \cdot b \cdot h^3} \cdot a(h+t)}{1 + \frac{12 \cdot P}{2 \cdot E \cdot b \cdot h^3} \cdot (a^2 + c^2)} \\ &= \frac{h+t}{\frac{a^2 + c^2}{a} \left( 1 + \frac{E \cdot b \cdot h^3}{6 \cdot P(a^2 + c^2)} \right)} \end{aligned}$$
 (6.19.)

Now,

PEEL LINE FORCE,  $P_f = \frac{P}{2 \cdot b} \cdot \theta$  (6.20.)

$$= \frac{P(h+t)}{2(a^2 + c^2) \cdot \frac{b}{a} \left[ 1 + \frac{E \cdot h^3}{6 \cdot \sigma_s \cdot 2c \cdot (a^2 + c^2)} \right]}$$
 (6.21.)

Therefore,

$$P_f = \frac{\sigma_s(h+t)}{\frac{(a^2 + c^2)}{a \cdot c} \left[ 1 + \frac{E \cdot h^3}{6 \cdot \sigma_s \cdot 2c \cdot (a^2 + c^2)} \right]}$$
 (6.22.)

Equation 6.22. is a more detailed calculation with two equal line forces at the end of the adhesive layer. However, the resulting plot, line peel force  $f$ (shear stress) - Figure 6.10., does not differ more than 8% from the nominal line peel force  $f$ (shear stress) shown in Figure 6.8.

Figures 6.6., 6.7. and 6.8. correctly predict that as the shear stress increases the extent of elastic rotation increases and thus, the peel stresses within the joint increase. These models also account for the thickness of the adherend material, joints incorporating thicker adherends undergoing more rotation and thus, inducing greater peel stresses. The problem with this approach is that it assumes that the joints rotate only elastically, which is incorrect, and it cannot explain the higher shear strengths attained by the joints with duplex and martensitic adherends. Now, because plastic deformation *does* occur, then the point at which the adherend begins to deform permanently must be significant to the joint performance, i.e. the yield strength of the adherend material must influence joint strength.

Now, it is interesting to compare the calculated normal stress of the adherend at fracture with the adherend yield strength (0.2% proof stress), or alternatively, compare the calculated shear stress of the joint at yield with the measured shear strength, see Table 6.5.

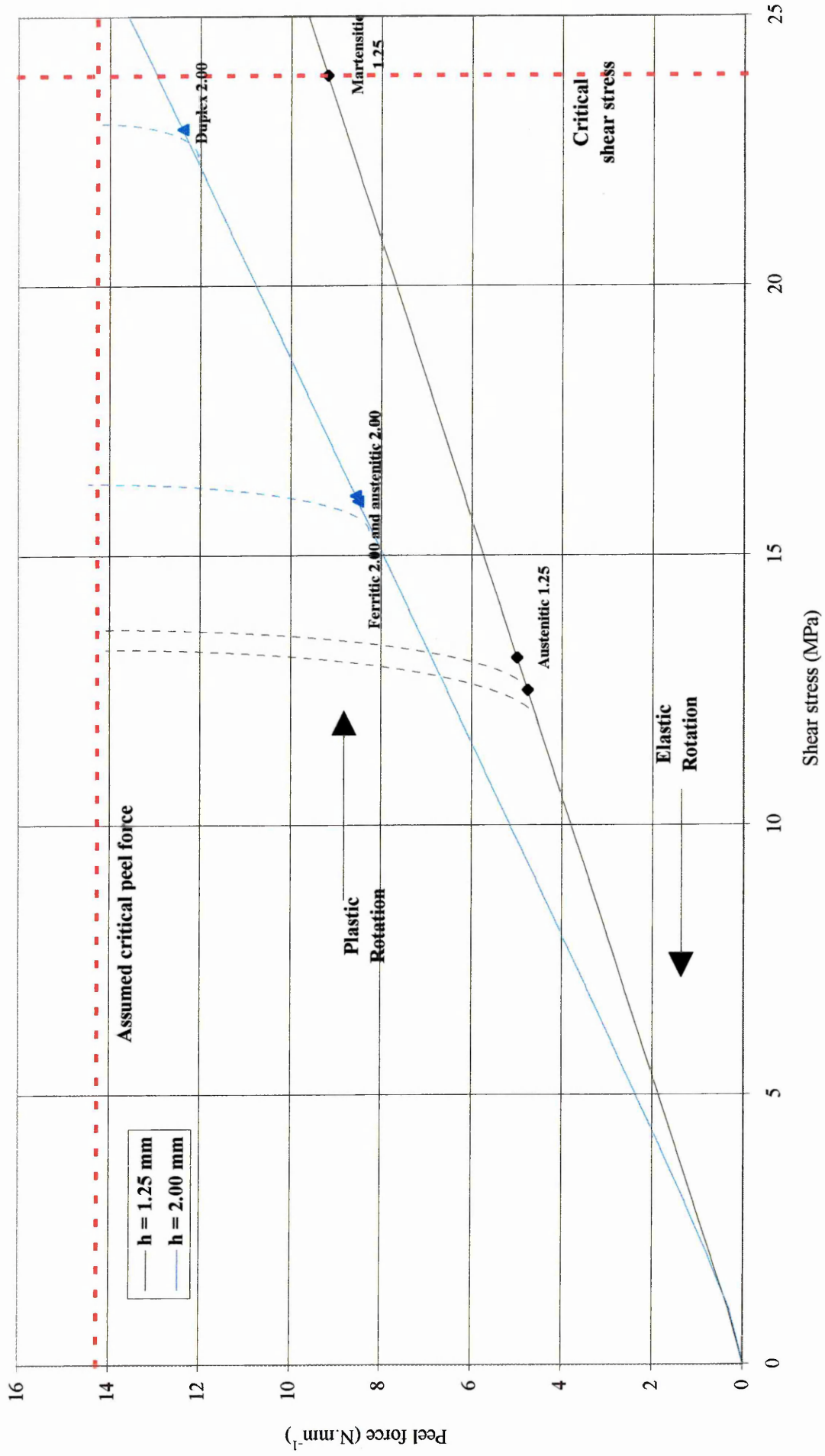


Figure 6.10. Peel force as a function of mean apparent shear stress.

**Table 6.5.** Theoretical shear stress at yield and the net section stress at fracture.

STEEL TYPE AND DESIGNATION	SURFACE FINISH	GAUGE h (mm)	0.2% PROOF STRESS $Y_s$ (MPa)	NET SECTION STRESS AT FRACTURE (MPa)	SHEAR STRESS AT YIELD (MPa)	MEASURED SHEAR STRENGTH $\sigma_s$ (MPa)
EN 1.4512 Ferritic	2B	2.00	340	320	17	16.0
EN 1.4462 Duplex	2D	2.00	540	458	27	22.9
AISI 304L Austenitic	2B	2.00	310	322	15.5	16.1
AISI 304L Austenitic	2B	1.25	310	419	9.7	13.1
AISI 304L Austenitic	BA	1.25	310	400	9.7	12.5
AISI 420 Martensitic	BA	1.25	1320	765	41.3	23.9

where,

$$\text{NET SECTION STRESS AT FRACTURE} = \frac{\sigma_s \cdot l}{h} \quad (\text{MPa}) \quad (6.23.)$$

and,

$$\text{SHEAR STRESS AT YIELD} = \frac{Y_s \cdot h}{l} \quad (\text{MPa}) \quad (6.24.)$$

From Table 6.5. The austenitic adherends (irrespective of thickness and surface finish) would be expected to plastically deform prior to joint fracture, since the measured shear strength at fracture had exceeded the predicted shear strength at yield. Contrary to this, because the measured shear strength of the joints incorporating the ferritic adherends was slightly lower than the predicted shear stress at yield, the ferritic adherends would be expected to show no evidence of plastic deformation on fracture. Similarly, the duplex and the martensitic adherends would be expected to show no plastic deformation on joint fracture, since the predicted shear stress at yield exceeded the measured shear strength at fracture, particularly in the case of the martensitic adherends (41.3 MPa *c.f.* 23.9 MPa). However, in reality all the adherends, with the exception of the martensitic, were plastically deformed during mechanical testing, see Table 6.6.

**Table 6.6.** Theoretical elastic rotation compared to actual plastic rotation.

<b>STEEL TYPE AND DESIGNATION</b>	<b>SURFACE FINISH</b>	<b>GAUGE (mm)</b>	<b>THEORETICAL ELASTIC ROTATION (degrees)</b>	<b>MEASURED PLASTIC ROTATION (degrees)</b>	<b>TOTAL ROTATION (degrees)</b>
EN 1.4512 Ferritic	2B	2.00	1.61	3.0	4.61
EN 1.4462 Duplex	2D	2.00	1.64	1.75	3.39
AISI 304L Austenitic	2B	2.00	1.61	3.5	5.11
AISI 304L Austenitic	2B	1.25	1.16	2.5	3.66
AISI 304L Austenitic	BA	1.25	1.16	2.5	3.66
AISI 420 Martensitic	BA	1.25	1.17	0	1.17

The theoretical elastic rotation was estimated from Figure 6.6. and the plastic rotation, causing permanently deformation, was measured directly from the fractured joints. The total rotation was therefore, the sum of the elastic and plastic rotation. In each case the theoretical elastic rotation was much smaller than the observed plastic deformation, with the exception of the martensitic material which showed no plastic deformation at all.

Since the martensitic adherends showed no permanent plastic deformation, this meant that the joints must have failed at stresses lower than that of the yield strength of the martensitic stainless steel, and the only rotation to have occurred could only have been elastic. Contrary to this, all the other adherend materials had suffered some permanent deformation, and this meant that the yield strength of the steel had been exceeded prior to fracture. Because the joints incorporating martensitic adherends gave the highest shear strength and suffered no plastic deformation, it was assumed that the point at which the adherends in a single lap joint yield must mark the onset of rapid fracture, since the joint rotation on plastic deformation will dramatically increase the peel stresses at the extremes of the joint overlap. Thus, joints incorporating 'low' yield strength adherends will fracture as a result of peel (peel dominated failure) immediately after the adherends plastically deform, and thus, there must be a critical peel stress and critical peel force at which the joint fractures. However, in joints incorporating 'high' yield strength adherends, the adherends may not yield at all and higher joint strengths will be realised, until the joint

finally fails by shear (shear dominated failure). Thus, in this case, there must be a critical shear stress at which the joint fractures. The assumed critical peel force and critical shear stress are given in Figure 6.10. at approximately  $14 \text{ N.mm}^{-1}$  and  $\sim 24 \text{ MPa}$ , respectively. The peel forces were calculated using the modified model - equation 6.22.

**Figure 6.10.** As the load increases the adherends begin to rotate elastically and peel stresses are introduced at the extremes of the overlap and they increase proportionately to the shear stress during elastic rotation - this is represented by the solid lines. The peel and shear stresses will continue to increase gradually, until failure eventually occurs either by peel at a critical peel force, or by shear at a critical shear stress. Thus, the elastic model explains the behaviour of the joints incorporating martensitic adherends since no plastic rotation was incurred; the joints failed by shear-dominated, adhesive-controlled failure at a critical shear stress of approximately  $24 \text{ MPa}$ . However, joints incorporating the other adherend materials all showed some evidence of plastic deformation, but the elastic model does not take into account the plastic rotation. Therefore, dotted lines are superimposed on Figure 6.10. to represent a sudden increase in the peel stresses due to plastic deformation of the adherend material to a critical point of rotation and explains the behaviour of joints with non-martensitic adherends; the joints failed by peel-dominated, adherend-controlled failure at an assumed critical peel force of approximately  $14 \text{ N.mm}^{-1}$ .

The total peel force at fracture (critical peel force) was calculated from the total joint rotation (Table 6.6.) and estimated to be somewhere between  $10$  and  $29 \text{ N.mm}^{-1}$  (see Table 6.7.). But, the critical peel force must be greater than  $12.5 \text{ N.mm}^{-1}$  to explain the plastic deformation of the duplex adherends (see Figure 6.10.). Thus, the critical peel stress was assumed to be approximately  $14 \text{ N.mm}^{-1}$ , slightly higher than  $12.5 \text{ N.mm}^{-1}$ .

Table 6.7. Total peel stress and total peel force at fracture .

STEEL TYPE AND DESIGNATION	SURFACE FINISH and GAUGE	MEASURED SHEAR STRENGTH (MPa)	TOTAL ROTATION From Table 6.6. (degrees)	TOTAL PEEL STRESS AT FRACTURE From Equation 6.12. (MPa)	TOTAL PEEL FORCE AT FRACTURE From Equation 6.14. (N.mm <sup>-1</sup> )
EN 1.4512 Ferritic	2B 2.00 mm	16.0	4.61	1.29	25.8
EN 1.4462 Duplex	2D 2.00 mm	22.9	3.39	1.35	27
AISI 304L Austenitic	2B 2.00 mm	16.1	5.11	1.44	28.8
AISI 304L Austenitic	2B 1.25 mm	13.1	3.66	0.84	16.8
AISI 304L Austenitic	BA 1.25 mm	12.5	3.66	0.80	16
AISI 420 Martensitic	BA 1.25 mm	23.9	1.17	0.49	9.8

From Table 6.7. the calculated peel force at fracture for the joints incorporating martensitic adherends (~10 N.mm<sup>-1</sup>) is below the assumed critical peel force (Figure 6.10.) and therefore the joints would be expected to fail by shear-dominated, adhesive-controlled failure and not by peel-dominated, adherend-controlled failure. N.B. It is interesting to note that the total peel force at fracture for the joints with martensitic adherends (9.8 N.mm<sup>-1</sup>) agrees with the peel force at the critical shear stress (see Figure 6.10.), ~9 N.mm<sup>-1</sup>. The calculated peel forces at fracture, for joints incorporating non-martensitic adherends, however, are considerable higher than the assumed critical peel force. But, the measured rotations may not be reliable because of the crude nature of the measuring technique employed.

In summary, when a single lap shear joint is loaded in tension a bending moment is induced and the joint starts to rotate first elastically and then plastically in an attempt to attain a common axis. For joints incorporating adherends of low stiffness (either too thin or with too low a yield point), as the joint rotates the adherends begin to yield plastically and severe peel forces are generated at the extremes of the joint overlap. As the load increases the adherends rotate further and the peel stresses at both ends of the overlap increase until cracks are initiated at the adhesive/adherend interface (at the extremes of the overlap, at right angles to the tensile axis). As the load increases further and the adherends deform

further, the approaching cracks propagate towards the centre of the joint at a critical peel force, where sudden failure occurs across the adhesive by shear as the two cracks approach one another.

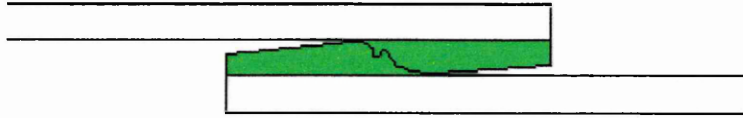


**Figure 6.11.** Loci of failure in lap joint due to joint rotation.

However, in joints incorporating stiffer adherends (thicker or of a higher yield point), as the joint rotates the adherends will elastically deform and may even plastically deform, but not to the critical peel stress, because the stiffness of the adherend prevents, or minimises, plastic deformation and the joint will tend to fail by shear when a critical shear stress has been exceeded. Since the only joints that did not plastically deform were those incorporating the martensitic adherends, it was assumed that the mechanism of failure in these joints was shear dominated failure within the adhesive and the joints failed when the critical shear stress was exceeded (~24 MPa). Since the other joints with the duplex, ferritic and austenitic adherends plastically deformed, the mechanism of failure in these joints was assumed to be controlled by the elastic/plastic behaviour of the adherend and to be peel dominated and fail at a critical peel force.

If the lap joints incorporating martensitic adherends failed due to the adhesive shearing and the remaining joints with the austenitic, ferritic and duplex adherends failed because of the peel stresses induced by plastic rotation, then surely it would be evident on the fracture faces. However, the fracture faces were almost identical; they all revealed a higher proportion of adhesive failure at the extremes of the joints which would suggest failure by peel. The central regions of the fracture faces, however, revealed predominantly interfacial failure with discrete areas of cohesive failure, more typical of shear failure.

So far, the models proposed take into account the adherend stiffness in terms of its thickness, but the inherent yield strength of the adherend material is not considered and this is too significant to ignore. The model must, somehow, take account of the yield strength of the adherend material as this dramatically influences the apparent shear strength of the lap joint. The shear strength as a function of the yield stress is given in Figure 6.12.

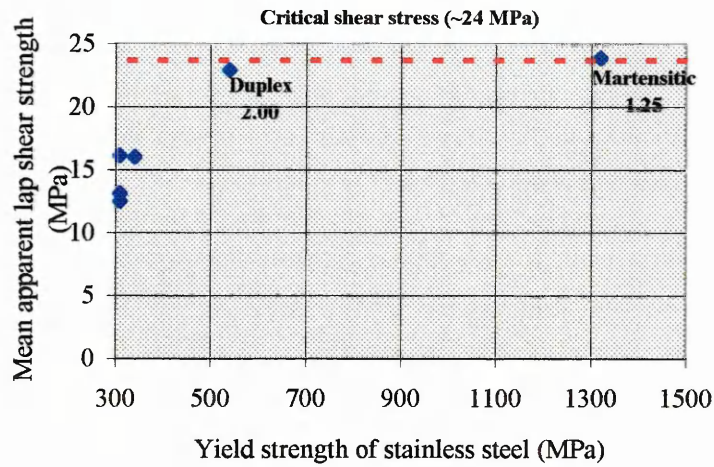


**Figure 6.12.** Mean apparent shear strength as a function of adherend yield strength.

## 6.5. CONCLUSIONS

1. Subtle differences in the chemical and physical make-up of the inherent surface oxides on the different grades of stainless steel do not observable influence initial single overlap shear strength.
2. Solvent wiping is a minimal but adequate means of cleaning stainless steel adherends prior to adhesive-bonding using epoxy systems, and does not appreciably affect initial single overlap shear strength.
3. The surface finishes typical of commercial stainless steel grades (2B, 2D and bright annealed) do not observably influence initial single overlap shear strength.
4. The mechanism by which a single lap shear joint fails is largely determined by the stiffness of the adherend material. Single overlap shear joints with adherends of low stiffness are more likely to fail as a result of critical peel stresses induced by joint rotation and plastic deformation (peel-dominated, adherend-controlled failure). And, single overlap shear joints incorporating 'stiff' adherends will resist plastic deformation to a higher stress, therefore the peel stresses will be minimised and joint failure is likely to be due to the adhesive shearing at a critical shear stress (shear-dominated, adhesive-controlled failure).

Joints incorporating thicker adherends should theoretically rotate more, but the stiffness imparted to the joint by the thicker adherends may be sufficient to resist plastic deformation. High yield strength adherends will impart stiffness to the joint, minimising the peel stresses at the extremes of the overlap, and thus, higher lap shear strengths will be obtained.

## **7.0. Room Temperature Creep and Dynamic Fatigue Performance of Adhesive-Bonded Stainless Steel Lap Joints.**

### *Abstract*

*Room temperature creep tests were conducted on AISI 304L stainless steel standard single-lap shear joints and single-lap box specimens, bonded with toughened epoxy DP 490. In addition, dynamic fatigue tests were carried out on single-lap box joints with (i) the hardened fillets of 'squeeze-out' adhesive removed and (ii) with the fillets un-removed. All tests were carried out at room temperature and 40-50 % relative humidity. Both joint designs showed a lot of scatter in the room temperature creep tests and the results were almost inconclusive. However, the box type specimens did exhibit a room temperature creep endurance limit at approximately 40% of the static failure load in tensile shear. The S-N curves produced for the joints tested, with and without the fillets, were similar, although the joints with the fillets left un-removed gave much more consistent results.*

## 7.1. INTRODUCTION

Adhesive joints are often expected to operate adequately in adverse environments, either chemically detrimental, at extreme temperatures (high or low), or both. Adhesive joints, particularly in structural applications, will also be required to function satisfactorily under both static and dynamic loading. The work presented in this chapter considers adhesive bonded single overlap joints subjected to static (room temperature creep) and dynamic (high cycle fatigue) loads. However, all the tests were conducted at ambient temperature and relative humidity, thus the effects of extreme temperatures and corrosive environments on the strength and durability of adhesive joints is not discussed. Room temperature creep is failure that occurs some time after the application of a constant load, and it usually occurs at loads lower than that needed to cause fracture under monotonic loading (11). Dynamic fatigue is the failure of a material as a result of persistent cyclic loading and it is responsible for a significant proportion of in-service failures. Fatigue is particularly important because failure will occur at stress levels much lower than the component can withstand under monotonic loading (11), leading to unexpected and often catastrophic failure. The dynamic fatigue performance of adhesives joints is good compared to other joining methods such as riveting, spot welding and mechanical fastening, because of the improved stress distribution within the adhesive joint. As a consequence, adhesives are often the preferred choice for applications involving cyclic loading, and thus, the dynamic fatigue properties of adhesive joints are very important to the design engineer. Figure 7.1. compares the fatigue performance of adhesive bonded and spot welded joints.

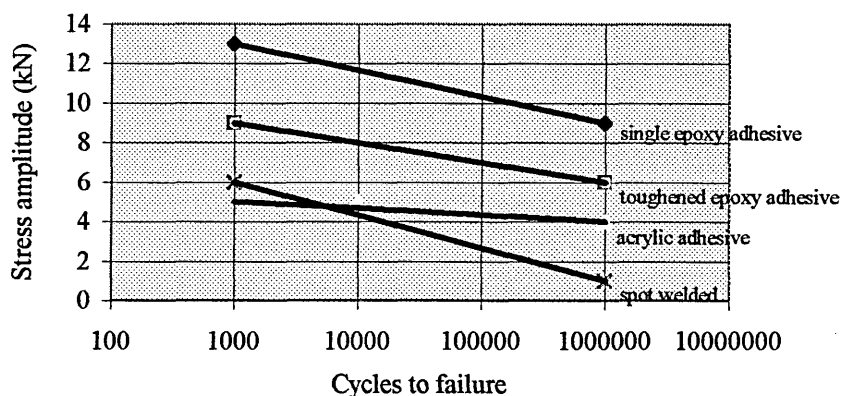


Figure 7.1. Dynamic fatigue of steel double-box hat structures (106).

## 7.2. EXPERIMENTAL WORK

### 7.2.1. TEST MATERIAL AND PIECE DIMENSIONS

Standard single overlap specimens were prepared from AISI 304L stainless steel (2B finish) by the procedure detailed in 3.2.1.1.1. *Single Lap Shear*. The box test pieces, which were manufactured by ADtranz, Sweden, were prepared from AISI 304L austenitic stainless steel with a 2B mat surface finish. The dimensions of the ADtranz test piece and a schematic of a bonded box joint are given in Figure 7.2.

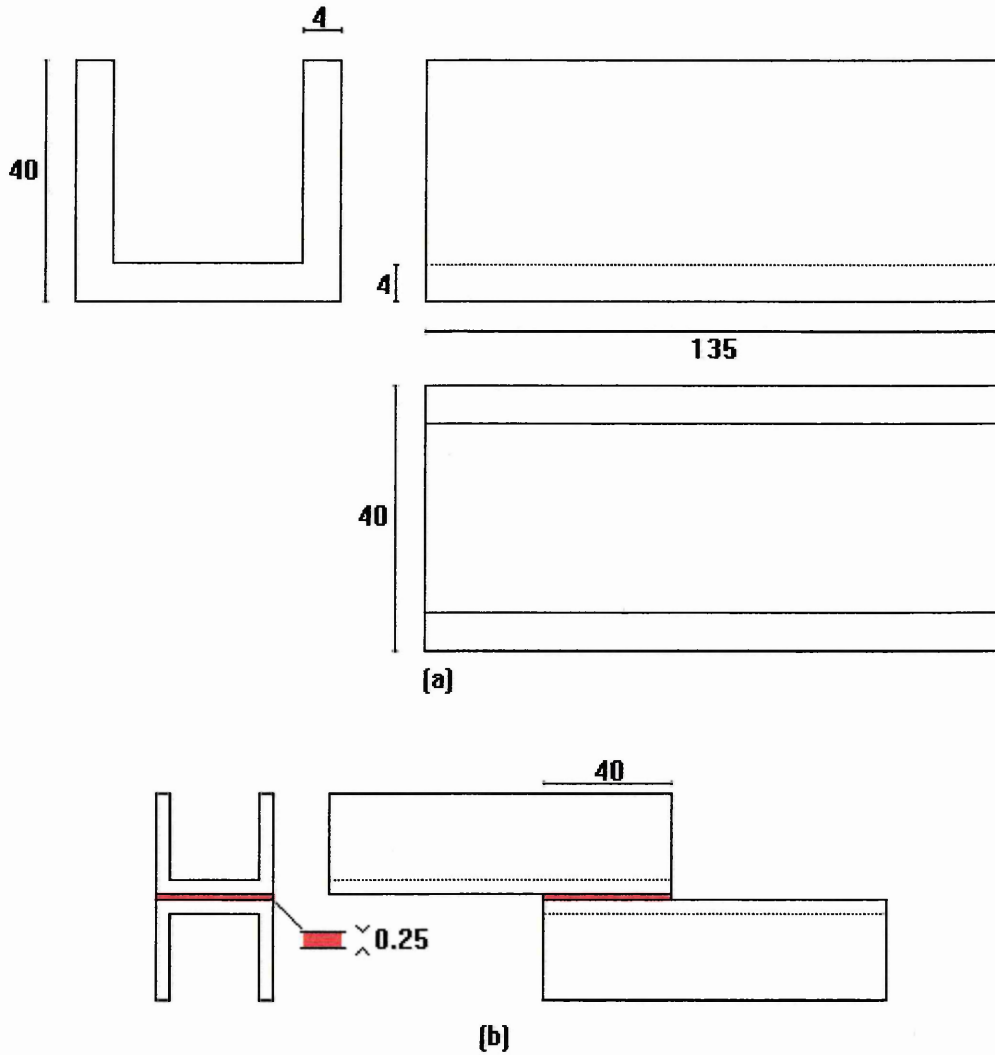


Figure 7.2. (a) ADtranz test piece dimensions (mm) and (b) assembled box joint.

### **7.2.2. SUBSTRATE SURFACE PRE-TREATMENT**

The stainless steel substrates were cleaned thoroughly following the procedure detailed in 3.2.1.2.1.1. *The Alkaline Degreasing Procedure*. Upon cooling, the surfaces were primed using a silane surface primer 3091 (see 3.2.1.2.1.4. *Priming*). The primed surfaces were wrapped in clean paper towel and allowed to stand overnight. The surfaces were then wiped with an acetone-wetted cloth, to remove traces of residual primer, and allowed to dry. The primed adherends were bonded within four days of priming.

### **7.2.3. JOINT ASSEMBLY AND CURING**

All joints were bonded using the toughened epoxy system DP 490. The single lap shear joints were assembled in accordance with the procedure given in 3.2.1.3. *Joint Assembly*, and the ADtranz box specimens were assembled in a similar fashion: 50 mm lengths of steel wire (no. 06 guitar string) were used to maintain a constant bondline of 0.25 mm; the wires were equally spaced out, in a direction parallel to the intended tensile axis. Wooden jigs were employed to ensure true joint alignment and ~1 kg weights were used to keep the bonded adherends together during the early stages of curing. Silicon-waxed release paper was located appropriately to prevent sticking in places where sticking was not desired.

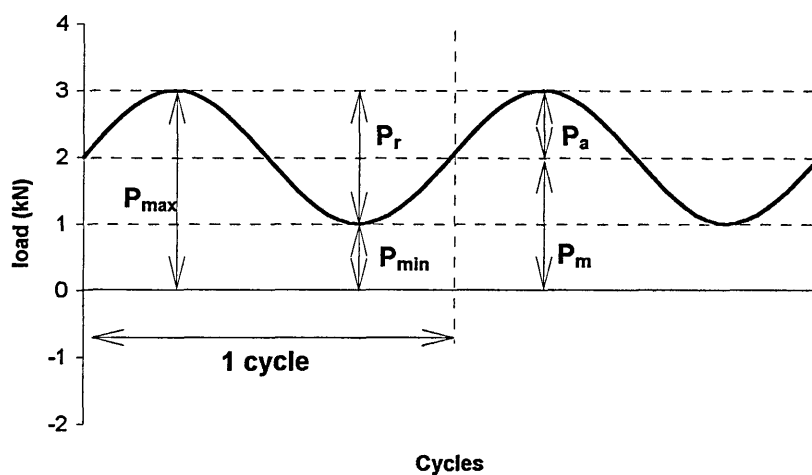
The bonded joints were allowed to stand undisturbed until they reached handling strength (~24 hours), and then stored for 7 to 10 days, depending upon the ambient temperature and relative humidity (laboratory air 19 to 25 °C and 40 to 60 % R.H.). After the curing time had elapsed the hardened joints were prepared for mechanical testing. Approximately half of the cured joints intended for dynamic fatigue testing were left with the fillets of hardened adhesive ('squeeze-out') un-removed. And for the other half of the batch, the fillets of hardened 'squeeze-out' were removed mechanically.

### **7.2.4. MECHANICAL TESTING**

Room temperature creep tests were conducted on a six-station rig in accordance with ASTM D 1780-94. Two joint types were tested: a standard 1.5 mm thick, single overlap shear joint (see Figure 3.1.) with a

12.5 mm overlap (bond area 312.5 mm<sup>2</sup>), and a 4 mm thick box joint with a 40 mm overlap (bond area 1600 mm<sup>2</sup>). The standard lap shear and the ADtranz box-lap shear joints were loaded in tension to a percentages of the mean static failure load under shear-tensile loading (8 kN and 50 kN, respectively), pre-determined from a sample size of six. The loaded joints were monitored and the times of failure recorded. Just prior to loading, lines were inscribed on the box joints, across the bondline, perpendicular to the tensile axis. Thus, any movement as a result of the adhesive creeping, could be detected and noted. N.B. The hardened fillets of adhesive ‘squeeze-out’ were not removed prior to testing.

Dynamic fatigue tests were carried out on AISI 304L ADtranz box-lap shear joints bonded with toughened epoxy DP 490. A servo-hydraulic machine was used for the tests, which were conducted in accordance with ASTM D 3166-93. The joints were loaded in tension and subjected to a fluctuating load of constant frequency until such a time when the joints failed. The number of cycles to failure was recorded and subsequently plotted as a function of the load range of the cycle. The applied cyclic load is represented in Figure 7.3.



where,  $P_{\max}$  = maximum load  
 $P_{\min}$  = minimum load  
 $P_r$  = load range  
 $P_m$  = mean load  
 $P_a$  = alternating load or load amplitude

**Figure 7.3.** Repeated load cycle.

A fluctuating load cycle is essentially made up of two components, a *mean*, or steady, load  $P_m$ , and an *alternating*, or variable, load  $P_a$ .

Where, the mean load is the algebraic mean of the maximum and minimum loads in the cycle,

$$P_m = \frac{P_{\max} + P_{\min}}{2} \quad (7.1.)$$

and the alternating load, or load amplitude, is half the load range,

$$P_a = \frac{P_r}{2} \quad (7.2)$$

where the load range  $P_r$  is given by,

$$P_r = P_{\max} - P_{\min} \quad (7.3.)$$

Thus, the load amplitude,

$$P_a = \frac{P_{\max} - P_{\min}}{2} \quad (7.4.)$$

Another important quantity often presented in fatigue data is the load ratio,

$$R = \frac{P_{\min}}{P_{\max}} \quad (7.5.)$$

The maximum load ( $P_{\max}$ ) was set at a percentage of the mean static failure load in uni-axial tension, determined previously from a sample size of six. The mean static failure load was 50 kN (mean apparent shear strength at failure 31.3 MPa). The minimum load ( $P_{\min}$ ) was then set to 10 % of the maximum load ( $R = 0.1$ ).

**Example:**

Mean static failure load of ADtranz box-lap joints in tension at  $1.5 \text{ mm.min.}^{-1}$  = 50 kN

Maximum load at 80% of mean failure load

$$P_{\max} = 50 \text{ (kN)} \times 0.8 = 40 \text{ kN}$$

Therefore, minimum load at 10% of maximum load

$$P_{\min.} = 40 \text{ (kN)} \times 0.1 = 4 \text{ kN}$$

Thus, load range

$$P_r = 40 \text{ (kN)} - 4 \text{ (kN)} = 36 \text{ kN}$$

Thus, load amplitude

$$P_a = \frac{40 \text{ (kN)} - 4 \text{ (kN)}}{2} = 18 \text{ kN}$$

Mean load

$$P_m = \frac{40 \text{ (kN)} + 4 \text{ (kN)}}{2} = 22 \text{ kN}$$

load ratio

$$R = \frac{4 \text{ (kN)}}{40 \text{ (kN)}} = 0.1$$

Fatigue tests were conducted at a constant test frequency of 20 Hz (1200 cycles per minute). The maximum load was set at a percentage of the mean static failure load (80, 70, 60, 50% etc.). S-N curves were then plotted; the number of cycles to failure as a function of the load range.

### 7.3. RESULTS

Tables 7.1. and 7.2., 7.3. and 7.4. detail the parameters of the room temperature creep, and dynamic fatigue tests, respectfully. Figure 7.4. shows room temperature creep performance of both standard single overlap shear test specimens and the box-lap shear joints. The S-N curves for the joints tested, both without and with fillets, are given in Figures 7.5. and 7.6., respectively.

**Table 7.1.** Room temperature creep performance of DP 490 epoxy-bonded AISI 304L stainless steel standard single overlap shear joints (t = 1.5 mm). Fillets un-removed.

PERCENTAGE OF MEAN STATIC FAILURE LOAD (%)	APPLIED LOAD (kN)	SHEAR STRESS (MPa)	TIME TO FAILURE (hr.)
80	6.4	20.5	1
80	6.4	20.5	1
80	6.4	20.5	5.5
80	6.4	20.5	7
80	6.4	20.5	10
60	4.8	15.4	239
60	4.8	15.4	400
60	4.8	15.4	431
50	4.0	12.8	358

**Table 7.2.** Room temperature creep performance of DP 490 epoxy-bonded AISI 304L stainless steel ADtranz box lap shear joints (t = 4 mm). Fillets un-removed.

PERCENTAGE OF MEAN STATIC FAILURE LOAD (%)	APPLIED LOAD (kN)	SHEAR STRESS (MPa)	TIME TO FAILURE (hr.)
80	40	25	10
80	40	25	20
80	40	25	285
70	40	25	16
70	35	21.9	300
60	30	18.8	260
60	30	18.8	300
60	30	18.8	334
40	20	12.5	4032 ↑
20	10	6.3	4032 ↑

**Table 7.3** Dynamic fatigue performance of DP 490 epoxy-bonded AISI 304L stainless steel

ADtranz box lap shear joints. Fillets removed prior to testing. Test frequency 20 Hz. R = 0.1

PERCENTAGE OF MEAN STATIC FAILURE LOAD (%)	MAXIMUM LOAD $P_{max}$ (kN)	MINIMUM LOAD $P_{min}$ (kN)	MEAN LOAD $P_m$ (kN)	LOAD RANGE $P_r$ (kN)	NUMBER OF CYCLES TO FAILURE ( $N_f$ )
80	40	4.0	22	36	28,170
80	40	4.0	22	36	23,570
80	40	4.0	22	36	137,740
80	40	4.0	22	36	157,810
80	40	4.0	22	36	69,160
80	40	4.0	22	36	66,150
80	40	4.0	22	36	342,700
70	35	3.5	19.25	31.5	218090
70	35	3.5	19.25	31.5	382490
70	35	3.5	19.25	31.5	181470
60	30	3.0	16.5	27	494680
60	30	3.0	16.5	27	252370
50	25	2.5	13.75	22.5	650850
50	25	2.5	13.75	22.5	4825630 ↑
50	25	2.5	13.75	22.5	1812270
50	25	2.5	13.75	22.5	426440
40	20	2.0	11	18	1000000 ↑
20	10	1.0	5.5	9	1000000 ↑

**Table 7.4.** Dynamic fatigue performance of DP 490 epoxy-bonded AISI 304L stainless steel

ADtranz box lap shear joints. Fillets left un-removed during testing. Test frequency 20 Hz. R = 0.1

PERCENTAGE OF MEAN STATIC FAILURE LOAD (%)	MAXIMUM LOAD $P_{max}$ (kN)	MINIMUM LOAD $P_{min}$ (kN)	MEAN LOAD $P_m$ (kN)	LOAD RANGE $P_r$ (kN)	NUMBER OF CYCLES TO FAILURE ( $N_f$ )
70	35	3.5	19.25	31.5	94010
70	35	3.5	19.25	31.5	96070
70	35	3.5	19.25	31.5	62480
70	35	3.5	19.25	31.5	61680
70	35	3.5	19.25	31.5	110390
60	30	3.0	16.5	27	461400
60	30	3.0	16.5	27	486460
60	30	3.0	16.5	27	328860
50	25	2.5	13.75	22.5	1062770
50	25	2.5	13.75	22.5	1645870
50	25	2.5	13.75	22.5	939060
40	20	2.0	11	18	4641740 ↑
40	20	2.0	11	18	4378720 ↑
40	20	2.0	11	18	9999990 ↑

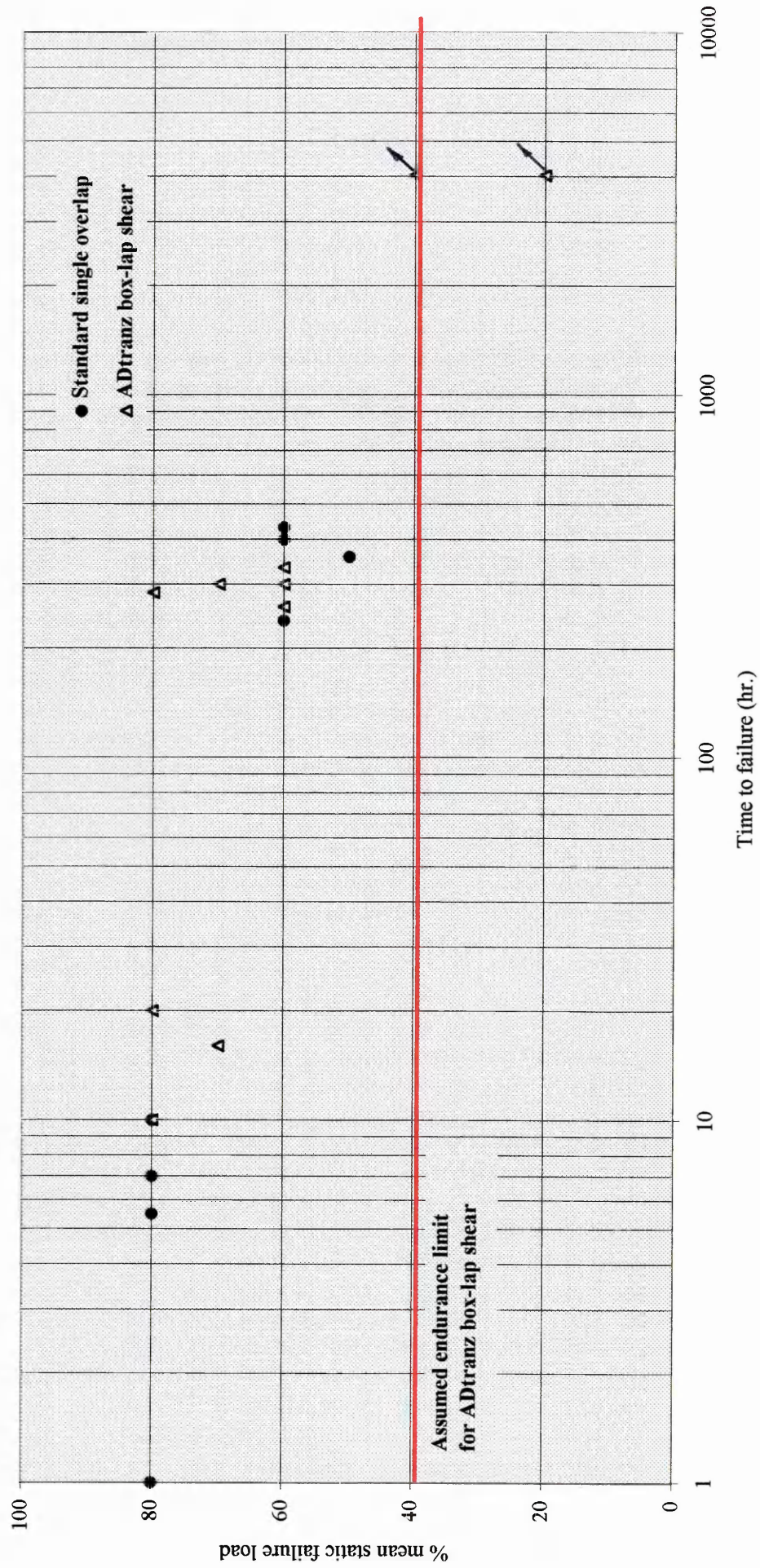


Figure 7.4. Room temperature creep performance of epoxy-bonded AISI 304L stainless steel lap joints. Fillets un-removed.

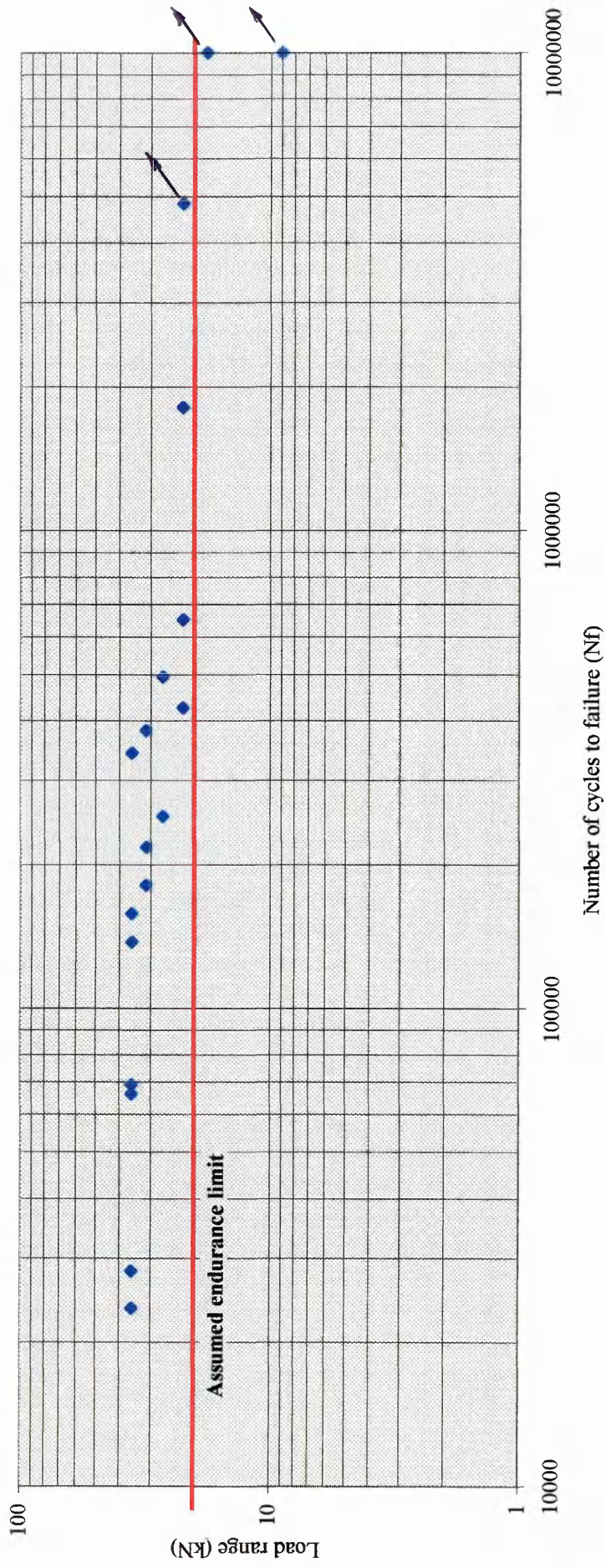


Figure 7.5. S-N curve for AISI 304L stainless steel, bonded with a toughened epoxy system. Fillets removed. ( $f = 20 \text{ Hz.}$ )  $R = 0.1$

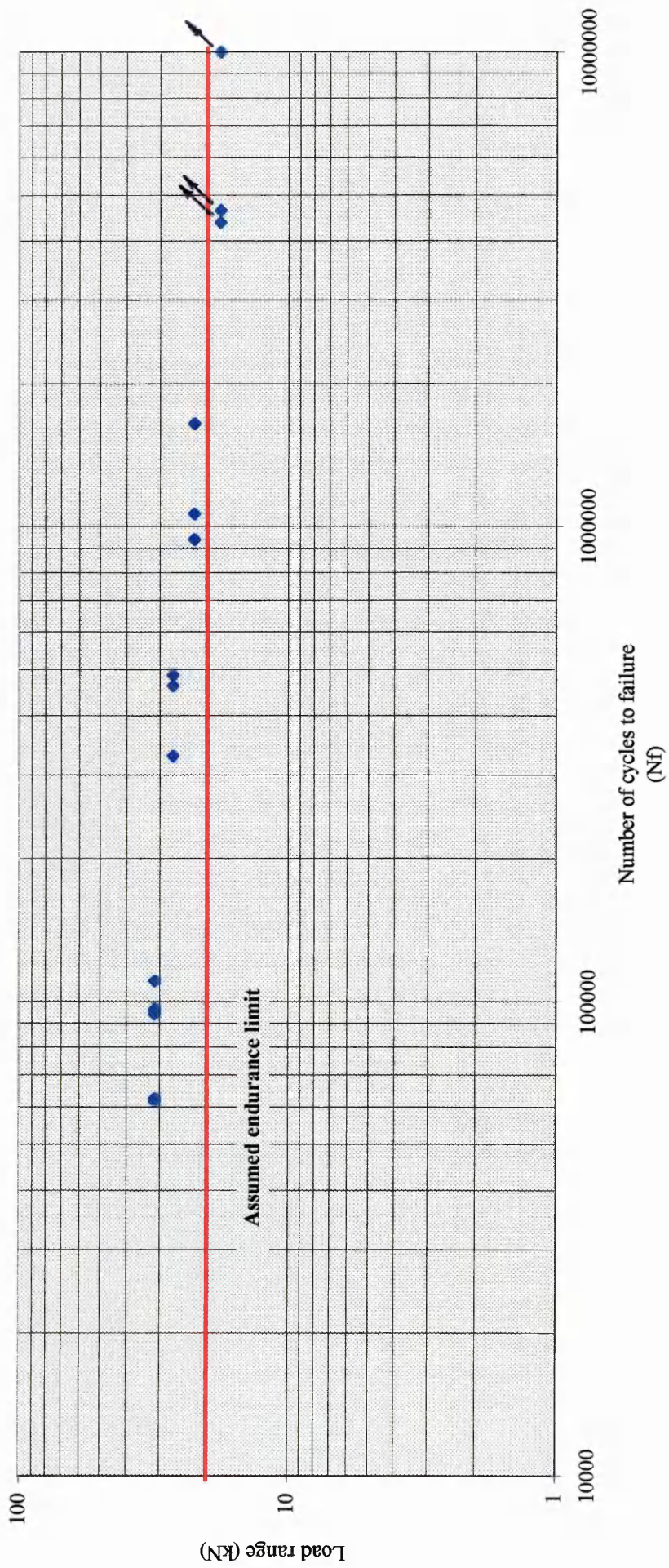


Figure 7.6. S-N curve for AISI 304L stainless steel, bonded with a toughened epoxy system. Fillets un-removed. ( $f = 20$  Hz.)  $R = 0.1$

## 7.4. DISCUSSION

### Room temperature creep

At the time the joints were loaded, the standard lap shear joints deformed the moment the load was applied, although the extent of deformation did not worsen with time and it did not appear to affect the longevity of the joints. There was no obvious deformation of the box lap joints observed at any time during the trial. Neither the standard lap shear nor the box lap joint types showed any observable deformation within the adhesive layer and no longitudinal displacement was recorded. There was a lot of scatter from both specimen types, particularly at 80% of the applied load; because the mean static failure load used (8 kN and 50 kN for the standard lap shear and the box lap shear joint types, respectively) was estimated from a sample size of six, the degree of scatter at this load level was expected. Two box lap joints loaded at 20 and 40% of the mean static failure load sustained the loads remarkable well (over six months without failure) showing no apparent damage - perhaps an endurance does exist. An endurance limit may be defined as a value of the applied load below which joint failure will not occur. There is much debate as to the existence of an endurance limit: Lewis *et al* (107, 108) calculated that an endurance limit would be about 35 to 45% of the short term joint strength (static strength); Wake *et al* (109, 110) concluded that, from both theoretical and experimental considerations, whether an endurance limit really does exist or not has yet to be firmly established. The room temperature creep results presented in this chapter, of course, do not confirm the existence of an endurance limit, but they do not disprove the existence of such a limit either. If it is assumed that an endurance limit does exist and that it is approximately 40% of the mean static failure load (see Figure 7.4.) then, with a safety factor of 2 this would provide the design engineer with a design load of about 10 kN or  $250 \text{ N.mm}^{-1}$  (10,000 N / joint width (40 mm)) for the ADtranz box specimens. Unfortunately, the joints loaded at 20 and 40% of the mean static load had to be dismantled (without fracture) after the 6 month period had elapsed, because the tests had already had more than their fair share of machine time, one of the problems with creep testing.

### Dynamic fatigue

Comparing the fatigue performances of ADtranz box lap joints with and without the fillets removed (Figures 7.5. and 7.6.). Removing the fillets of hardened squeeze-out prior to testing improved fatigue

performance both in terms of consistency and longevity. The increase in life was attributed to the fillets reinforcing the joint by minimising the peel stresses at the extreme of the overlap and thus postponing peel initiated failure. The improved consistency (and improved longevity) suggests that lap joints are sensitive to changes in fillet condition, i.e. cracks will develop sooner in joints without fillets at points of high localised stress i.e. corners, see Figure 7.7., and consistency is likely to be affected because the time the crack starts and the position of the starting point will be more unpredictable, than in joints with the fillets left un-removed. Figures 7.5. and 7.6. propose a fatigue endurance limit at a load range of approximately 20 kN, with a safety factor of 2 this would provide the design engineer with a design load of about  $250 \text{ N.mm}^{-1}$ .

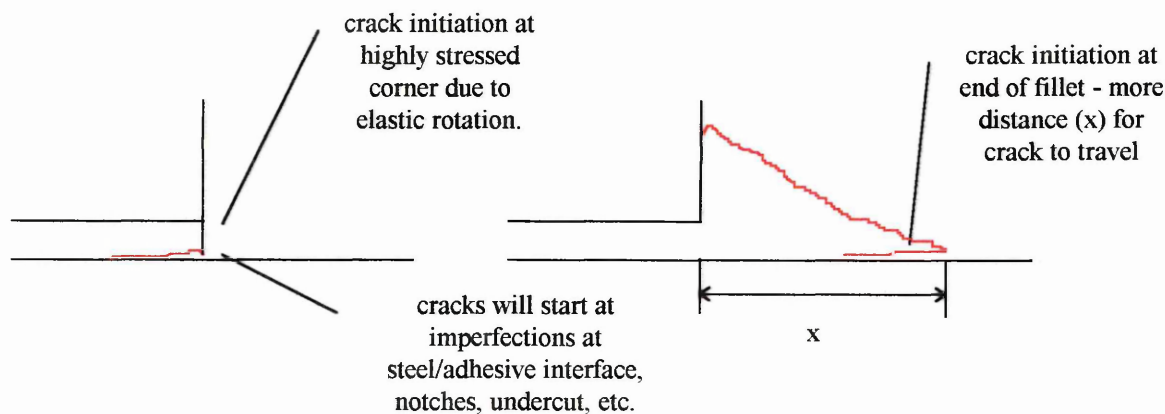


**Figure 7.7.** Effect of fillet condition on crack initiation.

But how does the fatigue performance of adhesive joints compare with that of spot welded, or for that matter, weldbonded joints? Weldbonding, referred to in 1.0. *Introduction*, is a hybrid of spot welding and adhesive bonding. Conveniently, Linder and co-workers (111) at The Swedish Institute for Metals Research and Ring Groth (112), 1000 km north of Stockholm, at Luleå University of Technology, conducted dynamic fatigue tests on spot welded and weldbonded ADtranz box lap shear joints, respectfully. The S-N curves for spot welded (111), weldbonded (112) and adhesive bonded joints (113) are presented in Figure 7.8. It is possible to compare the results of the adhesive bonded and the weldbonded lap joints because the bond areas were identical at  $1600 \text{ mm}^2$  ( $40 \times 40 \text{ mm}$ ). As for the spot welded joints, the overlap area was  $40 \times 40 \text{ mm}$  and the bond area, as defined by the diameter of the weld nugget, was  $9 \text{ mm}$ . Normal distances between spot welds in industrial, single-row, spot welded joints are about  $60 \text{ mm}$ , about 1.5 times greater than the overlap of the adhesive bonded and weldbonded

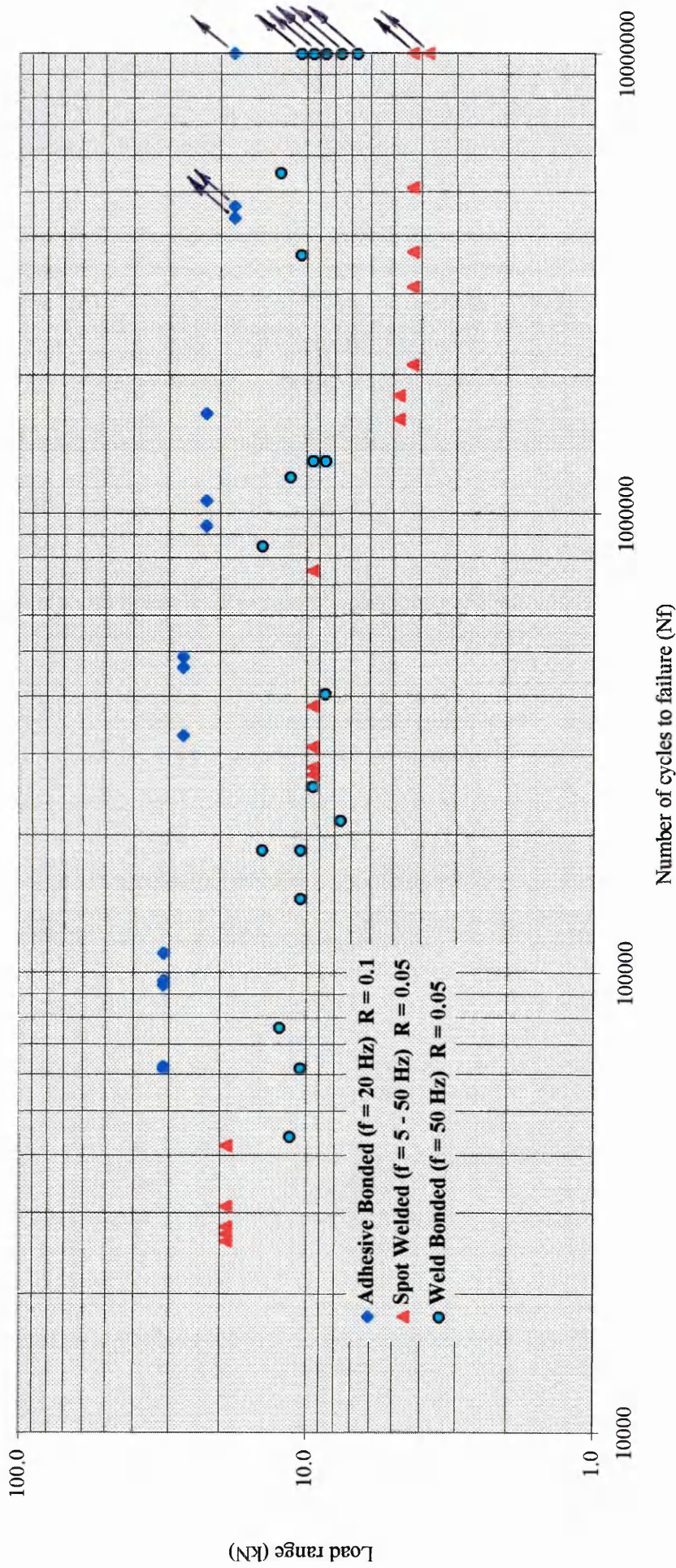


**Figure 7.8.** Fatigue performance of AISI 304L stainless steel ADtranz box-lap shear joints fabricated using different joining techniques. Fillets un-removed w.r.t. adhesive bonded joints.

joints, however, in standard 2-row spot welded joints, which are more common than single-row spot welded joints, the mean 2-row distance is approximately 40 mm. Thus, it is reasonable to compare the results of the spot welded joints with those of the adhesive bonded and weldbonded joints. The performance of the adhesive bonded joints (fillets un-removed) was attributed to the better stress distribution within the lap joint, compared to the spot welded and weldbonded joints. However, these test were all high cycle fatigue, but is joint behaviour any different at lower cycles?

The room temperature creep results for the ADtranz box lap shear joints (Figure 7.4.) showed the ability of reinforced lap joints to sustain low loads indefinitely, thus, time at load must be a very important factor and does it suggests that adhesive joints are highly frequency sensitive? Figure 7.9. compares the high cycle fatigue performance of ADtranz box lap joints (fillets un-removed - Figure 7.6.) (113) with the low cycle fatigue performance of single overlap joints (114). Crocombe's results (114) were chosen for comparison with the those of the ADtranz box lap shear joints because they represented single overlap specimens tested at an R value of 0.1. Although the bond area was greater for the ADtranz box lap shear joints, comparison is possible because a normalised load range is considered. The load range was normalised by dividing it by the static failure load,

$$\frac{P_r}{P_s}$$

- where,
- Ps for standard single overlap joints with 0.6 mm thick bondline = 10.1 kN.
  - Ps for standard single overlap joints with 0.165 mm thick bondline = 13.7 kN.
  - Ps for ADtranz box lap shear joints with 0.25 mm thick bondline = 50.0 kN.

From Figure 7.9., it is clear that the fatigue performance was not significantly effected by differences in the bondline thickness, therefore, the improved performance displayed by the ADtranz box lap joints was attributed to the test frequency. The reason for the difference in performance is possibly explained by Kinloch (11) - in low frequency tests the adhesive tends to creep quite markedly, not only near the ends but throughout the overlap. This progressive increase in the strain in the adhesive, due to the creep loads, results in joint fracture after a relatively few cycles. However, when tested at high frequency, the load is always being removed before the adhesive has time to creep and the accumulated creep strain is

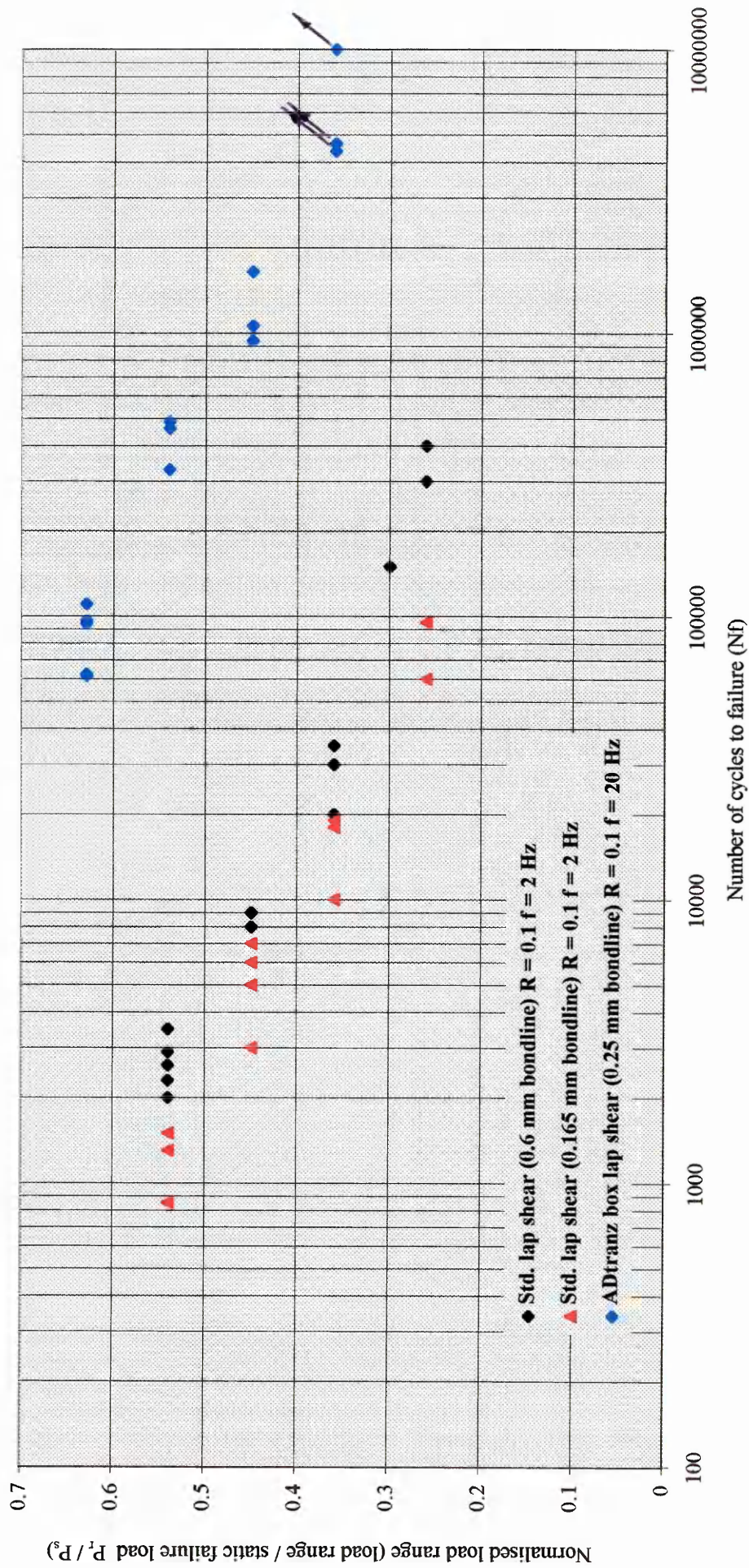


Figure 7.9. Comparison between high and low cycle fatigue performance of single overlap joints.

low and the joint survives for a long time. Perhaps this does explain the differences in the dynamic fatigue performances observed, but it is important to note that there are many other variables to consider before accurate comparisons can be made, for example, the type of adherend material, the condition of the fillets at the extremes of the overlap; the grade of steel used in the standard overlap shear joints is not identified and more attention was paid to the condition of the fillets, i.e. they had specific radii. The standard single over lap joint had also been modified to include a chamfer and the crosshead speeds used in the static tests were much slower than those of used for the ADtranz box lap joints, 0.1 to 0.2 mm.min<sup>-1</sup> c.f. 1.5 mm.min<sup>-1</sup>.

## 7.5. CONCLUSIONS

1. The room temperature creep data obtained for both specimen types, standard lap shear and box lap shear, correlated well, however, it is unfortunate that more tests were not carried out, especially standard lap shear.
2. Single overlap shear joints can withstand low loads (~ 20 to 40% mean static failure load) for considerable periods of time without fracture. Providing design engineers with a design load of about  $250 \text{ N.mm}^{-1}$ . There was good correlation between standard single overlap and ADtranz box overlap joints.
3. Single overlap shear type joints can withstand high cyclic loading at low loads (20 kN range) for a considerable number of cycles ( $10^7$ ). Providing design engineers with a design load of  $250 \text{ N.mm}^{-1}$ . However, when considering adhesives it is likely that joints will be sensitive to frequency and joints subjected to low cycle loads may fracture prematurely at even relatively low loads. Thus, dynamic fatigue tests must be conducted at a diverse range of test frequencies.
4. Adhesive bonded lap joints give an improved fatigue performance compared to spot welded and weldbonded lap joints due to the improved stress distribution within the overlap.
5. Leaving the fillets of hardened adhesive squeeze-out un-removed prior to testing will improve the dynamic fatigue performance in terms of consistency and longevity, because the fillets will minimise the peel stresses induced due to the adherend elastically rotating.

## 8.0. SURFACE CHARACTERISATION

### *Abstract*

*AISI 304L stainless steel adherends, intended for DP 490 epoxy-bonded adhesive joints, were subjected to a number of different surface pre-bonding treatments, in order to physically and/or chemically modify the surfaces, in an attempt to enhance the mechanical performance of the joints. The physical nature of the pre-treated adherends was characterised using Scanning Electron Microscopy (SEM) and surface profilometry, and the chemical nature was characterised using X-Ray Photoelectron Spectroscopy (XPS), Glow Discharge Optical Emission Spectroscopy (GDOES), and Energy Dispersive X-Ray Analysis (EDX). The subsequent fracture faces were examined using SEM and Fourier Transform Infra Red (FTIR) microscopy to determine the loci of failure.*

## 8.1. INTRODUCTION

The surface of the adherend is often treated prior to adhesive (metal-to-metal) bonding in order to optimise bond strength and prolong service life. Typical pre-treatments include degreasing to remove potential weak boundary layers, mechanical roughening to 'key' the surface, and chemical etching to promote a stable, resilient oxide. During the course of the experimental work, detailed in Chapters 3.0. to 7.0., a number of adherend surface pre-bonding treatments were considered. The pre-treatments used ranged from simple cleaning methods such as *Dry Wiping* to more thorough cleaning techniques such as *Alkaline Degreasing* and *Acid Rinsing*. While some of the substrates were just cleaned, other surfaces were physically modified, either by mechanical roughening in the form of *Alumina Blasting* or *Scotchbrite Abrading*, or by chemical roughening using, for example, *Acid Etching*. Thus, some form of surface characterisation was deemed necessary in order to investigate the contribution to, or detracting from, mechanical joint strength and durability afforded by the adherend surface condition. Surface profilometry and SEM were used to physically characterise the substrates in terms of surface roughness and the chemical nature of the surfaces was investigated using XPS, EDX, GDOES, and IR microscopy. The physical and chemical natures of the stainless steel substrates were examined prior to any surface pre-treatment and following pre-treatment, and the fracture faces of the failed joints were also examined using SEM and Infra Red microscopy to determine the loci of failure. The mechanical test results discussed in previous chapters (Chapters 3.0. to 7.0.) somewhat dictated the extent of the surface characterisation work carried out. From the results of the lap shear and peel tests it was impossible to discriminate between different surface pre-treatments, only contaminated (un-cleaned, *As Received*) surfaces adversely affected joint strength. It may be, however, that the lap shear and peel tests are insensitive to changes in the surface condition of the adherend, because in the wedge tests (see 5.0. *Environmental Durability of Adhesive Bonded Stainless Steel Joints*) discrimination between the different surface pre-bonding treatments was possible. During this project SEM was used extensively to physically characterise pre-bonded adherends and the subsequent fracture surfaces, however, the extent of chemical characterisation was limited. GDOES was employed to evaluate the cleaning efficiency of some of the pre-bonding treatments and FTIR microscopy to confirm interfacial failure within the adhesive (interfacial<sub>Adhesive</sub>) on the fracture faces. The XPS work carried out was limited due to lack of resources and financial restraint.

## 8.2. EXPERIMENTAL WORK

### 8.2.1. PHYSICAL CHARACTERISATION

Samples of 1.5 mm gauge AISI 304L stainless steel,  $\sim 25 \text{ mm}^2$ , were mechanically roughened by *Alumina Blasting* or *Scotchbrite Abrading*, or chemically roughened using *Acid Etching*, *Smutting* or the *Passivating* treatment (the pre-treatments are detailed in Chapters 3.0. to 5.0.). After cleaning and drying the samples, surface roughness profiles were recorded over a 10 mm traverse using a Talysurf profilometer. *As Received* surfaces were also included for comparison. The surface roughness of the substrates that had incurred no physical modification, for example *Alkaline Degreasing* and *Acid Rinsing*, were assumed to have the same surface roughness as the *As Received* material. The microscopic physical appearance of the mechanically and chemically roughened surfaces were recorded using SEM. The *Acid Etched*, *Smuted* and *Passivated* surfaces were gold coated prior to examination to minimise charging. *As Received* steel samples were also examined for comparison. Finally, the subsequent fracture faces of the failed joints were also examined using SEM to help determine the loci of failure.

### 8.2.2. CHEMICAL CHARACTERISATION

#### 8.2.2.1. XPS CHARACTERISATION OF PRE-BONDED ADHEREND

The *Alkaline Degreased* surface, in the primed and un-primed condition, and the *Alumina Blasted* surface in the un-primed condition were analysed by XPS, using the Microlab facility at S.H.U. Wide scans were obtained from the surfaces, together with specific elemental information where considered relevant.

#### 8.2.2.2. GDOES CHARACTERISATION OF PRE-BONDED ADHERENDS

Undoubtedly, one of the most significant factors effecting the efficiency of adhesive bonding is the degree of surface cleanliness. In 1965, Krieger and Wilson (115) developed a technique that measured the extent of surface contamination by the success by which indium adhered onto another solid surface. However, although repeatable results were obtained, the technique is somewhat cumbersome and out dated; modern surface analytical techniques such as XPS and FTIR are now considered more suitable

for quantifying surface contamination. However, if qualitative information will suffice, GDOES is a simple and quick means of evaluating surface cleanliness; it allows sampling of the surface analyte a few nanometers at a time and covers a penetration range of 0.005  $\mu\text{m}$  to 500  $\mu\text{m}$ . In this investigation GDOES was employed to qualitatively characterise the surface of AISI 304L stainless steel, prior to and after pre-treatment, to assess the cleaning efficiency of a number of pre-bonding treatments. The treatments considered were: *Solvent Wiping*; *Acetone/Inhibisol Rinsing*; *Alumina Blasting*; *Alkaline Degreasing*; *Acid Rinsing*; and *Acid Rinsing II*. *As Received* surfaces were also included for comparison. N.B. The treatment methods are detailed in Chapters 3.0. to 4.0.

### **8.2.2.3. EXAMINATION OF FRACTURE FACES USING INFRARED MICROSCOPY AND EDX**

FTIR microscopy was employed to chemically confirm the presence, or absence, of adhesive on some of the fracture faces in areas of suspected interfacial failure (interfacial<sub>Adhesive</sub>), observed both visually and using SEM. EDX was also used to confirm regions of interfacial<sub>Adhesive</sub> failure on the fracture faces.

### 8.3. RESULTS

#### 8.3.1. PHYSICAL CHARACTERISATION

##### 8.3.1.1. SURFACE ROUGHNESS VALUES

Several surface pre-bonding treatments were considered in Chapters 3.0. to 7.0. Table 8.1. lists those treatments used to roughen the adherend surface (chemically or mechanically), together with their measured surface roughness value; *Scotchbrite Abrading*, *Alumina Blasting*, *Acid Etching* ( $H_2SO_4$  - smut removed), *Smutting* ( $H_2SO_4$  - smut intact), and *Passivating*. The surface roughness value of the *As Received* surface is included for comparison and may be assumed to represent the surface roughness of all the remaining 'non-physically modified' surfaces.

**Table 8.1.** Surface roughness' of pre-treated surfaces. Assessment length = 10 mm.

SURFACE CONDITION	SURFACE ROUGHNESS PARAMETER Ra ( $\mu\text{m}$ )
<i>As Received</i>	0.1
<i>Scotchbrite Abraded</i>	0.2
<i>Alumina Blasted</i>	1.1
<i>Acid Etched</i>	1.8
<i>Smuted</i>	NA
<i>Passivated</i>	0.4

**Ra** arithmetic average roughness = arithmetic average deviation from the mean line with assessment length.

N.B. A reliable value could not be obtained for the *Smuted* surface, the oxide was not hard enough to tolerate the diamond stylus.

Using the surface roughness of the *Alkaline Degreased* surface as a control ( $Ra = 0.1 \mu\text{m}$ ). *Scotchbrite Abrading* effectively doubled the surface roughness ( $Ra = 0.2 \mu\text{m}$ ). However, this increase was inconsequential in comparison to that afforded by *Alumina Blasting* ( $Ra = 1.1 \mu\text{m}$ ) and, especially, by *Acid Etching* ( $Ra = 1.8 \mu\text{m}$ ). The *Passivated* surface was surprisingly smooth at  $Ra = 0.4 \mu\text{m}$ .

### 8.3.1.2. SCANNING ELECTRON MICROSCOPY

The physical nature of the *As-Received* surface is shown in Plate 8.1. Plates 8.2. to 8.6. show the affects of mechanical and chemical roughening, *Scotchbrite Abrading*, *Alumina Blasting*, *Acid Etching*, *Smutting* and *Passivating*.

Plate 8.1.



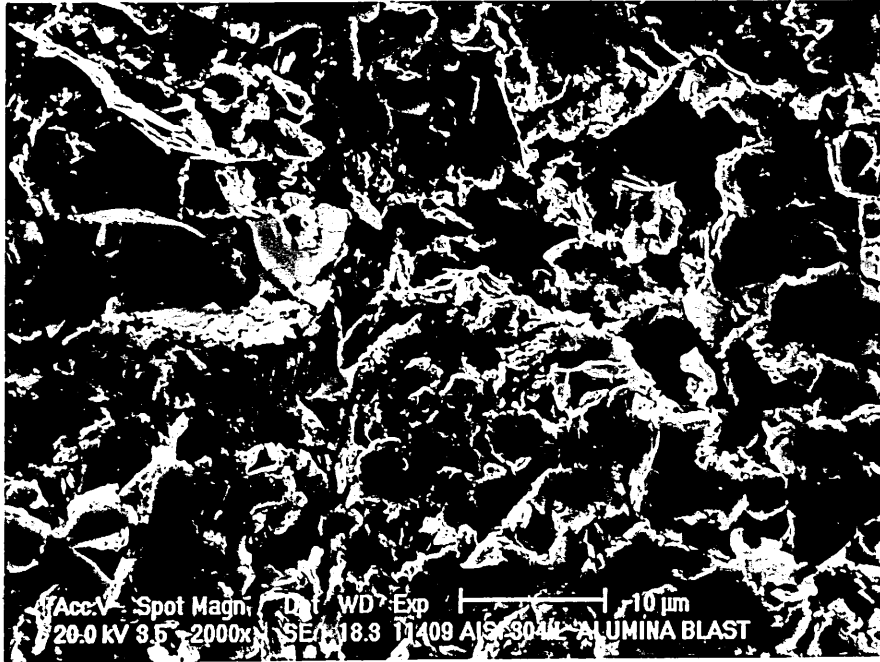
Scanning electron micrograph of AISI 304L stainless steel with a 2B surface finish. Surface condition *As Received* ( $R_a = 0.1 \mu\text{m}$ ).

Plate 8.2.



Scanning electron micrograph of AISI 304L stainless steel with *Scotchbrite Abraded* surface ( $R_a = 0.2 \mu\text{m}$ ).

Plate 8.3.



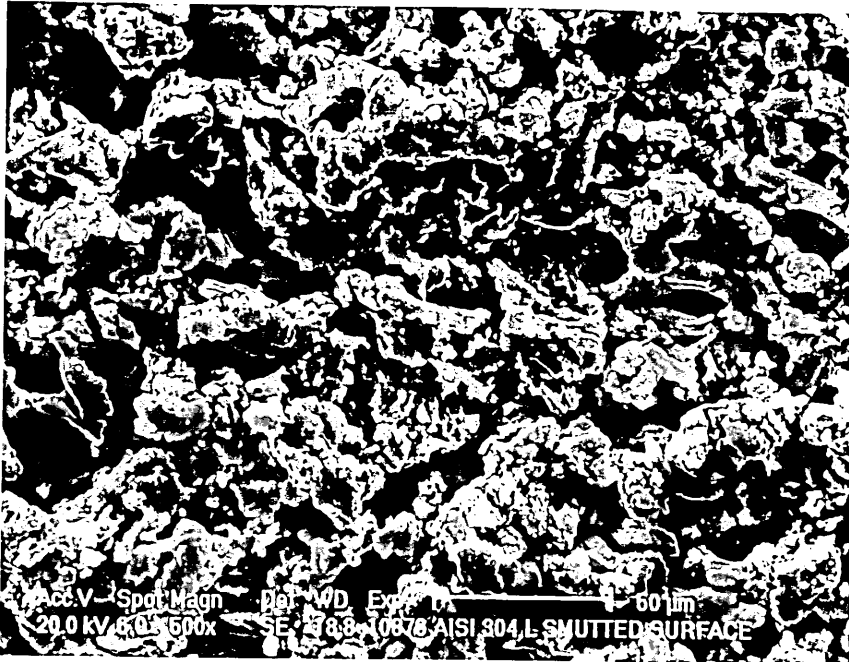
Scanning electron micrograph of AISI 304L stainless steel with *Alumina Blasted* surface ( $R_a = 1.1 \mu\text{m}$ ).

Plate 8.4.



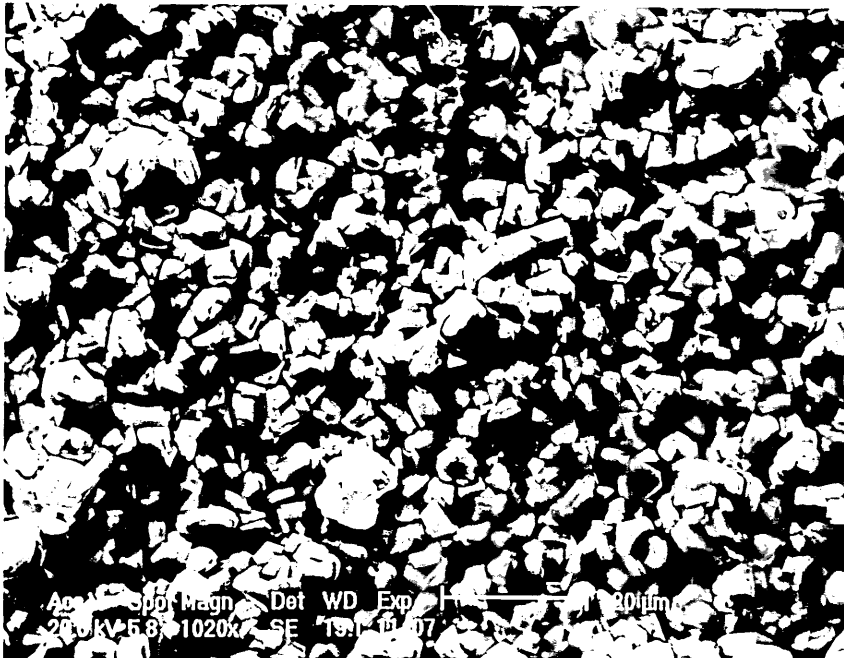
Scanning electron micrograph of AISI 304L stainless steel with *Acid Etched* ( $\text{H}_2\text{SO}_4$  - smut removed) surface ( $R_a = 1.8 \mu\text{m}$ ).

Plate 8.5.



Scanning electron micrograph of AISI 304L stainless steel with *Smutted* ( $H_2SO_4$  - smut un-removed) surface.

Plate 8.6.



Scanning electron micrograph of AISI 304L stainless steel with *Passivated* surface.

**Plate 8.1.** The *As Received* surface consisted of re-crystallised, equi-axed austenite grains, 5 to 20  $\mu\text{m}$  in size. The re-crystallisation occurred during annealing after cold rolling, although the rolling direction can still just be made out in the micrograph, running bottom left to top right, transgranularly engraved on the faces of flattened grains. The grain boundary areas showed signs of attack, i.e. the flattened grains were observed in relief, a result of the acid pickling process which was employed to produce the desired mat (2B) finish.

**Plate 8.2.** The *Scotchbrite Abraded* surface consisted of a plethora of scratches running in essentially the same direction; left to right in the micrograph. Although the scratches were many, they were very fine (0.5 to 2  $\mu\text{m}$ ) and there appeared to be little penetration into the surface of the steel.

**Plate 8.3.** The *Alumina Blasted* surface showed heavy deformation; an explosion of new surface had been exposed by the action of the hard alumina grit. Large (~10  $\mu\text{m}$ ), flake-like areas of deformed steel, in random directions, dominated the surface of the steel.

**Plate 8.4. and 8.5.** On the *Acid Etched* surface, the extent to which the acid attacked the steel surface was such that the grain boundary network could no longer be discerned. Deep angular craters were observed in the surface (5 to 10  $\mu\text{m}$  across), and the once whole grains showed heavy localised corrosion, pitting. The *Smutted* surface was very similar to that of the *Acid Etched* surface, showing the same signs of vigorous chemical attack.

**Plate 8.6.** The *Passivated* surface was very different from the *Acid Etched* and *Smutted* surfaces. The acid attack appeared to have been less vigorous; the surface consisted of nodular grains, generally < 5  $\mu\text{m}$ , with smooth, moulded features unlike the sharp, angular features observed on the *Acid Etched* and *Smutted* surfaces.

## **8.3.2. CHEMICAL CHARACTERISATION**

### **8.3.2.1. CHARACTERISATION OF PRE-BONDED ADHEREND**

Figures 8.1. to 8.4. are XPS spectra obtained from the surface of AISI 304L stainless steel (2B finish) in the *Alkaline Degreased* (primed and un-primed) and *Alumina Blasted* condition.

Figure 8.1. shows a wide scan spectrum of a silane primed *Alkaline Degreased* surface. The counts for carbon and oxygen (at 280 and 535 eV, respectively), were higher than those from the un-primed surface and silicon was present at a binding energy of 155 eV; this was attributed to the silane primer. There was one significant difference between the spectra from the *Alkaline Degreased* surfaces and the *Alumina Blasted* surface, the *Alumina Blasted* surface gave counts for aluminium at a binding energy of 120 eV (Figure 8.2.) and an increased oxygen count at 532 eV, (Figure 8.3.); this was attributed to residual aluminium oxide ( $\text{Al}_2\text{O}_3$ ) from the blasting process. It is worth noting that the presence of aluminium in a stainless steel/adhesive structural assembly would be unacceptable, due to the potential for galvanic corrosion. Figure 8.4. shows two chromium peaks from the steel surface.

### **8.3.2.2. EVALUATION OF SURFACE CLEANING METHODS USING GDOES**

The qualitative depth profile of the *As Received* surface and those of the surfaces pre-treated by *Alkaline Degreasing*, *Acid Rinsing*, *Acid Rinsing II*, *Alumina Blasting*, *Acetone/Inhibisol Rinsing* and *Solvent Wiping* are given in Figures 8.5. to 8.11. It is not possible to quantify surface contamination by GDOES, since the contamination layers, which are a only few nanometers in thickness, are beyond the resolution capabilities of this instrument. Thus, the spectra produced give only qualitative information, although, this is sufficient to allow discrimination between the different cleaning methods. The spectrum representing the *As Received* surface (Figure 8.5.) shows heavy contamination from carbon, oxygen, nitrogen, sodium, sulphur, hydrogen, chlorine, calcium, and silicon. The point at which the iron peak (from the bulk composition) becomes constant represents the extent of the surface layers. The spectrum representing the *Alkaline Degreased* surface (Figure 8.6.) shows light contamination with respect to carbon, silicon, and calcium. The *Acid Rinsed* surface (Figure 8.7.) gave a spectrum very similar to that

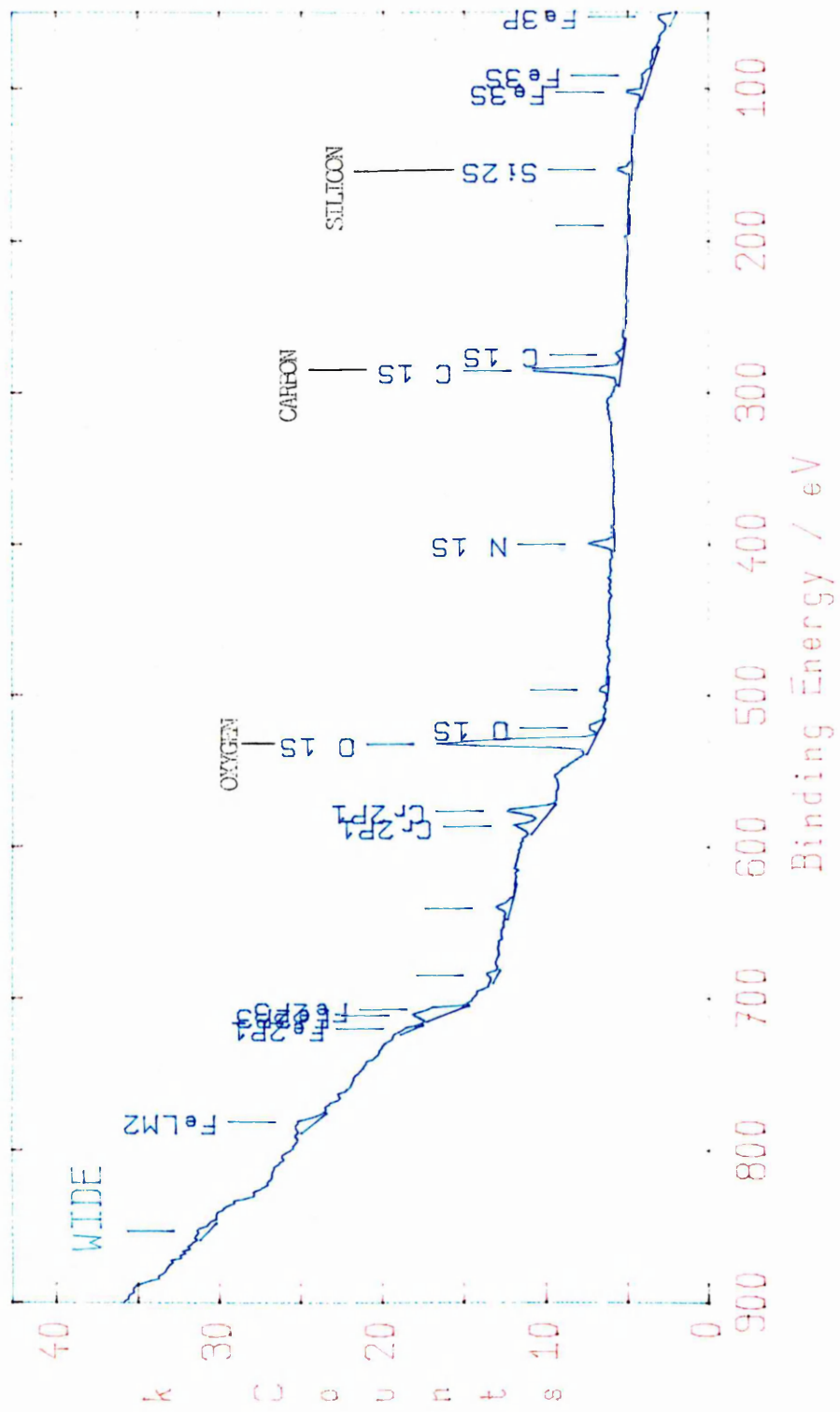


**Figure 8.1.** XPS wide scan of AISI 304L stainless steel (2B) surface. *Alkaline Degreased and silane primed.*

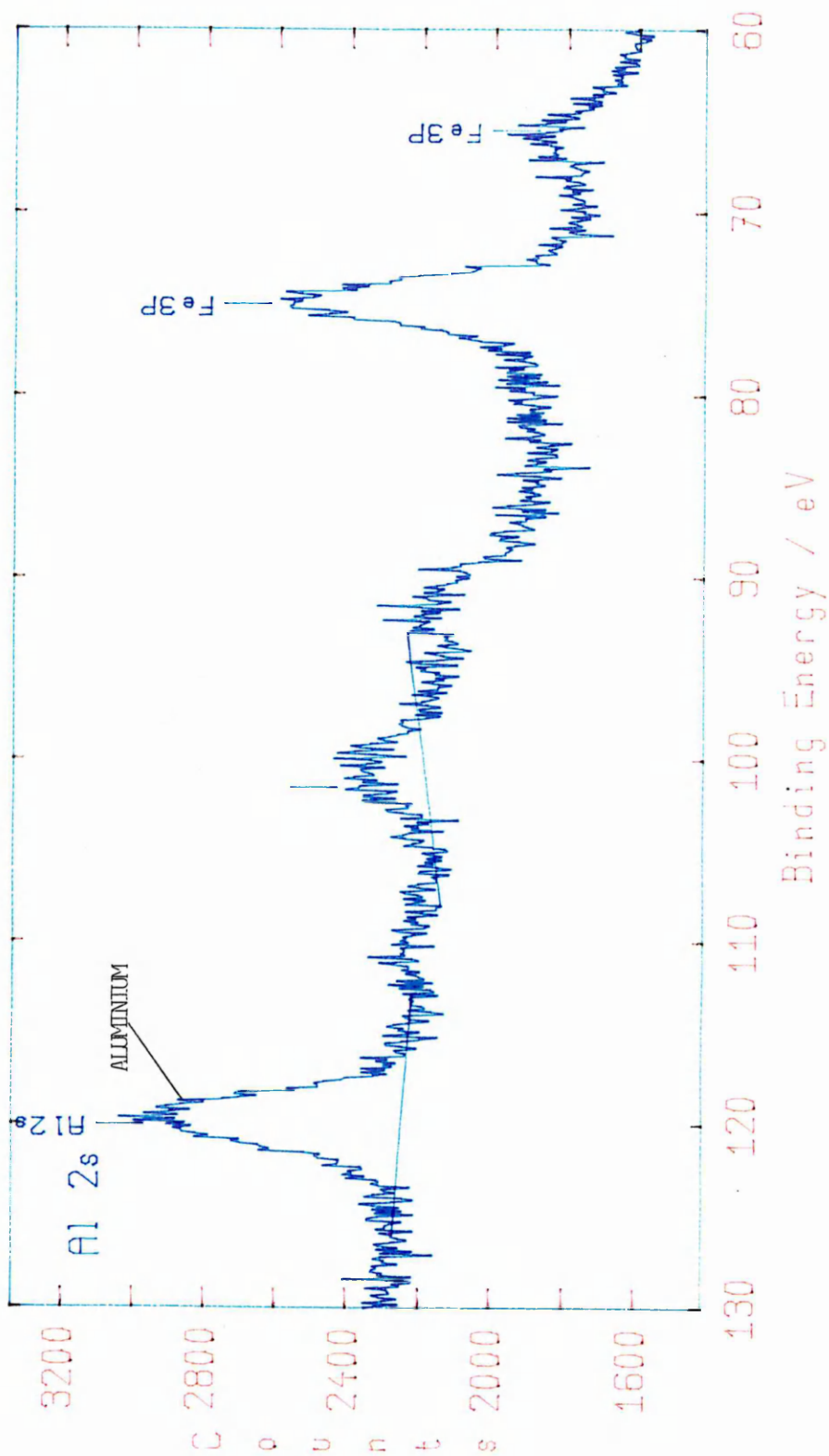


**Figure 8.2.** XPS elemental data of AISI 304L stainless steel (2B) surface. Alumina Blasted.

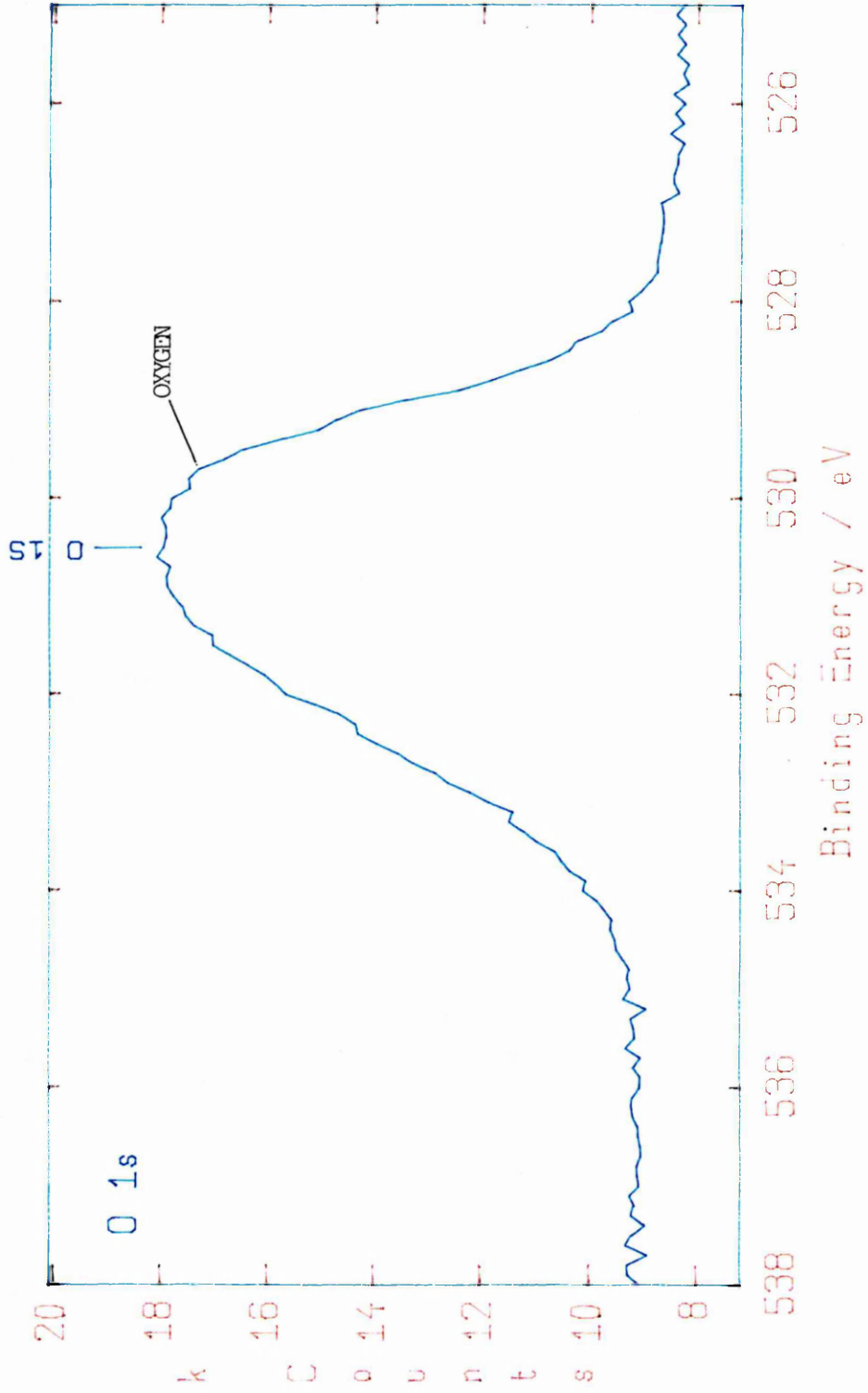


**Figure 8.3.** XPS elemental data of AISI 304L stainless steel (2B) surface. Alumina Blasted.

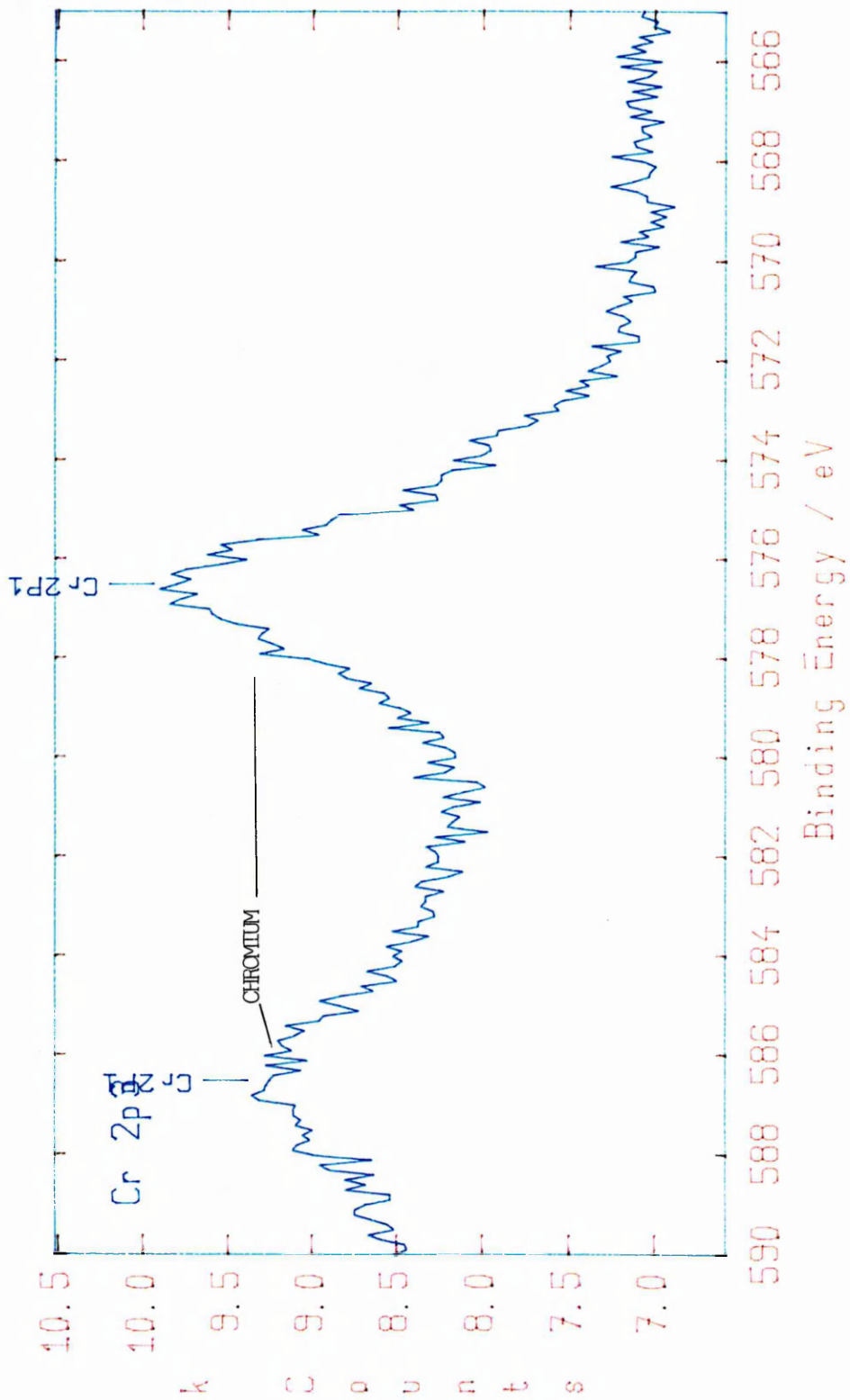


**Figure 8.4.** XPS elemental data of AISI 304L stainless steel (2B) surface. *Alkaline Degrease (un-printed).*

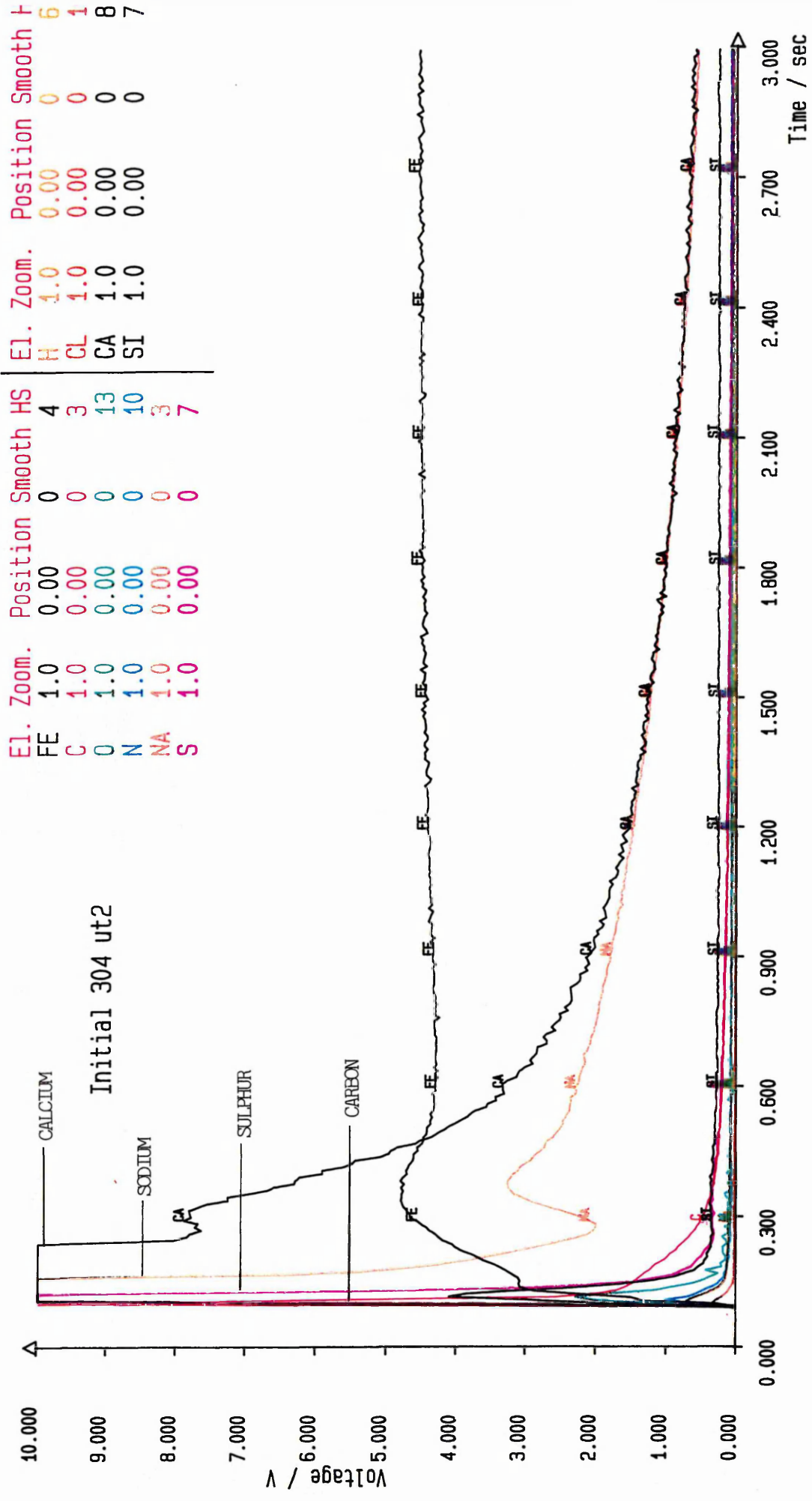


Figure 8.5. GDOES qualitative depth profile from AISI 304L stainless steel (2B) surface. As Received.

Initial 304 ad 2

El.	Zoom.	Position	Smooth	HS	El.	Zoom.	Position	Smooth	HS
FE	1.0	0.00	0	4	H	1.0	0.00	0	6
C	1.0	0.00	0	3	CL	1.0	0.00	0	10
O	1.0	0.00	0	13	CA	1.0	0.00	0	8
N	1.0	0.00	0	10	SI	1.0	0.00	0	7
NA	1.0	0.00	0	3					
S	1.0	0.00	0	7					

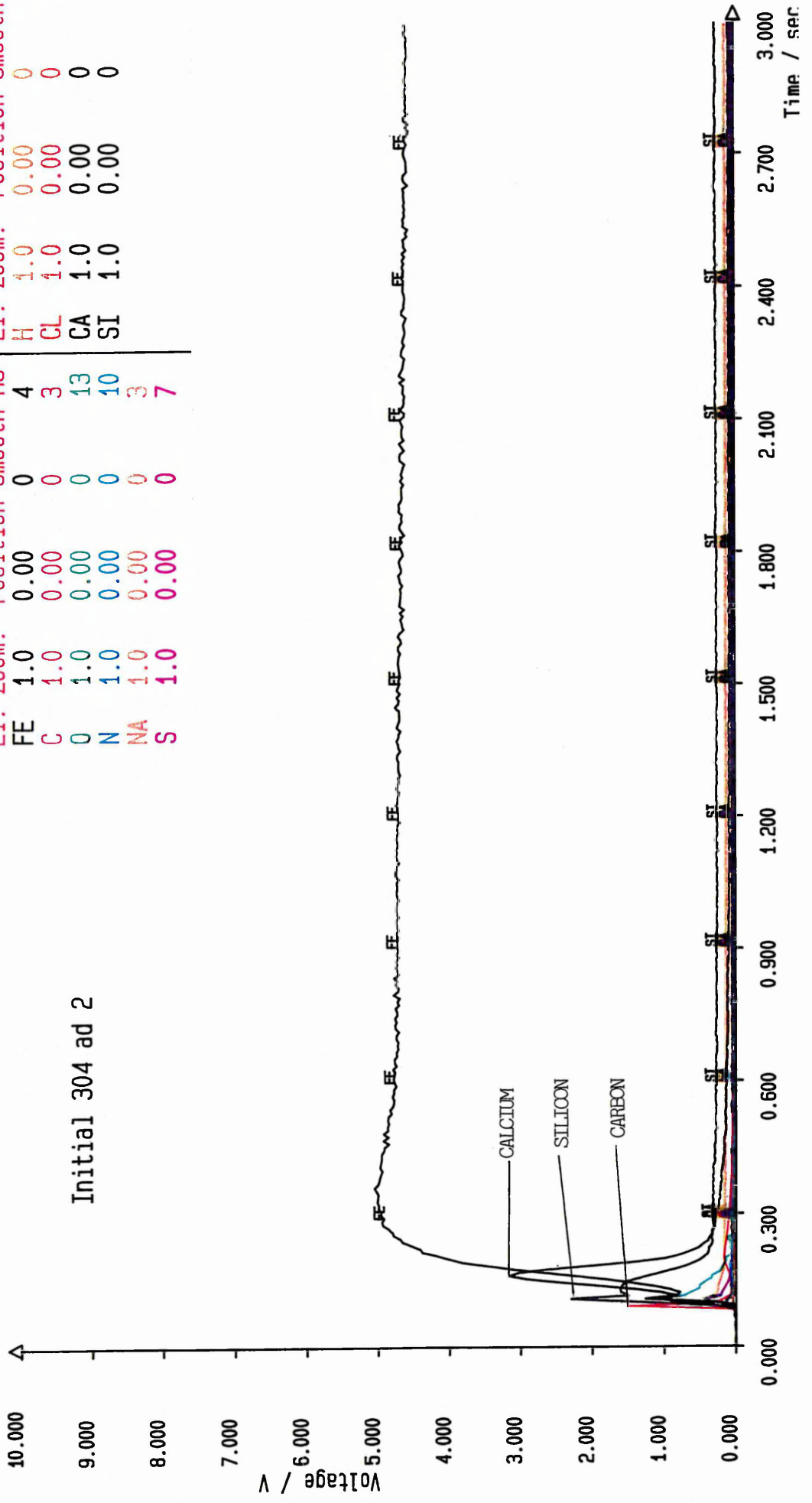


Figure 8.6. GDOES qualitative depth profile from AISI 304L stainless steel (2B) surface. Alkaline Degreased.

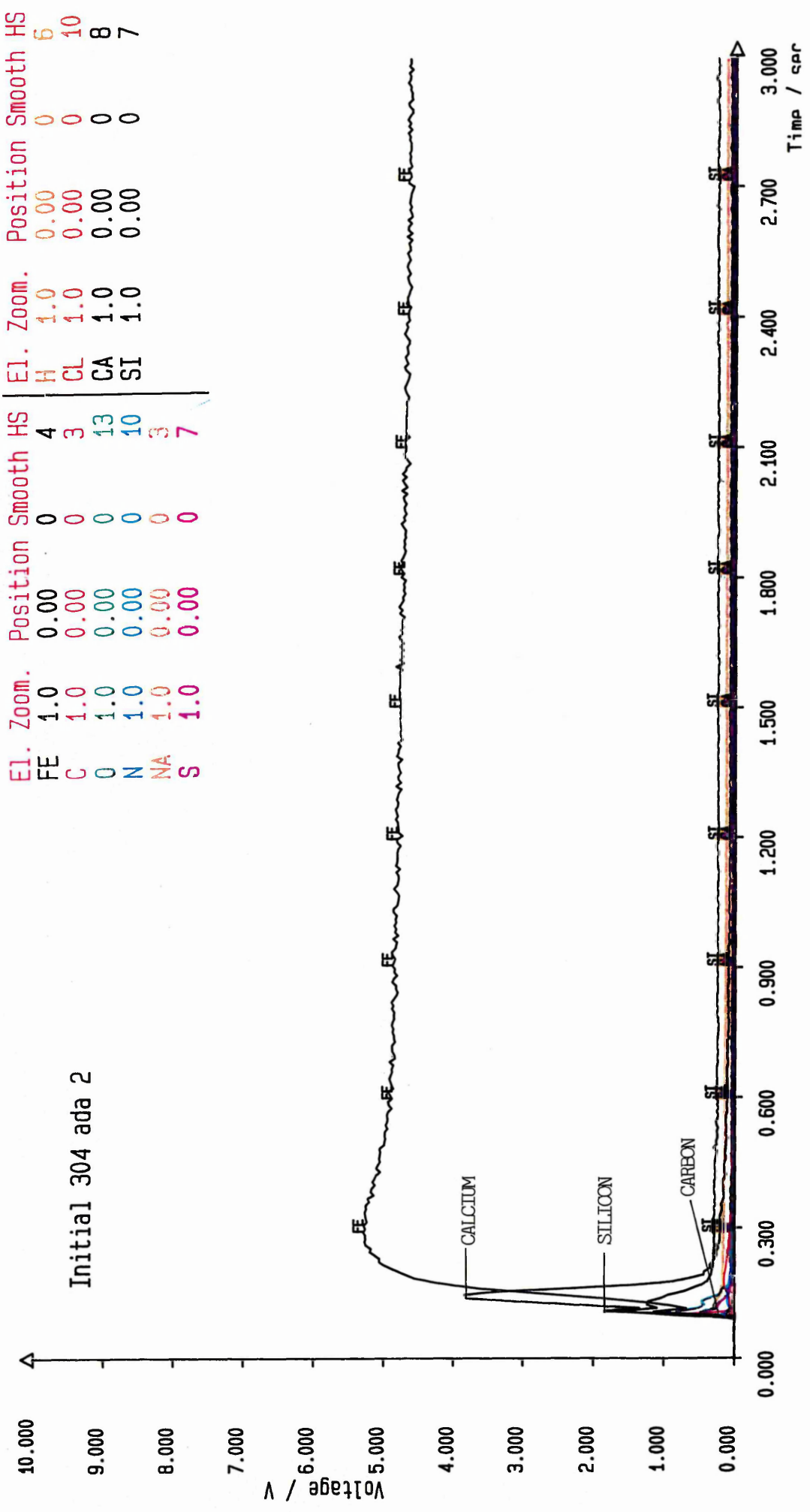


Figure 8.7. GDOES qualitative depth profile from AISI 304L stainless steel (2B) surface. Acid Rinsed.

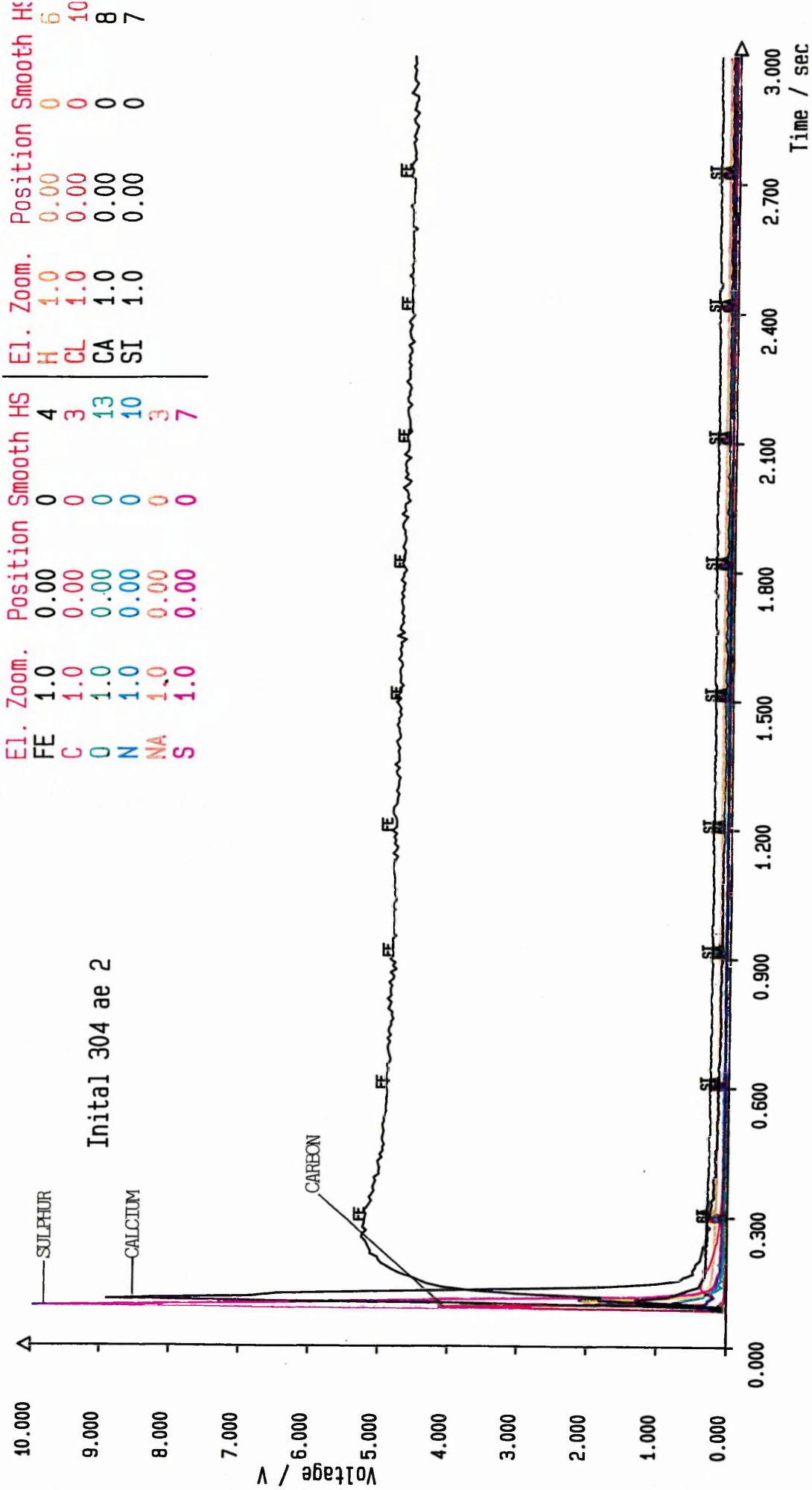


Figure 8.8. GDOES qualitative depth profile from AISI 304L stainless steel (2B) surface. Acid Rinsed II.

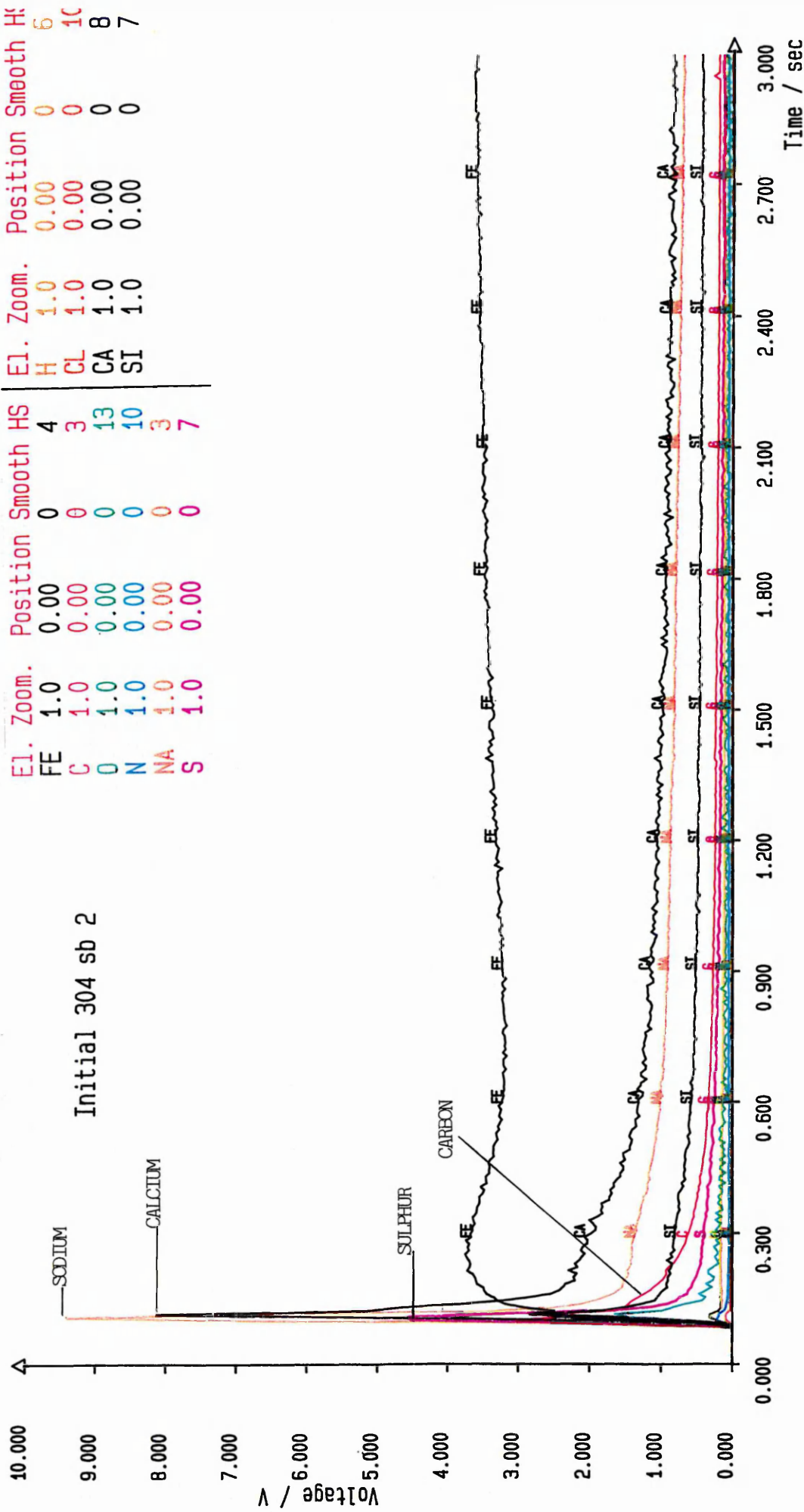


Figure 8.9. GDOES qualitative depth profile from AISI 304L stainless steel (2B) surface. Alumina Blasted.

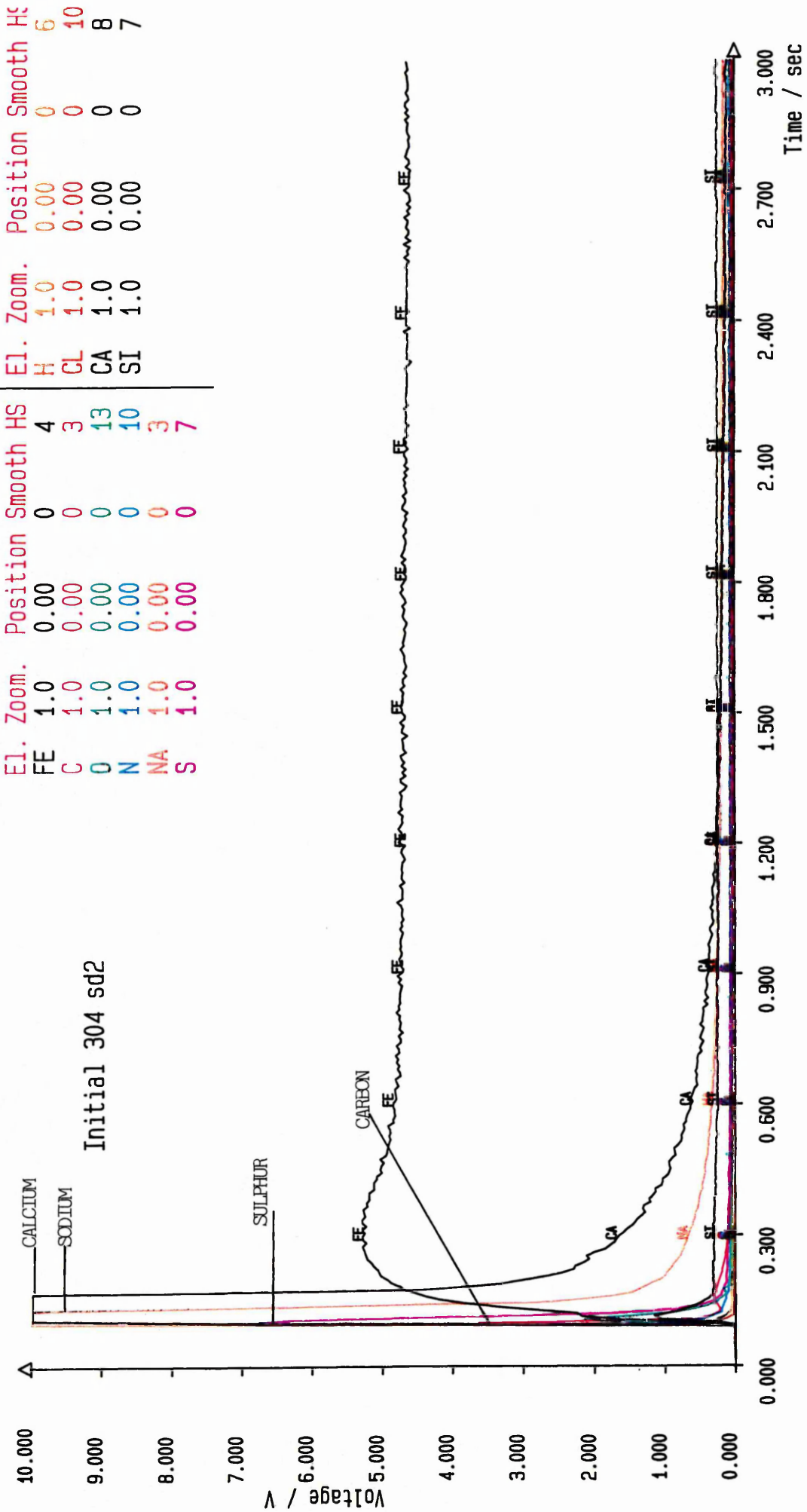


Figure 8.10. GDOES qualitative depth profile from AISI 304L stainless steel (2B) surface. Acetone/Inhibisol Rinsed.

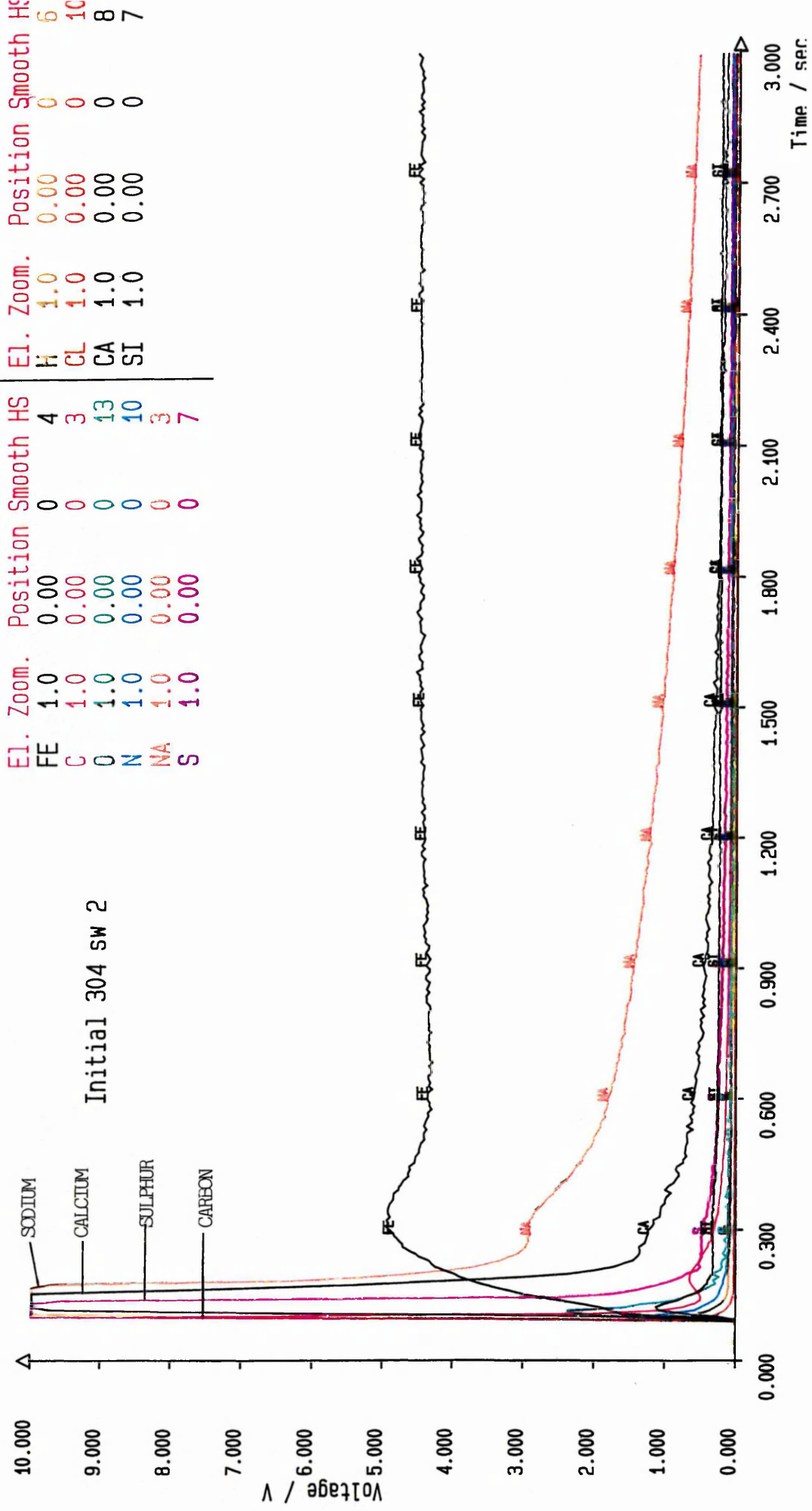


Figure 8.11. GDOES qualitative depth profile from AISI 304L stainless steel (2B) surface. Solvent Wiped.

obtained from the *Alkaline Degreased* surface, but showing less counts from carbon. The *Acid Rinsed II* treatment removed most of the contamination (Figure 8.8.), but high levels of carbon, sulphur and calcium were still present. The spectrum representing the *Alumina Blasted* surface (Figure 8.9.) showed the presence of calcium, sodium, carbon and sulphur, although the thickness was much reduced. The spectra obtained from the surfaces subjected to *Acetone/Inhibisol Rinsing* (Figure 8.10.) and *Solvent Wiping* (Figure 8.11.) were similar to that representing the *Alumina blasted* surface, although the reduction in thickness of the contamination was not as pronounced.

### **8.3.2.3. EXAMINATION OF FRACTURE FACES USING INFRARED MICROSCOPY AND EDX**

During the visual examination of the fracture faces of the failed joints, a large proportion of interfacial failure within the sub-surface region of the adhesive (interfacial<sub>Adhesive</sub> failure) was recorded. FTIR microscopy and EDX were employed to chemically verify that the thin interfacial layer was indeed adhesive. Figure 8.12. shows a FTIR spectrum taken from a fracture face with predominant interfacial<sub>Adhesive</sub> failure. The peaks between 2800 and 3000 wavenumbers are indicative of CH groups from the epoxy system DP 490. Figures 8.13a., 8.13b. and 8.13c. are EDX spectra taken from the adherend, the adhesive, and from an area of interfacial<sub>Adhesive</sub> failure, respectfully.

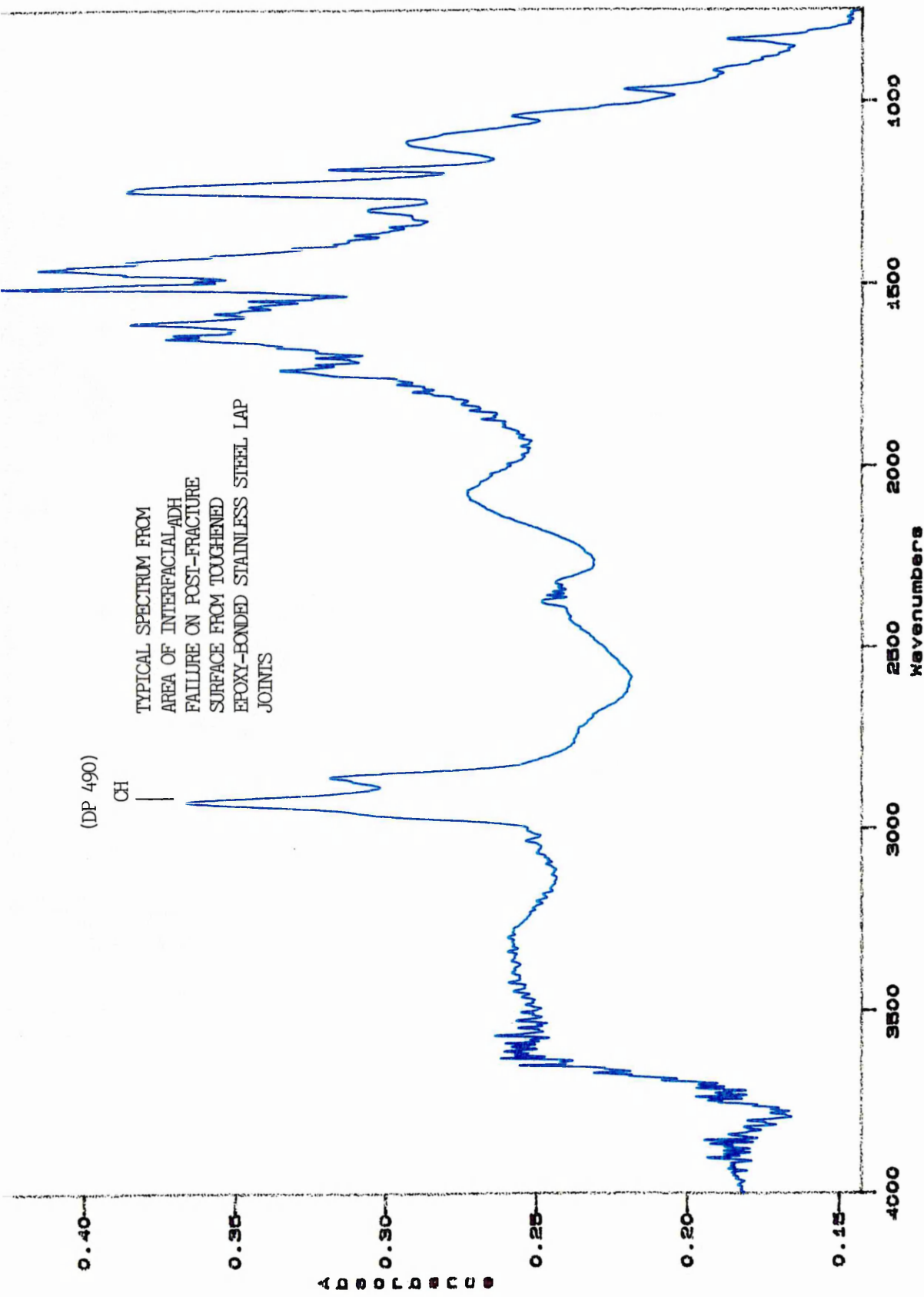


Figure 8.12. Infra red spectrum taken from fracture face of DP 490-bonded AISI 304L adhesive joint, showing evidence of interfacial adhesive failure.

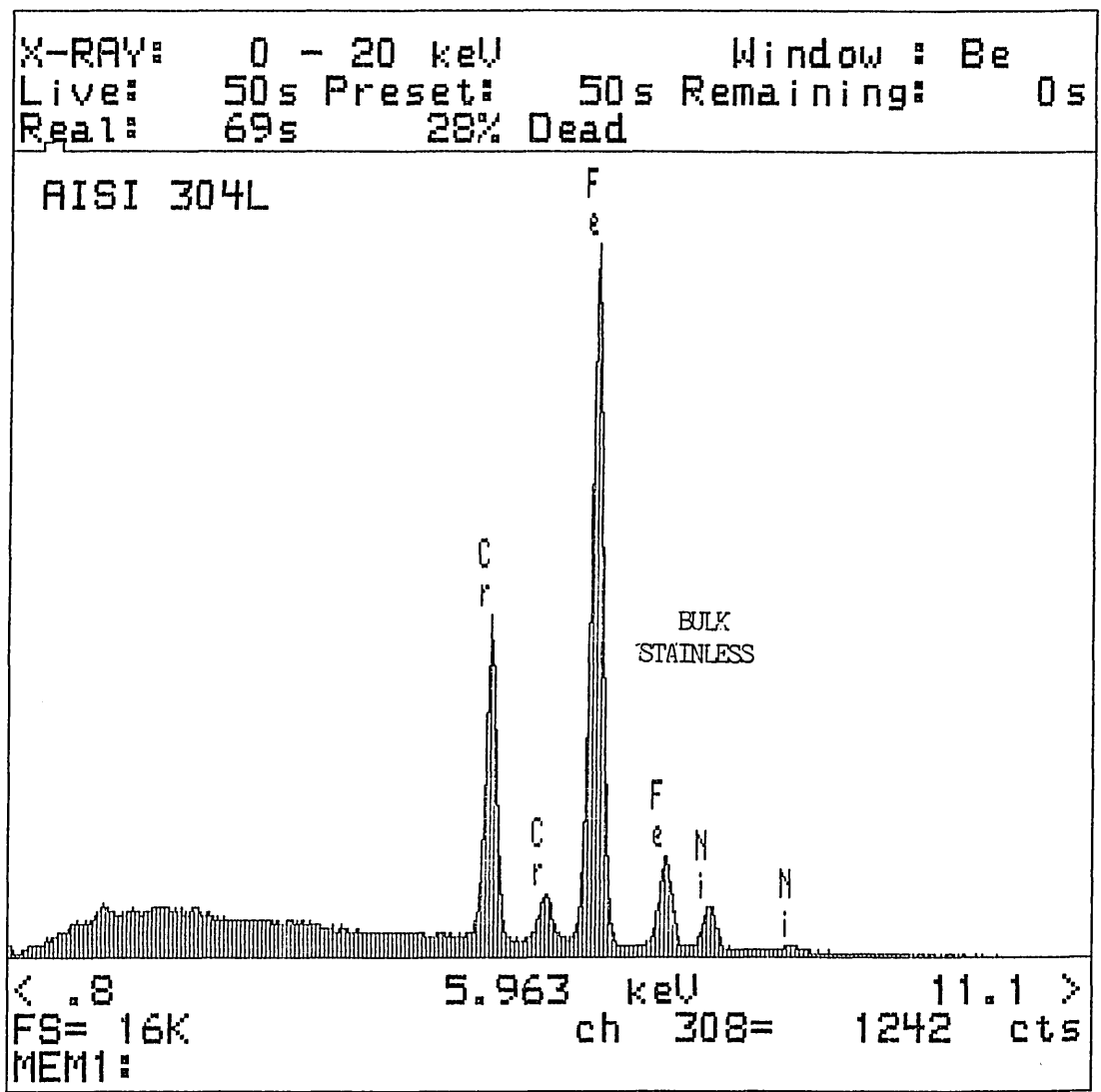


Figure 8.13a. EDX analysis of AISI 304L stainless steel surface. Indicative of adhesive failure.

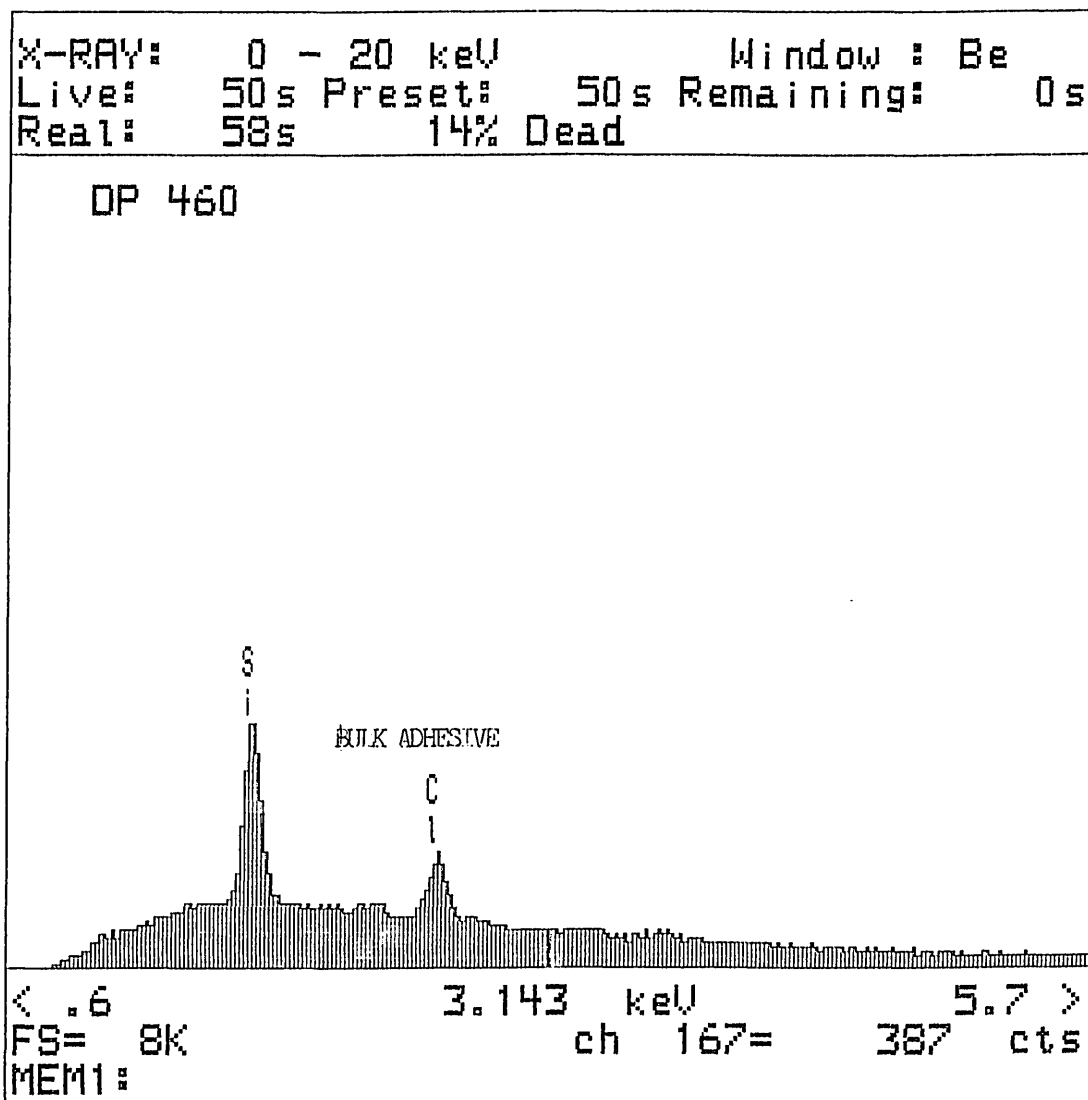


Figure 8.13b. EDX analysis of DP 490 toughened epoxy on fracture surface. Indicative of cohesive<sub>Adhesive</sub> failure.

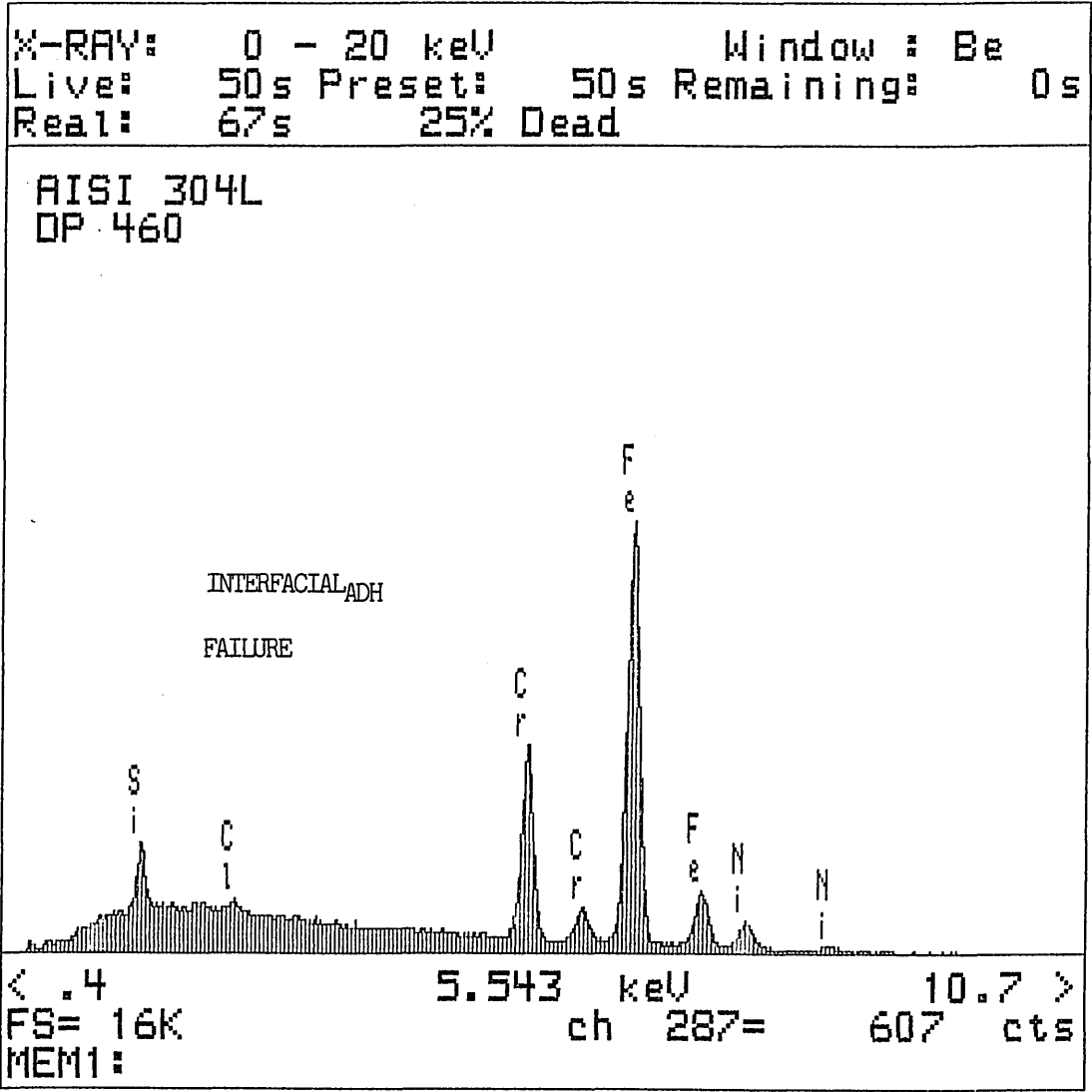


Figure 8.13c. EDX analysis of suspected interfacial failure on fracture face. Indicative of interfacial<sub>Adhesive</sub> failure.

## 8.4. DISCUSSION

During the course of the project a number of adherend surface pre-treatments were implemented in an attempt to optimise the bond strength and enhance the mechanical performance of stainless steel adhesive joints, and this warranted some form of surface analysis to characterise the pre-bonded adherends, both physically and chemically. In addition to this, it was necessary to physically and chemically characterise the post-fracture surfaces to ascertain the nature and locus of failure.

**Physical characterisation** Surface profilometry was employed to measure the surface roughness' of the pre-bonded adherends in order to equate these to the measured joint strengths. The Talysurf equipment used was reliable, quick (all surfaces measurements done in about 2 hours) and easy to operate. SEM was employed to evaluate and record the morphology and topography of pre-bonded surfaces and it was also used successfully to characterise the post-fracture surfaces as it proved to be an excellent means of examining fractures to determine the loci of failure; cohesive<sub>Adhesive</sub> and adhesive failure were easily distinguishable under relatively high magnification, interfacial<sub>Adhesive</sub>, however, was more difficult to discern. One can be taught to drive an SEM after about 10-15 hours instruction, there is no, or very little, sample preparation necessary and the resulting micrographs provide a hard copy fingerprint of the adherend surface.

It was impossible to discriminate between the different surface pre-treatments using the mechanical test results (single lap shear and floating roller peel), with the exception of the *As Received* surfaces which gave inferior joint strengths. However, during the Boeing wedge crack extension tests, joints incorporating adherends, either mechanically roughened by *Alumina Blasting* or chemically roughened by *Acid Etching* or *Passivating*, performed much better than the other joints. This was thought to be due to the surface macro-roughness acting as a hindrance to crack propagation, i.e. the crack tip is forced to change direction against the peel stresses and follow the surface profile of the roughened adherend as it propagates between the adhesive and the adherend during adhesive failure. Complimentary to this, SEM revealed the increase in surface area available for chemical bonding and the depth of penetration available for mechanical interlocking, created by mechanical and chemical roughening, which would also explain the wedge test results.

**Chemical characterisation** Although the equipment was not fully utilised XPS did provide some useful elemental information; the presence of silane primer on primed surfaces was chemically verified and traces of alumina were discovered on *Alumina Blasted* surfaces. GDOES analysis was found to be suitable for qualitatively evaluating surfaces subjected to different cleaning regimes. However, if quantitative analysis is required then XPS is a more appropriate technique; GDOES can provide quantitative information, but the elements to be quantified must be calibrated against a known standard. EDX analysis was used successfully to chemically verify interfacial failure within the adhesive (interfacial<sub>Adhesive</sub>) on post-fracture faces. IR spectroscopy was also employed to verify interfacial<sub>Adhesive</sub> failure. Loci of failure within the metallic surface oxide layer (interfacial<sub>Oxide</sub> failures) would be difficult to detect using any of the surface analytical techniques discussed. The only way of accurately evaluating interfacial<sub>Oxide</sub> failure is to fracture the bonded joint and examine the resultant fracture faces in situ under vacuum.

## 8.5. CONCLUSIONS

1. Pre-bonded adherends can be physically characterised using SEM and surface profilometry, and post-fracture surfaces can be physically characterised using SEM.
2. For quantitative chemical characterisation of pre-bonded adherends and post-fracture surfaces XPS must be considered, however, if qualitative information will suffice, pre-bonded adherends can be characterised using GDOES. FTIR and EDX are suitable techniques for chemically evaluating post-fracture surfaces.
3. Interfacial failure within the surface layers of the adhesive (interfacial<sub>Adhesive</sub>) can be chemically verified using FTIR and EDX analysis.

## 9.0. DISCUSSION

**Adhesive screening** At the start of this project a review of literature was undertaken to provide a background into adhesive bonding and to enable the starting point of the experimental work to be established. It soon became apparent from the literature that the epoxy family of adhesives offered the ultimate in terms of structural performance and that they have been, and are being, used successfully to bond metallic substrates. Unfortunately, the literature regarding adhesive bonding of metals was dominated by aluminium adhesive joints; occasionally there were references to mild steel adhesive joints, titanium adhesive joints and sometimes even stainless steel adhesive joints, but most of the time it was aluminium adhesive joints. This is not surprising because a lot of time, money and effort has been spent researching and developing aluminium adhesive joints for the aerospace industries, because of the weight saving benefits they offer. Aluminium, like stainless steel, is protected from corrosion by a very thin metallic oxide layer, which is self-repairing when damaged. In order to optimise the strength and durability of aluminium adhesive joints, the aluminium substrates (adherends) were chemically treated to modify and develop the inherent oxide into one much thicker and more tenacious, and this worked very well for aluminium. Thus, a starting point was established, a screening program. Six candidate adhesives or adhesive systems (4 epoxies (2 of which were toughened), a polyurethane and an acrylic) were selected; all adhesives supplied by 3M UK plc. One adherend material was chosen, a commercial grade austenitic stainless steel AISI 304L, but a number of adherend surface pre-treatments were included in the schedule. Two mechanical tests were decided upon, single overlap shear and floating roller peel, to discriminate between the different adhesives and the different adherend surface pre-treatments. The joints bonded with epoxy systems gave the highest shear strengths (Figure 3.10.), although the polyurethane-bonded joints gave an outstanding performance in the peel tests (Figure 3.13.). One adhesive was finally selected, because of its shear and peel performance, its ease of application and cost, and also because of its compatibility with a stainless steel surface (measured by the proportion of cohesive failure on the post-fracture surface); toughened epoxy system DP 490. Although the adhesive screening procedure was relatively straight forward, the contributions to joint strength afforded by the adherend pre-bonding treatments was less conclusive. In the lap shear tests there was a slight improvement for those joints incorporating *Acid Rinsed* adherends, and modifying the surface roughness of the adherend proved to be of some benefit to peel performance, possibly due to an increase

in the degree of mechanical interlocking. Generally, roughening the surface, mechanically or chemically, improved joint performance and consistency, and again, this was attributed to mechanical interlocking or to the cleaning proficiency of the roughening treatments. In conclusion, if stainless steels are to be joined using adhesives, with the intention of employing the resulting fabrications in structural applications, toughened epoxy systems must be considered, and physical and/or chemical modifications to the adherend surface may improve initial joint strengths and durability. N.B. there were two important observations in the screening schedule: the adherend material plastically deformed during the lap shear test; and removing the fillets of hardened adhesive 'squeeze-out' from the perimeter of the bonded lap joint prior to testing, resulted in a 25% reduction in the measured shear strength. The plastic deformation of the adherend was explained by the rotation of the lap joint in tension because of a bending moment induced due to the asymmetry of the load axis. This would give rise to intense tensile forces (peel forces) at the extremes of the overlap which may initiate premature joint failure, and this would explain the reduction in strength of joints with the fillets removed, i.e. the presence of the fillets must minimise the peel stresses at the extremes of the overlap.

**The importance of surface cleanliness** It is well known, not only by those in the adhesives community, but by everyone, that dirty surfaces are impossible, or at least, very difficult to stick together. Surface contamination can act as a weak boundary layer, preventing chemical intimacy between adhesive and adherend, and consequently adversely affecting bond strength. To investigate the extent to which weak boundary layers affected bond strength, single overlap shear tests were conducted on AISI 304L stainless joints bonded with the toughened epoxy DP 490 and incorporating adherends subjected to different degrees of surface preparation (Figure 4.1.). Only joints incorporating *As Received* surfaces and those minimally cleaned by *Dry Wiping* gave inferior joint strengths. Joints with adherends cleaned using solvent degreasing and acid rinsing methods gave reasonable joint strengths, as did those with chemically and mechanically roughened adherends (*Smutted* and *Alumina Blasted*); in the latter case the joint strengths were attributed to mechanical interlocking and to the effective cleaning action of the roughening techniques. Etching stainless steel in 30% sulphuric acid at 70 °C results in the formation of a black, velvety oxide on the surface of the steel known as smut. Smut is easily removed, either chemically or mechanically, and it is thought by some (11) to adversely affect joint strength. However,

as mentioned above, joints incorporating *Smuted* adherends gave reasonable joint strengths. At high magnification the *Smuted* surfaces appeared sponge-like and it was assumed that the joint strength was due to mechanical interlocking achieved as a result of the liquid adhesive deeply penetrating the smut layer before starting to harden. Although reasonable joint strengths were attained the loci of failure were predominantly within the oxide layer, proving that smut is indeed weakly adhered to the steel surface. Again the failure was thought to be initiated by peel stresses at the extremes of the overlap induced during joint rotation, resulting in failure at the weakest bond in the joint, the steel/oxide interface. Priming the surface of the adherend using a silane primer prior to bonding did little to improve the initial shear strength, or indeed, detract from it. The problem with priming metallic surfaces, however, is controlling the concentration, the amount and the uniformity of the primer applied, using primers, therefore, may be detrimental to joint strength, because excess primer may act as a weak boundary layer to adhesion if non-uniformly applied. In conclusion, surface contamination will provide a barrier to adhesion if present in sufficient quantities and will adversely affect bond strength. However, for stainless steels the cleaning procedure need not be that elaborate, degreasing using solvents and weak acids appears to be sufficient. Primers are reported to improve joint performance, particularly durability and this may be the case, but they may also be detrimental to bond strength if applied incorrectly; the thickness of the primer, its concentration and distribution are very important factors, for example, if the primer layer is too thick this can impart brittleness to the joint and consequently reduce the bond strength; this was the case during supplementary peel tests, where the loci of failure were observed on the post-peel fracture surfaces to be within the primer layer. The peel tests, like the lap shear tests, failed to conclusively discriminate between primed, non-primed and over primed surfaces. However, one of the advantages of priming is that it provides a protective layer on the surface of newly cleaned and prepared adherends, which means that treated adherends can be stored for sometime before they are bonded. During this stage of the experimental work, the significance of the adhesive thickness (bondline) was evaluated using single overlap shear and floating roller peel tests. Increasing the bondline in the lap shear tests resulted in a decrease in bond strength (Figure 4.2.). This, result was expected as the increased bondline would mean an increase in the magnitude of the bending moment which would adversely affect bond strength. However, the results of the peel tests were inconclusive and this was contrary to what was expected. The peel strength was expected to increase with increasing

bondline thickness (116-122); essentially as the thickness of the adhesive layer is increased in the peel test a larger volume of adhesive is subjected to deformation per unit area of detachment so that the total energy expended in peeling increases. However, at large thickness' the energy dissipated during peel then becomes independent of the overall thickness of the adhesive, since the dissipation process no longer involves the entire layer of adhesive (11).

**Environmental durability** To investigate the environmental durability of adhesive bonded stainless steel, single overlap shear and floating roller tests were carried out before, during and after ageing. The joints were aged in ambient conditions and in a humid environment (98% R.H.). The adherend material used was AISI 304L (2B) stainless steel, pre-treated by *Alkaline Degreasing* and priming with a silane primer. Boeing wedge crack extension tests were also conducted using a number of different environments, ambient, humid, sub-zero, and immersed in water. The toughened adhesive DP 490 was the preferred adhesive selection, but the polyurethane was also considered in light of its excellent performance in the floating roller peel tests. The curing time recommended by 3M for the DP 490 system, 7 to 10 days at 20°C proved to be about right, the lap shear tests gave low shear strengths when the joints were under-cured (one day), although handling strength had developed. Ageing the lap joints in ambient and at 98% R.H. did little to detract from the shear strength. A strong, durable bond must have been attained initially between the adhesive and the adherent and this intimacy had apparently remained un-compromised even within a humid environment. Similarly, the floating roller peel strength remained reasonably constant with time, appearing not to be affected even in high humidity conditions. However, peel tests conducted before the recommended curing cycle had elapsed (one day) gave higher peel strengths. This was attributed to the liquid adhesive adequately wetting the surface of the stainless steel and developing strong durable bonds during the initial stages of the curing cycle. However, as the curing cycle continued the subsequent increase in cross-linking may have resulted in the redundancy of some of the original durable bonds between the adhesive and the adherend, in order to facilitate cross-linking. Thus, the peel strength of a fully cured joint may be less than that of one partially cured. Although the results of the lap shear and peel tests were almost inconclusive, those of the Boeing wedge test were very different. In ambient conditions the joints bonded with the toughened epoxy DP 490 and incorporating adherends with mechanically or chemically roughened surfaces

(*Alumina Blasted*, *Acid Etched* and *Passivated*), experienced hardly any crack growth after about 1 month of ageing (Figure 5.6.). This was attributed to surface roughness providing obstacles to crack propagation and sites for mechanical interlocking. In addition, the surface area and surface energy would be greater to accommodate more chemical bonds and render the surface more adhesive-receptive. The integrity of the bonds may also benefit from the degree of surface cleanliness provided by the roughening treatments. However, un-primed joints incorporating *Alkaline Degreased* adherends experienced slightly more crack growth, but the joints with *Alkaline Degreased* and primed adherends experienced about 13 mm crack growth after about 2 weeks. This was attributed to brittle failure within the primer layer (interfacial<sub>Prim.</sub>). Joints incorporating mechanically and chemically roughened adherends, aged in a high relative humidity environment (Figure 5.7.), proved to be more resistant or tolerant to the ingress of moisture, whereas joints with *Alkaline Degreased* adherends experienced greater crack growth and priming the surface did little to improve the durability of the joint. Joints bonded with the polyurethane system 3532 (Figures 5.8. and 5.9) generally gave a poorer performance than those bonded with DP 490, particularly in the high humidity environment. This suggests that the interfacial bond strength to resist crack propagation between adhesive and adherend is higher and less susceptible to the ingress of water in joints bonded with the epoxy DP 490, and that the DP 490 is inherently tougher than the polyurethane 3532. Once again, joints incorporating mechanically or chemically roughened adherends generally performed better for the same reasons as discussed above, with the exception of joints with *Passivated* adherends aged in ambient conditions, which gave a poor performance. Considering joints bonded with the toughened epoxy DP 490 at a sub-zero temperature of -16°C (Figure 5.10.). There was no crack extension in joints incorporating *Alumina Blasted* adherends and this was attributed to the toughness of the epoxy and to the extent of mechanical interlocking afforded by the roughened surface. The short term durability of joints incorporating *Alkaline Degreased* surfaces was much improved by priming with the silane and the Accomet C primers; no crack extensions were observed after 120-180 hours at -16°C, respectively. Although the primers became less effective with time and crack extensions were observed after ~1000 hours. Considering joints bonded with DP 490 immersed in de-ionised water at room temperature (Figure 5.11). Joints incorporating *Alumina Blasted* adherends proved by far to be the most durable, no crack extension was incurred after 1000+ hours. Although, joints incorporating *Alkaline Degreased* adherends primed with Accomet C

showed some crack growth, the extension was gradual, so the Accomet C primer must have contributed to the bond strength and the moisture resistance at the adhesive/adherend interface. Joints with *Alkaline Degreased* and un-primed adherends performed poorly under water, and priming with a silane primer did little to improve joint durability. In conclusion, the durability of adhesive joints will be improved by roughening the surface of the adherends, either by mechanical or chemical means. The integrity of the bond and the extent of bonding is determined by several factors: mechanical interlocking; surface cleanliness; surface energy; and surface area. Priming the surface of the adherend prior to bonding will to some extent improve joint durability by increasing the strength and resistance of the chemical bonds at the adhesive/adherend interface. However, priming the pre-bonded surface may be detrimental to joint durability and impart brittleness to the joint if the thickness of the primer layer is excessive. Finally, the Boeing wedge crack extension test is a more suitable means of assessing joint durability than either the single overlap shear or the floating roller peel tests. This is because, in the wedge tests, the joints are stressed and aged, simultaneously, rather than tested at ambient temperature and relative humidity after a finite ageing time has elapsed; the former test is more typical of in-service life.

**Significance of the adherend material** The majority of the experimental work presented in this thesis has considered only one adherend material; a low carbon, austenitic stainless steel AISI 304L. However, because there are a number of different types of stainless steels, it was decided to compare the single overlap shear strengths of adhesive bonded stainless steel joints incorporating different grades of stainless steel. The grades considered; austenitic, ferritic, martensitic and duplex, were selected to represent the four main families of stainless steels. Two adherend thicknesses were considered, 2 mm and 1.25 mm. Only one adhesive was employed in the investigation, the toughened epoxy DP 490. The different grades of stainless steel had different surface finishes, i.e. 2B, 2D, and bright annealed, and the surfaces were only subjected to a minimal degree of surface preparation, *Solvent Wiping*. Reasonable joint strengths were obtained for all the joint combinations considered. The chemical and physical nature of the surfaces of the grades of the stainless steels included in the evaluation did not appear to enhance or detract from joint strength. In addition, *Solvent Wiping* was proven to be a sufficiently thorough cleaning procedure for stainless steels, at least with respect to initial joint strength. The shear strengths of joints with 2 mm thick adherends were approximately 25% higher than those of joints

incorporating 1.25 mm adherends. The most surprising result of the tests, however, was the significant difference in lap shear strength observed between joints incorporating different grades of stainless steel.

Consider a single overlap joint loaded in tension. Because the directions of the two forces ( $P \leftarrow \rightarrow P$ ) are not co-linear a bending moment is induced as the load is increased and the joint rotates to bring the line of action closer to the centre of the adherends in order to reduce the value of the bending moment. At this point the joint becomes analogous with the deflection of a fixed beam under load. The elastic rotation was modeled as a function of the shear stress using equation 6.11. The derivation is given in Chapter 6.0.

$$\theta_{TOTAL} = \frac{h+t}{a \cdot \left[ 1 + \frac{E \cdot h^3}{6 \cdot \sigma_s \cdot l \cdot a^2} \right]} \quad (6.11.)$$

The elastic model (Figure 6.6.) predicts that lap joints incorporating thick adherends will rotate more than joints with thinner adherends due to the increased asymmetry of the load axis. The model was also used to estimate the nominal line peel stress and nominal line peel force at the centre of the overlap as a function of the shear stress (Figures 6.7. and 6.8.). Equation 6.22. is a model that provides an alternative means of determining the line peel force at the extremes of the joint overlap.

$$P_f = \frac{\sigma_s(h+t)}{\frac{(a^2 + c^2)}{a \cdot c}} \cdot \left[ 1 + \frac{E \cdot h^3}{6 \cdot \sigma_s \cdot 2c \cdot (a^2 + c^2)} \right] \quad (6.22.)$$

Equation 6.22. is a more detailed calculation with two equal line forces at the end of the adhesive layer. However, the resulting plot, line peel force f(shear stress) - Figure 6.10., does not differ more than 8% from the nominal line peel force f(shear stress) shown in Figure 6.8.

However, the problem with the two models is that plastic rotation is not considered. To help explain joint behaviour, the supposed plastic rotations are superimposed on the elastic model represented in Figure 6.10. Considering joints incorporating 'high' yield strength adherends such as martensitic stainless steel. As the load increases the joint will rotate elastically and peel stresses will be introduced at the extremes of the overlap. However, because the high yield strength of the adherend imparts

stiffness to the joint, plastic rotation will be prevented or minimised and the peel stresses will not be critical, instead the joint will fail by a shear-dominated, adherend-controlled mechanism at a critical shear stress (the elastic model explains the behaviour of joints with martensitic adherends). Considering joints with 'low' yield strength adherends, however. As the load is increased the joint rotates and peel stresses are introduced at the extremes of the overlap due to elastic rotation. At higher loads plastic rotation occurs as the adherend yields and the peel stresses at the extremes of the overlap will increase dramatically, which will lead to peel-dominated, adherend-controlled failure at a critical peel force.

As the thickness of the adherend material increases the magnitude of the bending moment increases, but at the same time the increase in thickness imparts stiffness to the joint and elastic and plastic rotation is minimised, therefore, higher joint shear strengths will be realised in joints with thicker adherends because premature failure due to rotation-induced peel stresses will be avoided and failure will be controlled by the shear properties of the adhesive, when a critical shear stress is reached. Whereas, in joints with thinner adherends, although the bending moment decreases, adherends are susceptible to plastic deformation which will result in failure at lower loads due to peel.

In summary, lap shear strengths will be higher for joints incorporating stiffer adherends, where the stiffness of the joint is increased, by increasing the adherend thickness and/or by incorporating inherently stiffer, high yield strength, adherends. Although the bending moment will be greater in joints with thicker adherends, joint rotation will be less because the thickness of the adherend will impart stiffness to the joint and, therefore, resist rotation. Lap joints incorporating high yield strength adherends will also give higher joint strengths, because of the stiffness imparted to the joint by the inherent yield strength of the adherend material to resist rotation. Failure will be by shear-dominated, adhesive-controlled failure. However, joints with low yield strength and/or thin adherends, where the rigidity or stiffness of the joint is much reduced, will rotate plastically and premature failure by peel-dominated, adherend-controlled failure will ensue. N.B. The two different scenarios, shear-dominated, adhesive-controlled failure and peel-dominated, adherend-controlled failure, are extreme examples. In reality, joint failure will be partially due to a shear component and partially due to a peel component.

Using the elastic model, Figure 9.1. shows the effect of adherend thickness on elastic joint rotation. It is clear that elastic rotation will increase to an optimum as the thickness of the adherend increases because of the increased asymmetry of the joint. However, at greater adherend thicknesses elastic joint rotation will be less due to the stiffness imparted to the joint by the thickness of the adherend. The experimental work carried out in this study considered only two adherend thicknesses and therefore it is impossible at this stage to confirm the prediction of the elastic model at large adherend thicknesses. Further experimental work is therefore necessary to determine the single overlap shear strengths for joints incorporating adherends of different thicknesses, ranging from 4 mm to 20 mm. Different stainless steel grades should also be incorporated in the test programme to investigate further the significance of the adherend yield strength. In addition, the actual rotation of the joints during testing must be measured accurately to compare with the predicted rotation.

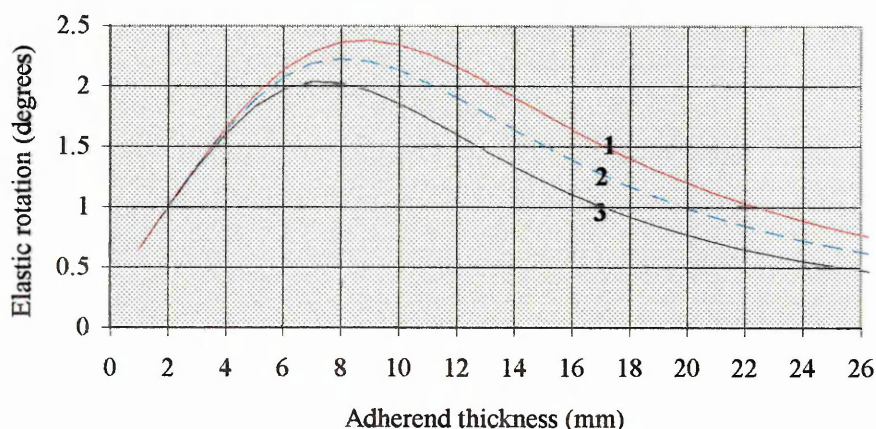


**Figure 9.1.** Effect of adherend thickness on elastic joint rotation:

- 1 - shear stress 25 MPa;
- 2 - shear stress 20 MPa;
- 3 - shear stress 15 MPa.

**Room temperature creep and dynamic fatigue performance** During the room temperature creep tests considerable scatter was observed, particularly with the standard single overlap shear tests (Figure 7.4.). The bending moment experienced by the standard single overlap shear was apparent, although the reinforced ADtranz test specimens gave no evidence of bending of the adherends during the tests. An endurance limit was observed, however, at approximately 40% of the static strength of the ADtranz

specimens. The dynamic fatigue tests were much more conclusive (Figures 7.5. and 7.6.). Considerable scatter was observed for the box lap shear joints with the adhesive fillets removed prior to testing, however, better and more consistent results were obtained from the fatigue tests of the ADtranz joints tested with the fillets left un-removed. This was attributed to the improved peel stress distribution at the extremes of the overlap because of presence of the adhesive fillets. A fatigue endurance limit was experienced for the ADtranz boxed joints, both with and without the hardened adhesive fillets, at a load range of approximately 20 kN, ~ 40% of the mean static strength. In comparison to spot welded and weldbonded joints, adhesive bonded joints performed much better and this was attributed to the improved stress distribution within the joint (Figure 7.8.). The results of the room temperature creep tests suggested that time at load is a very important factor, thus, dynamic fatigue performance is very likely to be sensitive to the test frequency. Figure 7.9. compares the high cycle fatigue performance of ADtranz box lap shear joints with the low cycle fatigue of standard single overlap shear joints. Possibly, joints will fail sooner at low test frequencies due to accumulated creep strain, which is much lower at high test frequencies and, thus, the joints will survive longer (11). The dynamic fatigue test programme presented in this thesis needs to be expanded to include tests conducted over a range of frequencies, from 2 to 100 Hz.

**Surface Characterisation** Throughout the experimental work several stainless steel surface pre-treatments have been considered and thus a number of different techniques were employed to physically and chemically characterise the pre-bonded surfaces and the post-fracture faces. SEM and surface profilometry are useful techniques for characterising the physical nature of pre-bonded adherends, and SEM is an excellent means of examining fracture faces to determine the loci of failure. IRS and EDX analysis were both used successfully to chemically verify the presence of a thin adhesive layer on post-fracture faces denoting interfacial <sub>Adhesive</sub> failure. XPS is used to provide elemental information of the top 5 nm, and is widely employed to evaluate pre-bonded adherends, however, it is less suitable for post-fracture analysis because of problems with the adhesive charging. GDOES analysis was employed successfully to evaluate the cleaning efficiency of different pre-bonding treatments. However, if quantitative analysis is required then XPS is a more appropriate surface analytical technique. GDOES

can provide quantitative information, but the elements to be quantified must be calibrated against a known standard.

In summary, the work presented in this dissertation has shown that toughened epoxy systems offer the ultimate in mechanical performance and are compatible with, and suitable for bonding, stainless steels. The surface of stainless steel must be cleaned prior to bonding to optimise the interfacial bond strength between adhesive and adherend, although the cleaning procedure need not be too stringent. Surface roughening by mechanical or chemical means is beneficial to joint durability because it increases the surface area available for chemical bonding, increases the surface energy to render it more adhesive-receptive, creates sites for mechanical locking, and cleans the surface of the steel sufficiently well. Priming the pre-bonded steel surface prior to bonding may promote and maintain stable chemical bonds between the adhesive and adherend, however, the primer may impart brittleness to the joint if the thickness of the layer is excessive. The thickness of the adherend will contribute to the stiffness of the joint, but the inherent yield strength of the adherend is much more significant. The degree of rotation experienced by lap joints in tension will greatly depend on the point at which the adherend plastically deforms, since this will immediately lead to a critical peel stress at the extremes of the overlap and the joint will fail prematurely by peel-dominated, adherend-controlled failure. However, if the yield strength of the adherend is sufficiently high to resist plastic rotation, then a higher joint strength will be reached before the joint fails by shear-dominated, adhesive-controlled failure. The peel stress distribution at the extremes of the overlap is also reduced by leaving the fillets of hardened squeeze-out intact. N.B. The contribution to joint stiffness afforded by the inherent yield strength of the adherend is in agreement with other workers (123, 124). Finally, in both room temperature creep and dynamic fatigue tests of single overlap shear joints an endurance limits were observed for the ADtranz box lap shear joints at 40% of the mean static strength. In addition, adhesive bonded joints were shown to perform better than spot welded and weldbonded joints under dynamic loading, and are likely to be very dependent upon the test frequency; low cycle fatigue is possibly more detrimental to the fatigue life of the joint than high cycle fatigue.

## 10.0. CONCLUSIONS

The results of the work presented in this thesis has led to the following conclusions:

1. Standard single overlap shear and floating roller peel tests can be used to discriminate between different adhesive systems, but these tests are less sensitive to the surface condition of the adherend and the test environment. The Boeing wedge crack extension test is more reliable for evaluating different surface pre-treatments and service environments.
2. If stainless steels are to be joined successfully using adhesives with the intention of employing the resulting fabrications in structural applications, toughened epoxy systems must be considered to be the ultimate adhesives, because of their high shear strength and ability to form strong, durable bonds with the stainless steel surface.
3. The surface condition of the pre-bonded stainless steel is an important consideration. A degree of surface cleanliness is required to optimise the chemical intimacy between the adherend and the adhesive to ensure strong and durable bonds; roughening the surface of the steel prior to bonding by mechanical or chemical means will improve the environmental durability of adhesive bonded joints; surfaces primers are important for protecting the chemical integrity of freshly pre-treated adherends until the time when they are bonded, although care must be exercised during the application of the primer to control the thickness and distribution because an excessive primer layer can impart brittleness to the joint.
4. Etching stainless steel in sulphuric acid can result in the formation of an iron oxide (smut) on the surface of the etched steel. Although high lap shear strengths may be realised, the oxide is weakly adhered to the metal surface, as the loci of failures was observed to be at the metal / metal oxide interface. The bond between the adhesive and the metallic oxide proved to be more resilient than the bond between the metal and its oxide.

5. Although the results of the lap shear and peel tests after ageing in ambient and high humidity environments were high, the susceptibility of adhesive joints to moisture ingress was clear from the wedge test results. Surface pre-treatments can be employed to optimise joint durability, although there is still much work to be done in this area, for example, modifying adhesive formulations.

6. The stiffness of the adherend material significantly influences lap shear strength. Stiffness is imparted to the joint by the thickness of the adherend and its inherent yield strength, and will resist joint rotation and, thus, minimise the peel stresses at the extremes of the overlap which will result in premature joint failure. Elastic rotation of the single overlap joint can be modeled as a function of the shear stress by:

$$\theta_{TOTAL} = \frac{h+t}{a \cdot \left[ 1 + \frac{E \cdot h^3}{6 \cdot \sigma_s \cdot l \cdot a^2} \right]} \quad (6.11.)$$

7. The line peel force and the line peel stress acting on the extremes of the overlap during elastic rotation of a single overlap joint can also be modeled as a function of the shear stress by:

$$P_f = \frac{\sigma_s(h+t)}{\frac{(a^2 + c^2)}{a \cdot c}} \cdot \left[ 1 + \frac{E \cdot h^3}{6 \cdot \sigma_s \cdot 2c \cdot (a^2 + c^2)} \right] \quad (6.22.)$$

8. Single overlap shear joints with adherends of low stiffness are more likely to fail as a result of critical peel stresses induced by joint rotation and plastic deformation (peel-dominated, adherend-controlled failure). And, single overlap shear joints incorporating ‘stiff’ adherends will resist plastic deformation to a higher stress, therefore the peel stresses will be minimised and joint failure is likely to be due to the adhesive shearing at a critical shear stress (shear-dominated, adhesive-controlled failure).

Joints incorporating thicker adherends should theoretically rotate more, but the stiffness imparted to the joint by the thicker adherends may be sufficient to resist plastic deformation. High yield strength

adherends will impart stiffness to the joint, minimising the peel stresses at the extremes of the overlap, and thus, higher lap shear strengths will be obtained.

9. Single overlap shear joints can withstand low loads (~40% mean static failure load) for considerable periods of time without fracture. Providing design engineers with a design load of about  $250 \text{ N.mm}^{-1}$ . There was good correlation between standard single overlap and ADtranz box overlap joints.

10. Single overlap shear type joints can withstand high cyclic loading at low loads (20 kN range) for a considerable number of cycles ( $10^7$ ). Providing design engineers with a design load of  $250 \text{ N.mm}^{-1}$ . However, when considering adhesives it is likely that joints will be sensitive to frequency and joints subjected to low cycle loads may fracture prematurely at even relatively low loads. Thus, dynamic fatigue tests must be conducted at a diverse range of test frequencies.

11. Dynamic fatigue performance of adhesive joints is favourable compared to that of spot welded (111) and weldbonded joints (112). However, adhesive bonded joints are likely to be sensitive to the test frequency and particularly susceptible at low test frequencies.

12. Removing the fillets of hardened adhesive squeeze-out from around the perimeter of the joint prior to testing will reduce the static strength and the dynamic fatigue strength of single overlap joints because the intensity of the peel stresses at the extremes of the overlap will be intensified.

## 11.0. FUTURE WORK

### 1. Comparative Analysis

**Static tests** The standard single overlap shear testing programme should be expanded to include a wide range of adherend thicknesses, from 4 to 20 mm, to confirm the predictions of the elastic model described in Chapter 6.0. Different stainless steel grades should also be incorporated in the schedule to further evaluate the contribution to joint stiffness afforded by the yield strength of the adherend.

**Room temperature creep** The room temperature creep work programme should be extended to firmly establish a room temperature creep endurance limit, and elevated temperature creep of standard overlap shear joints needs to be considered.

**Dynamic fatigue** The fatigue work programme should be extended to determine S-N data for adhesive bonded single overlap joints incorporating AISI 304L stainless steel adherends tested over a full range of frequencies, to study the effect of test frequency on fatigue strength. S-N data should also be determined for adhesive bonded single overlap joints incorporating adherends of different thicknesses and made from different stainless steel grades to establish a relationship between adherend yield strength and fatigue strength: high and low cycle fatigue should be considered, i.e. two extreme test frequencies shall be used.

### 2. Fracture Mechanics Approach

A primary consideration in designing adhesive joints is the possibility of crack growth within the adhesive or at the interface, which can prove catastrophic if the fracture resistance of the adhesive or interface is exceeded. Thus, it is desirable to explain the fracture toughness in terms of a crack growth parameter that reaches a critical value for catastrophic growth. One such parameter is the strain energy release rate ( $G$ ); the amount of energy dissipated per unit amount of crack extension. Strain energy release rate data should be obtained for adhesive bonded joints incorporating adherends made from different stainless steel grades over a range of test frequencies using double cantilever beam (DCB) specimens as shown in Figure 11.1.

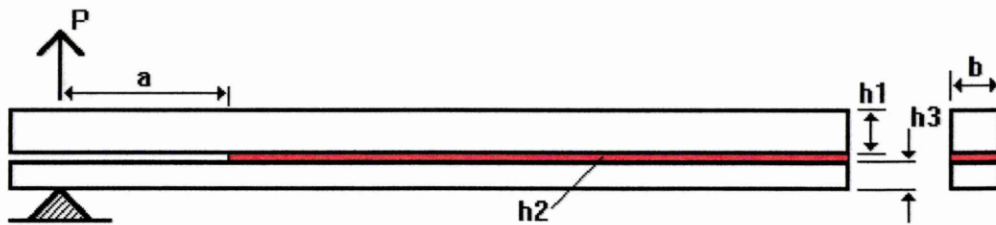


**Figure 11.1. Double cantilever beam (DCB) specimen:**

The DCB specimen operates under Mode I loading, but can be modified to operate in mode I/II and Mode I/III mixed modes, thus, the joint fracture toughness can be obtained for all three modes. This is important since any of the modes can operate and may lead to failure in adhesive assemblies. To model the dynamic fatigue behaviour of stainless steel adhesive joints, DCB tests, at a range of frequencies, should be run concurrently to the high and low cycle fatigue tests and should incorporate different stainless steel grades.

## REFERENCES

1. Kinloch, A. J. Durability of Structural Adhesives (Ed. A. J. Kinloch), App. Sci. Pub. (1983).
2. Brockmann, W., Hennemann, O. D., Kolleck, H., Matz, C. Int. J. Adhesion and Adhesives 6, 3 (1986).
3. Fay, P. Materials World: Bonding and Joining. Aug. (1994).
4. Kennedy, J. Materials World: Automotive Materials Dec. (1993).
5. Brockmann, W. Durability of Structural Adhesives (Ed. A. J. Kinloch), App. Sci. Pub. (1983).
6. Budde, I., Hahn, O. Welding in the World 30, 12 (1992).
7. Wines, B. L. Automotive Engineering 97, 7 (1989).
8. Gaskin, G. B., Brown, S. R. 23<sup>rd</sup> Int. SAMPE Tech. Con. (1991).
9. Bouquet, F., Cuntz, J. M., Coddet, C. J. Adhesion Sci. Technol. 6, 2 (1992) .
10. Lees, W. A. Adhesives in Engineering Design, The Design Council. (1984.)
11. Kinloch, A. J. Adhesion and Adhesives: Science and Technology, Chapman and Hall. (1987).
12. Avesta Sheffield AB Annual Report. (1994).
13. Allen, K.W. Appendix 1: Fundamental Aspects of Adhesion, in Adhesives in Engineering Design. (Lees, W. A.). The Design Council, London. (1984).
14. Lieng-Huang Lee. Recent Studies in Polymer Adhesion Mechanisms in Adhesive Bonding (Ed. Lieng-Huang Lee). Plenum Press, New York. (1991).
15. Wake, W. C. Lecture Series No. 4: Adhesives. The Roy. Inst. of Chemistry. (1966).
16. Lieng-Huang Lee, The Chemistry and Physics of Solid Adhesion, in Fundamentals of Adhesion (Ed. Lieng-Huang Lee). Plenum Press, New York (1991).
17. Gutowski, W. Thermodynamics of Adhesion in Fundamentals of Adhesion (Ed. Lieng- Huang Lee). Plenum Press, New York (1991).
18. Good, R. J. and Chaudhury, M. K. Theory of Adhesive Forces Across Interfaces: 1, in Fundamentals of Adhesion (Ed. Lieng-Huang Lee). Plenum Press, New York (1991).
19. Good, R. J., Chaudhury, M. K. and Oss, C. J. Theory of Adhesive Forces Across Interfaces: 2, in Fundamentals of Adhesion (Ed. Lieng-Huang Lee). Plenum Press, New York (1991).
20. Tabor, D. Winterton, R. H. S. Proc. Roy. Soc. A312, 435 (1969).
21. Israelachvili, J. N. and Tabor, D. Proc. Roy. Soc. A331, 19 (1972).
22. Johnson, K. L., Kendall, K. and Roberts, A. D. Proc. Roy. Soc. A324, 301 (1971).
23. Voyutskii, S. S. Autohesion and Adhesion of High Polymers. Interscience, New York. (1963).
24. Deryaguin, B.V. Research 8, 70. (1955).

25. Deryaguin, B.V., Krotova, N. A., Karassev, V. V., Kirillova, Y. M. and Aleinikova, I. N. Proc. of the 2<sup>nd</sup> International Congress on Surface Activity - III. Butterworths, London. (1957).
26. Deryaguin, B. V. and Smilga, V. P. Adhesion, Fundamentals and Practice. McLaren and Son, London. (1969).
27. Pauling, L. The Nature of the Chemical Bond. Cornell University Press, New York. (1960).
28. Good, R. J. Treatise on Adhesion and Adhesives. Vol. 1: Theory. (Ed. Patrick, R. L.). Marcel Dekker, New York. (1967).
29. Fowkes, F. M. Physicochemical Aspects of Polymer Surfaces. Vol. 2. (Ed. Mittal, K. L.). Plenum, New York. (1983).
30. Callister, Jr., W. D. Materials Science and Engineering: An Introduction. John Wiley and Sons. (1985).
31. Crisp, S., Prosser, H. J., Wilson, A. D. J. Mater. Sci. 11, 36 (1976).
32. Sugama, T., Kukacka, L. E., Carciello, N., J. Mater. Sci. 19, 4045 (1984).
33. Chu, H. T. Eib, N. K., Gent, A. N., Henrikssen, P. N. Advances in Chemistry Series 174 (Ed. Koenig, J. L.). American chemical Society, Washington D. C. (1979).
34. Klein, I. E., Shgaron, J., Yaniv, A. E., Dodiuk, H., Katz, D. Int. J. Adhesion and Adhesives 3, 159 (1983).
35. Kusaka, I. and Suetaka, W. Spectrochim. Acta 36A, 647 (1980).
36. Hirschfelder, J. O., Curtiss, C. F. and Bird, R. B. Molecular Theory of Gases and liquids. Wiley, New York (1954).
37. Fowkes, F. M. and Maruchi, S. Org. Coatings Plastics Chem. 37, 605 (1977).
38. Fowkes, F. M. and Mostafa, M. A. Ind. Eng. Chem. Prod. Res. Dev. 17, 3 (1978).
39. Fowkes, F. M. Rub. Chem. Technol. 57, 328 (1984).
40. Fowkes, F. M., Tischler, D. O., Wolfe, J. A., Lannigan, L. A., Ademu-John, C. M. and Halliwell, M. J. J. Polymer Sci., Polymer Chem. Ed 22, 547 (1984).
41. Fowkes, F. M., Sun, C.Y. and Joslin, S. T. Corrosion Control Organic Coatings (Ed. Leidheiser, H.), NACE, Houston, Texas (1981).
42. Rance, D. G. Thermodynamic Approach to Adhesion Problems, in Industrial Adhesion Problems (Ed. Brewis, D. M. and Briggs, D.), Orbital Press, Oxford (1985).
43. De Gennes, P. G., The Dynamics of Wetting in Fundamentals of Adhesion (Ed. Lieng-Huang Lee), Plenum Press, New York (1991).
44. Young, T. Trans. Roy. Soc. 95, 65 (1905).
45. Wenzel, R. N. Ind. Eng. Chem. 28, 988 (1936).
46. Dupré, A., Theorie Mechanique de la Chaleur, p. 393, Gauthier-Villars, Paris (1869).
47. Fox, H. W. and Zisman, W. A., J. Colloid Sci. 5, 514 (1950).

48. Fox, H. W. and Zisman, W. A., *J. Colloid Sci.* 7, 109 (1952).
49. Fox, H. W. and Zisman, W. A., *J. Colloid Sci.* 7, 428 (1952).
50. Shafrin, E. G. and Zisman, W. A., *J. Phys. Chem.* 64, 519 (1960).
51. Zisman, W. A. in *Advances in Chemistry Series 43* (Ed. Gould, R. F.), American Chemical Society, Washington, p.1 (1964).
52. Schonhorn, H., *J. Phys. chem.* 71, 4578 (1967).
53. Livey, D. T. and Murray, P., *J. Am. Ceram. Soc.* 39, 363 (1956).
54. Benson, C. C., Freeman, P. I. and Dempsey, E., *J. Am. Ceram. Soc.* 46, 43 (1963).
55. Bryant, P. J., Gutshall, P. L. and Taylor, L. H., *Wear* 7, 118 (1964).
56. Shields, J., *Adhesives Handbook*, 3<sup>rd</sup> Ed., Butterworths (1984).
57. Rosty, R., Wagner, R. J., Wegman, R. F., Bodnar, M. J. *Hi-Tech Review* 16 (1984).
58. Shields, J. *Adhesive Bonding: Engineering Design Guides 02*, The Design Council, Oxford Uni. Press (1974).
59. Saunders, D. *TWI Bulletin* 3 (1994).
60. Atkins, R.W., Greenwood, L., Punter, T.J. (1973). Unpublished.
61. Jennings, C.W. *J. Adhesion* 4 25 (1972).
62. Allen, K. W., Alsalim, H. S. *J. Adhesion* 8, 183 (1977).
63. Gettings, M., Kinloch, A. J. *Surf. Interf. Anal.* 1, 5, 165 (1979).
64. Gettings, M., Kinloch, A. J. *Surf. Interf. Anal.* 1, 6, 189 (1979) 6.
65. Pocius, A. V., Almer, C.J., Waid, R.D., Wilson, T.H., Davidian, B. E. *SAMPE J.*, 11 (1984).
66. Rogers, N. L. (Bell Helicopter Company, Texas, U.S.A.) 21<sup>st</sup> National Symposium. (1976).
67. Ross, M. C., Wegman, R. F., Bondnar, M. J. and Tanner, W. C., *SAMPE J.* 6, 2, 12 (1974).
68. Ross, M. C., Wegman, R. F., Bondnar, M. J. and Tanner, W. C., *SAMPE J.* 6, 4, 14 (1974).
69. Ross, M. C., Wegman, R. F., Bondnar, M. J. and Tanner, W. C., *SAMPE J.* 6, 3, 20 (1974).
70. Kaelble, D. H. and Dynes, P. J., *J. Colloid Interf. Sci.* 52, 562 (1975).
71. Leffler, B. *Stainless Steels and their Properties*, Avesta Sheffield AB Research Foundation, Kopieringen, Stockholm (1996).
72. Llewellyn, D. D. *Steels Metallurgy and Applications* 2<sup>nd</sup> Ed., Butterworth Heinemann (1994).
73. Bottrell, N. L., *Preparation of Surfaces for adhesive bonding*, Sheet Metal Industries (1965).
74. Haak, R. P. and Smith, T., *Int. J. Adhesion and Adhesives* 3, 15 (1983).
75. Gaillard, F. and Romand, M., *Surf. Interf. Anal.* 12 (1988).

76. Baun, W. L. Air Force Mats. Lab., Tech. Report TR-79-4138 (1979).
77. Baun, W. L., Solomon, J. S. Air Force Mats. Lab., Tech. Report TR-79-4165 (1979).
78. Sterett, T. L. Int. J. Adhesion and Adhesives 1, 298 (1981).
79. Gaillard, F., Romand, M. J. *Materiaux et Techniques* 3-4, 141 (1987).
80. Comyn, J. *Durability of Structural Adhesives* (Ed. A. J. Kinloch), App. Sci. Pub. (1983).
81. Boiziau, C., Lécayon, G. Int. J. Adhesion and Adhesives 6, 207 (1986).
82. Gaskin, G. B., Pilla, G. J., Brown, S. R. J. *Testing and Evaluation* 22, 3 (1994).
83. De Lacy, H. and Tavakoli, M., proceedings from EURADH '96 p. 503 (1996).
84. Gauthier, M. M. *ASM Engineered Materials Handbook*, Vol. 3, 2 (1990).
85. Landrock, A. H. *Adhesives Technology Handbook*, Noyes Pub.(1985).
86. *ASM Engineered Materials Handbook*, Vol. 3, *Glossary of Terms* (1990).
87. Goddard, T. J., Norris, T. S., Maddison, A., Beevers, A. Oxford Poly., ADENG Report OPSG/1/90, Sect. 2 (1990).
88. Brockmann, W. G. *Structural Adhesives in Engineering*, IMechE Conf. Pub. (1986-6).
89. Dillard, D. A. *ASM Engineered Materials Handbook*, Vol. 3, Sect. 5: Testing and analysis; Introduction (1990).
90. Sancaktar, E. *ASM Engineered Materials Handbook*, Vol. 3, Sect. 5: Testing and Analysis; Static and Dynamic Fatigue Testing (1990).
91. Lee, R. J. DTI Report: The Performance of Adhesive Joints, Sect. 2 (1994).
92. Joseph, R., Bell, J. P., McEvily, A. J., Liang, J. L. J. *Adhesion*, 41 (1993).
93. Su, N., Mackie, R. I., Harvey, W. J. Int. J. Adhesion and Adhesives 12, 2 (1992).
94. Mackie, R. I., Su, N. J. *Adhesion* 42 (1993).
95. Harris, J. A., Fay, P. A. Int. J. Adhesion and Adhesives 12, 1 (1992).
96. Liechti, K. M. *ASM Engineered Materials Handbook*, Vol. 3, Sect. 5: Testing and Analysis; Fracture Testing and Failure analysis (1990).
97. Czanderna, A. W. *Ion Spectroscopies for Surface Analysis* (Ed. Czanderna, A. W., Hercules, D. M.), Plenum Pub. (1990)
98. Boyes, R. *The Manufacture and Durability of Adhesive Bonded Stainless Steel Joints - Ph.D. Transfer Report*, Commercial in confidence, MRI, SHU (1995).
99. Davis, G. D. *ASM Engineered Materials Handbook*, Vol. 3, Section 4: Surface Considerations; Surface Analysis Techniques and Applications (1990).
100. Bryant, R. W., Dukes, W. A. *British J. of Applied Physics* 16, 101 (1965).
101. Bryant, R. W., Dukes, W. A. *Applied Polymer Symposium* 3, 81 (1966).

102. McCann, S. B.Eng. (Hons.) Materials Engineering Final Year Project Report, The Effect of Surface Modification on the Environmental Durability of Stainless steel Adhesive Joints, SHU (1997).
103. Brewis, D. M. and Briggs, D. Industrial Adhesion Problems, Chapter 1. (Ed. D. M. Brewis and D. Briggs), Orbital Press (1985).
104. Goland, M. and Reissner, E. Stresses in Cemented Joints, J. Appl. Mech. (Trans. ASME), Vol. 66 (1944).
105. Adams, R. D. ASM Engineered Materials Handbook, Vol. 3, Section 5: Testing and Analysis; Failure Strength Tests and their Limitations (1990).
106. Jones, T. B. and Williams, N. T., SAE International Congress and Exposition, Detroit, USA (1986).
107. Lewis, A. F. Adhesives Age 15, 38 (1972).
108. Lewis, A. F., Kinmouth, R. A. and Krehling, R. P. J. Adhesion 3, 249 (1972).
109. Wake, W. C., Allen, K. W. and Dean, S. M. Elastomers: Criteria for Engineering Design p. 311 (Ed. C. Hepburn and R. J. W. Reynolds), Applied Science Pub., London (1979).
110. Allen, K. W., Smith, S. M., Wake, W. C. and van Raalte, A. O. Int. J. Adhesion Adhesives 5, 23 (1985).
111. Linder, J., Melander, A., Larsson, M. and Bergengren, Y. Fatigue Data and Design Methods for Spot welded Austenitic and Duplex Stainless Sheet Steels, Stainless Steels in Transport Industry, Proceedings of the Ni - Seminar, Report MTR 1/98 (Ed. M. Alenius, M. Lokka, H. Hänninen) (1998).
112. Ring Groth, M. Weldbonded Stainless Steel Joints - Strength and Fatigue Properties, Stainless Steels in Transport Industry, Proceedings of the Ni- Seminar, Report MTR 1/98 (Ed. M. Alenius, M. Lokka, H. Hänninen) (1998).
113. Boyes, R. Ph.D. Thesis, Adhesive Bonding of Stainless Steel: Strength and Durability, Chapter 7: Static and Dynamic Fatigue Performance of Adhesive-Bonded Stainless Steel Lap joints, MRI, SHU (1998).
114. Crocrombe, A. D. Fatigue Failure in Adhesively Bonded Structures: Structural Adhesives in Engineering V (5<sup>th</sup> International Conference), Proceedings p. 80 (1998).
115. Krieger, G. L., Wilson, G. J. Materials Research and Standards (1965).
116. Gent, A. N. and Hamed, G. R. Polymer Eng. Sci. 17, 462 (1977).
117. Gent, A. N. and Hamed, G. R. Plast. Rub. Proc. 3, 17 (1978).
118. Gardon, J. L. J. Appl. Polymer Sci. 7, 643 (1963).
119. Johnston, J. Adhesives Age 11 (4), 20 (1968).
120. Aubrey, D. W., Welding, G. N. and Wong, T. J. Appl. Polymer Sci. 13, 2193 (1969).
121. Igarashi, T. J. Polymer Sci., Polymer Phys. Ed. 13, 2129 (1975).

122. Yamamoto, Y., Yamakowa, S. and Tsuru, S. J. *Polymer Sci., Polymer Phys. Ed.* 18, 1847 (1980).
123. Karachalios, V. K. and Adams, R. D. The Effect of Adherend Plasticity and Overlap Length on the Failure of Single Lap Joints: *Structural Adhesives in Engineering V (5<sup>th</sup> International Conference)*, Proceedings p. 98 (1998).
124. Hadavinia, H., Steidler, S., Durodola, J. and Beevers, A. Stiffness Sensitivity of Adhesive Bonded Coach Joints in Automotive Structures: *Structural Adhesives in Engineering V (5<sup>th</sup> International Conference)*, Proceedings p. 156 (1998).